NASA TECHNICAL MEMORANDUM

NASA TM X-73349

(NASA-TM-X-73349-Vol-4) SPACELAB EXPERIMENT COMPUTER STUDY. VOLUME 4: SPACELAB USER COST DATA (CENTRAL EXPERIMENT COMPUTER) (NASA) 803 p HC A99/MF A01 CSCL 22B
N77-13100
Unclas
G3/15 57000

SPACELAB EXPERIMENT COMPUTER STUDY
Vol IV: Spacelab User Cost Data (Central Experiment Computer)

By James L. Lewis, Bobby C. Hodges, and James O. Christy
Data Systems Laboratory

April 1976

NASA

George C. Marshall Space Flight Center
Marshall Space Flight Center, Alabama

TECHNICAL REPORT STANDARD TITLE PAGE

1. REPORT NO. NASA TM X-73349	2. GOVERNMENT ACCESSION NO.	3. RECIPIENT'S CATALOG NO.
4. TITLE AND SUBTITLE SPACELAB EXPERIMENT COMPUTER STUDY Vol. IV: Spacelab User Cost Data (Central Experiment Computer)		5. REPORT DATE April 1976
		6. PERFORMING ORGANIZATION CODE
7. AUTHOR(S) James L. Lewis, Bobby C. Hodges, and James O. Christy		8. PERFORMING ORGANIZATION REPORT #
9. PERFORMING ORGANIZATION NAME AND ADDRESS George C. Marshall Space Flight Center Marshall Space Flight Center, Alabama 35812		10. WORK UNIT NO.
		11. CONTRACT OR GRANT NO.
12. SPONSORING AGENCY NAME AND ADDRESS National Aeronautics and Space Administration Washington, D. C. 20546		13. TYPE OF REPORT & PERIOD COVERED Technical Memorandum
		14. SPONSORING AGENCY CODE

15. SUPPLEMENTARY NOTES

This is Volume IV of five volumes.

16. ABSTRACT

The purpose of this study was to provide a quantitative cost for various Spacelab flight hardware configurations, along with varied software development options. The three major conclusions reached as a result of this study are as follows:

1. Spacelab program cost for software development and maintenance is independent of experimental hardware and software options.

2. Distributed standard computer concept simplifies software integration without a significant increase in cost.

3. Decision on flight computer hardware configuration should not be made until payload selection for a given mission and a detailed analysis of the mission requirements are completed.

This report is published in five volumes: Volume I contains the Executive Summary (Presentation); Volume II, Study Elements and Approach; Volume II, Spacelab Cost Data; Volume IV, Spacelab User Cost Data (Central Experiment Computer); and Volume V, Spacelab User Cost Data (Distributed Computer).

This is Volume IV: Spacelab User Cost Data (Central Experiment Computer).

17. KEY WORDS		18. DISTRIBUTION STATEMENT Unclassified-Unlimited	
19. SECURITY CLASSIF. (of this report) Unclassified	20. SECURITY CLASSIF. (of this page) Unclassified	21. NO. OF PAGES 799	22. PRICE NTIS

MSFC - Form 3292 (Rev December 1972) For sale by National Technical Information Service, Springfield, Virginia 22151

SPACELAB EXPERIMENT COMPUTER STUDY

TABLE OF CONTENTS

PAGE INTENTIONALLY BLANK

ii

Technical Memorandum X-73349

SPACELAB EXPERIMENT COMPUTER STUDY

Volume IV: Spacelab User Cost Data (Central Experiment Computer)

SECTION 1 Option IA1 - Central with Mini, Central Software Development by Central Group

1.1 <u>Costing Method</u>

ASSUMPTIONS

- o STIL facility hardware used to maximum extent in lieu of purchasing added hardware.
- o Mini's required are procured such that they are built compatible with existing STIL interface hardware to accommodate real-time simulations for software checkout and verification.
- o DEP mini's are procured that have existing cross support software (assembler, link editor, Fortran Compiler) that will execute on the STIL Host (S360)
- o All DEP mini's are assumed to be procured from different vendors and are not software compatible
- o A centralized group of programmers will develop all software.

Cost Element 4.1 <u>Experiment Application Software Development</u>

Cost Factors

1. Software Development
2. Common Software
3. Host Computer Time
4. Simulation Computer Time
5. Host Computer Time DEP Software
6. Simulation Computer Time DEP Software
7. Travel
8. Training

(1) <u>Software Development</u>

(A) = ((Number of Statements) (Cost/Statement)) Per Flight Per Yr.

Number of Statements = GDC Estimate = ((New Flights) - (Previous Yr. Common)) Per Yr.

Cost/Statement = $45 (Requirements, Code, and Verification) $15 Per Statement is Applied to Integrated Verification (See 4.3 (1))

(1) Total = ((#10) ($45)) Per Yr.

(2) <u>Common Software</u>

(A) ((Number of Statements) (Cost/Statement)) Per Yr. for 5 years Starting in FY81.

Number of Statements = 10% of new Development per Flight Per Yr. Reducing 2% Per Yr. to 0% - Yearly Totals are Accumulative and Accumulated Total is Subtracted from Subsequent Years Required Development.

Cost/Statement = $5 (Document and Place in Library)

(2) Total = ((#5) ($5)) Per Yr.

(3) Host Computer Time

(A) = ((Host Time) (Cost/Hr.)) Per New Flight Per Yr.

Host Time = ((# Instructions) ÷ ((# Instructions/Module)

(Hrs. /Module))

= (# of Modules) (Hrs. /Module)

Hrs. /Module = 18 Compiles/Module @ 3 Mins. /Compile + 9 Functional Simulations @ 12 Mins. / Run + 1 Data Reduction for 75% of Simulation Runs @ 10 Mins. Each

= (54 Mins.) + (108 Mins.) + (70 Mins.)

= 3. 87

Host Cost/Hr. = ((10% Maintenance) + (Operations) + (Consumables)) ÷ (2080 Hrs. /Shift)

= (2. 43) + (57. 69) + (63. 05) = $123. 22/Hr.

# of Modules = #8

(3) Total = (3. 87) (#8) ($123. 22)/Yr.

(4) Simulation Computer Time

(A) = (# of Hrs. /Module) (Cost/Hr.) (# of Modules)

# of Hrs. = 4 Simulations at 60 Min. /Simulation (Includes Set-Up, Runs, and Run Evaluations)

Cost/Hr. = (10% (Maintenance (CDMS, CID, SIMULATION COMPUTER)) + (Consumables) + (Operations)) ÷ 2080 Hrs.

= ($8) + (0) + ((2) ($40K)) ÷ 2080

= ($8) + ($38.46)

= $46.46/Hr.

(4) # of Modules = #8

(4) Total = (($46.46) (#8) (4 Hrs.)) Per Yr.

(5) Host Computer Time DEP Software

(A) = ((Host Time/Module) (#Modules) (Cost/Hr.)) Per Flight/Yr.

Host Time = (# Modules) (Time/Module)

Time/Module = 18 Compiles/Module @ 3 Mins. /Compile
+ 3 Data Reduction Runs/Module @ 10 Mins. /Run

= 84 Mins. /Module

Cost/Hr. = $123.22 (Same as 4.1 (3))

# of Modules = #9

(5) Total = ((1.4 Hrs.) (#9) ($123.22)) /Yr.

(6) Simulation Computer Time DEP Software

(A) =((# of Hrs.) (Cost/Hr.) (# of Modules)) Per Flight/Yr.

# of Hrs. = 7 Simulations at 60 Mins. /Simulation
(Includes Set-up, etc.)

9 Functional Simulations = 3 Realtime Simulations.
Assume no Functional Simulators for DEP.

Cost/Hr. = $46.46 (Same as 4.1 (4))

(6) Total = ((7 Hrs.) ($46.46) (#9)) Per Yr.

(7) Travel

(A) = ((Number of Man Yrs.) (Travel Cost/Man Yr.))/Yr.

Number of Man Yrs. = Number of Man Yrs. Required as Determined by Number of New Instructions.

Travel/Man Yr. = Number of Trips ((Cost of Ticket) + (Number of Days) (Cost Day))

Number of Trips = 4/Man Yr.

Cost of Ticket = $150

Cost/Day = $12.50 Per Diem + $12.50 for Car = $25

Number of Days = 365

Travel = 4(($150) + (365) ($25))

= $600 + $9,125 = $9,725/Man/Yr.

(7) Total = 0 for This Option

(8) Training

(A) = (Number of Programmers) (Cost/Programmer)

Number of Programmers = Number of Programmers Required by Number of New Instructions.

Cost of Programmer = Engineering Estimate $500/Man

(8) Total = 0 for This Option

Cost Element 4.2 Experiment Application Software Maintenance

Cost Factors

1. Experiment Unique Software
2. Experiment Common Software
3. Host Computer Time
4. Simulation Computer Time
5. Host Computer Time DEP Software
6. Simulation Computer Time DEP Software
7. Travel

(1) Experiment Unique Software

(A) = (# of Statements) (Rate of Change) (Cost/Statement)

(Number of Statements) (Rate of Change) = #13

Rate of Change = Engineering Estimate Based on Past Programs = $0% for 1st Re-Fly, 30% for 2nd Re-Fly, 20% for 3rd Re-Fly, 10% for all Subsequent Re-Flys.

Cost/Statement = $45 (See 4.1 for Rationale)

(1) Total = ((#13) ($45)) Per Yr.

(2) Experiment Common Software

(A) = ((# of Statements) (Change Rate) (Cost/Statement)) Per Yr.

Rate of Change = Engineering Estimate = 1%

Cost/Statement = $60 (Due to Verification Necessary for Multi-Use)

(2) Total = ((#6) (1%) ($60)) Per Yr.

(3) Host Computer Time

(A) = (#Modules) (#Hrs. /Module) (Cost/Hr.)

#Modules = Line (#14)

Hrs. /Module = 3.87 (See 4.1 for Rationale)

Cost/Hr. = $123.22 (See 4.1 for Rationale)

(3) Total = ((#14) (3.87) ($123.22)) Per Yr.

(4) Simulation Computer Time

(A) = ((#Modules) (#of Hrs. /Module) (Cost/Hr.)) Per Yr.

Modules = Line (#14)

Hrs. /Module = 4 Hrs. (See 4.1 for Rationale)

(4) Total = ((#14) (4) ($46.46)) Per Yr.

(5) Host Computer Time DEP Software

(A) ((Host Time/Module) (#Modules) (Cost/Hr.)) Per Yr.

Host Time/Module = 1.4 Hrs. (See 4.1 for Rationale)

Modules = Line (#15)

Cost/Hr. = $123.22 (See 4.1 for Rationale)

(5) Total = ((1.4) (#15) ($123.22)) Per Yr.

(6) Simulation Computer Time DEP Software

(A) ((# of Hrs.) (Cost/Hr.) (#Modules)) Per Yr.

# of Hrs. = 7 (See 4.1 for Rationale)

Cost/Hr. = $46.46 (See 4.1 for Rationale)

(6) Total = ((7) ($46.46) (#15)) Per Yr.

(7) Travel

(A) ((Number of Man Yrs.) (Travel Cost/Man Yr.))/Yr.

Number of Man Yrs. = Number of Man Yrs. Required as Determined by Number of Instructions to be Maintained.

Travel = $9, 725 Man/Yr.

(7) Total = 0 for This Option

Cost Element 4.3 EAS Software Integrated Verification

Cost Factors

1. Integrated Verification

2. Host Computer Time

3. Simulation Computer Time

4. Integrated Verification Simulation Software

(1) Integrated Verification

(A) = ((# of Modules) (Cost/Module)) Per Flight/Yr.

# of Modules = #21

Cost/Module = (# of Statement) (Cost/Statement)

# of Statements = 100/Module

Cost/Statement = $15 ($60 Estimated Total Cost Per Statement for Central Development Less $45 for Development)

= $1,500/Module

(1) Total = ((#21) ($1,500))/Yr.

(2) Host Computer Time

(A) = (# Hrs.) (Cost/Hr.)

(2) Total = (0) For This Function (Has Been Included in Required Host Runs 4.1)

(3) Simulation Hardware Time

(A) = (# Hrs./Module) (Cost/Hr.) (# Module)

Hrs./Module = 2 Simulations/Module at 60 Min. Per Simulation (Includes Set-Up, etc.)

Cost/Hr. = $46.46 (See 4.1 (4) B)

Modules = #21

(3) Total = ((2) (#21) ($46.46)) Per Yr.

(4) Integrated Verification Simulation Software

(A) = ((# of Modules) (Cost/Module)) Per Yr.

# of Modules = #29

Cost/Module = $1,500 (See 4.3 (1) for Rationale

(4) Total = ((#29) ($1,500)) Per Yr.

Cost Element 4.4 — Preflight Checkout Software Development

Cost Factors

1. Software Development
2. Common Software
3. Host Computer Time
4. Simulation Computer Time
5. Travel

(1) Software Development

(A) = ((Number of HOL Statements) (Cost/Statement)) Yr.

(1) Total = ((#22) ($30))/Yr.

(2) Common Software

(2) Total = 0 for This Option

(3) Host Computer Time

Host Computer Time = ((Host Time)) (Cost/Hr.)
Ref. 4.1 (3)

(A) = ((3.87) (# Modules) ($123.22))/Yr.

(3) Total = ((3.87) (#22 ÷ 100) ($123.22)) Per Yr.

(4) Simulation Computer Time

(A) = (# Hrs./Module) (Cost/Hr.) (# Modules)
Ref. 4.1 (4)

(4) Total = (4) ($46.46) (#22 ÷ 100) Per Yr.

U.S. DEPARTMENT OF COMMERCE
Technology Administration
National Technical Information Service
Springfield, VA 22161 (703) 487-4650

Figur. .5

NMFS Mean Sea Surface Temperature Map for September, 1978

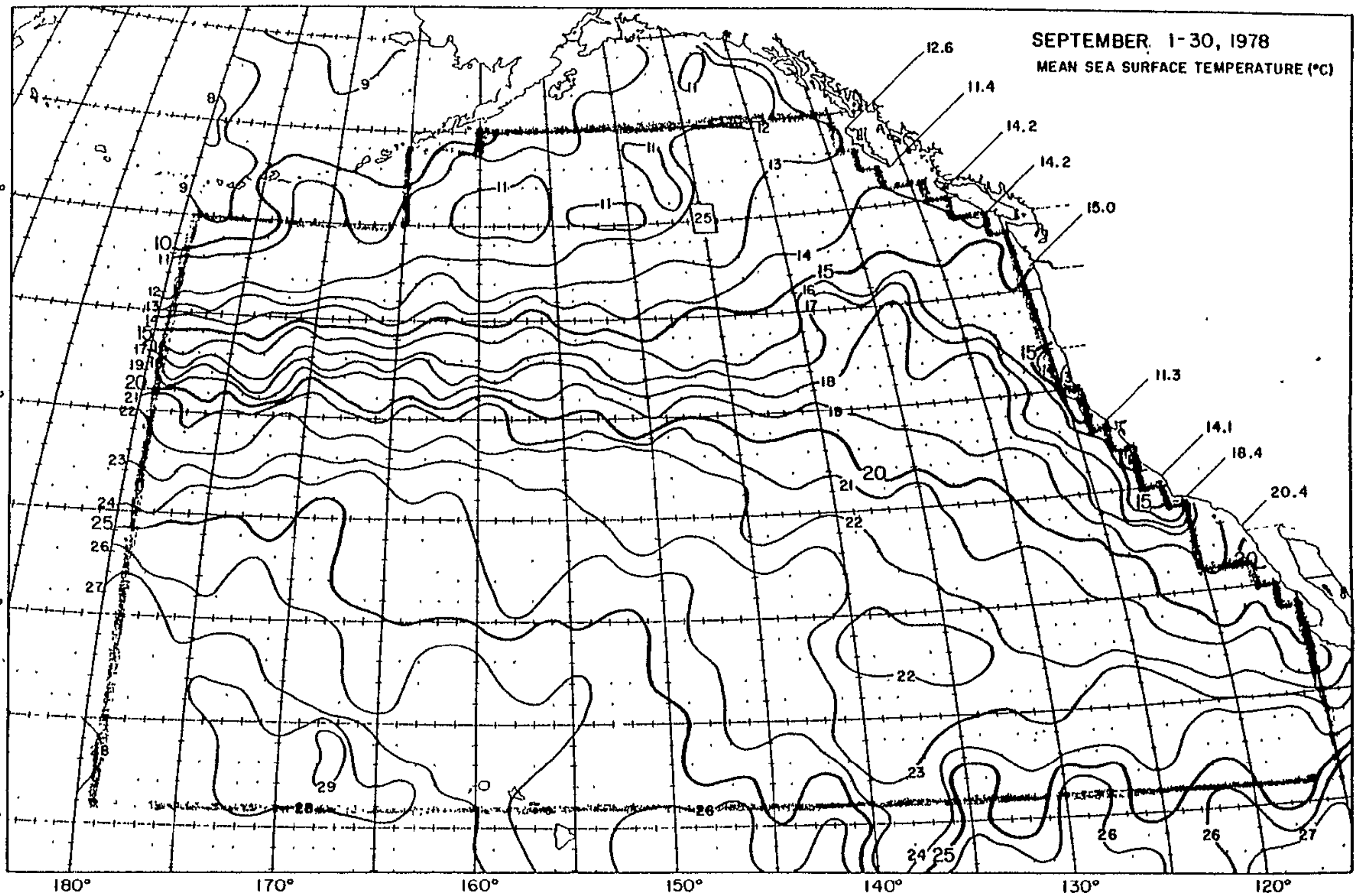

Figure 14

Sample Output from Program MATCH

```
BUOY       44001       212     0   19    46    JSTAT =   1    NTOT =   6

INTERPOLATED MEASUREMENTS
     23.2        .0  1013.7      4.4    91.0      .0       .0       .0       .0
       .0        .0      .0       .0      .0      .0     23.0       .0       .0
MAXIMUM VALUES OVER SIX-HOUR RANGE
     23.5        .0  1014.8      5.3   114.2      .0       .0       .0       .0
       .0        .0      .0       .0      .0      .0     23.3       .0       .0
MINIMUM VALUES OVER SIX-HOUR RANGE
     22.8        .0  1012.8      4.2    54.6      .0       .0       .0       .0
       .0        .0      .0       .0      .0      .0     22.9       .0       .0
STANDARD DEVIATIONS
       .2        .1      .0       .4    20.1      .0       .0       .0       .0
       .0        .0      .0       .0      .0      .0       .1       .0       .0
```

TABLE 3

Buoys Used in Program LOCATE

Buoy ID	North Latitude	West Longitude
41001	35.0	72.0
41002	32.3	75.3
41004	32.6	78.7
42001	26.0	90.0
42002	26.0	93.5
42003	26.0	86.0
44001	38.7	73.6
44002	40.1	73.0
44003	40.8	68.5
44004	39.0	70.0
46001	56.0	148.0
46002	42.5	130.0
46003	52.0	156.0
46004	51.0	136.0
46005	46.0	131.0
46006	41.0	138.0
46007	59.2	152.7
46008	57.1	151.7
46009	60.2	146.8

Figure 13.10. Orbit 1212, 38° N, Nominal and Interim

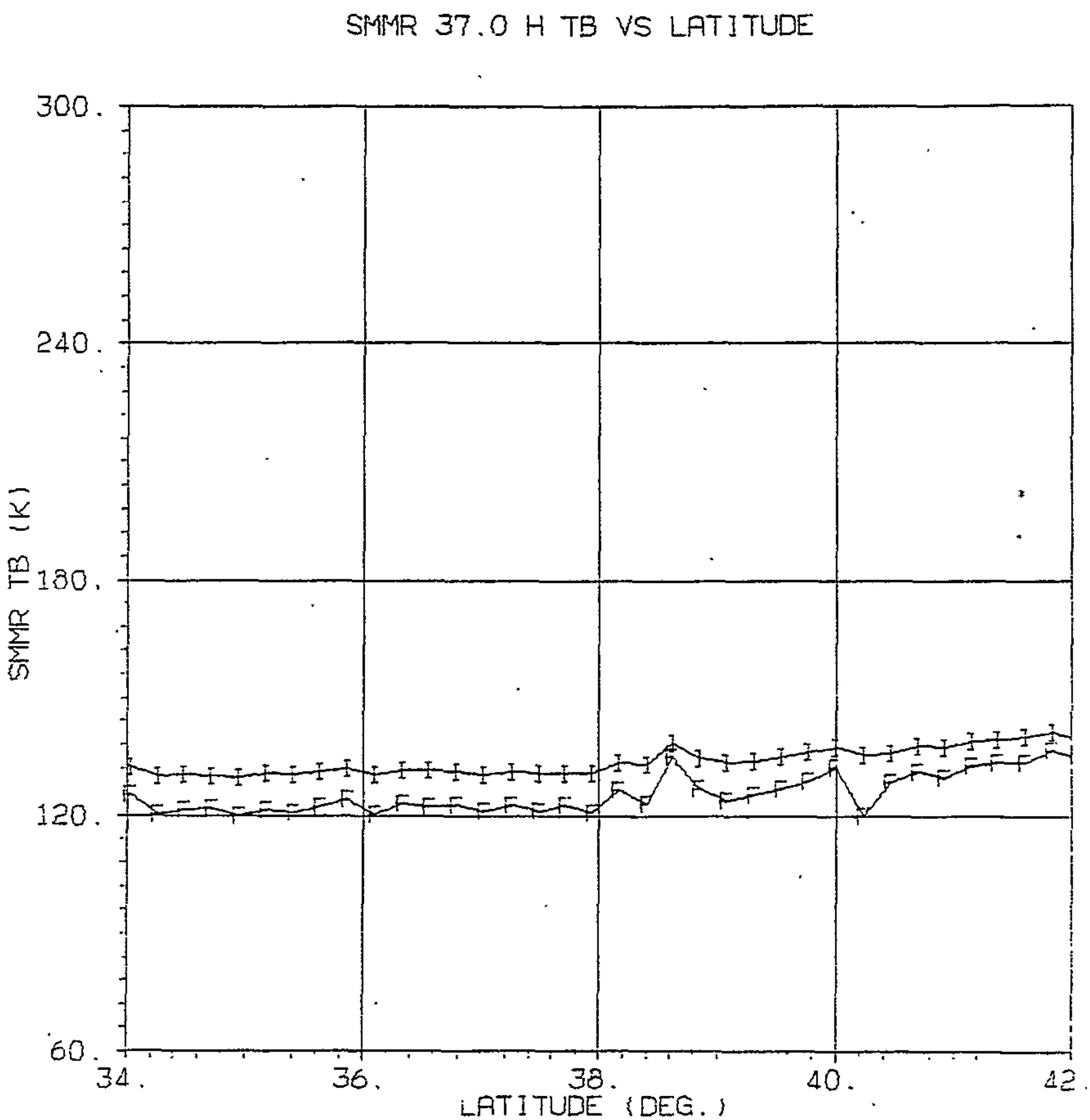

Figure 13.9. Orbit 1212, 38° N, Nominal and Interim

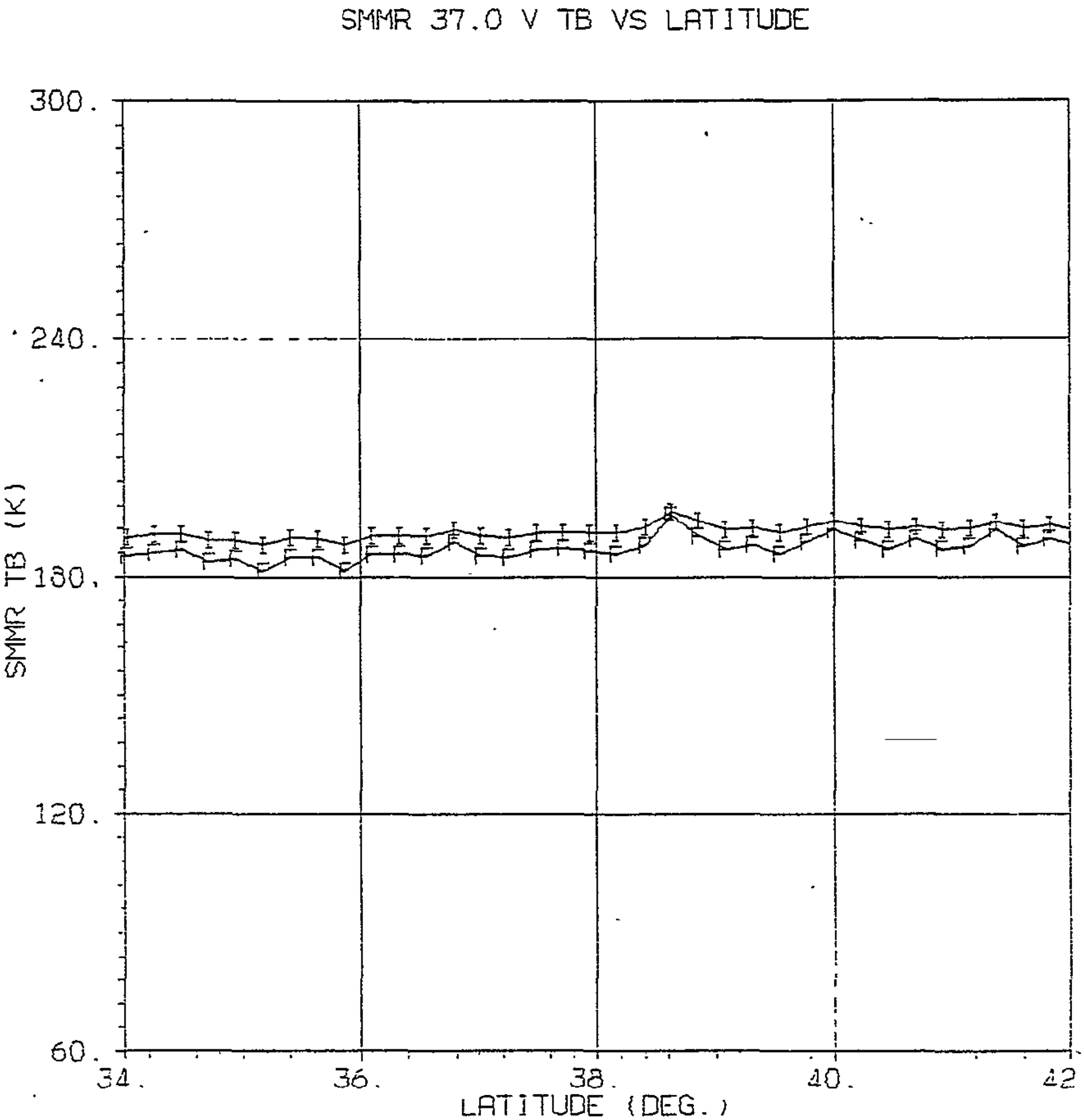

Figure 13.8. Orbit 1212, 38° N, Nominal and Interim

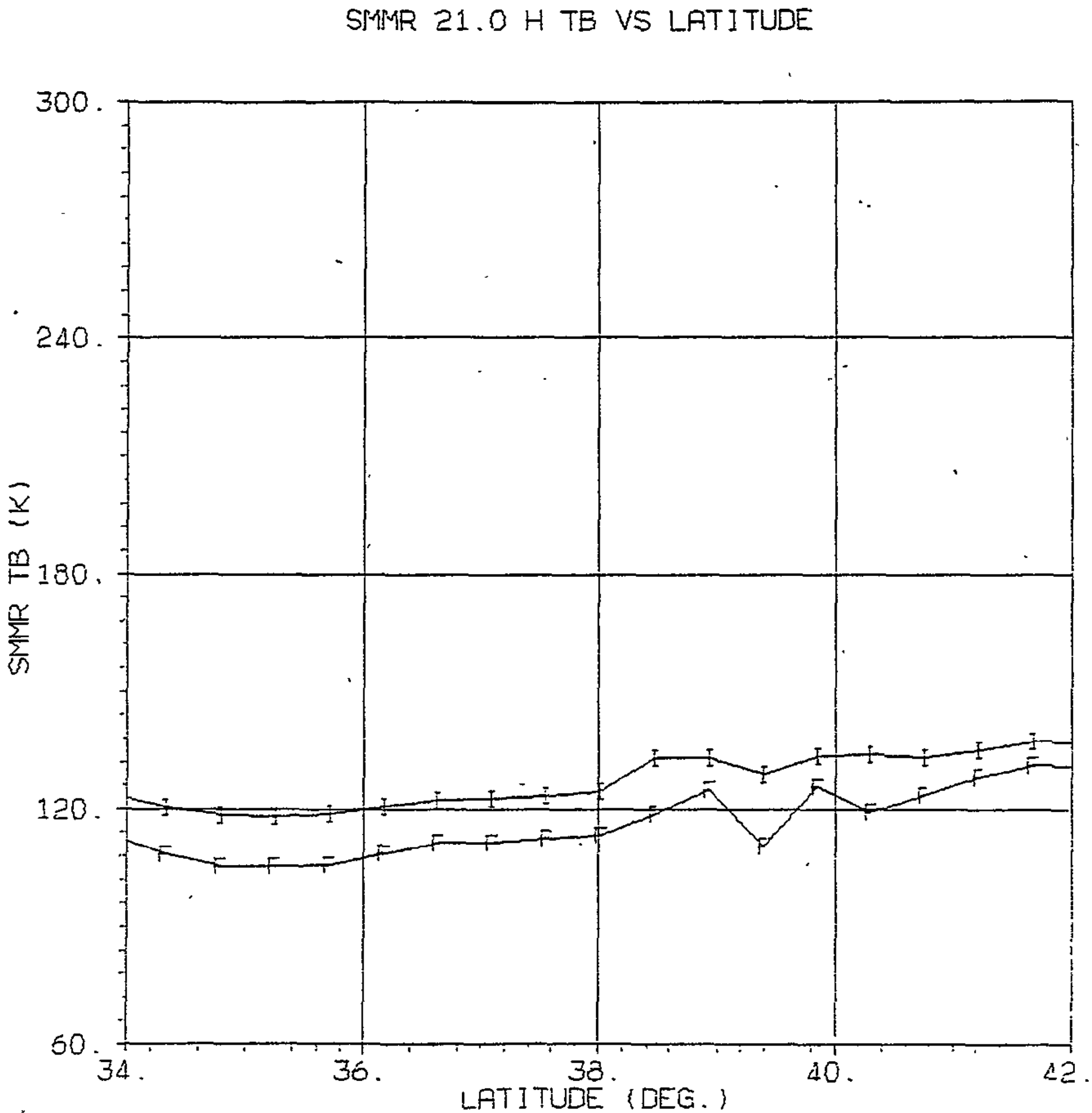

Figure 13.7. Orbit 1212, 38° N, Nominal and Interim

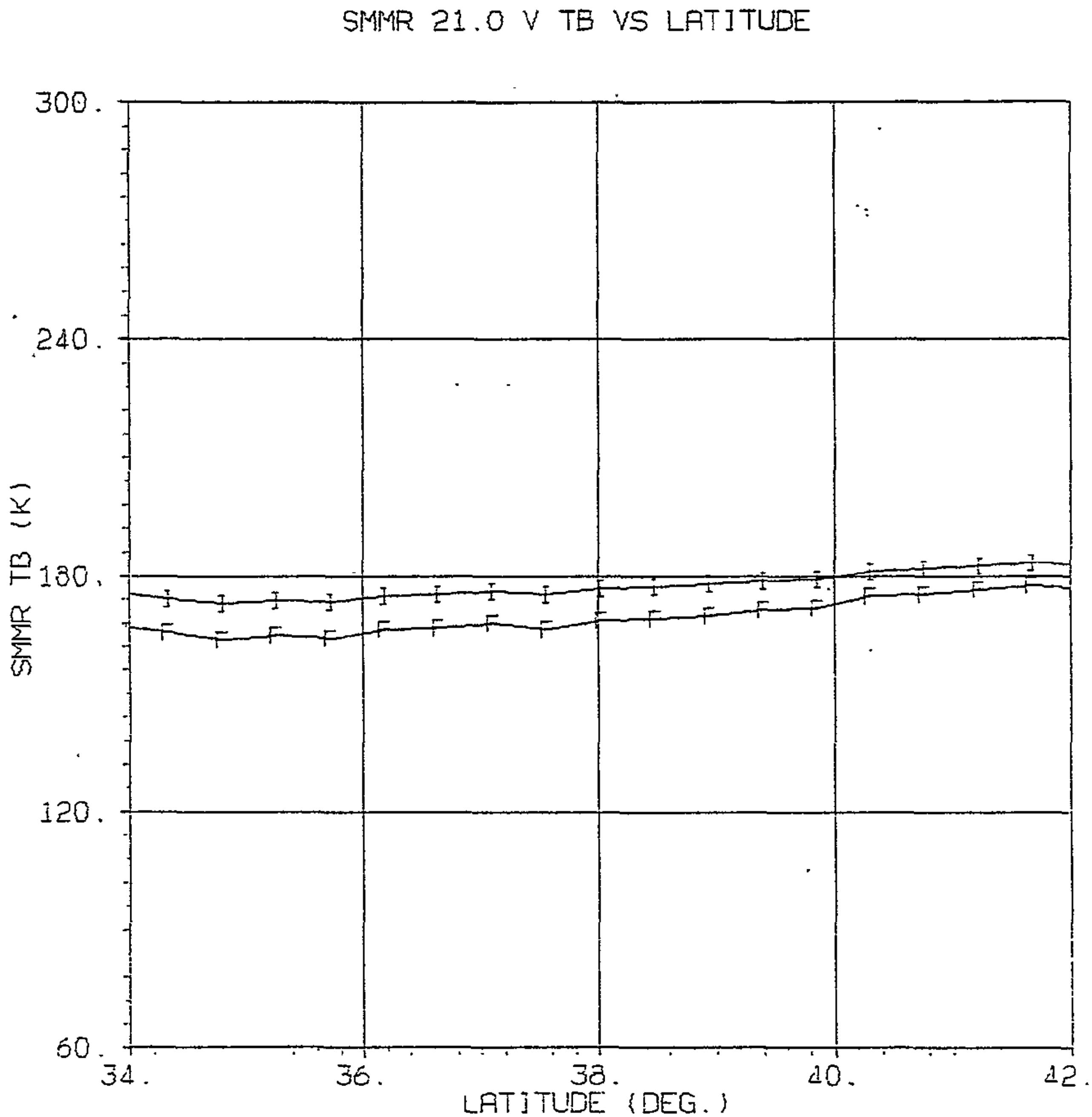

Figure 13.6. Orbit 1212, 38° N, Nominal and Interim

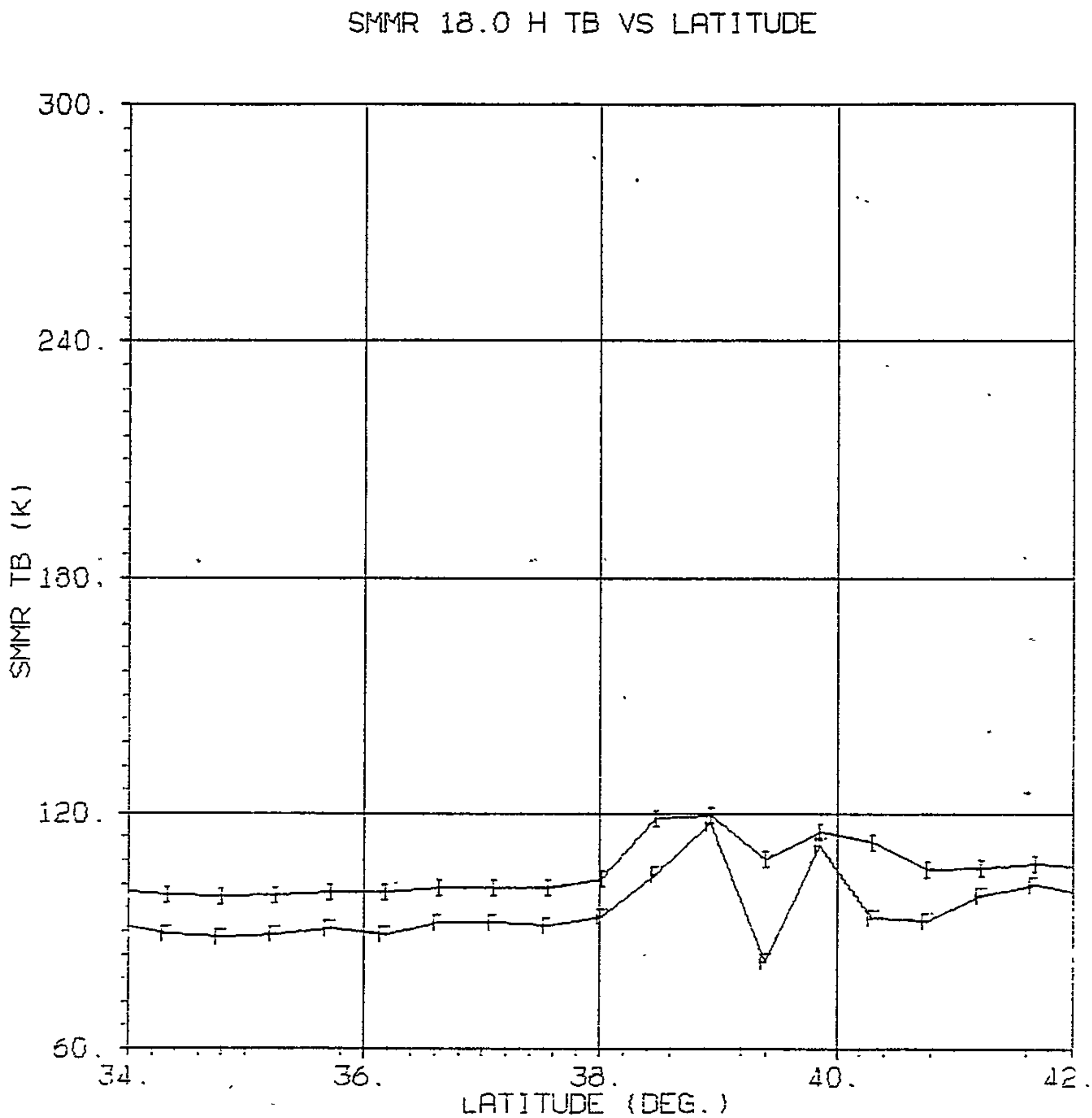

Figure 13.5. Orbit 1212, 38° N, Nominal and Interim

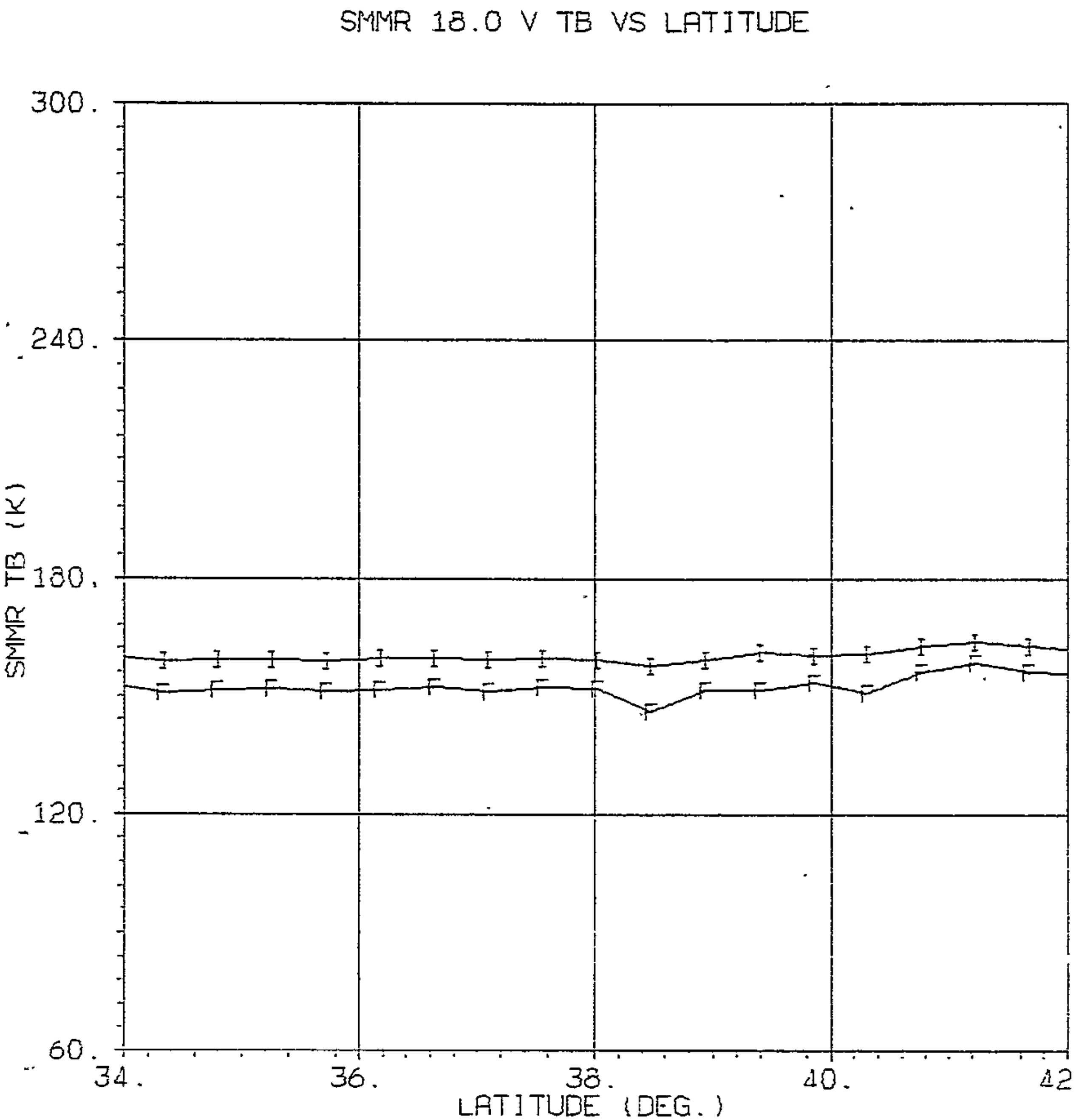

Figure 13.4. Orbit 1212, 38° N, Nominal and Interim

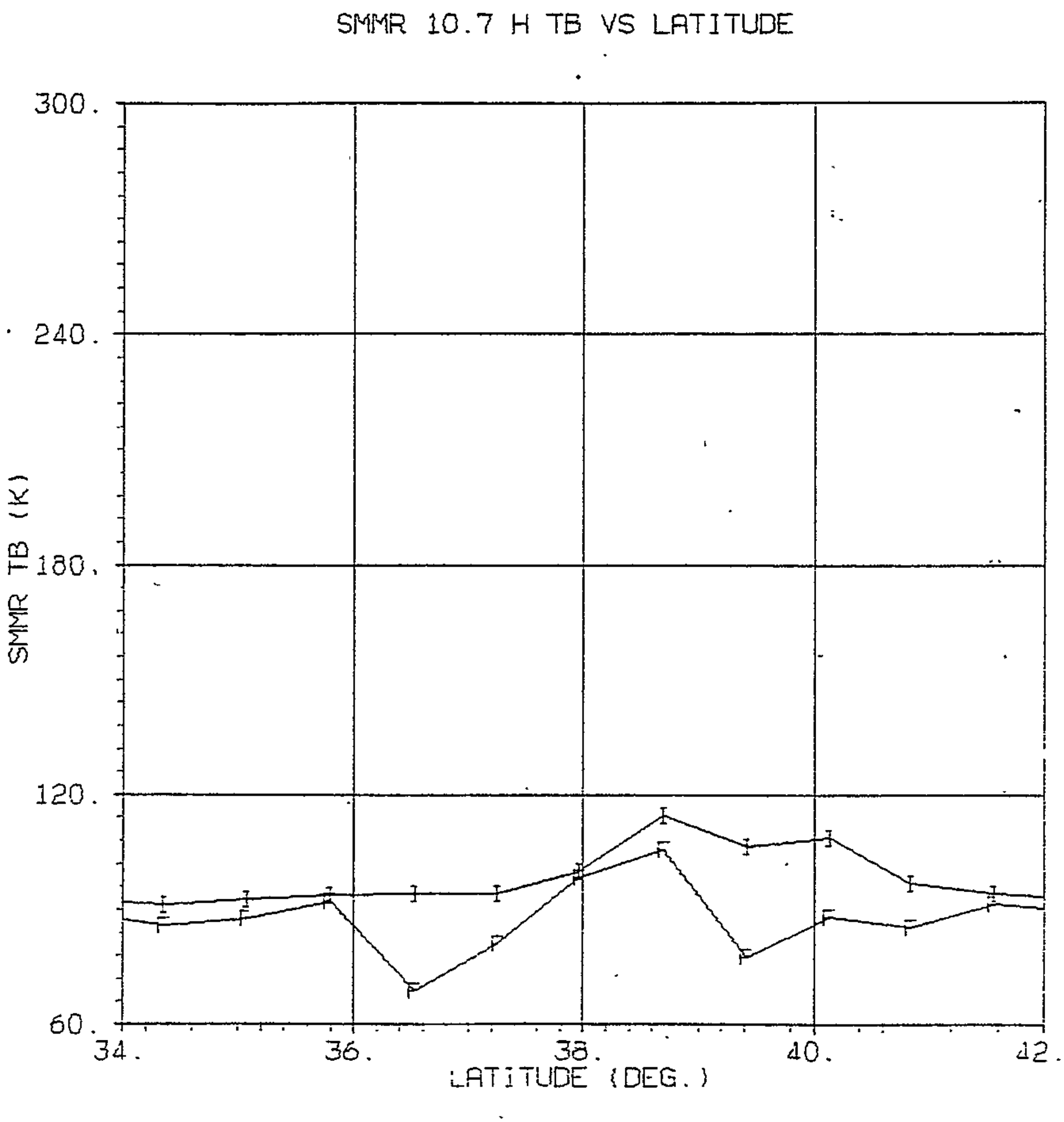

Figure 13.3. Orbit 1212, 38° N, Nominal and Interim

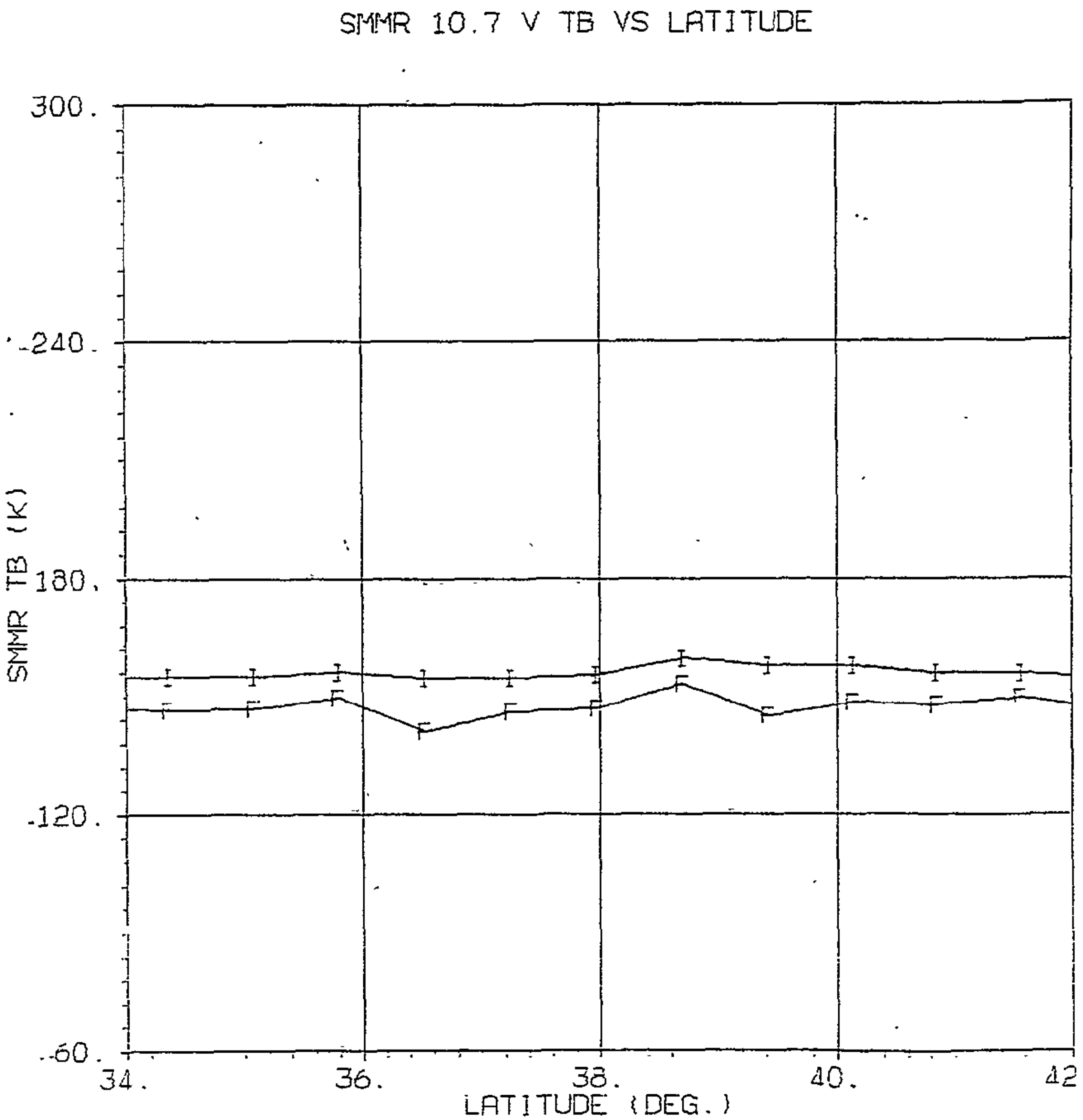

Figure 13.2. Orbit 1212, 38° N, Nominal and Interim

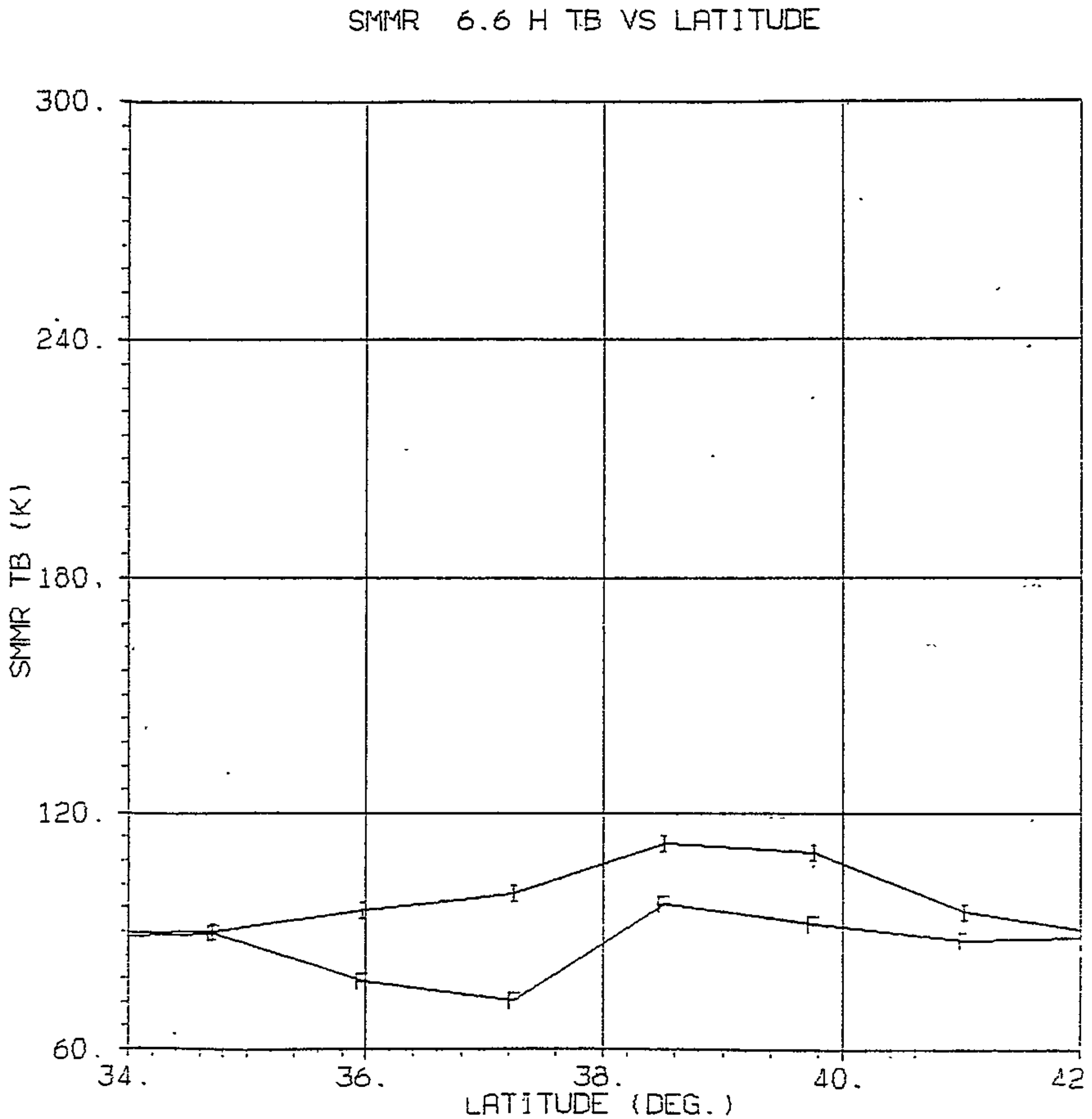

Figure 13.1. Orbit 1212, 38° N, Nominal and Interim

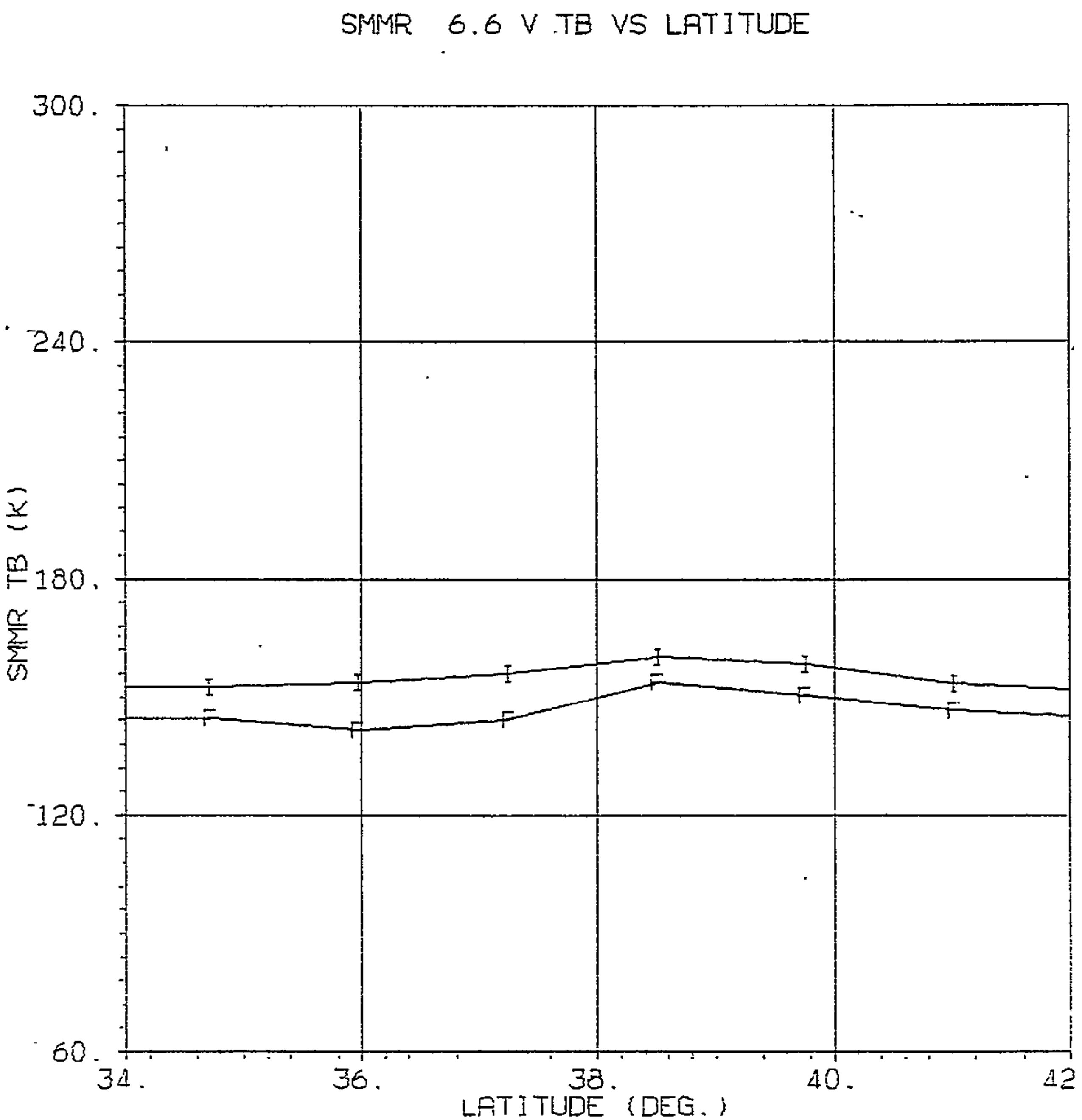

Figure 12.10. Orbit 1212, 38° N, Cross and Interim

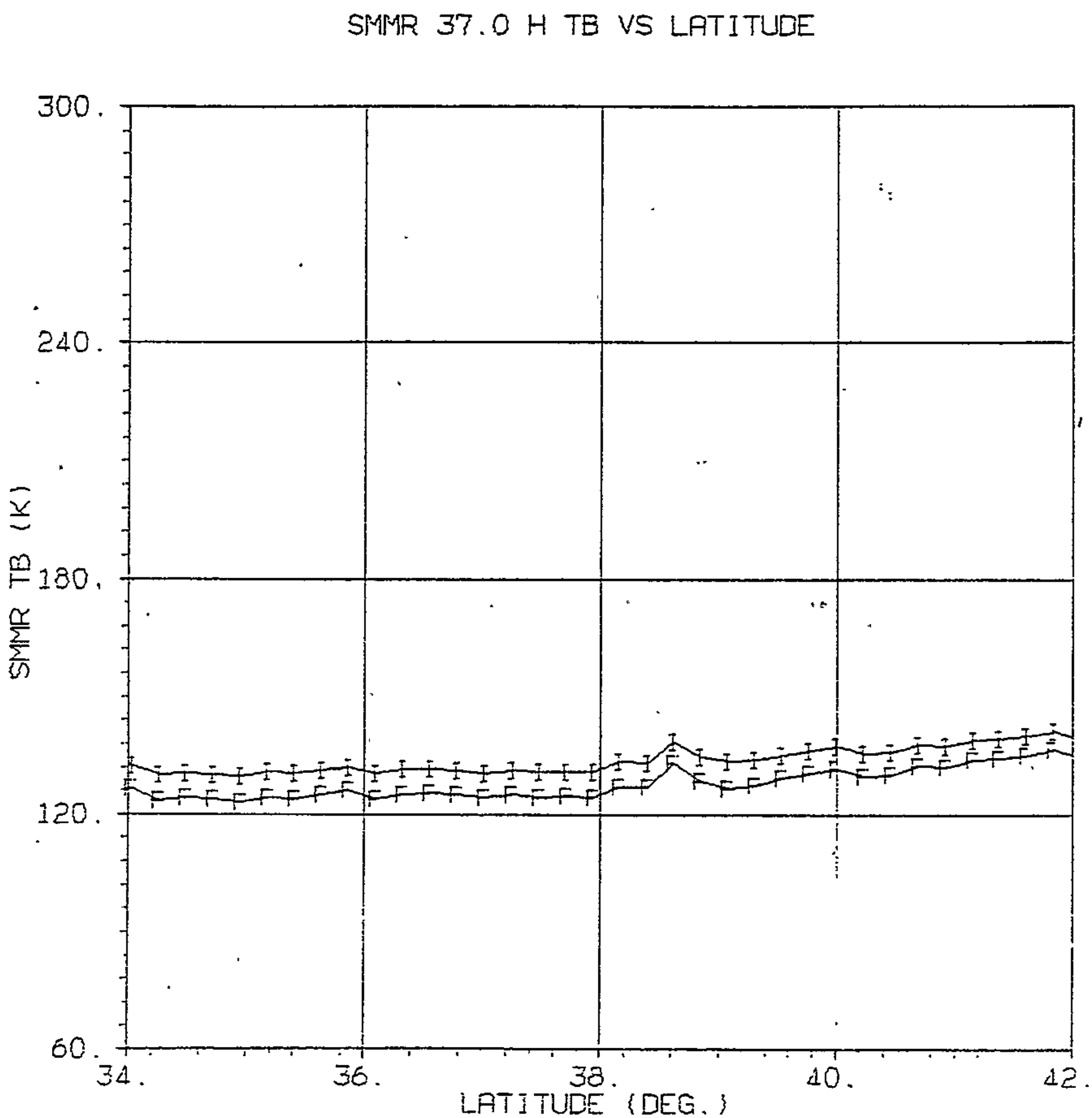

Figure 12.9. Orbit 1212, 38° N, Cross and Interim

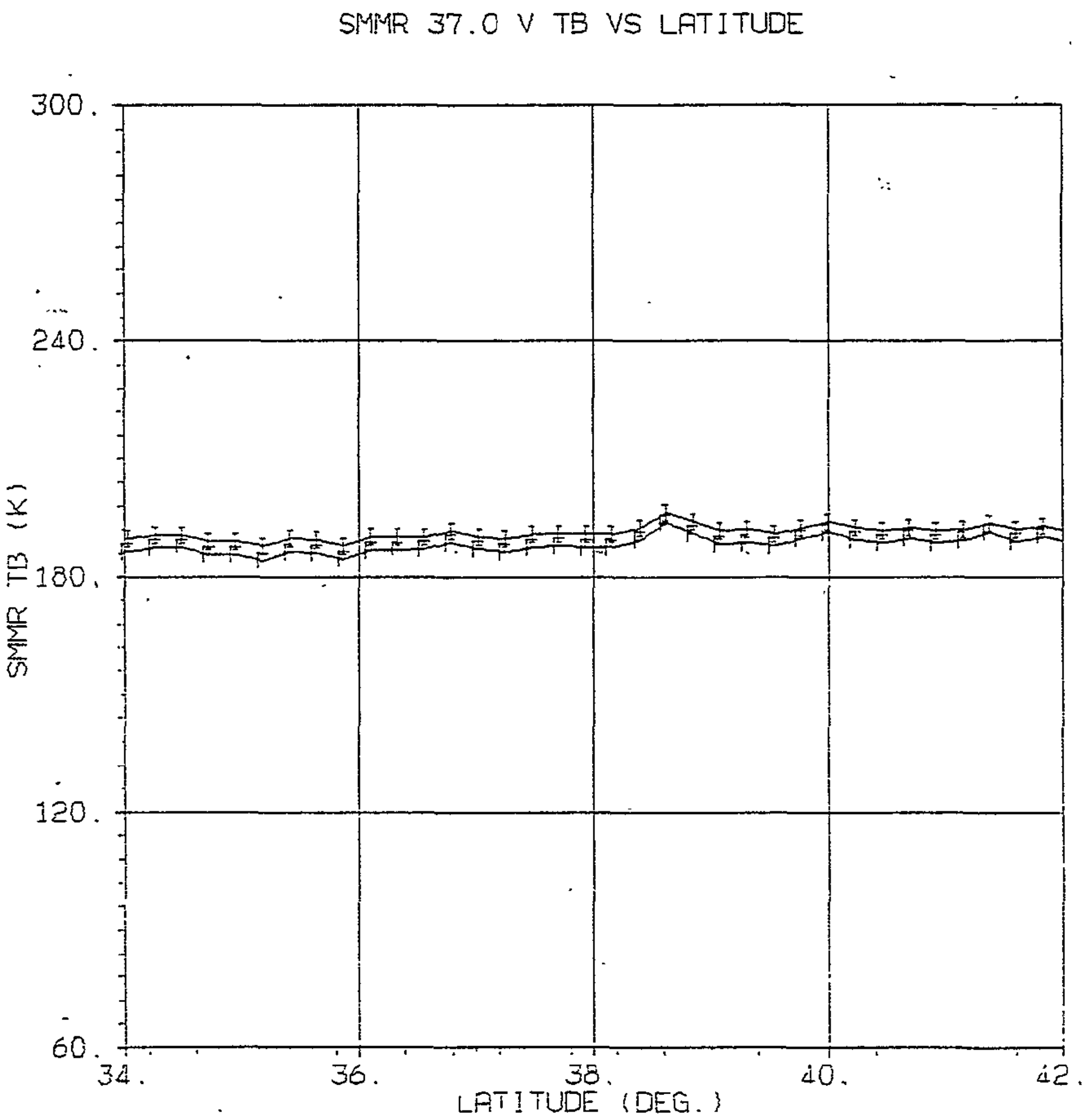

Figure 12.8. Orbit 1212, 38° N, Cross and Interim

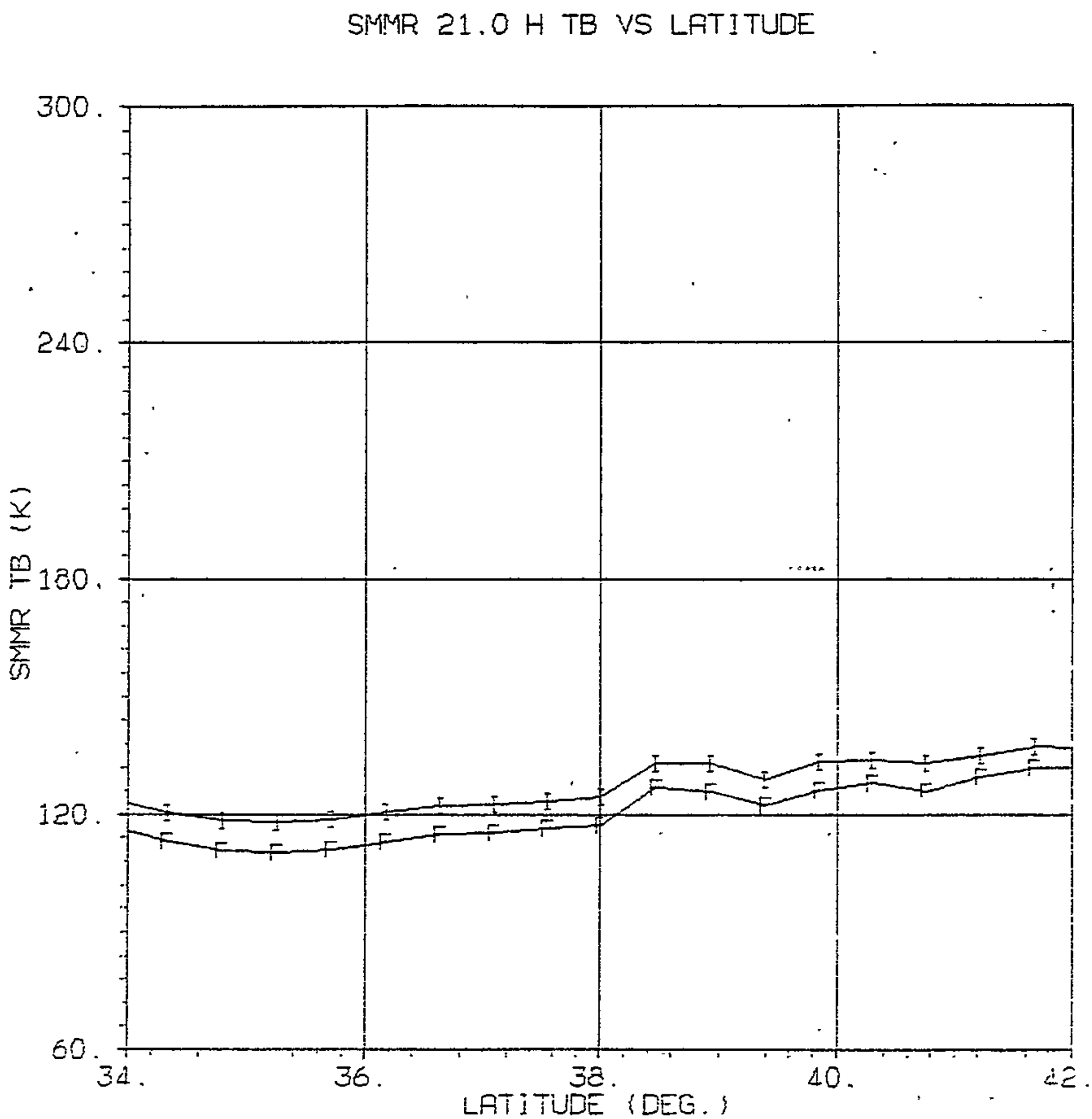

Figure 12.7. Orbit 1212, 38° N, Cross and Interim

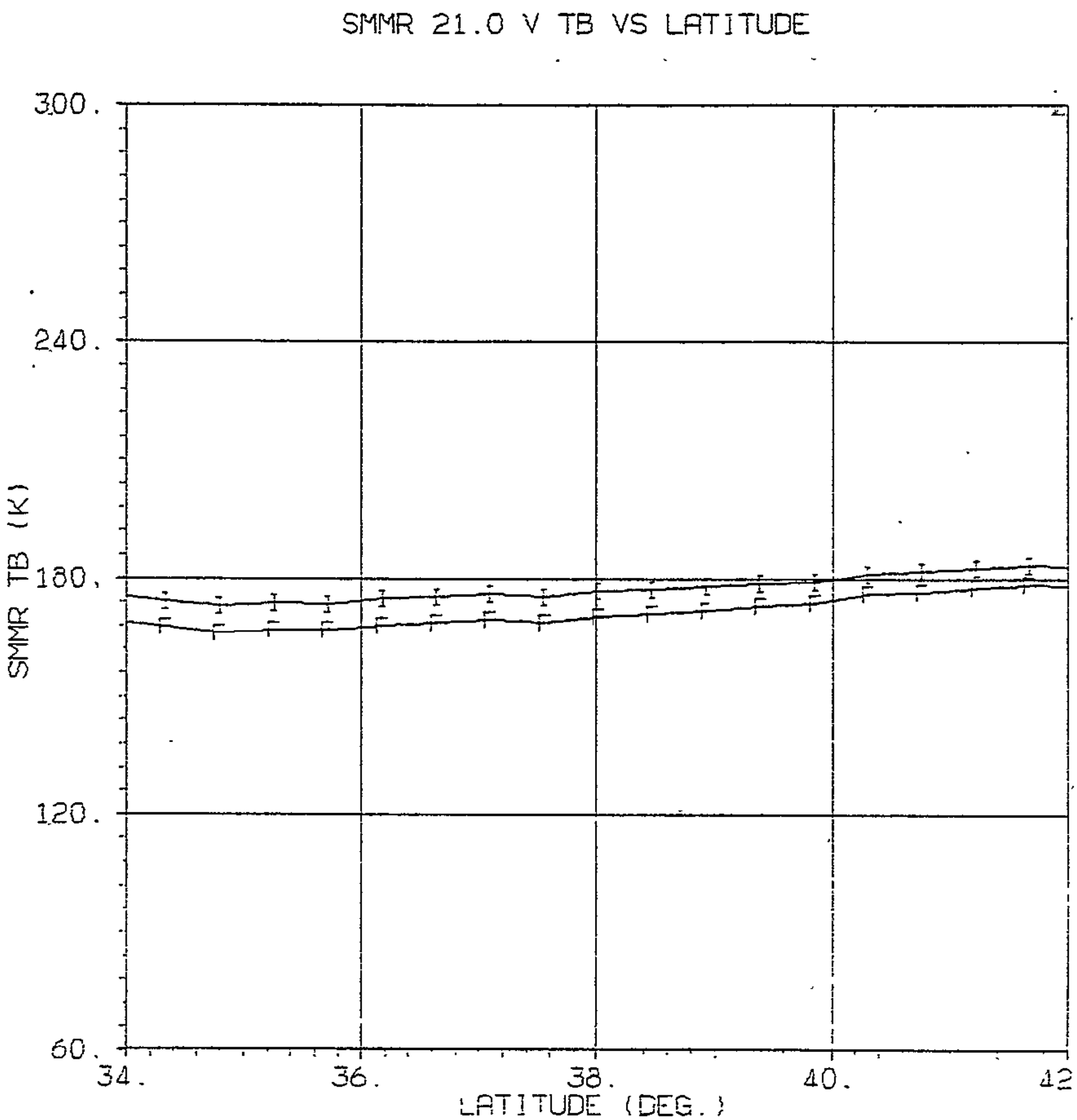

Figure 12.6. Orbit 1212, 38° N, Cross and Interim

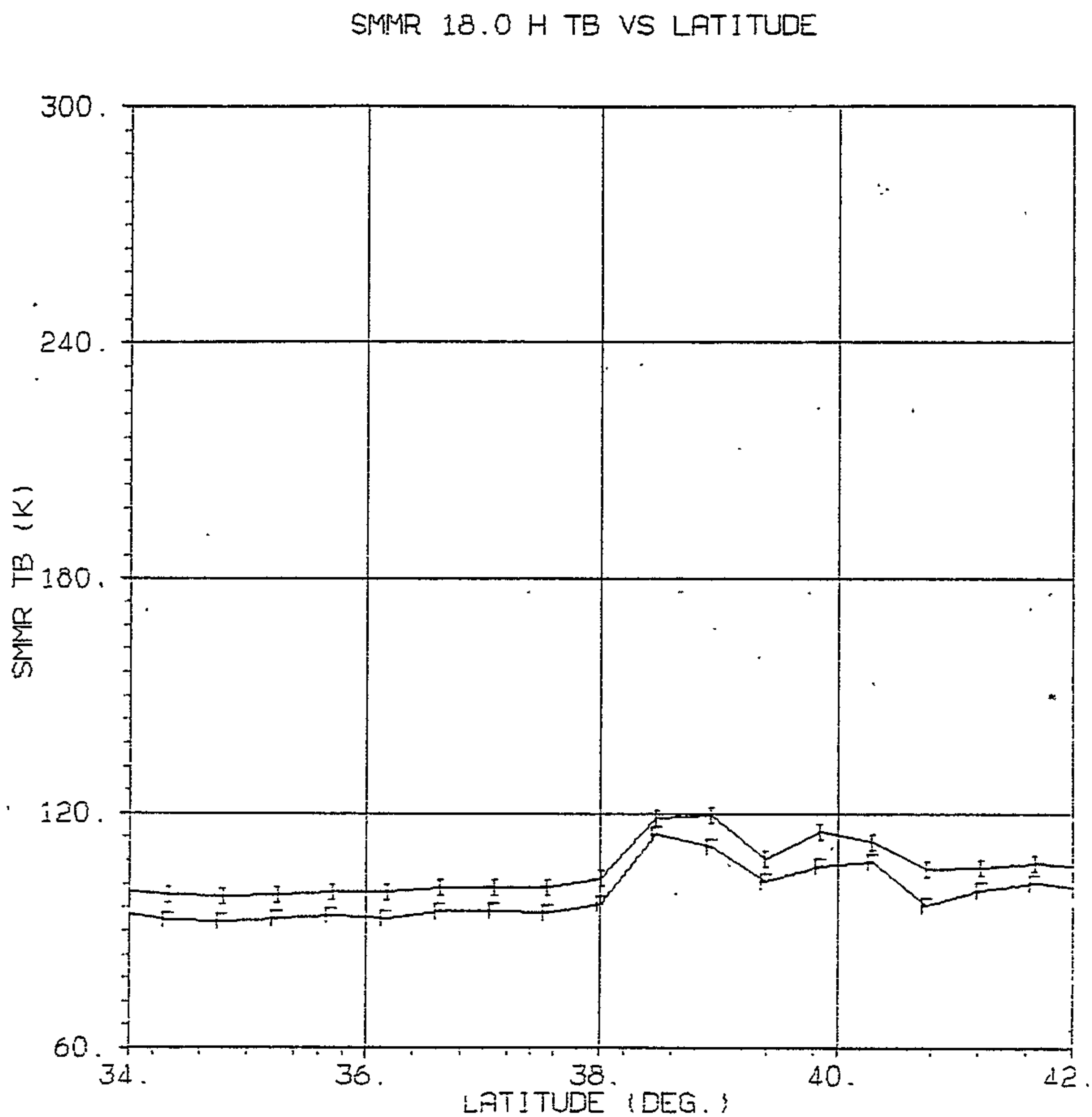

Figure 12.5. Orbit 1212, 38° N, Cross and Interim

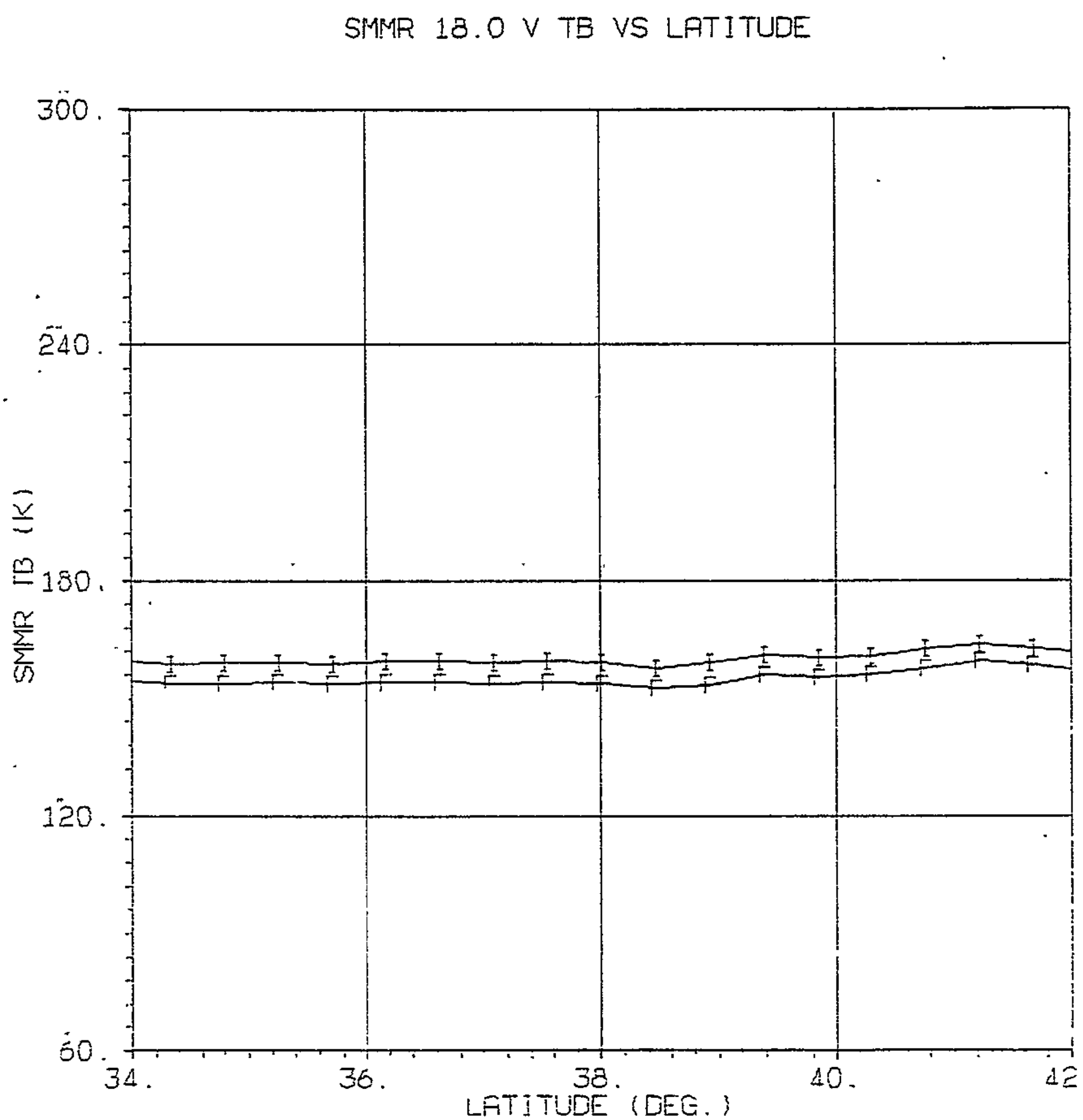

Figure 12.4. Orbit 1212, 38° N, Cross and Interim

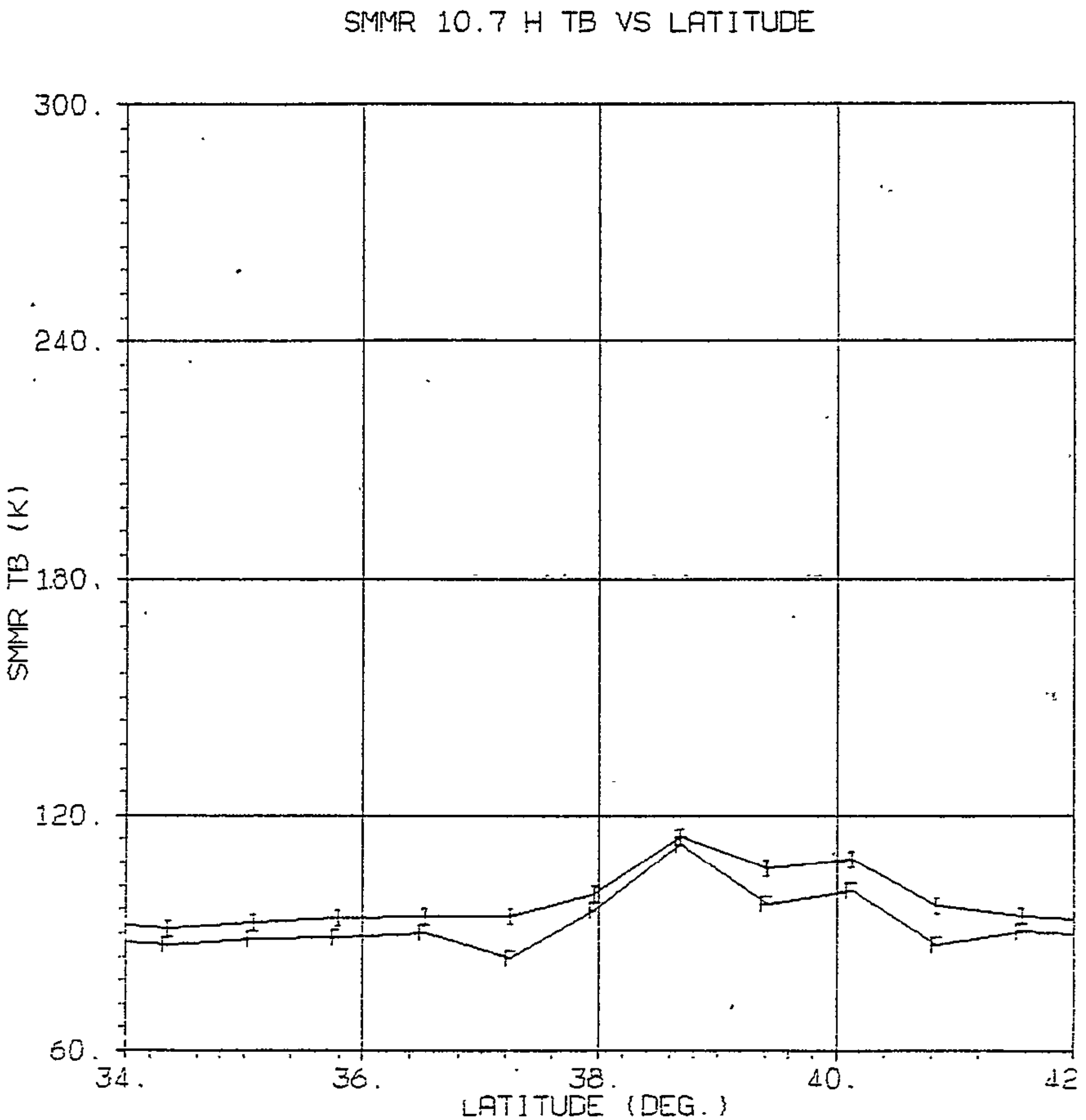

Figure 12.3. Orbit 1212, 38° N, Cross and Interim

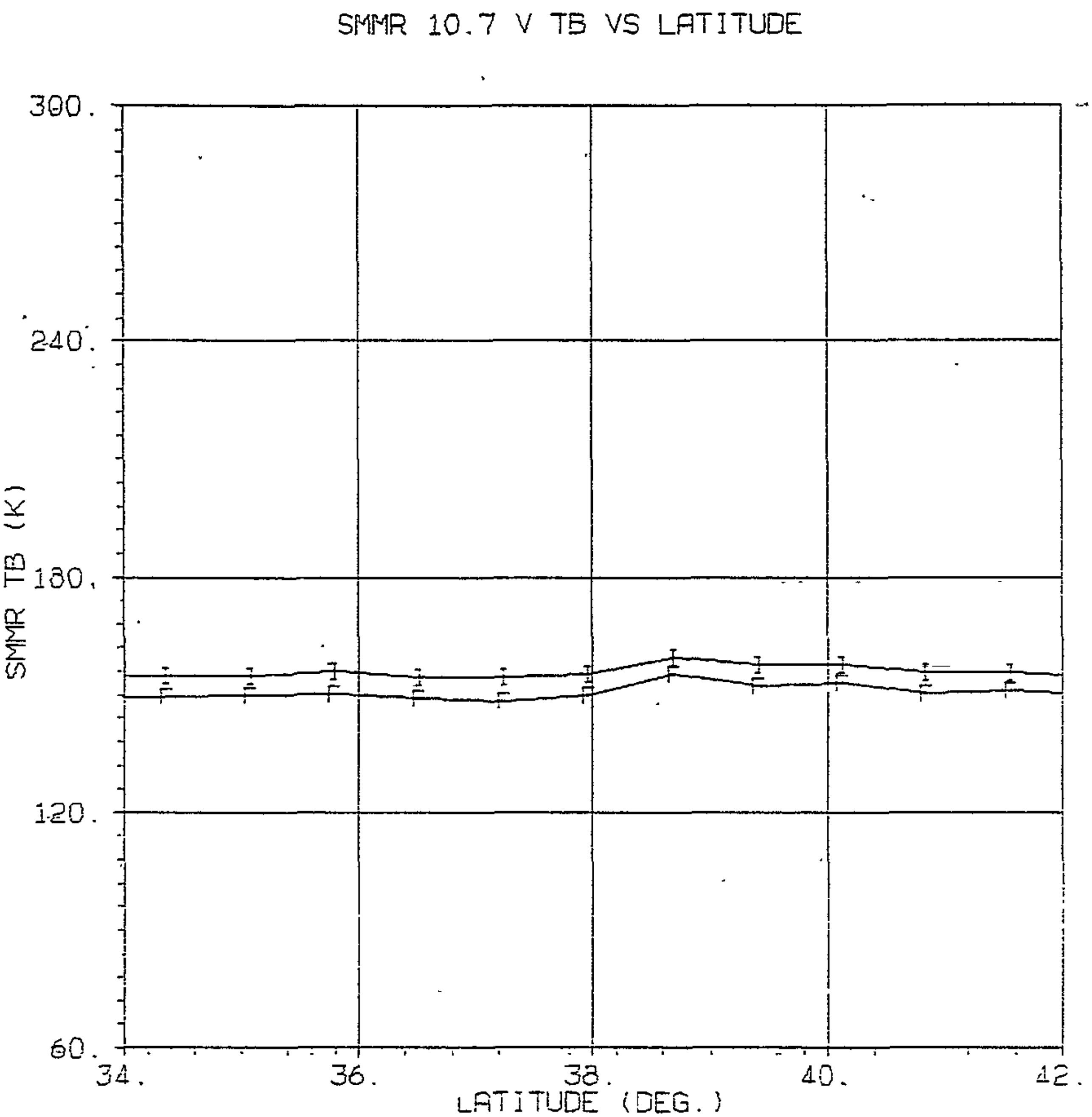

Figure 12.2. Orbit 1212, 38° N, Cross and Interim

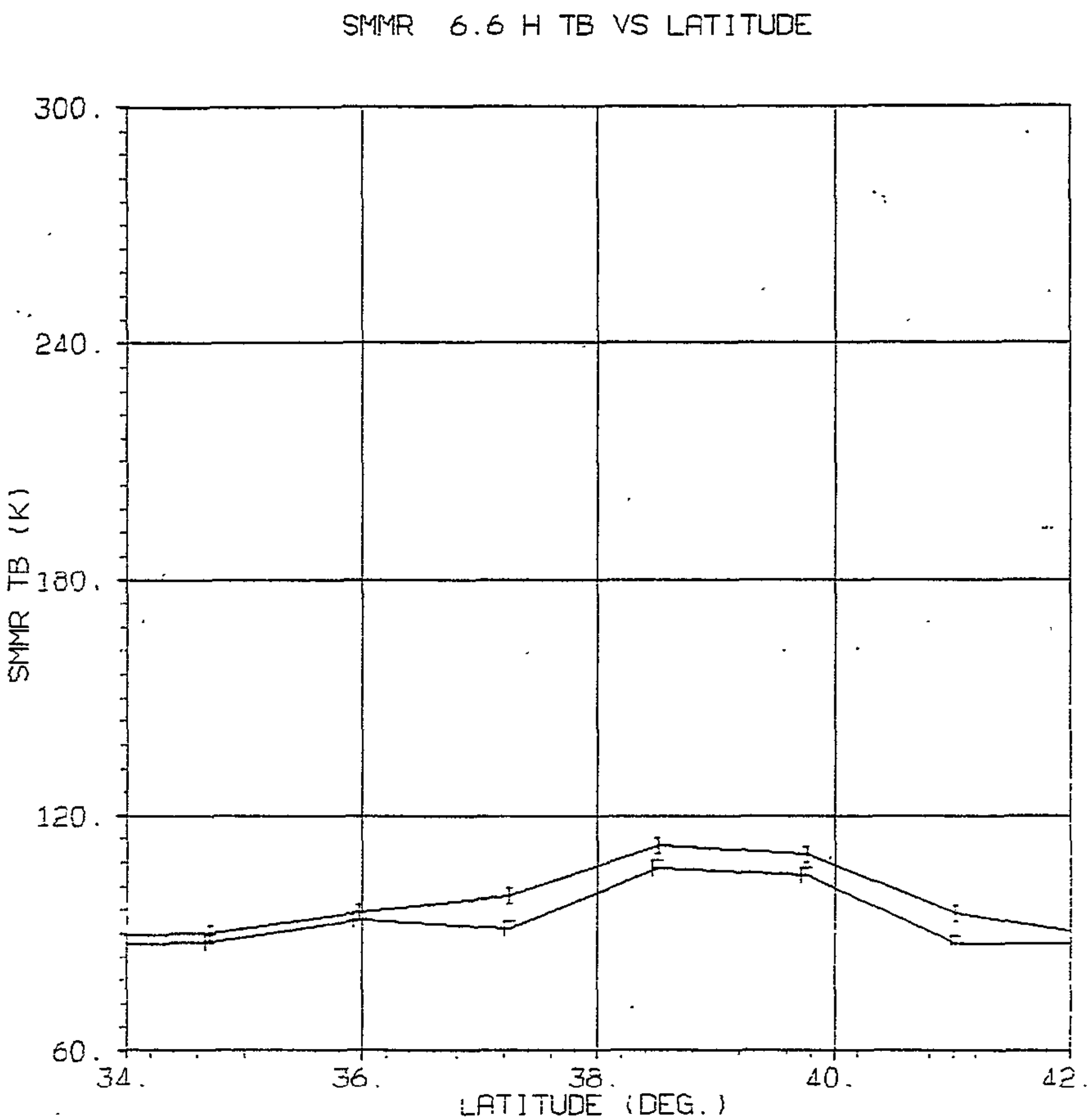

Figure 12.1. Orbit 1212, 38° N, Cross and Interim

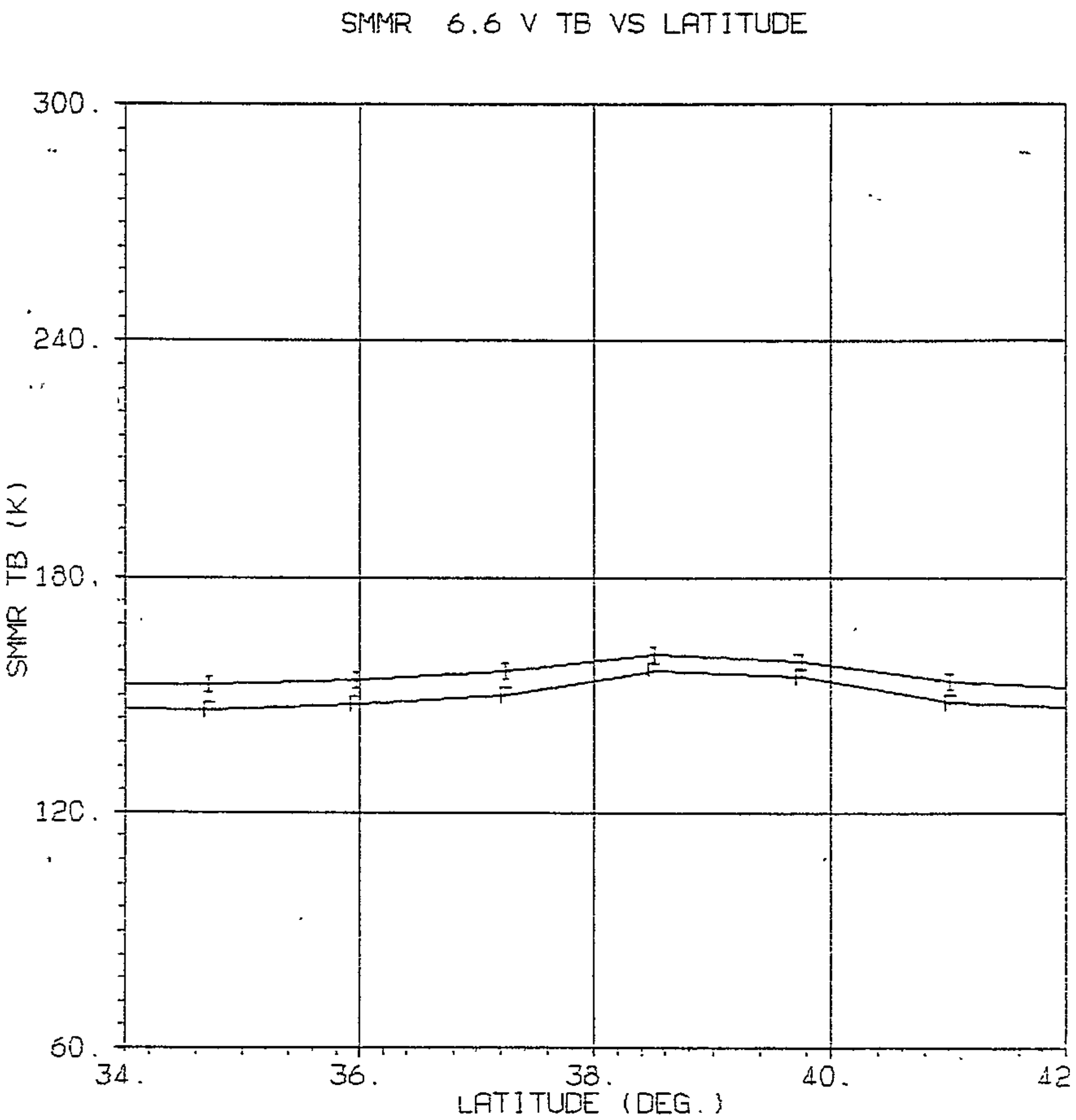

Figure 11.10. Orbit 1212, 38° N, Box and Interim

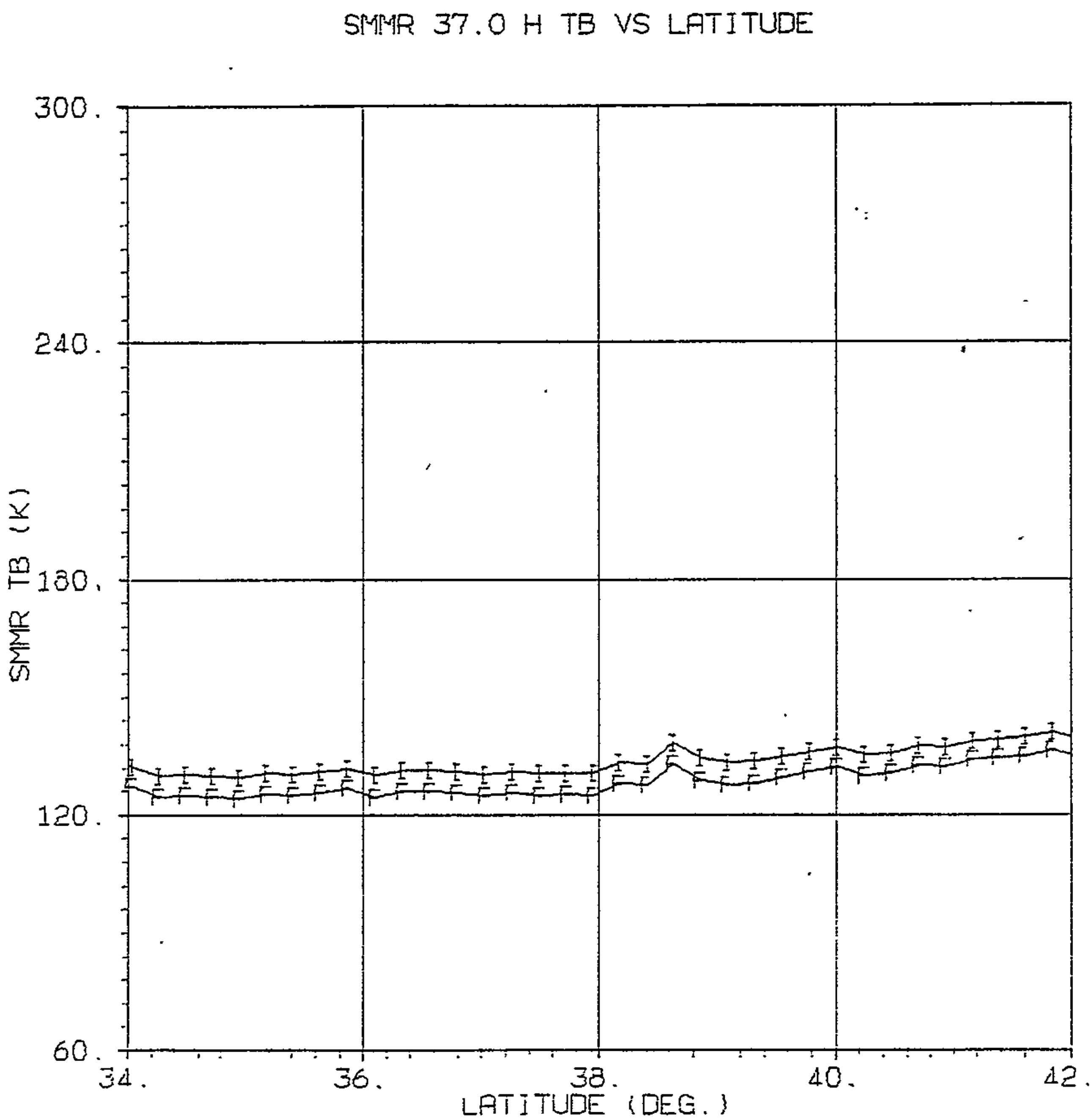

Figure 11.9. Orbit 1212, 38° N, Box and Interim

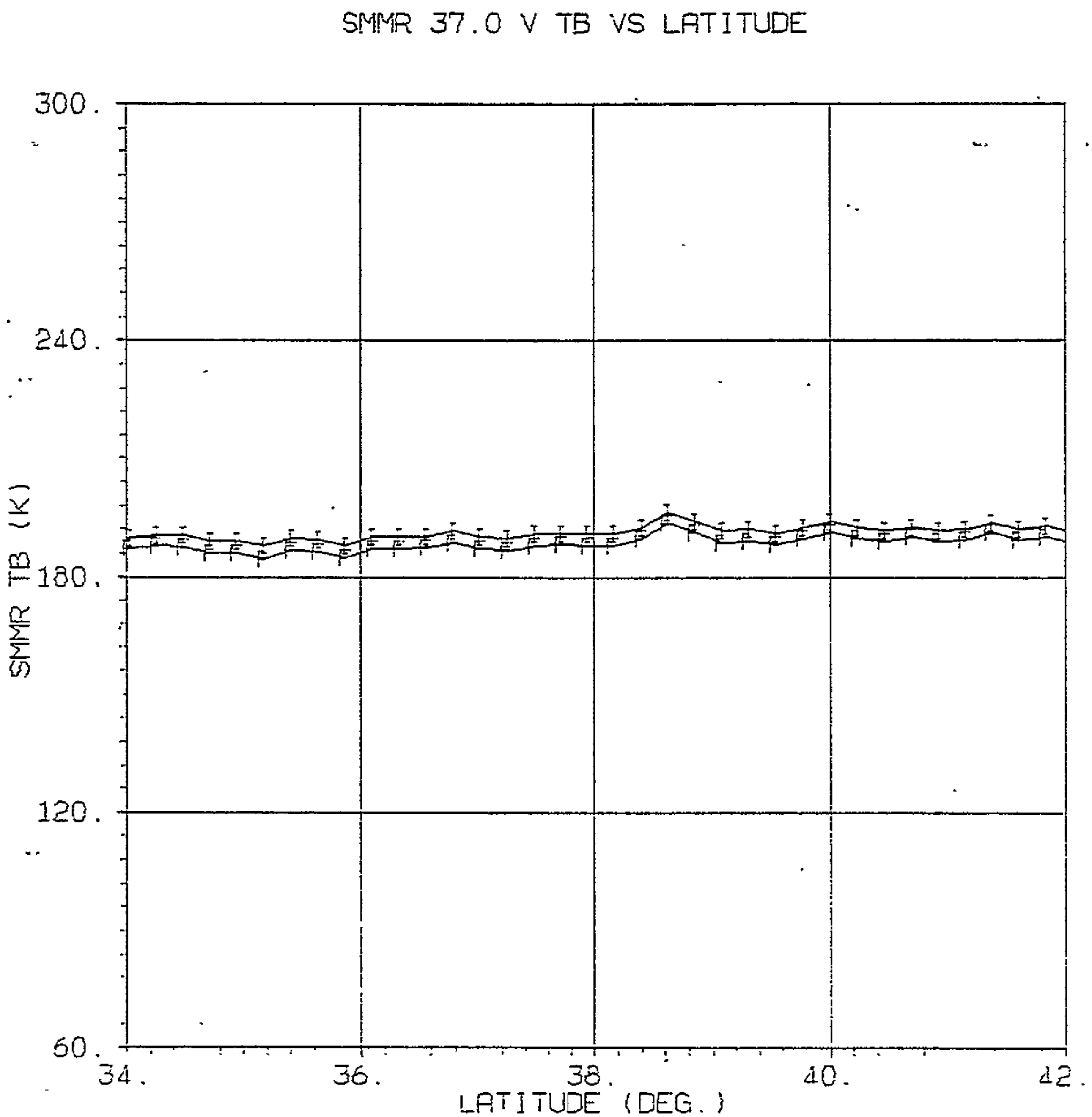

Figure 11.8. Orbit 1212, 38° N, Box and Interim

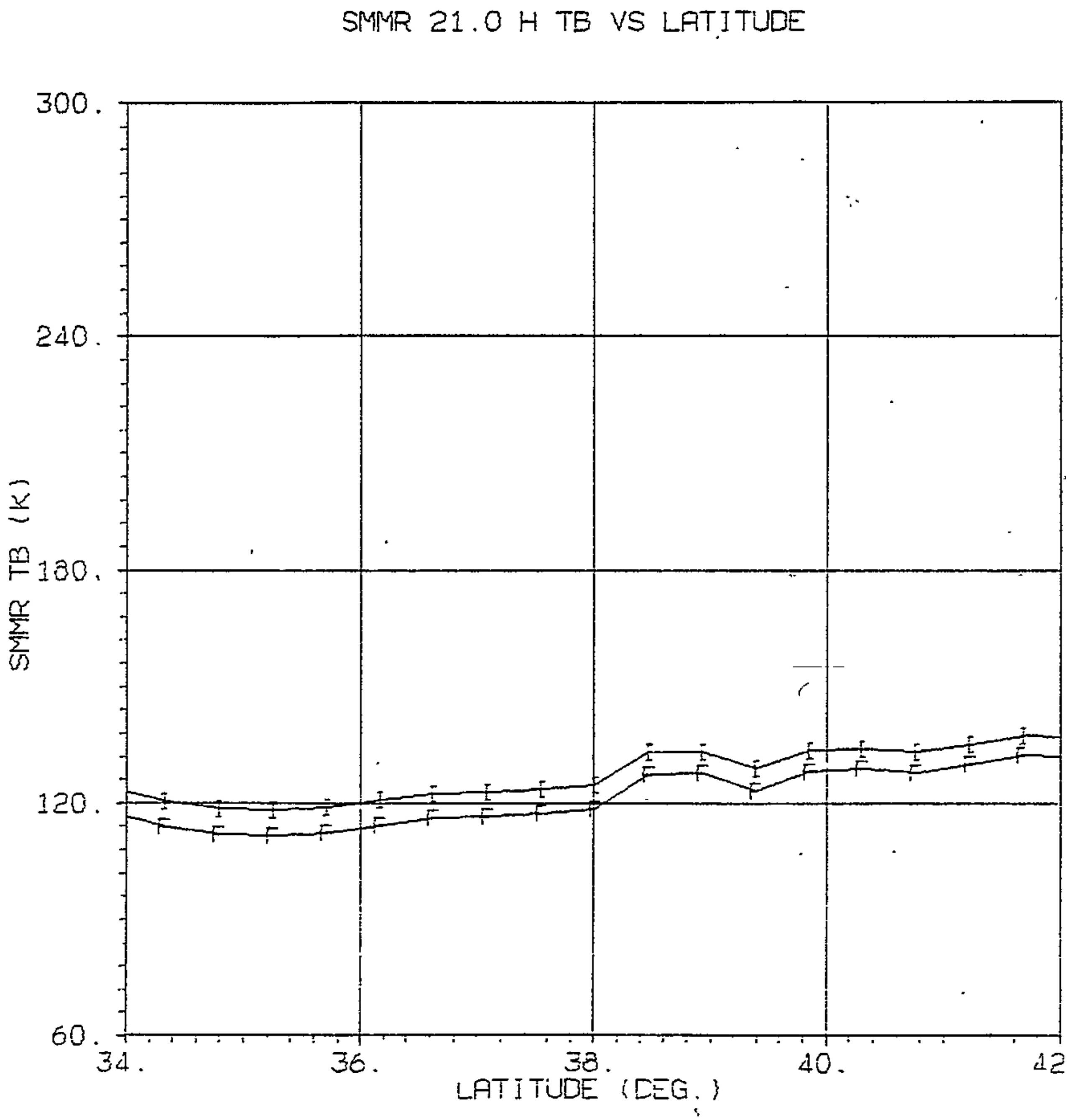

Figure 11.7. Orbit 1212, 38° N, Box and Interim

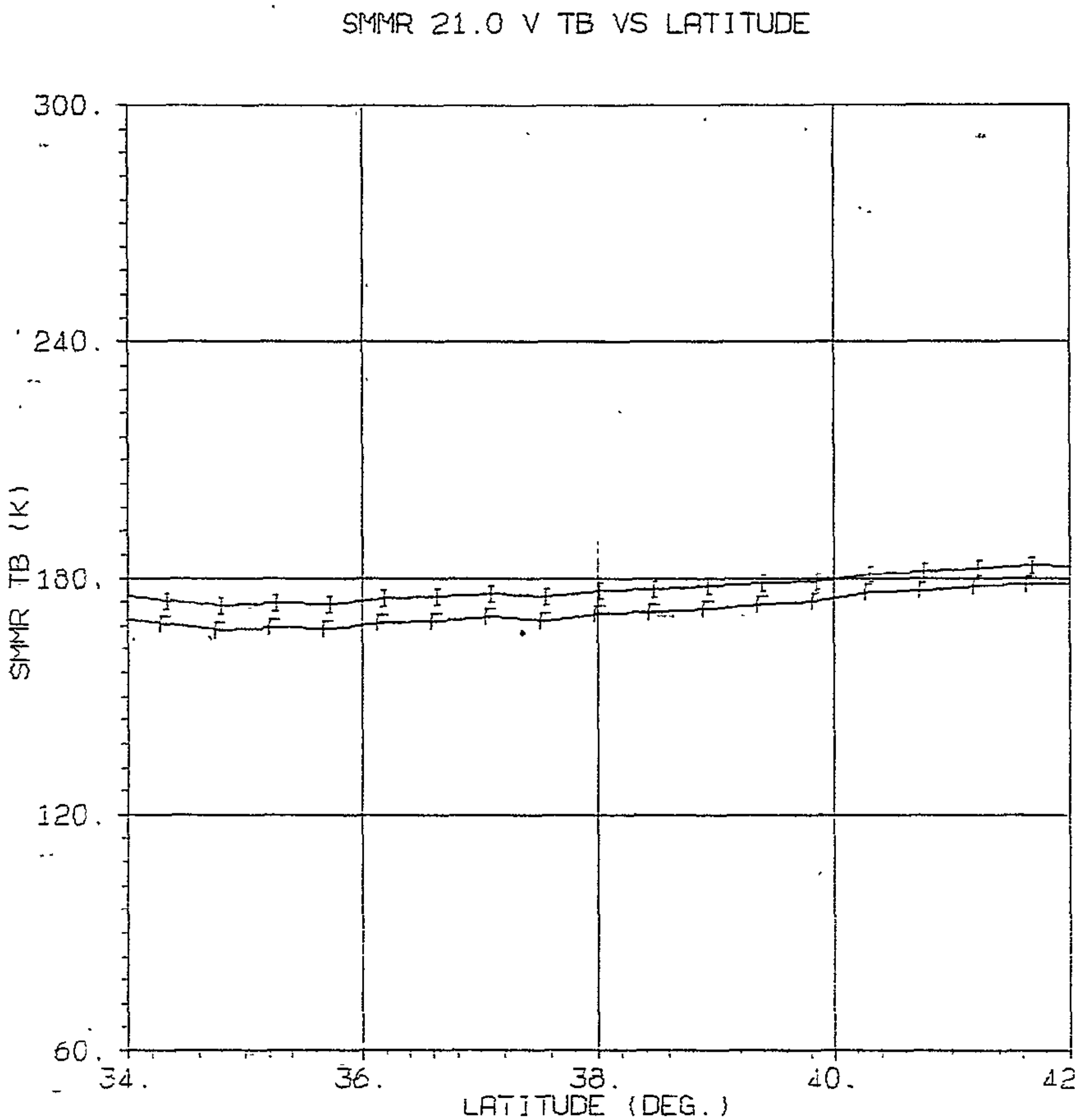

Figure 11.6. Orbit 1212, 38° N, Box and Interim

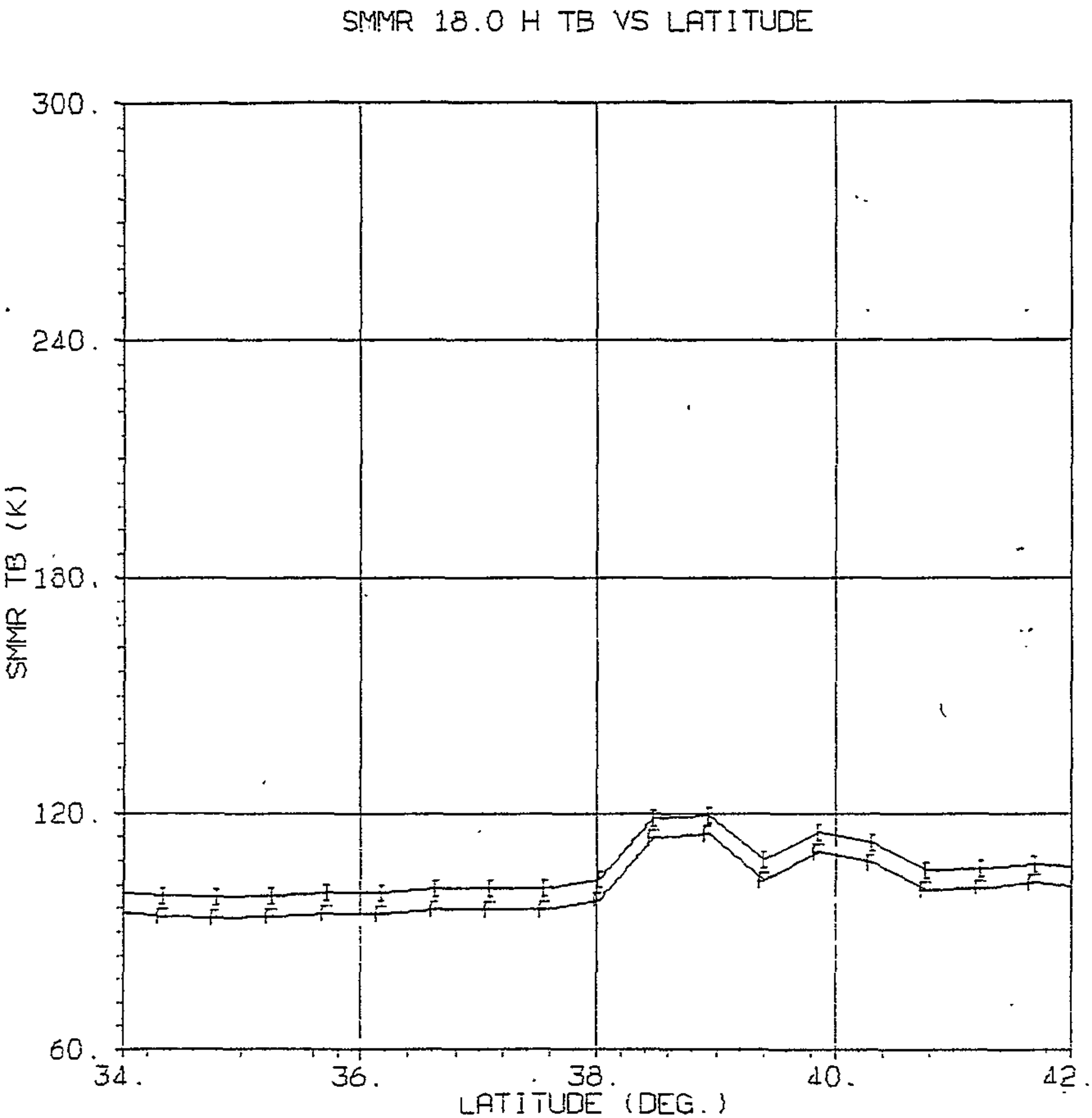

Figure 11.5. Orbit 1212, 38° N, Box and Interim

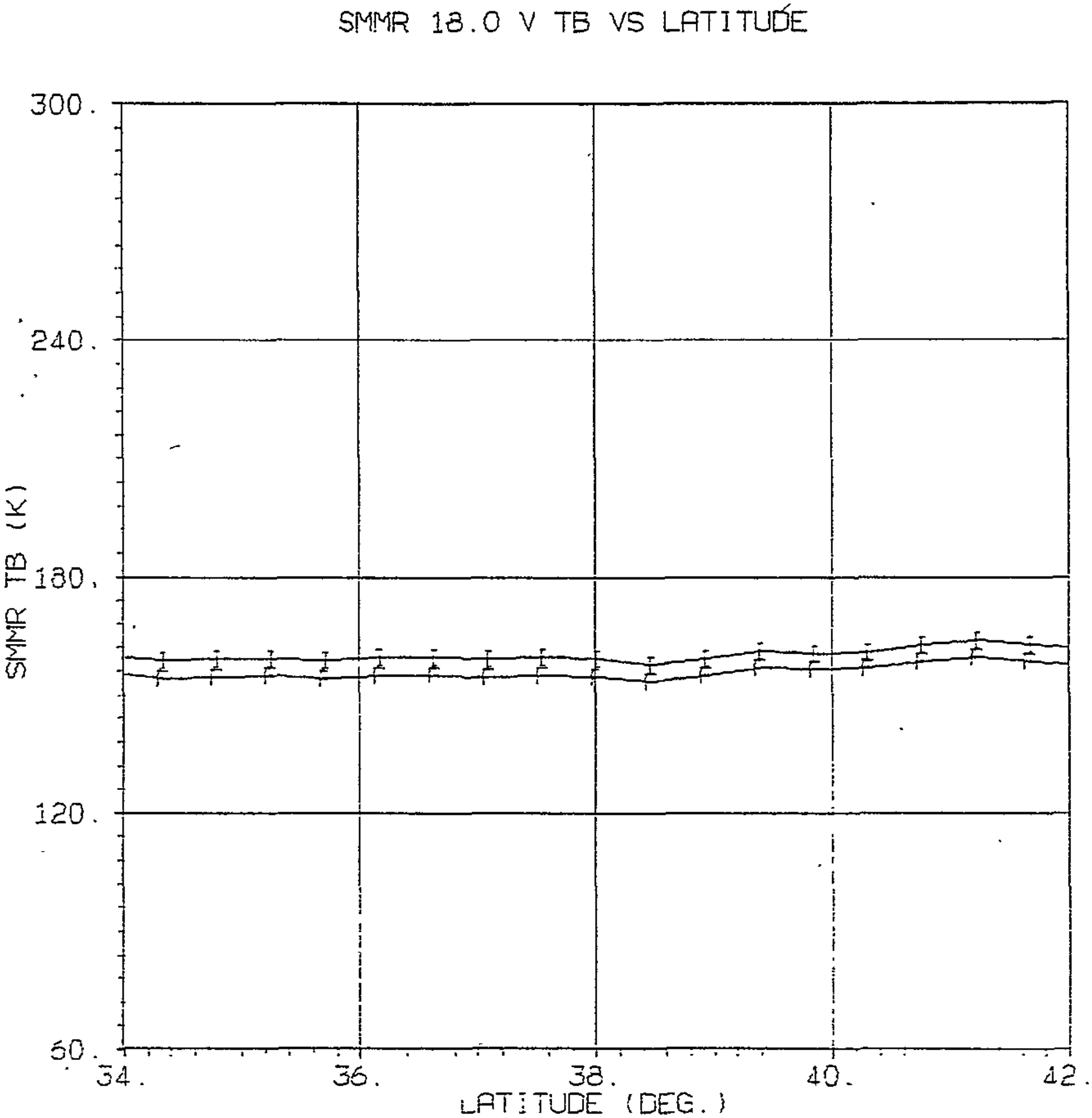

Figure 11.4. Orbit 1212, 38° N, Box and Interim

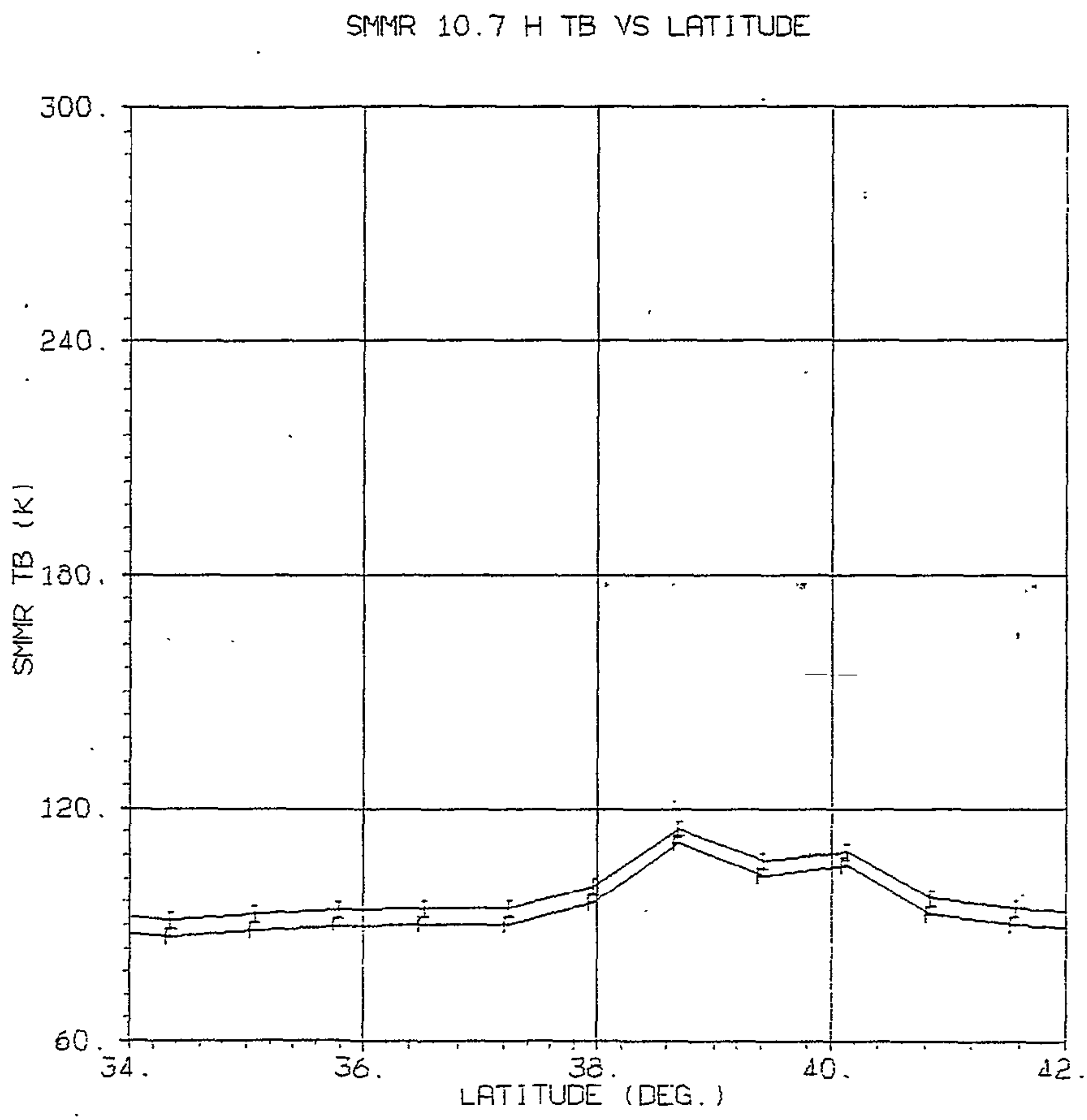

Figure 11.3. Orbit 1212, 38° N, Box and Interim

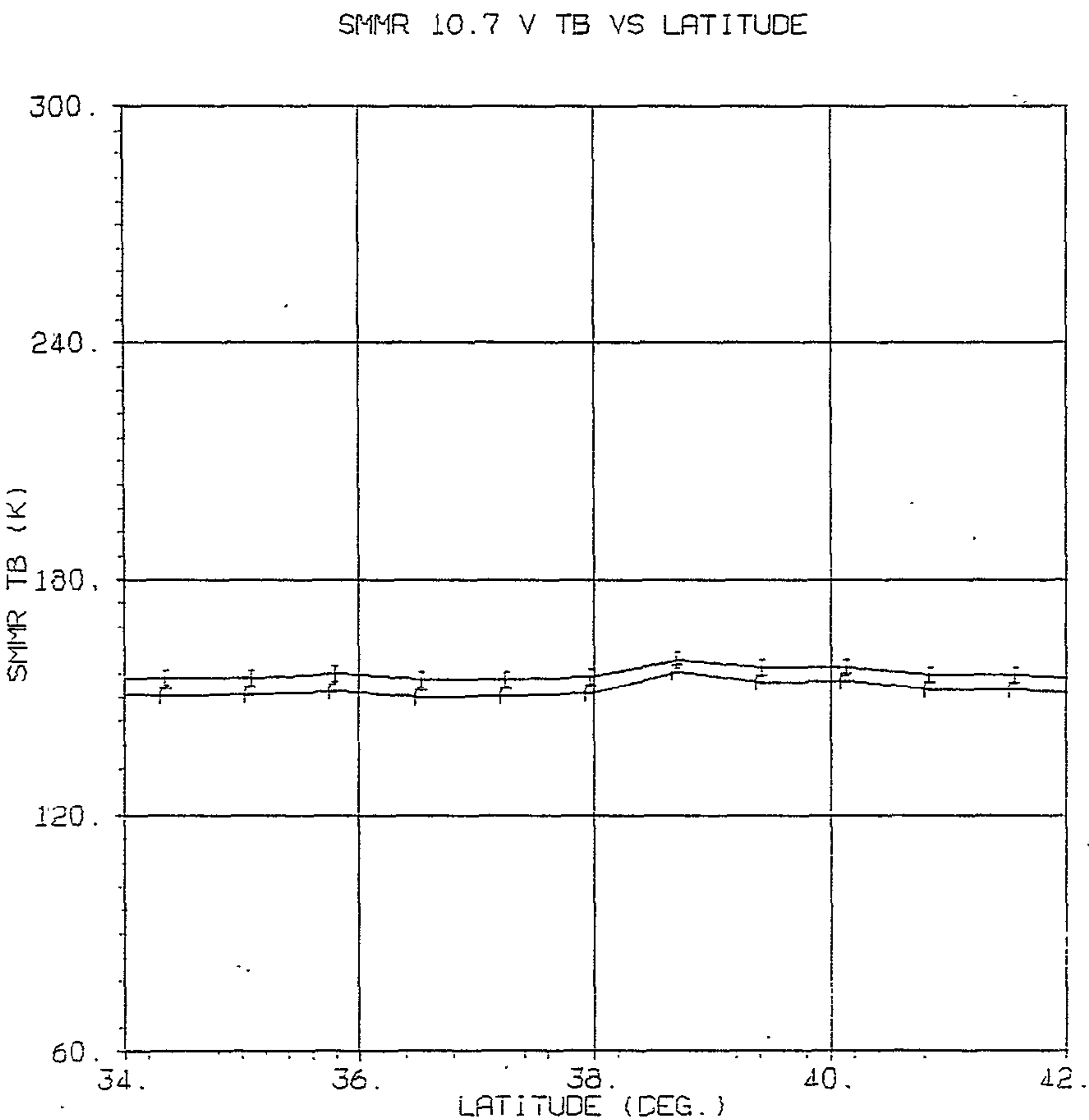

Figure 11.2. Orbit 1212, 38° N, Box and Interim

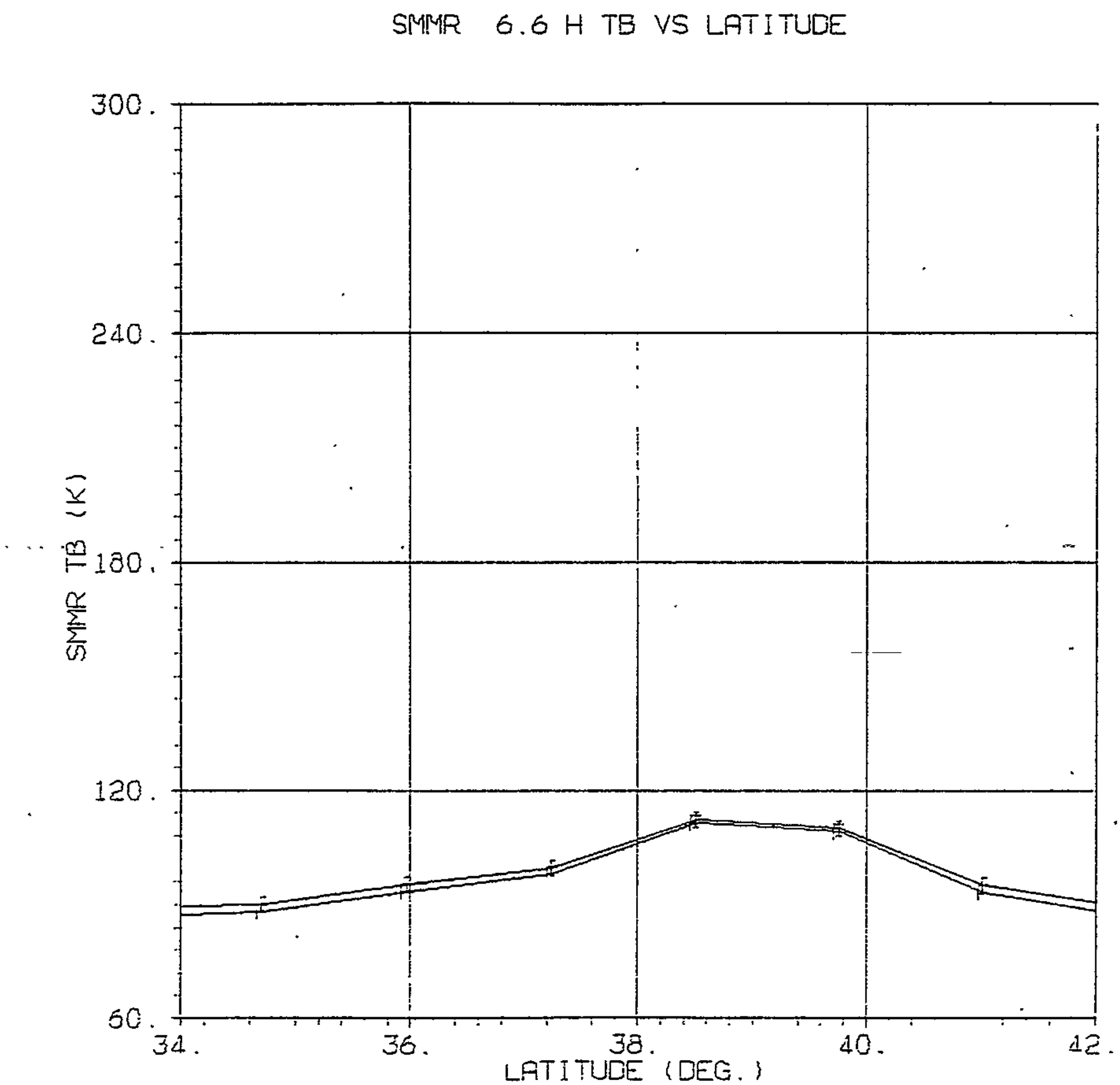

Figure 11.1. Orbit 1212, 38° N, Box and Interim

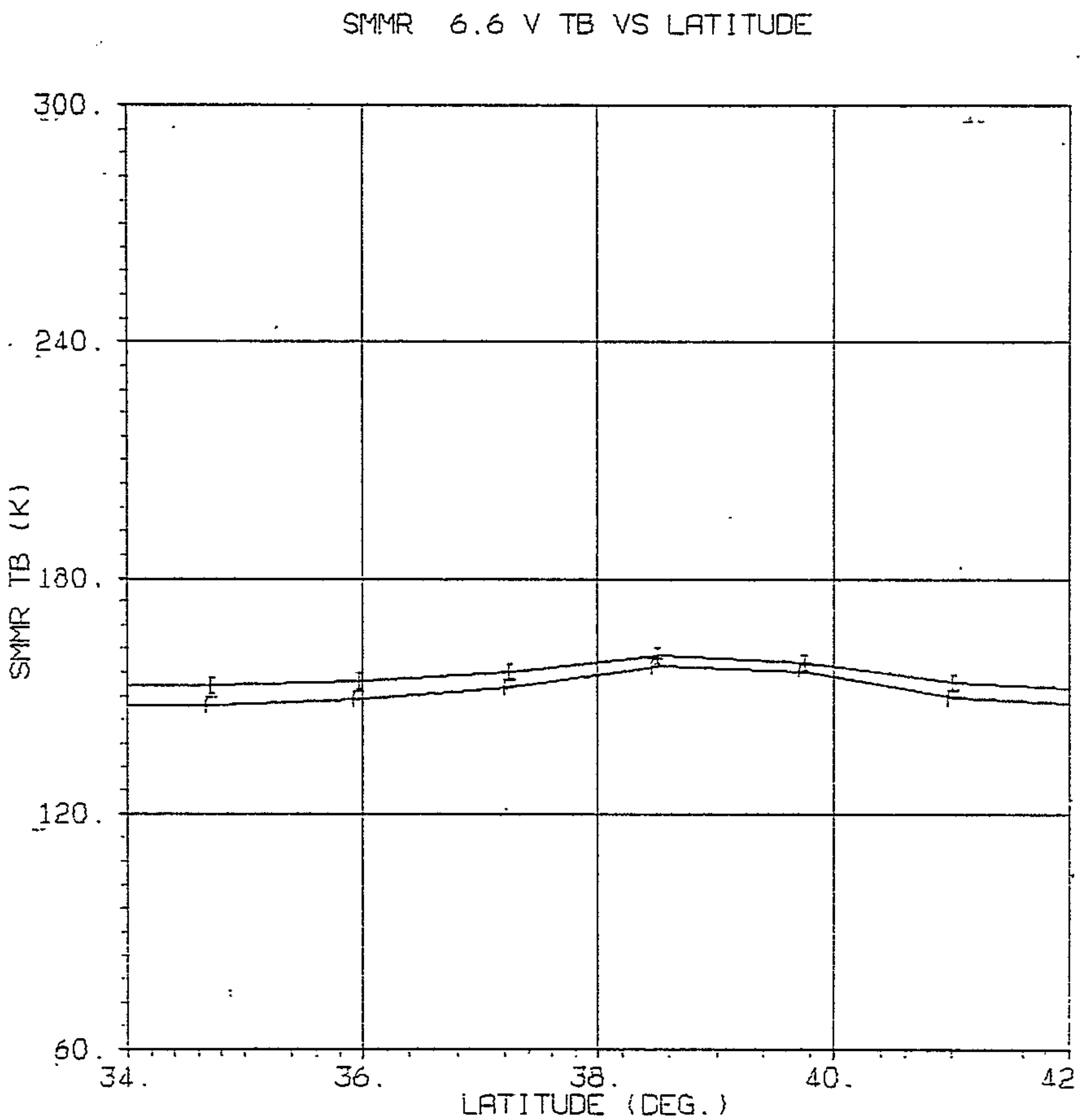

Figure 10.10 Orbit 1212, 55° N, Nominal and Interim

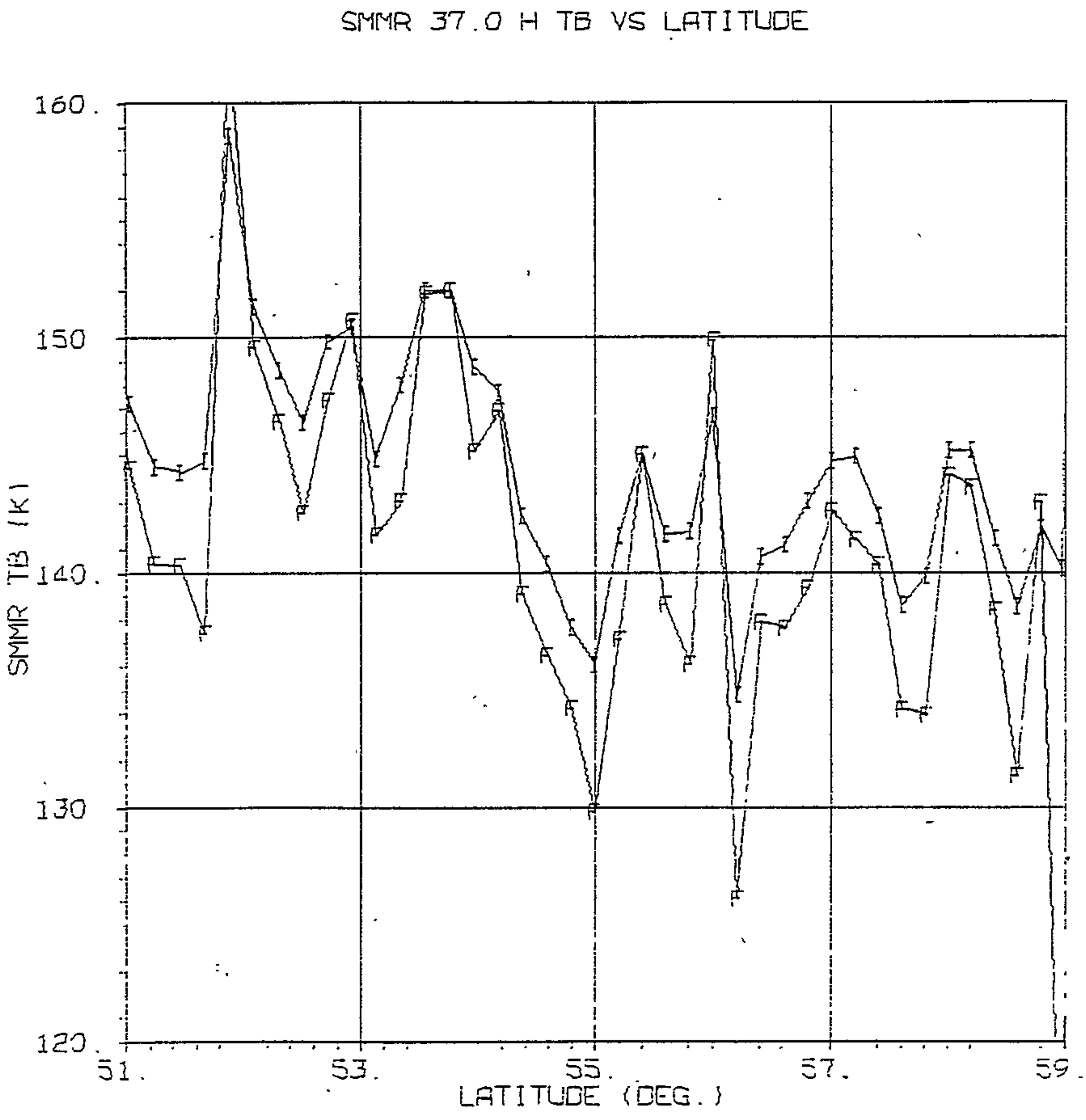

Figure 10.9. Orbit 1212, 55° N, Nominal and Interim

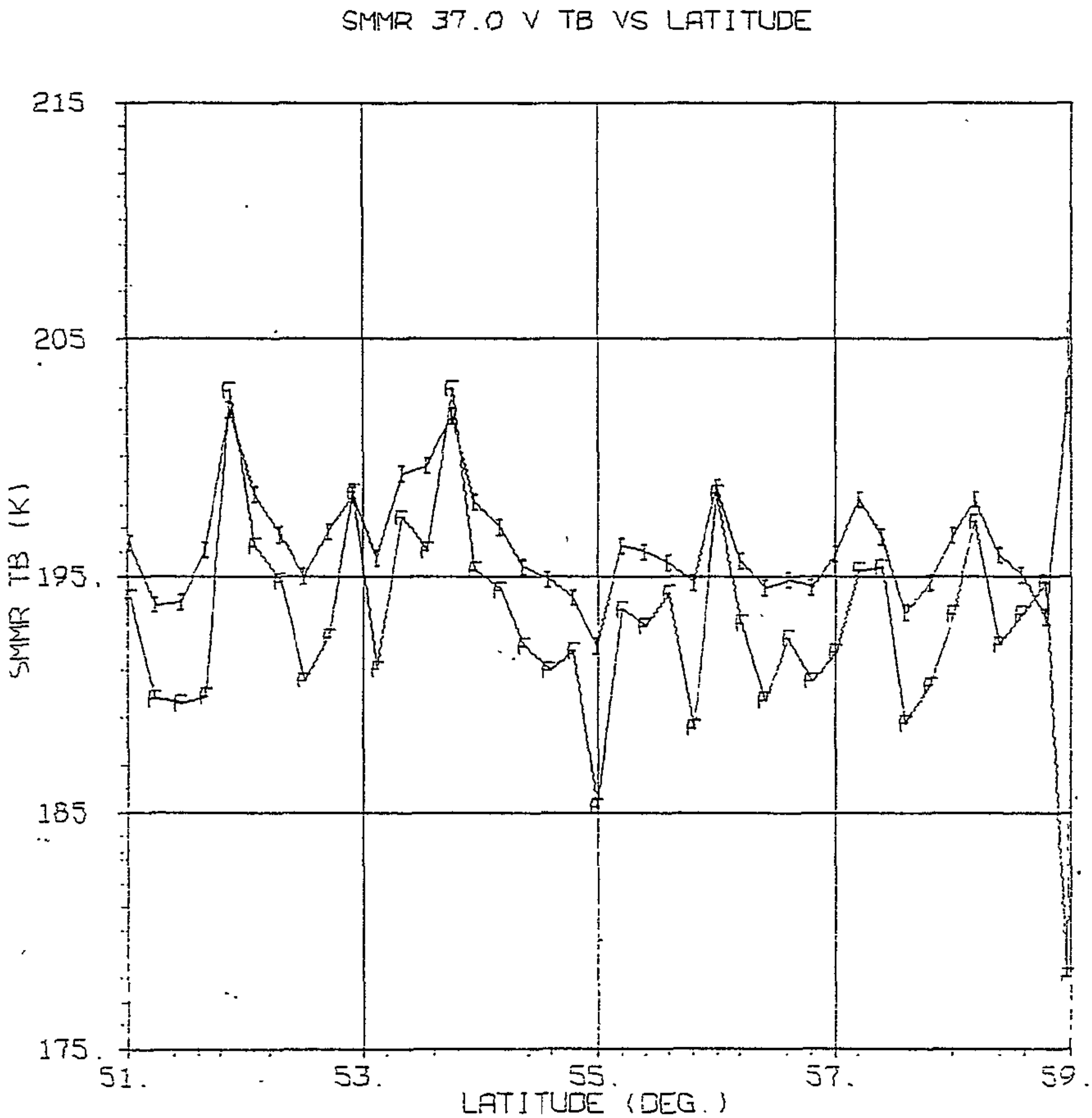

Figure 10.8. Orbit 1212, 55° N, Nominal and Interim

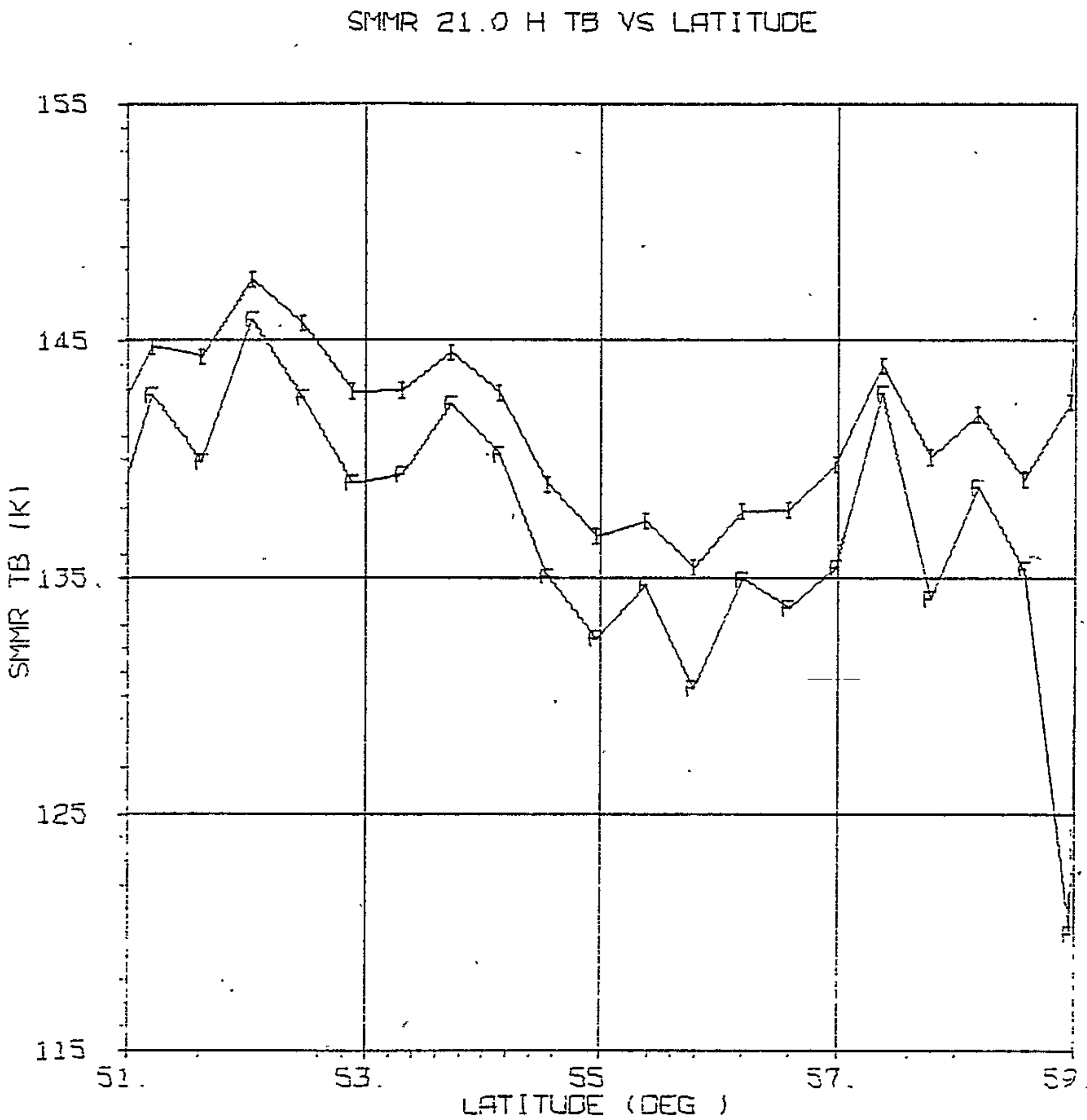

Figure 10.7. Orbit 1212, 55° N, Nominal and Interim

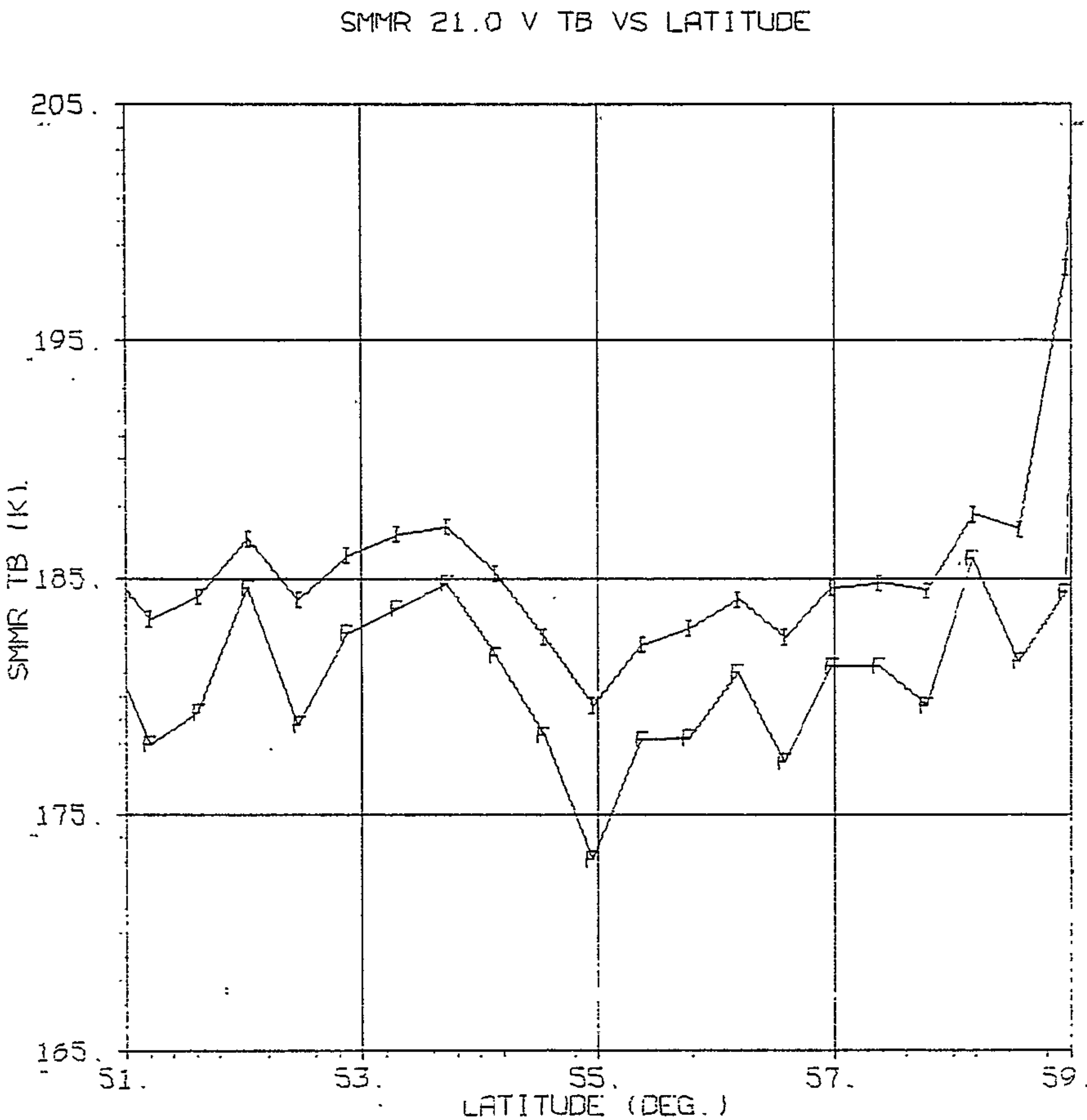

Figure 10.6. Orbit 1212, 55° N, Nominal and Interim

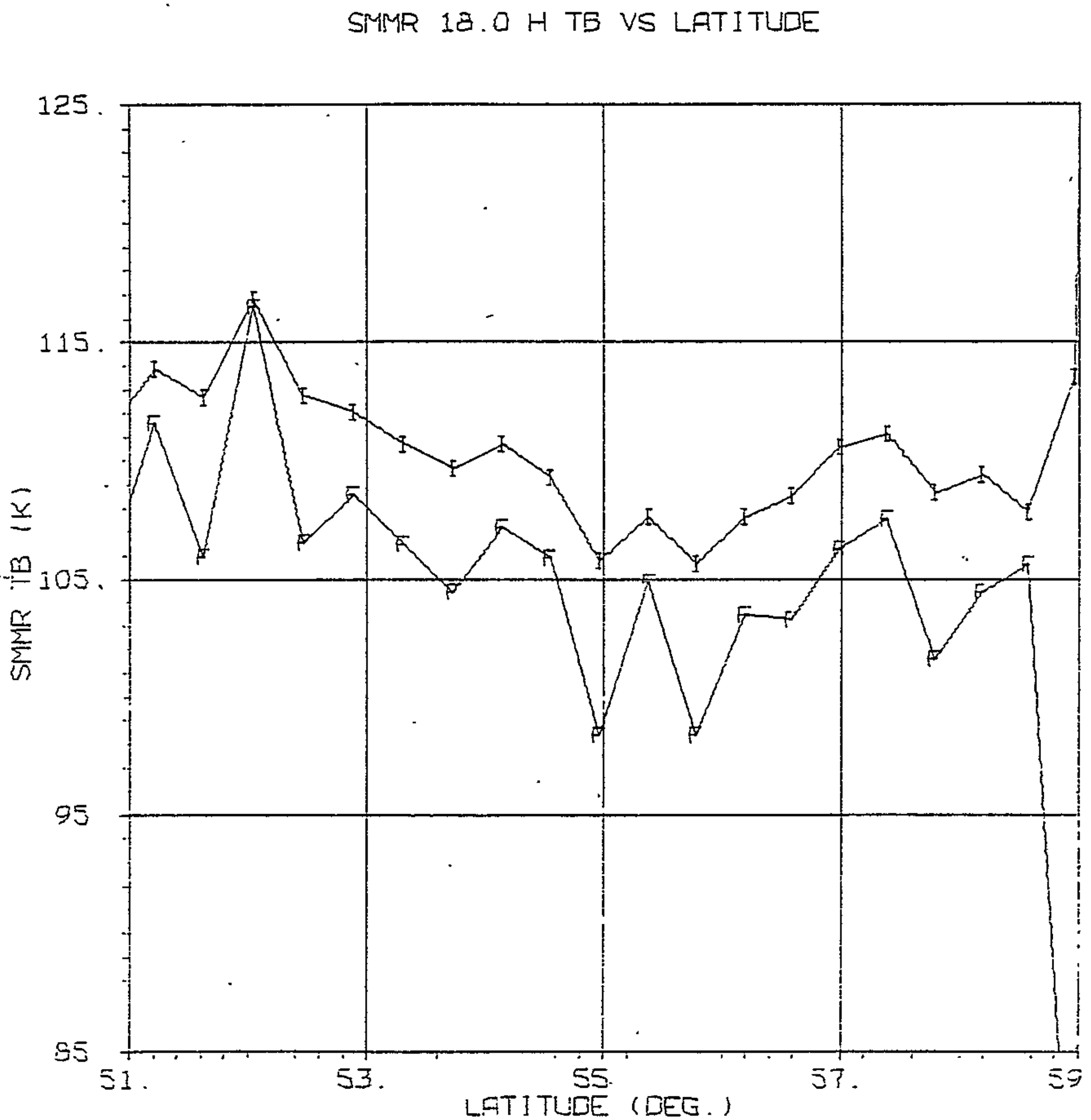

Figure 10.5. Orbit 1212, 55° N, Nominal and Interim

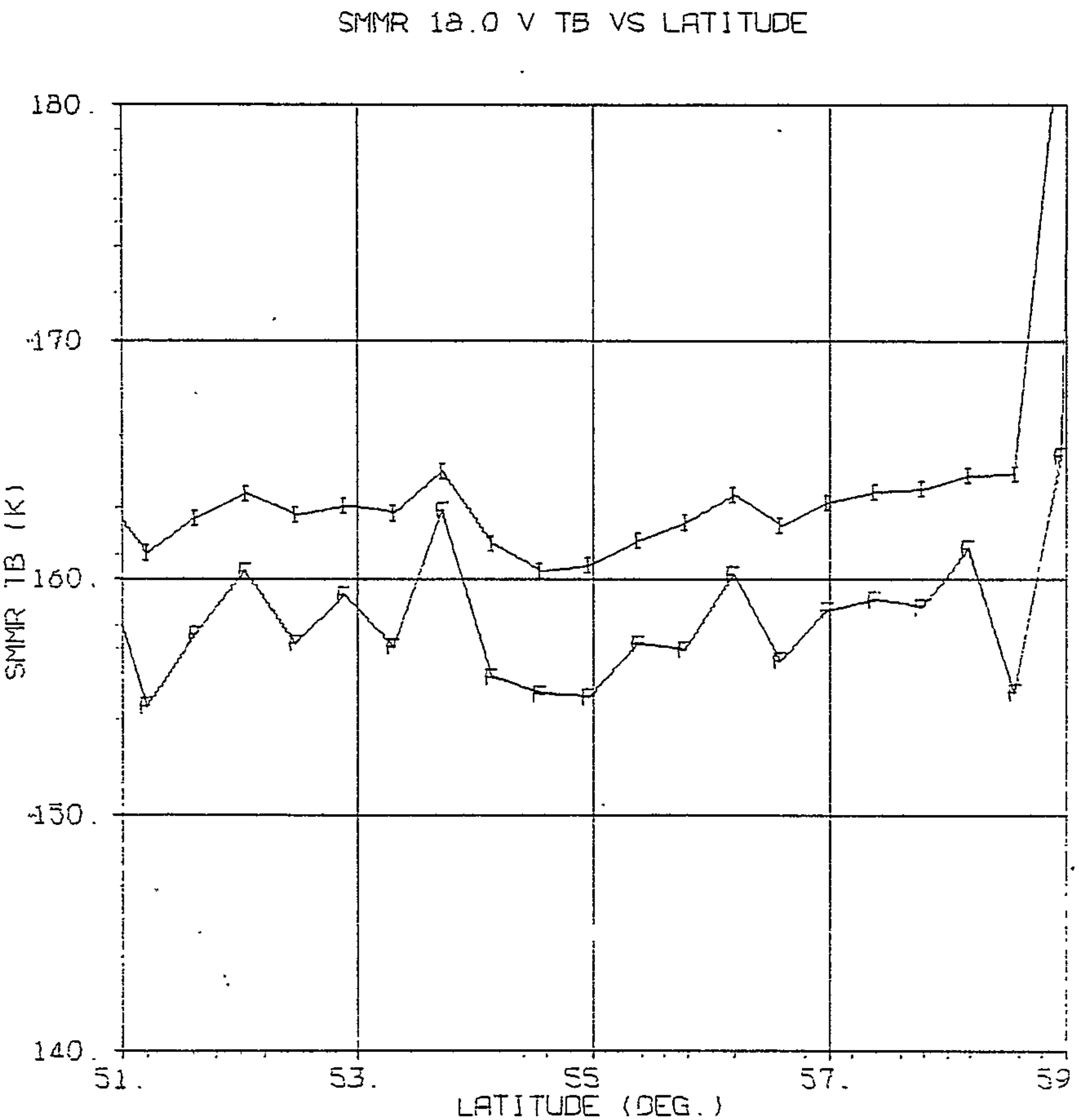

Figure 10.4. Orbit 1212, 55° N, Nominal and Interim

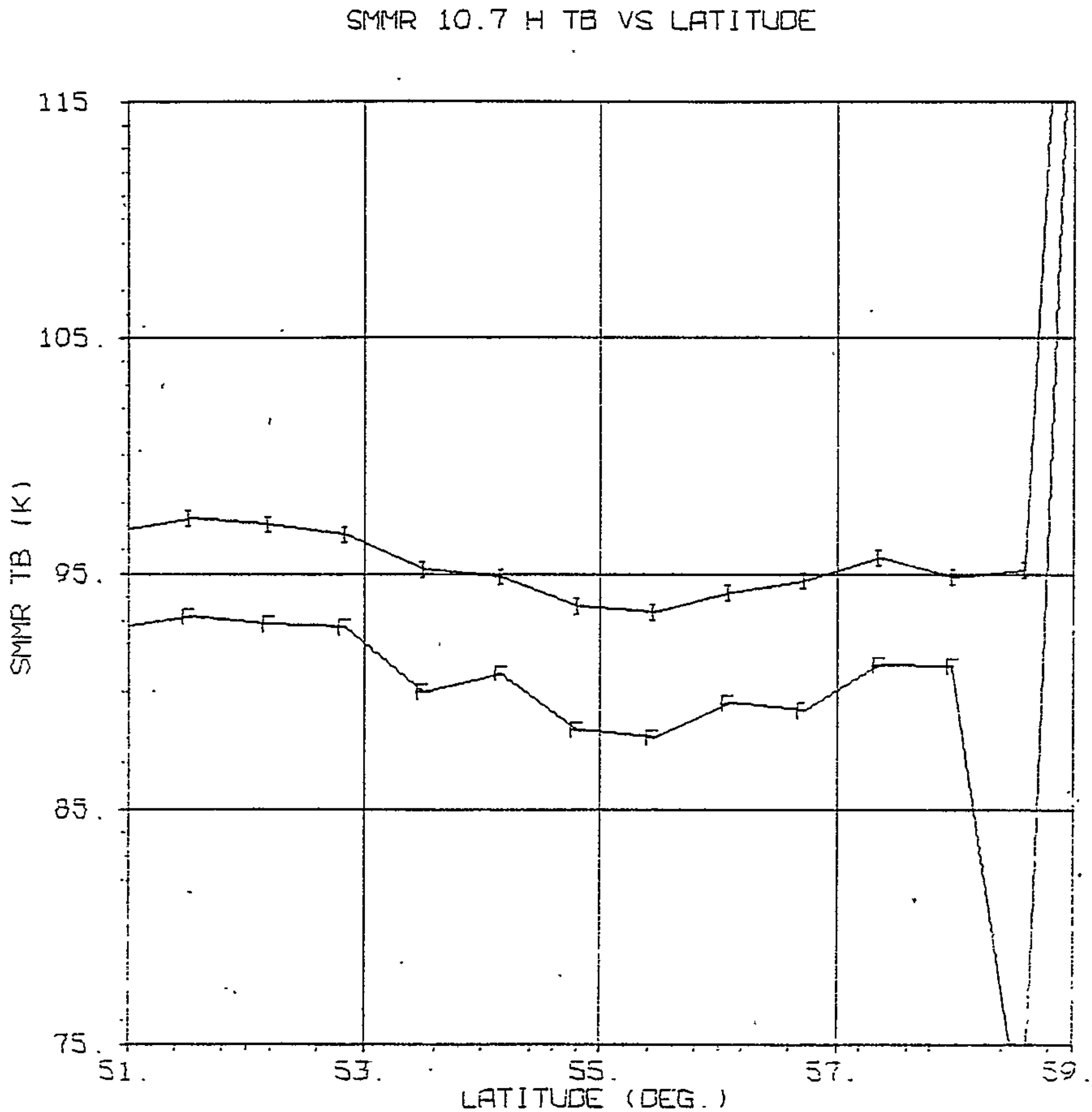

Figure 10.3. Orbit 1212, 55° N, Nominal and Interim

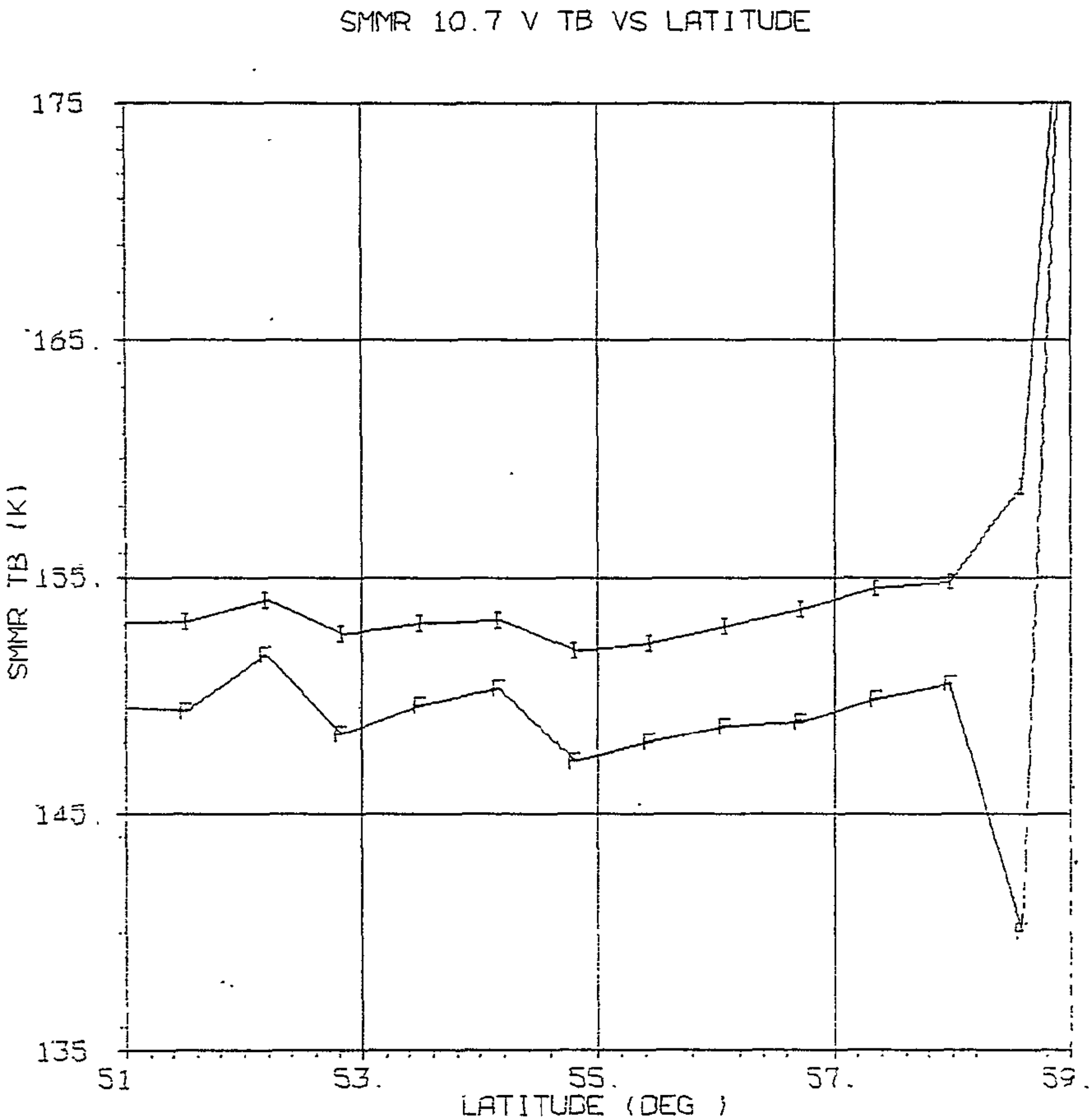

Figure 10.2. Orbit 1212, 55° N, Nominal and Interim

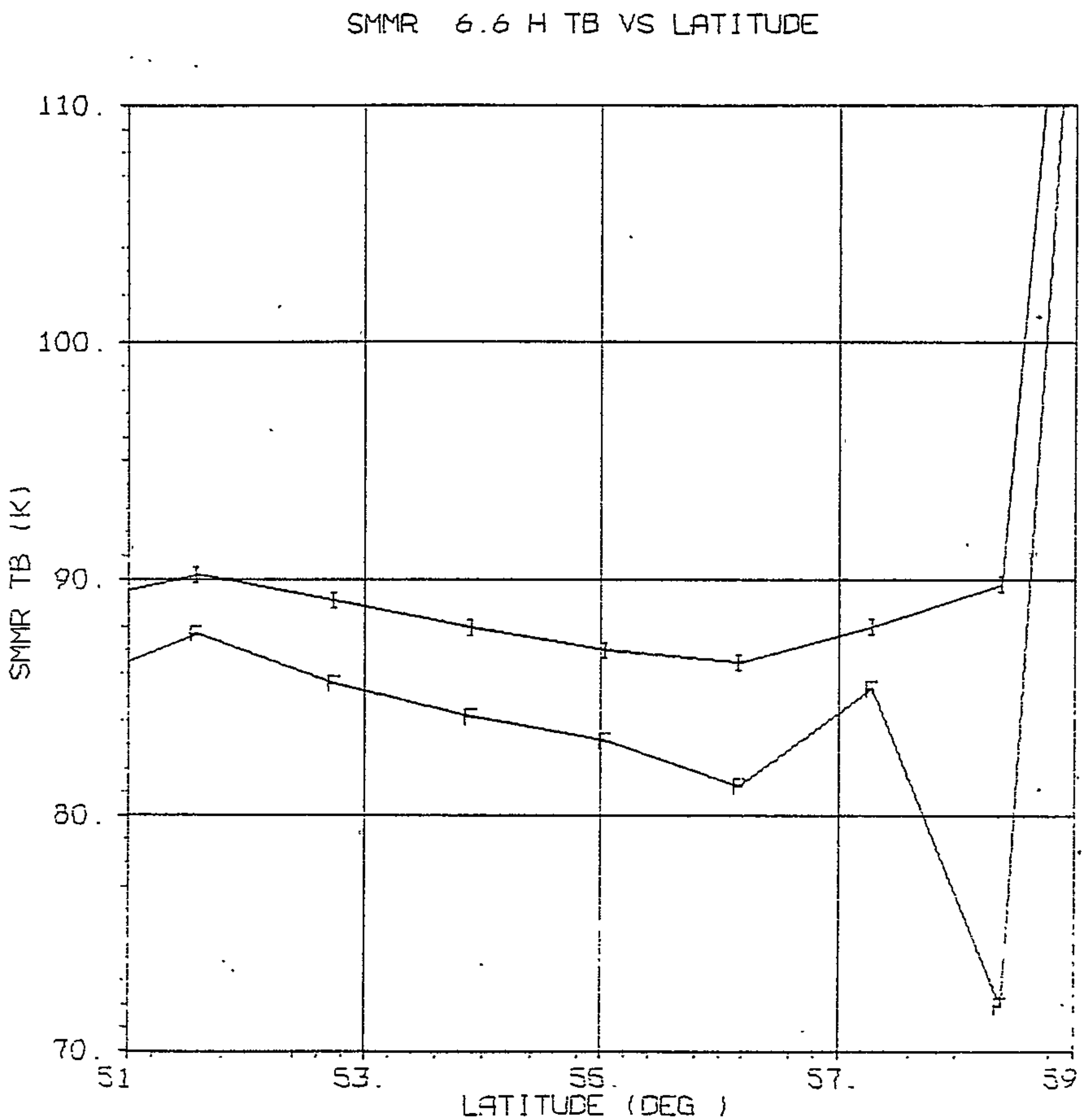

Figure 10.1. Orbit 1212, 55° N, Nominal and Interim

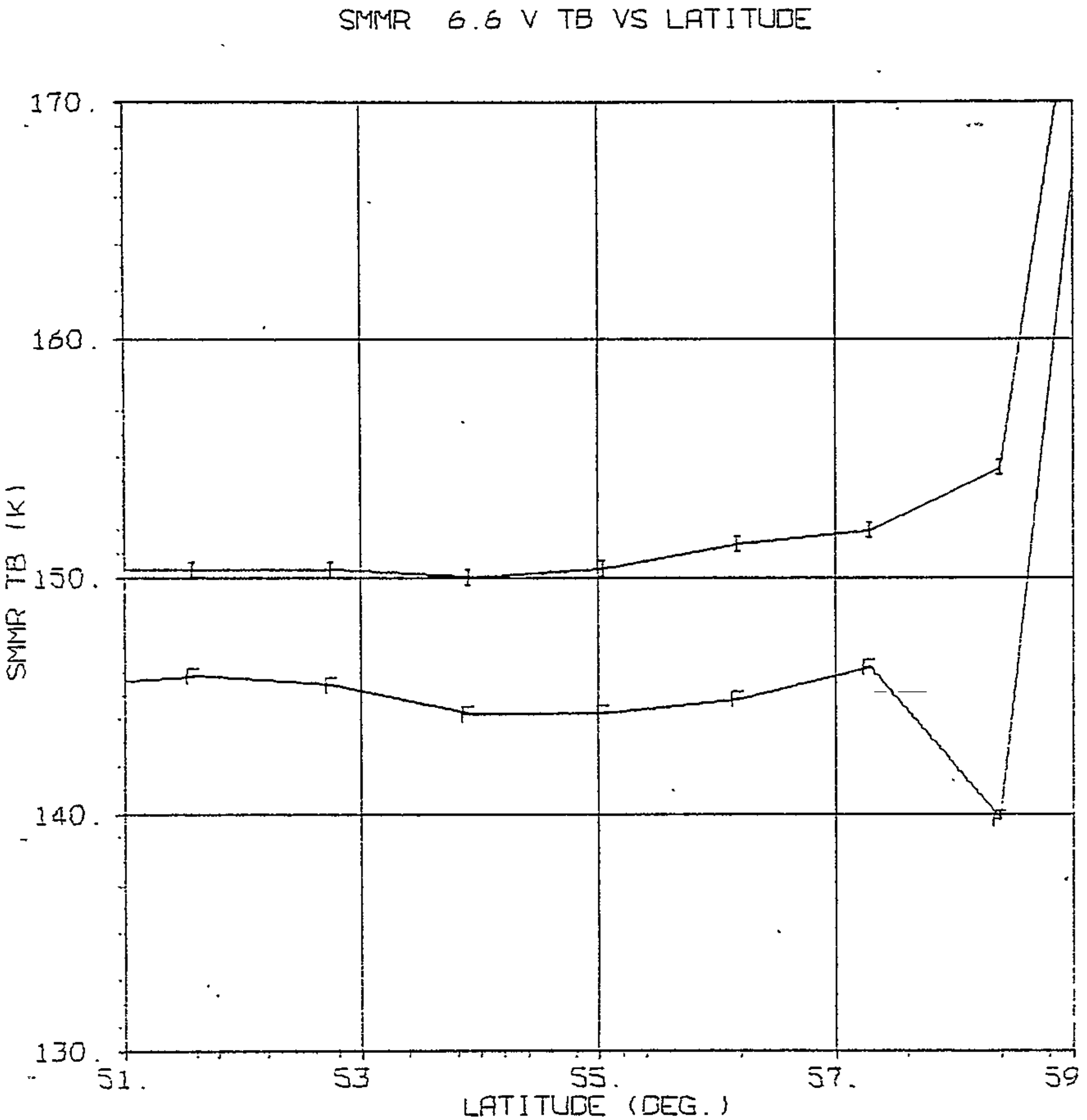

Figure 9.10. Orbit 1212, 55° N, Cross and Interim

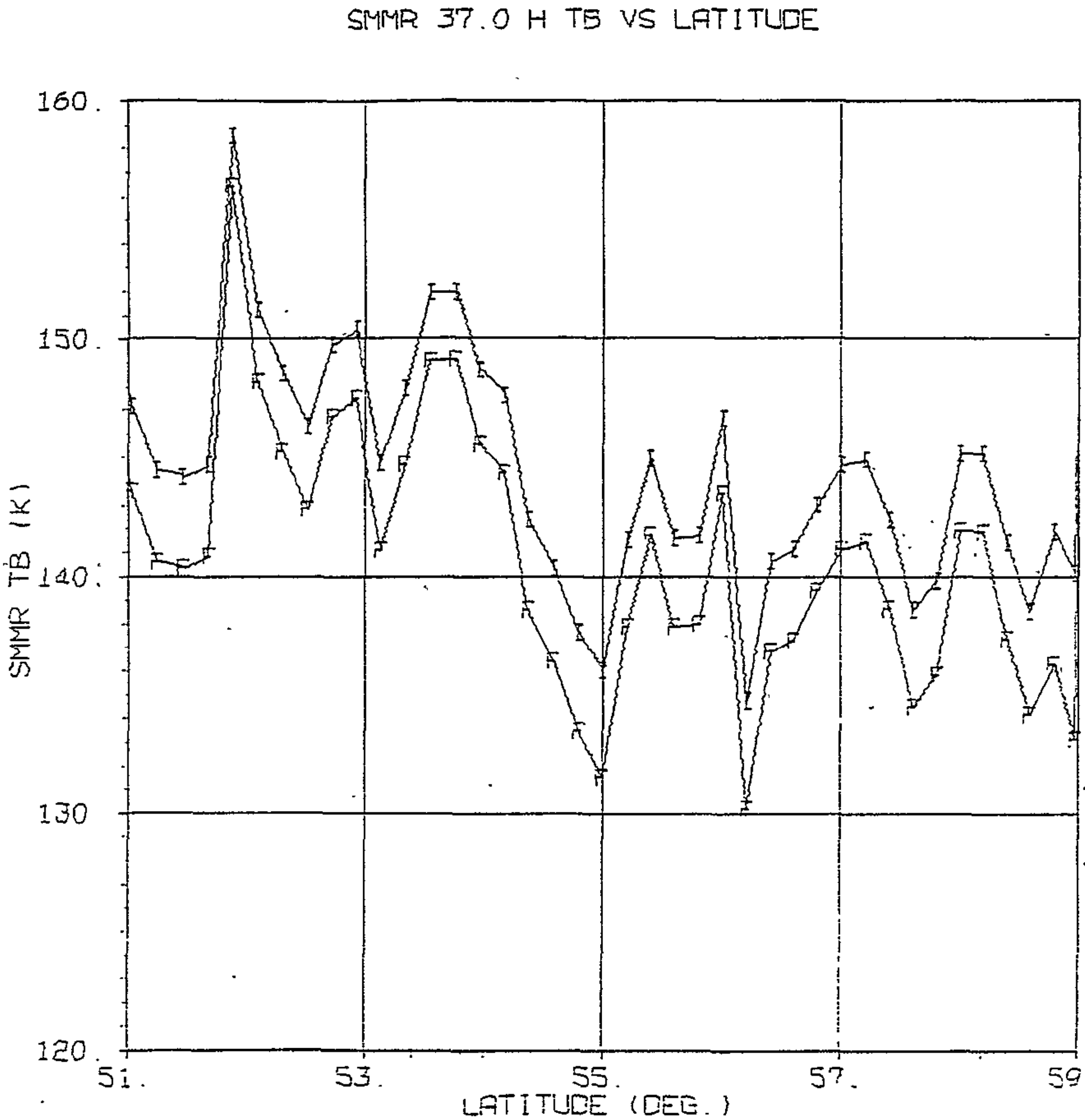

Figure 9.9. Orbit 1212, 55° N, Cross and Interim

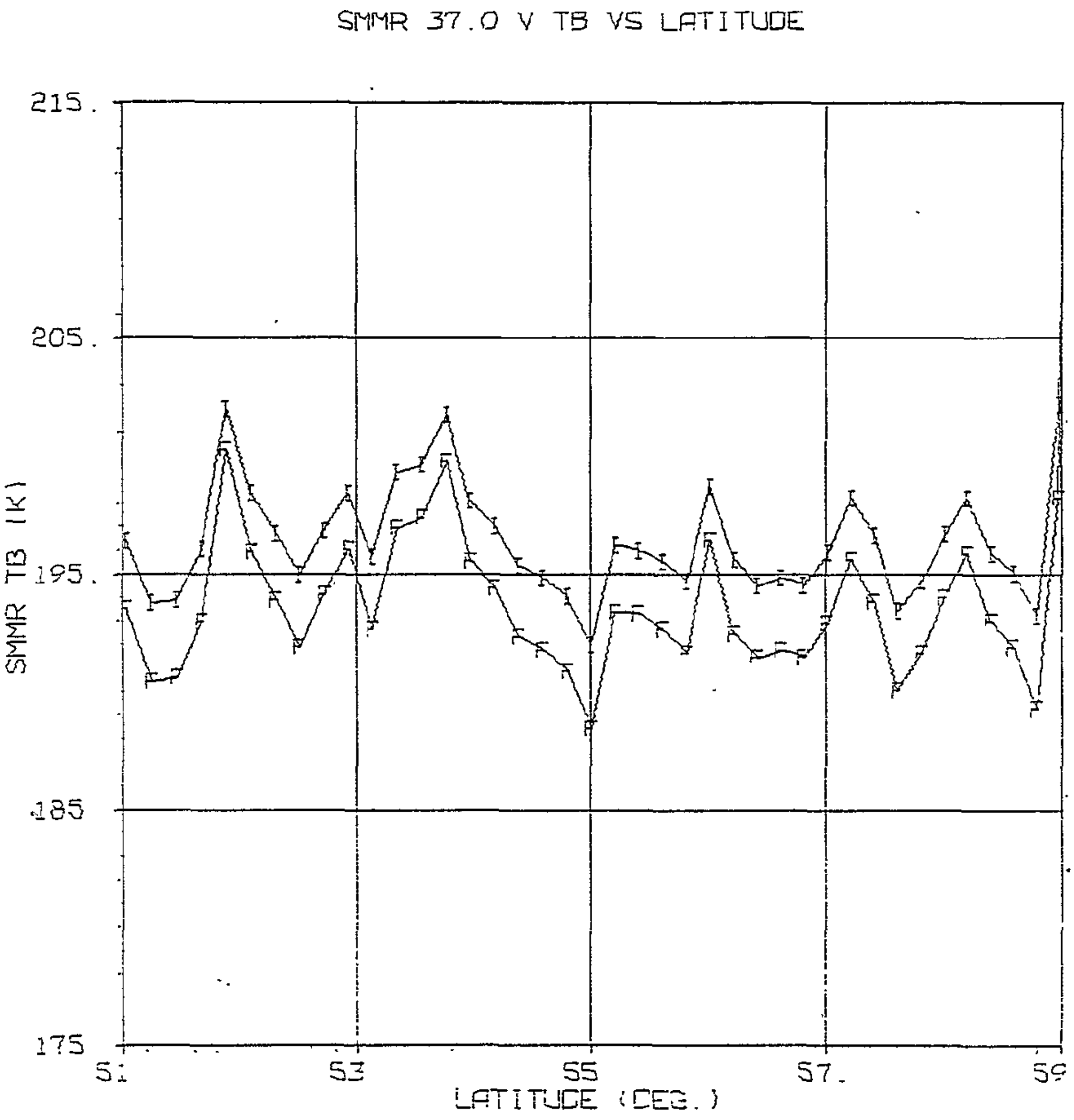

Figure 9.8. Orbit 1212, 55° N, Cross and Interim

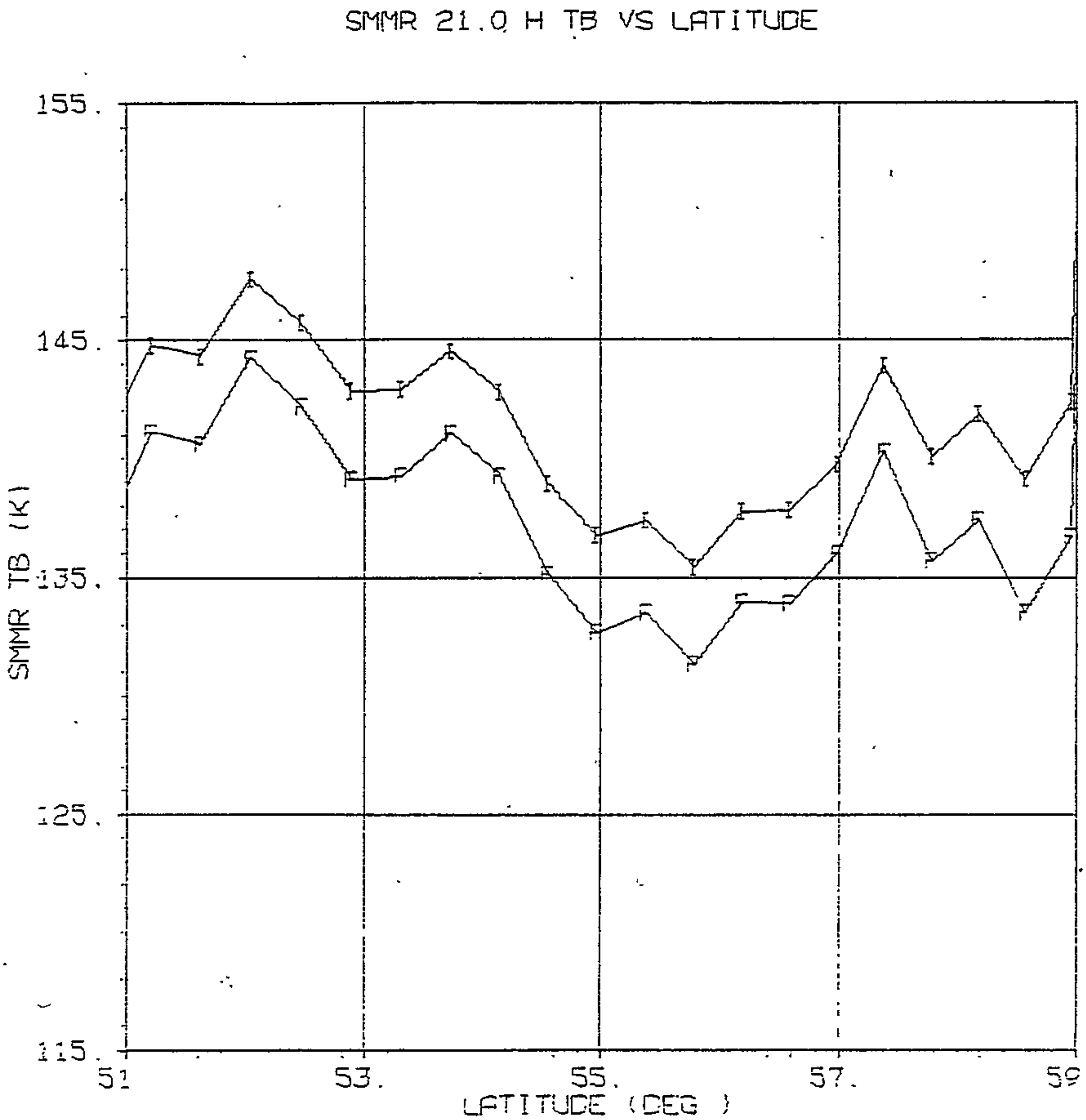

Figure 9.7. Orbit 1212, 55° N, Cross and Interim

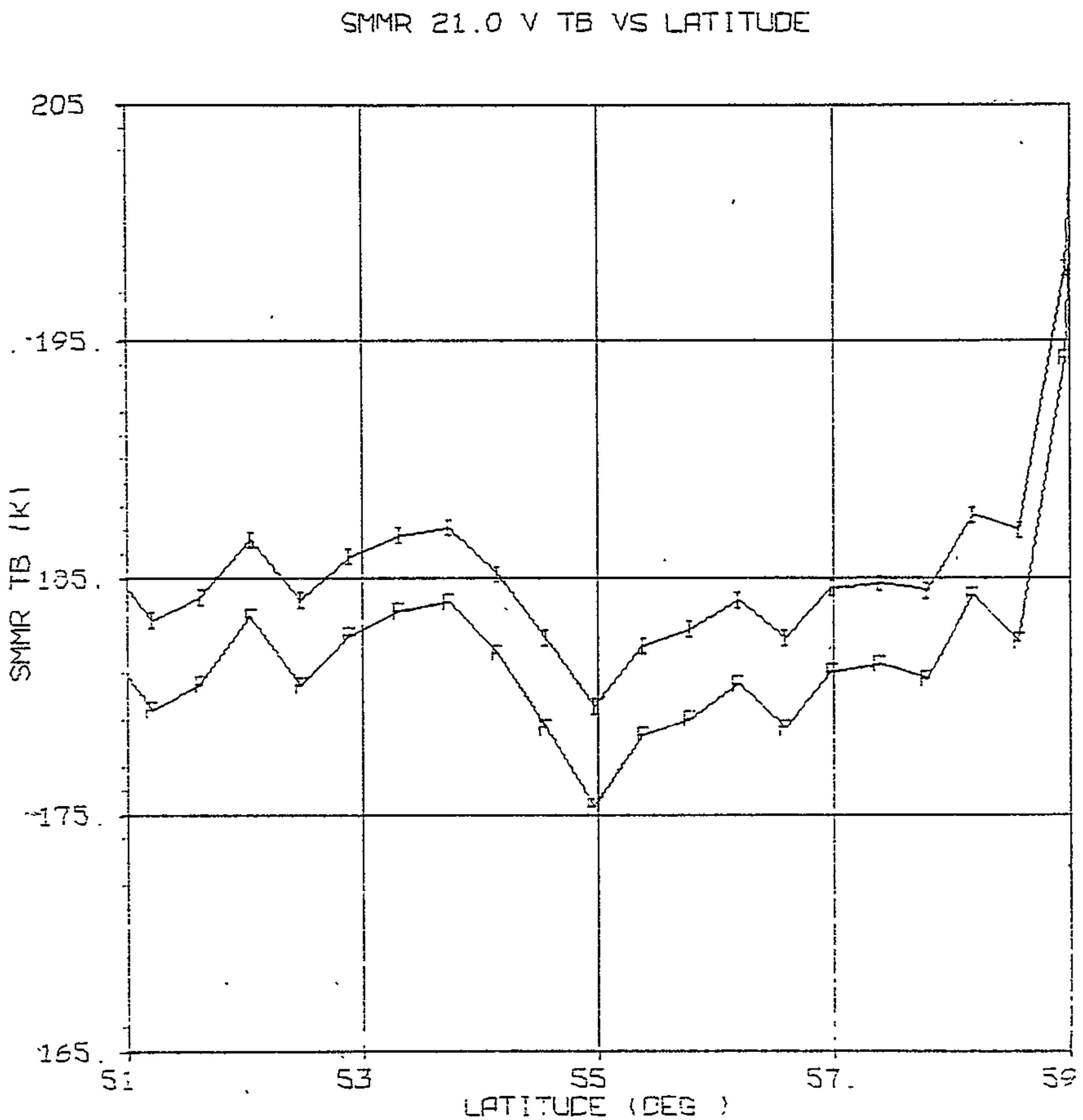

Figure 9.6. Orbit 1212, 55° N, Cross and Interim

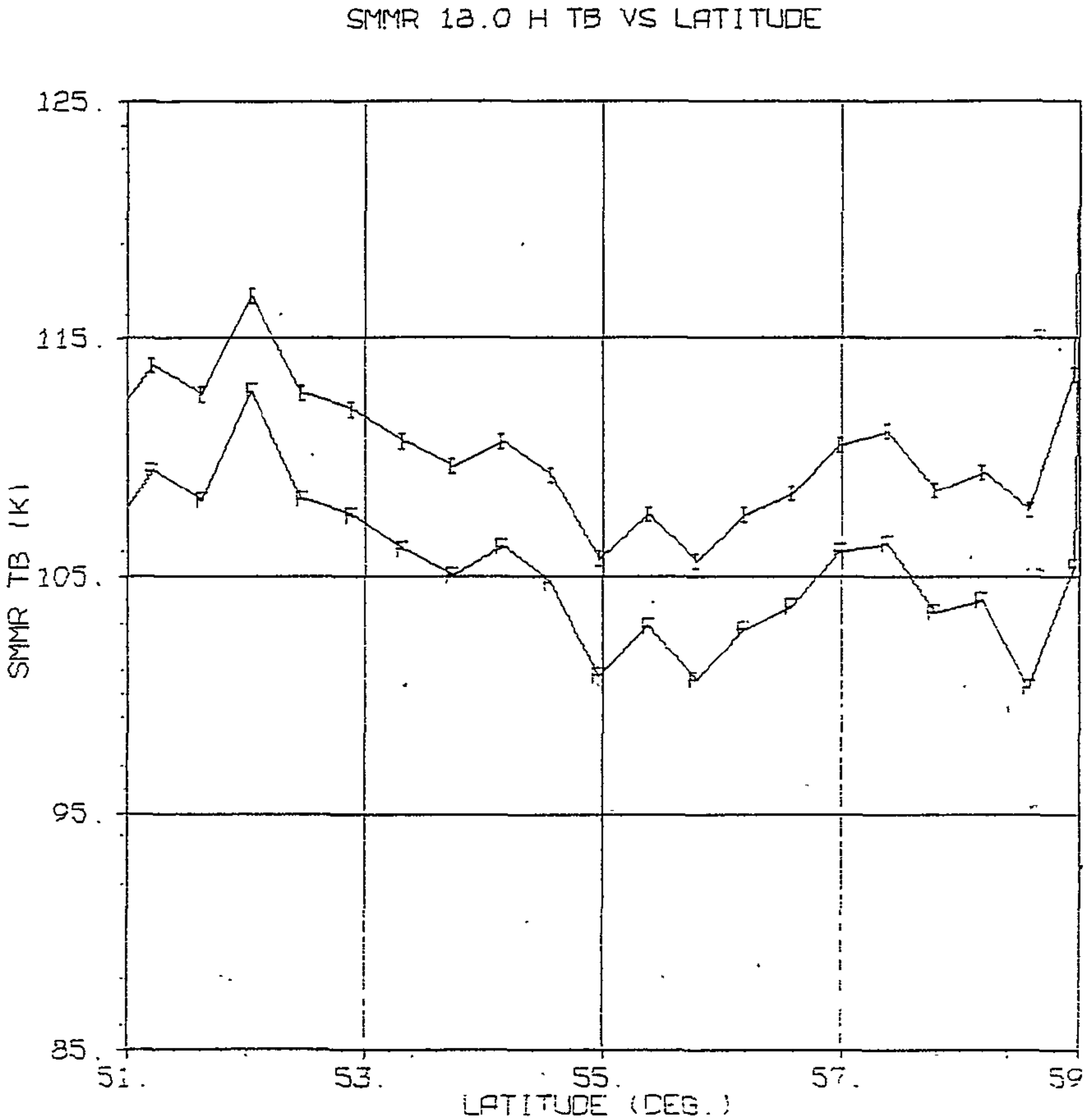

Figure 9.5. Orbit 1212, 55° N, Cross and Interim

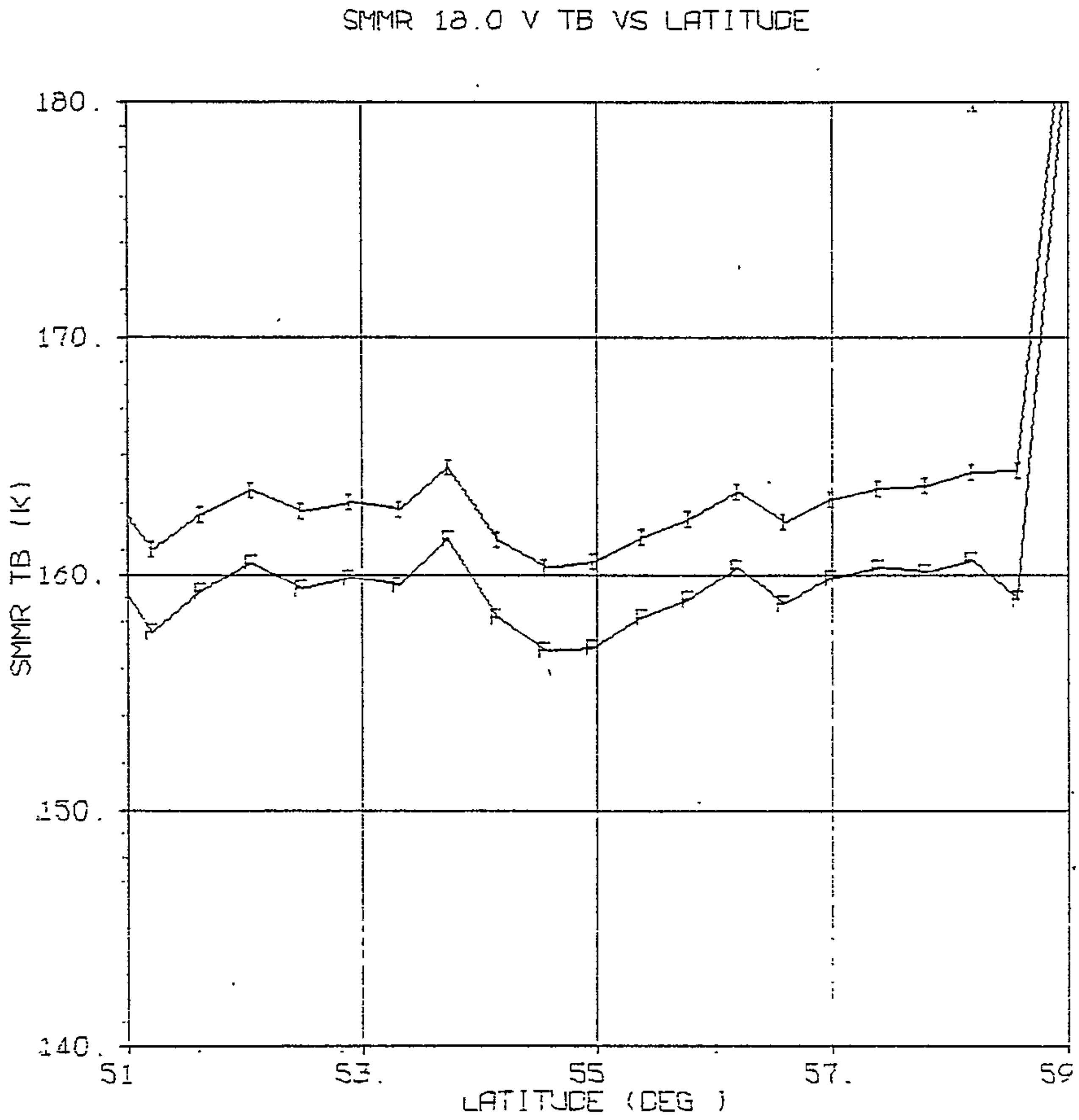

Figure 9.4. Orbit 1212, 55° N, Cross and Interim

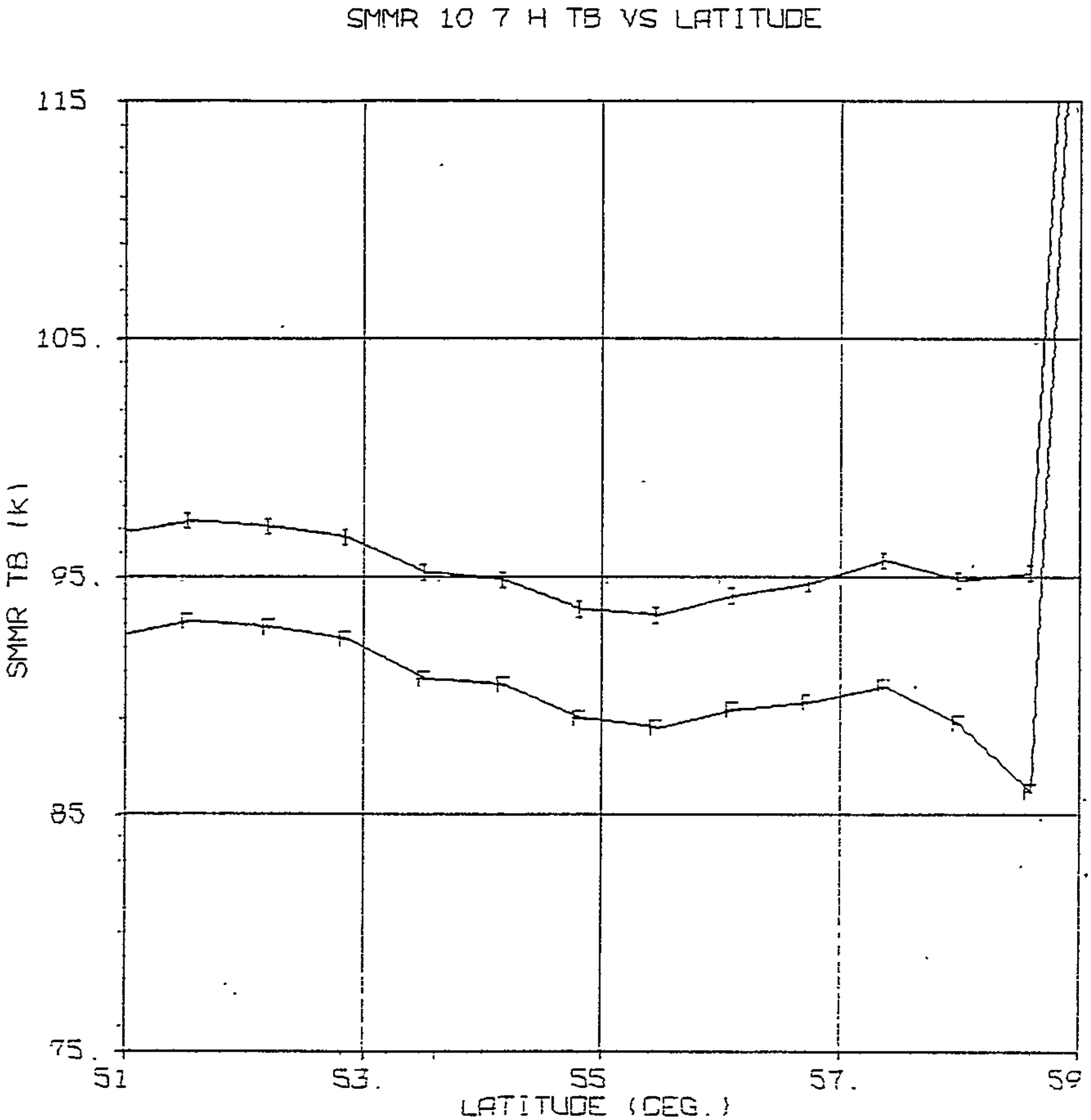

Figure 9.3. Orbit 1212, 55° N, Cross and Interim

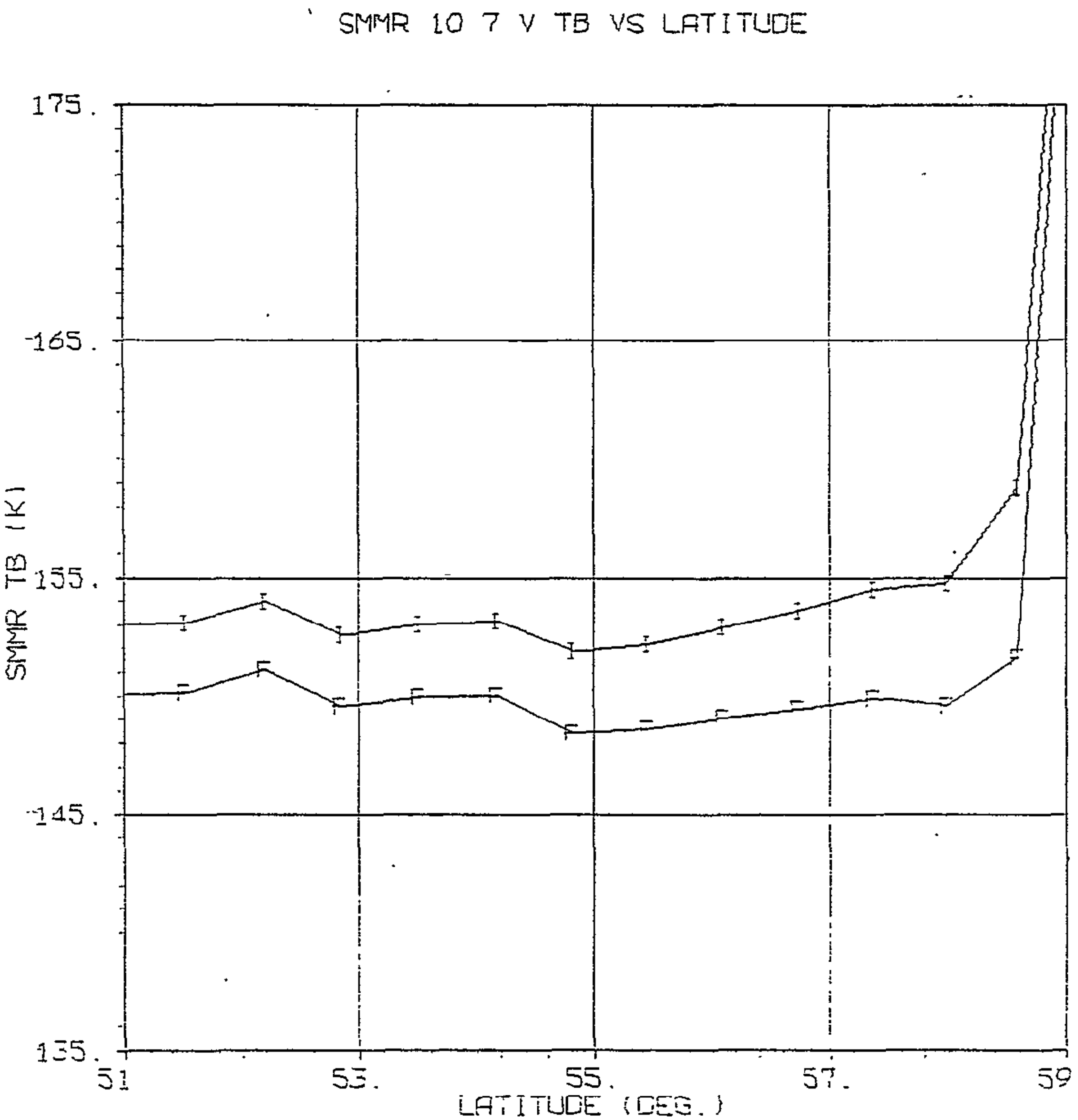

C-2

Figure 9.2. Orbit 1212, 55° N, Cross and Interim

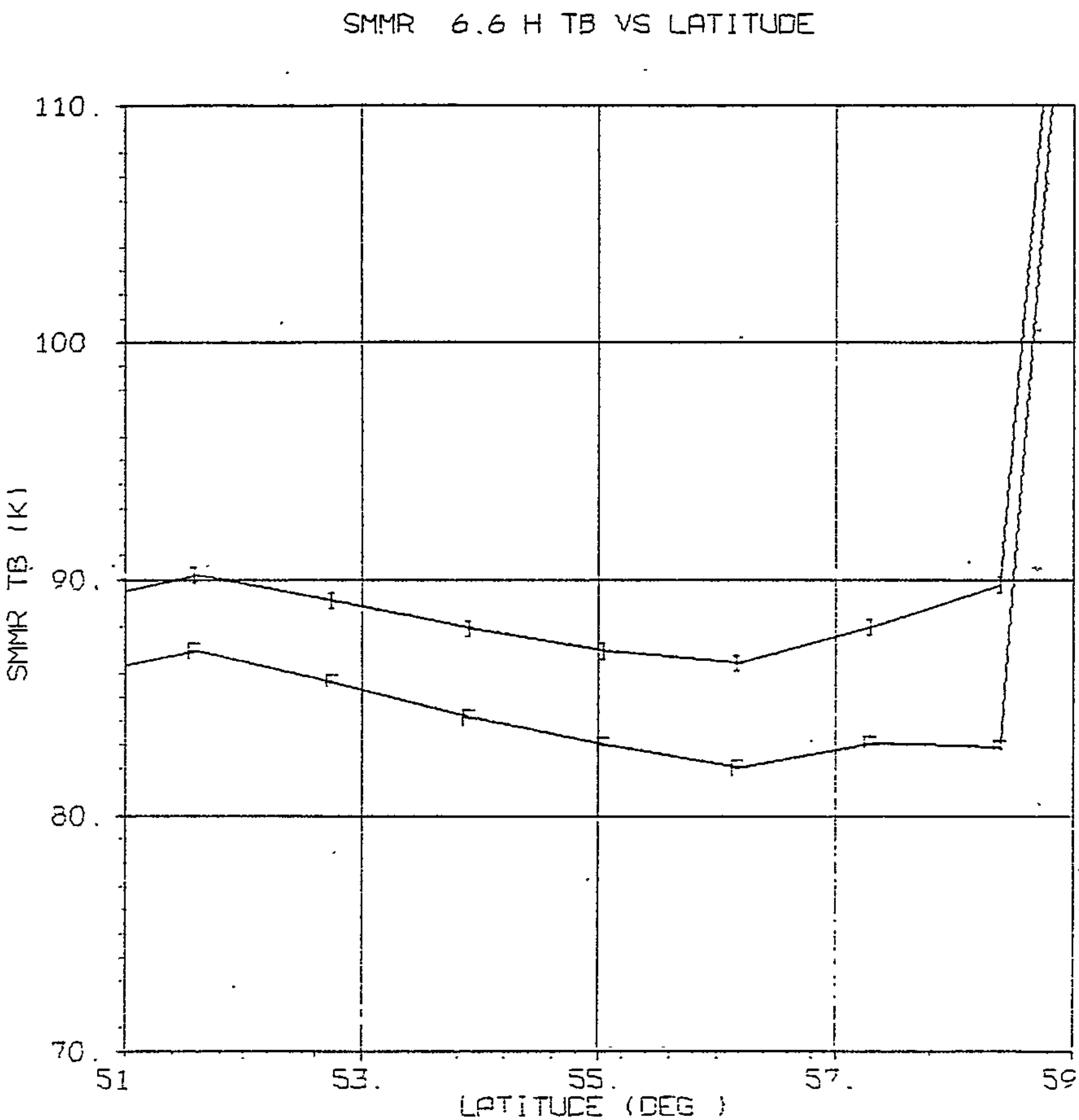

Figure 9.1. Orbit 1212, 55° N, Cross and Interim

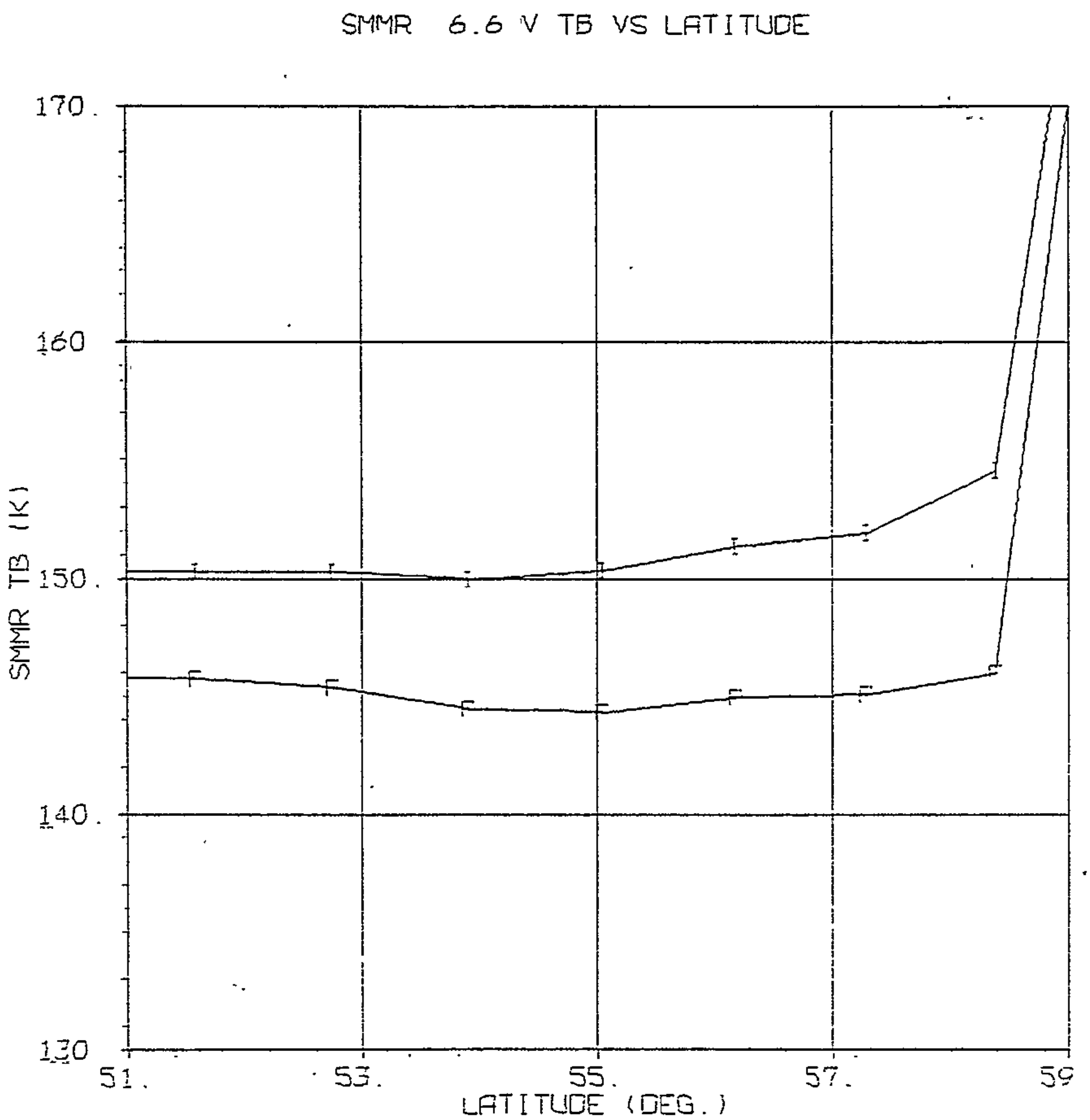

Figure 8.10. Orbit 1212, 55° N, Box and Interim

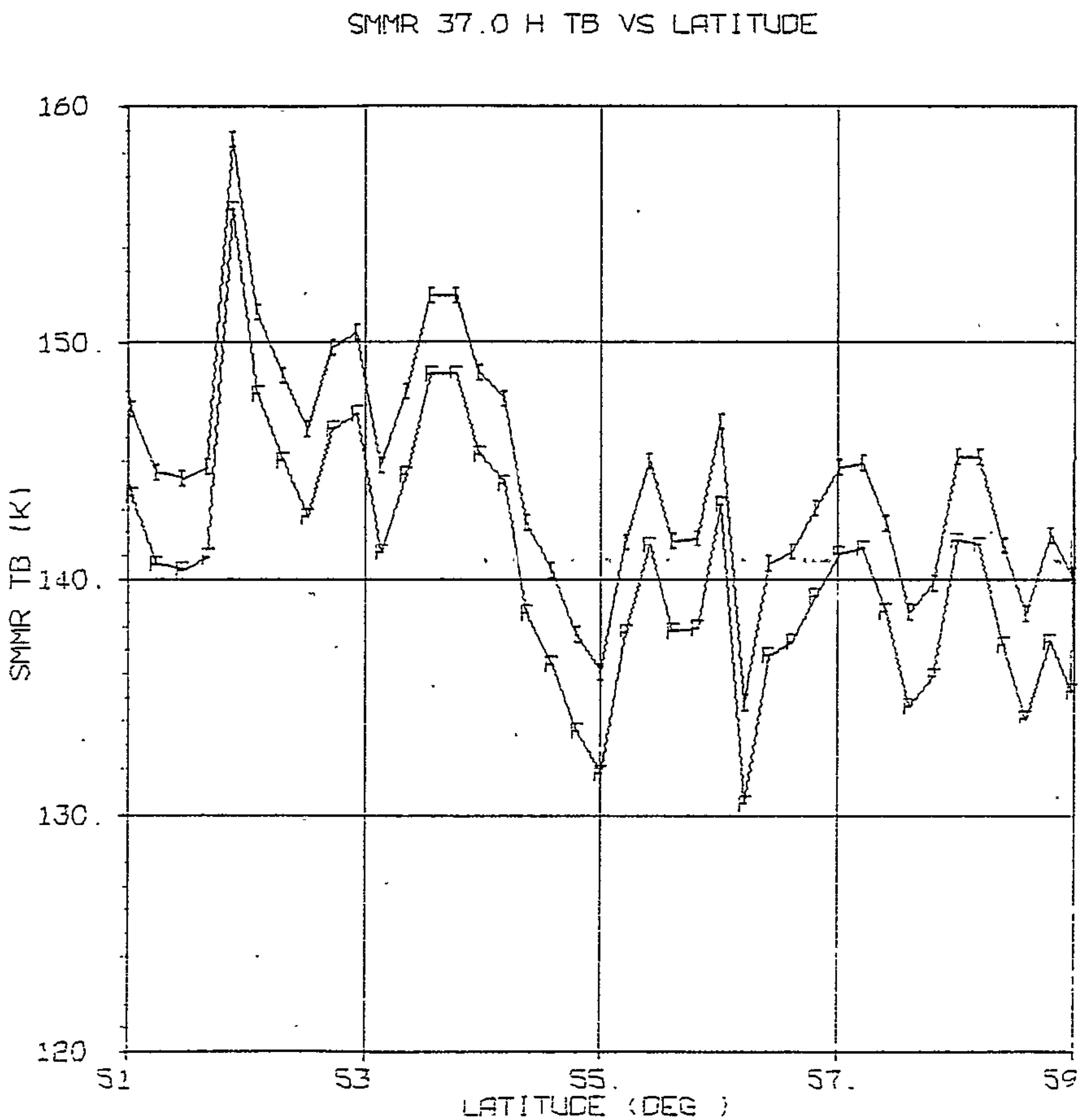

Figure 8.9. Orbit 1212, 55° N, Box and Interim

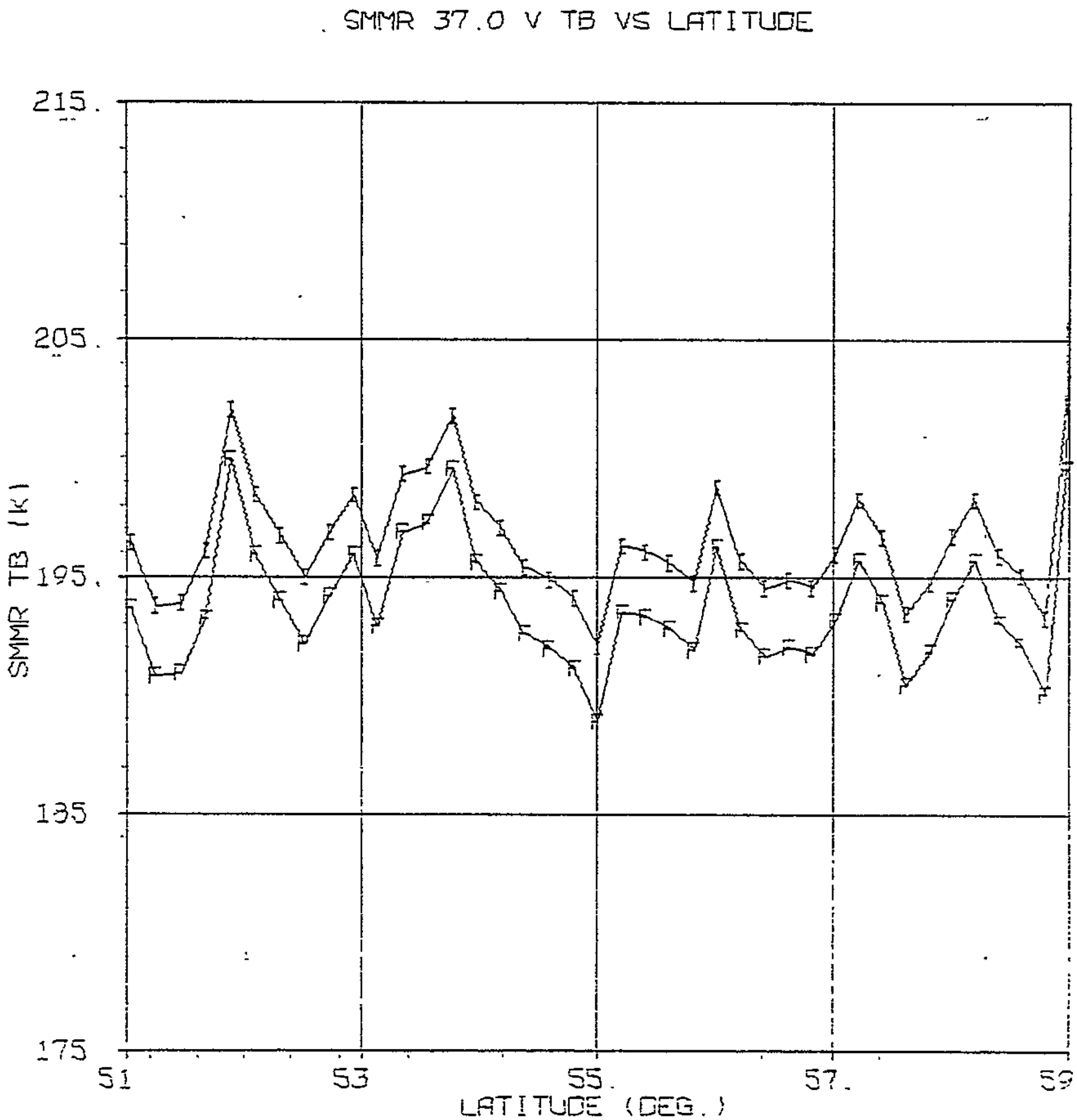

Figure 8.8. Orbit 1212, 55° N, Box and Interim

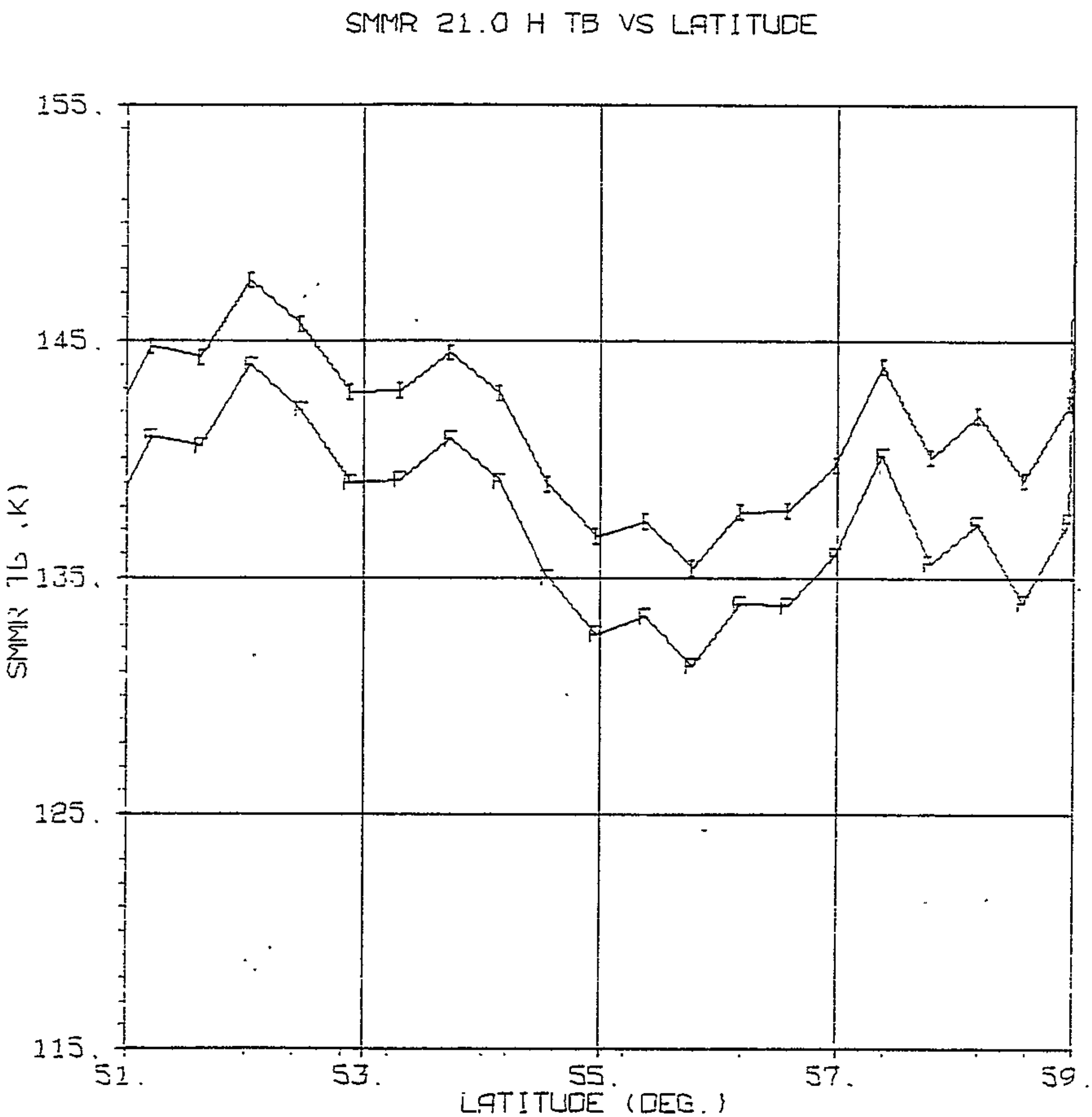

Figure 8.7. Orbit 1212, 55° N, Box and Interim

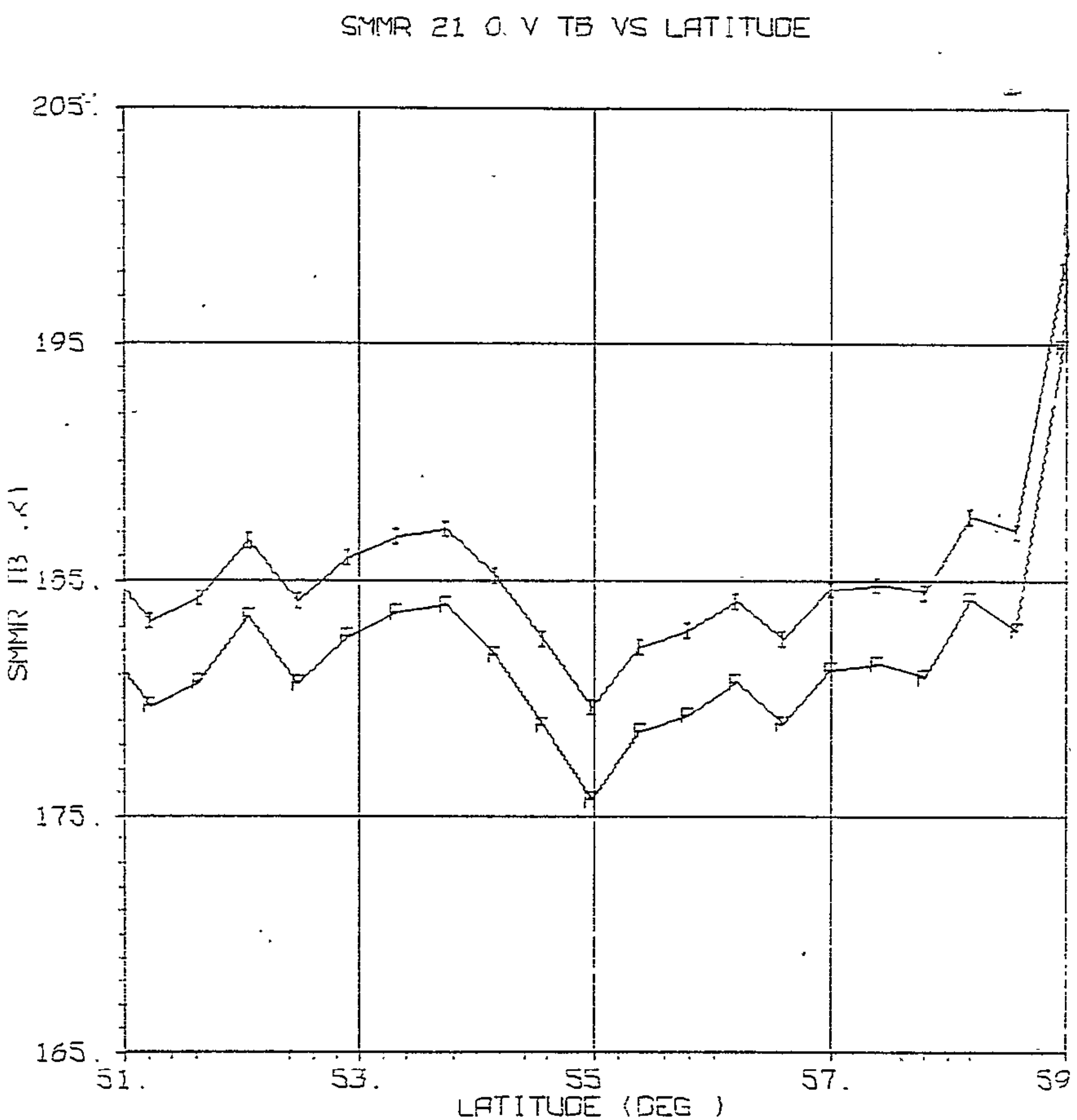

Figure 8.6. Orbit 1212, 55° N, Box and Interim

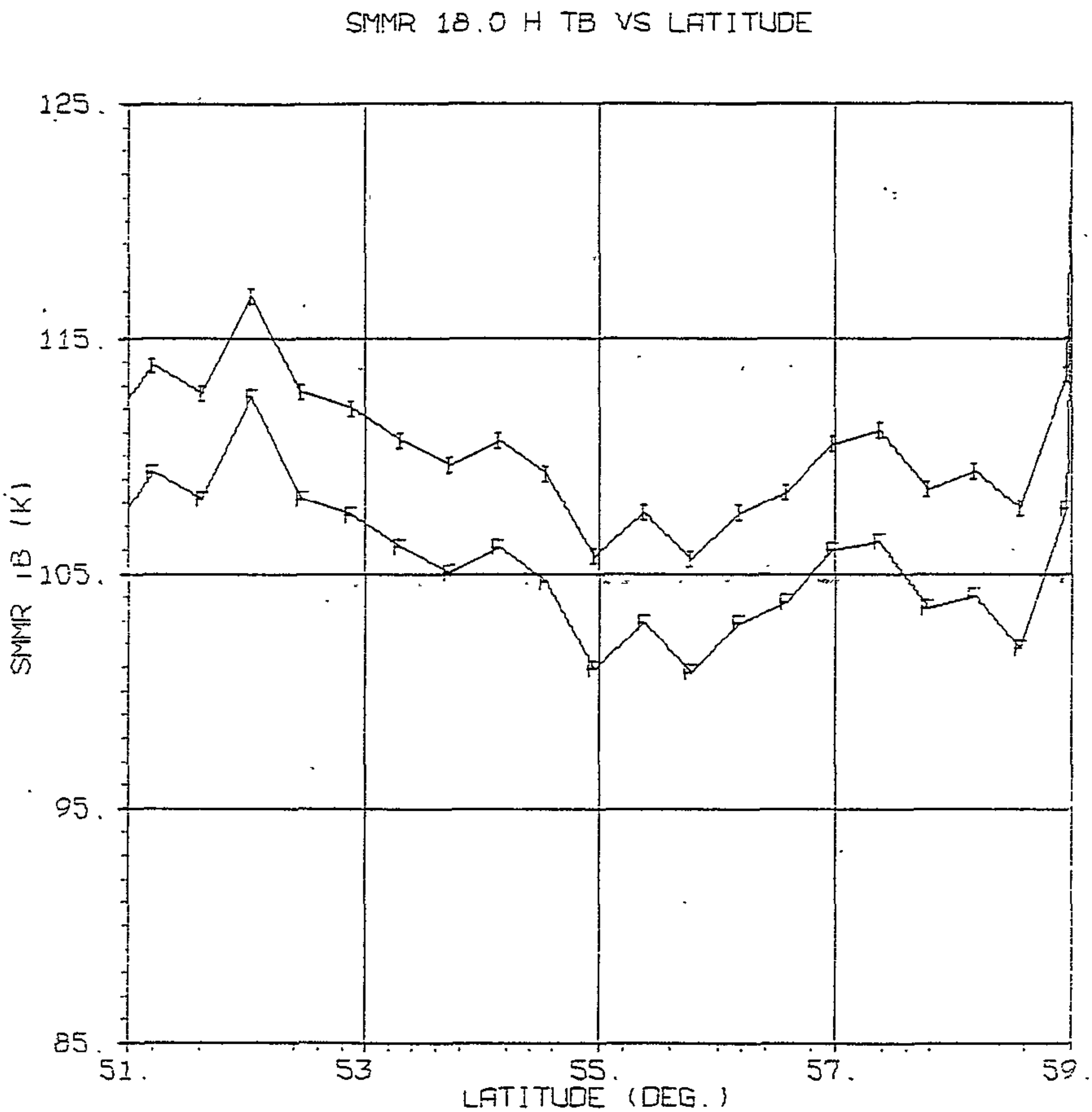

Figure 8.5. Orbit 1212, 55° N, Box and Interim

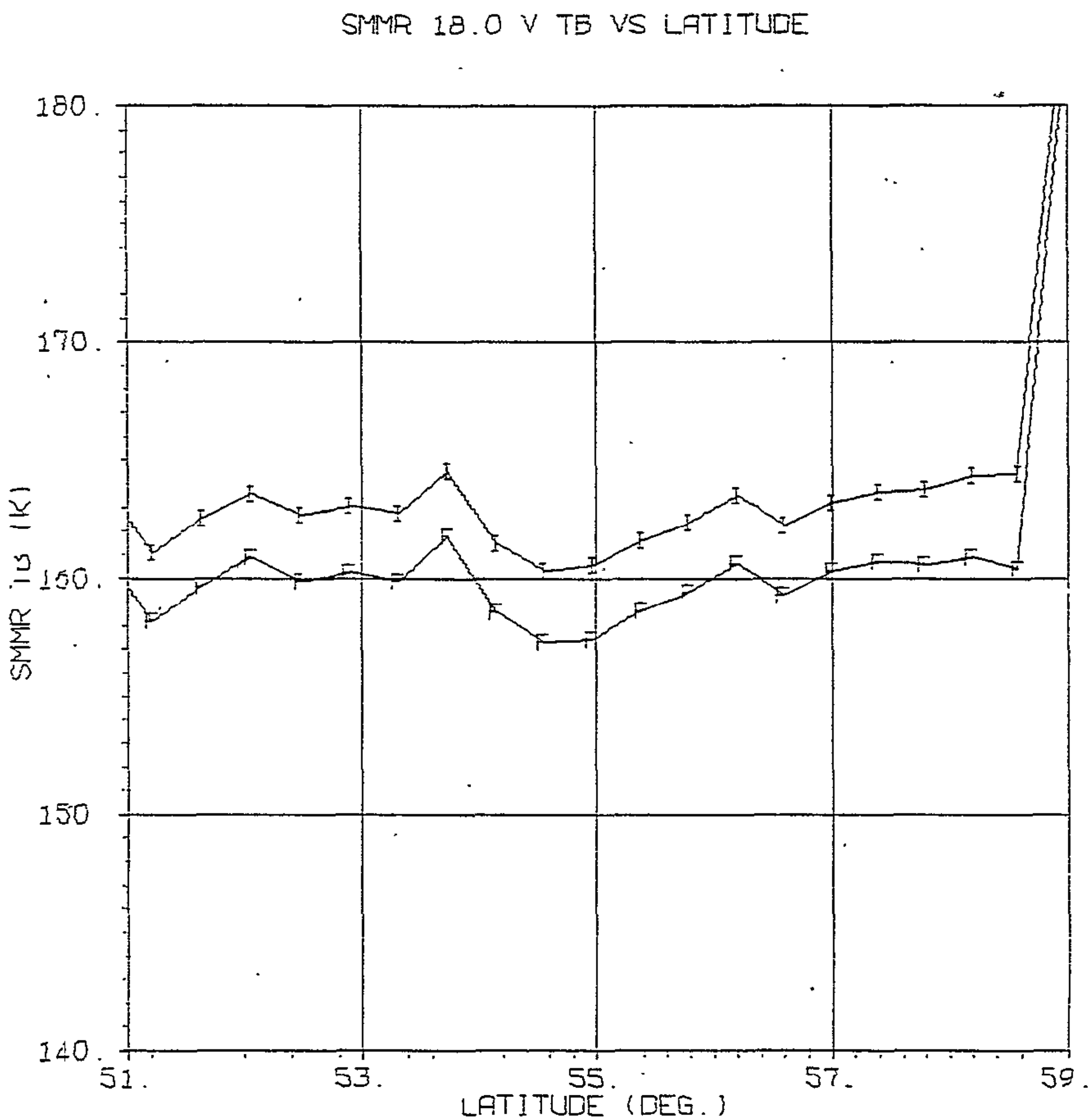

Figure 8.4. Orbit 1212, 55° N, Box and Interim

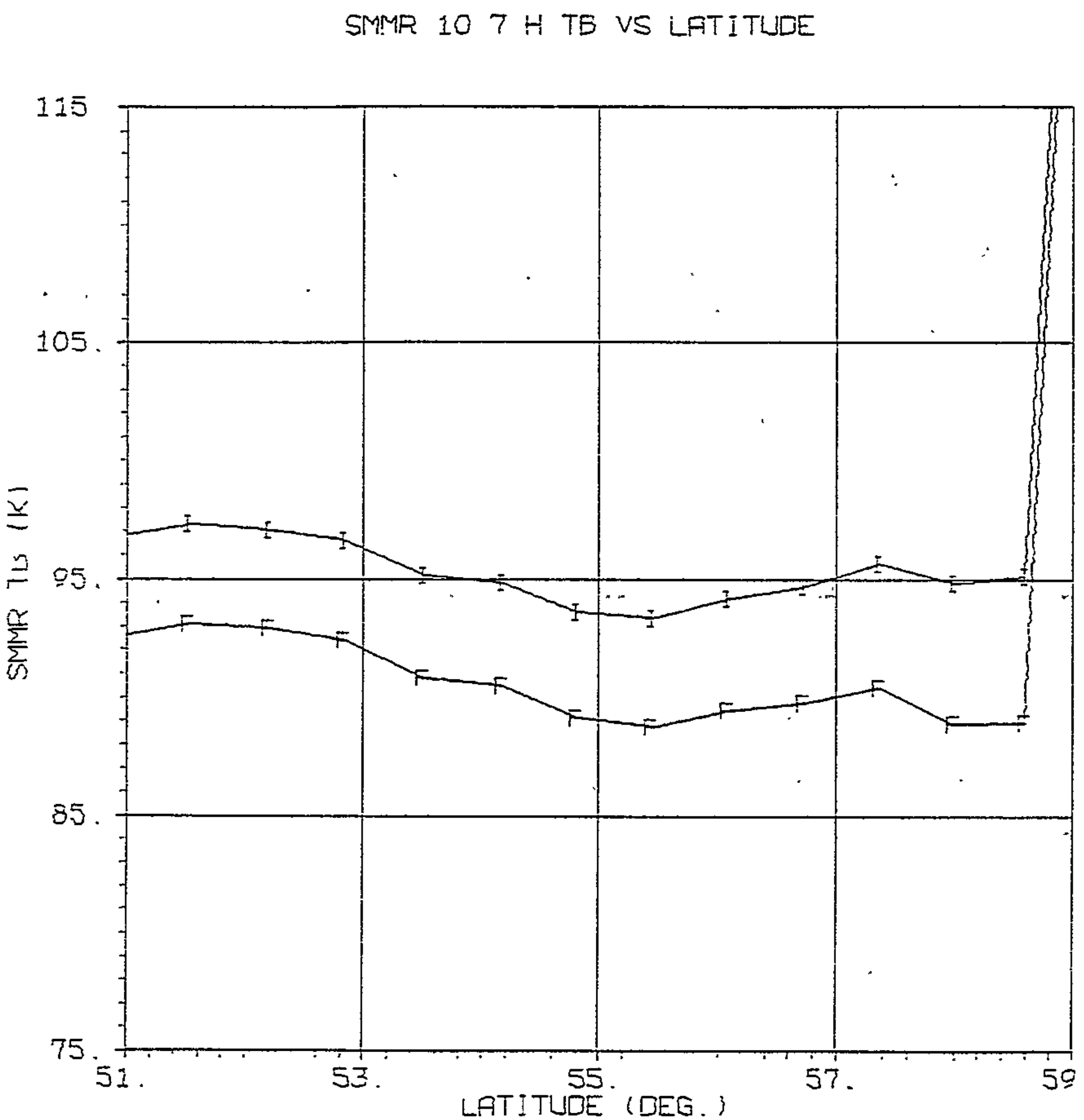

Figure 8.3. Orbit 1212, 55° N, Box and Interim

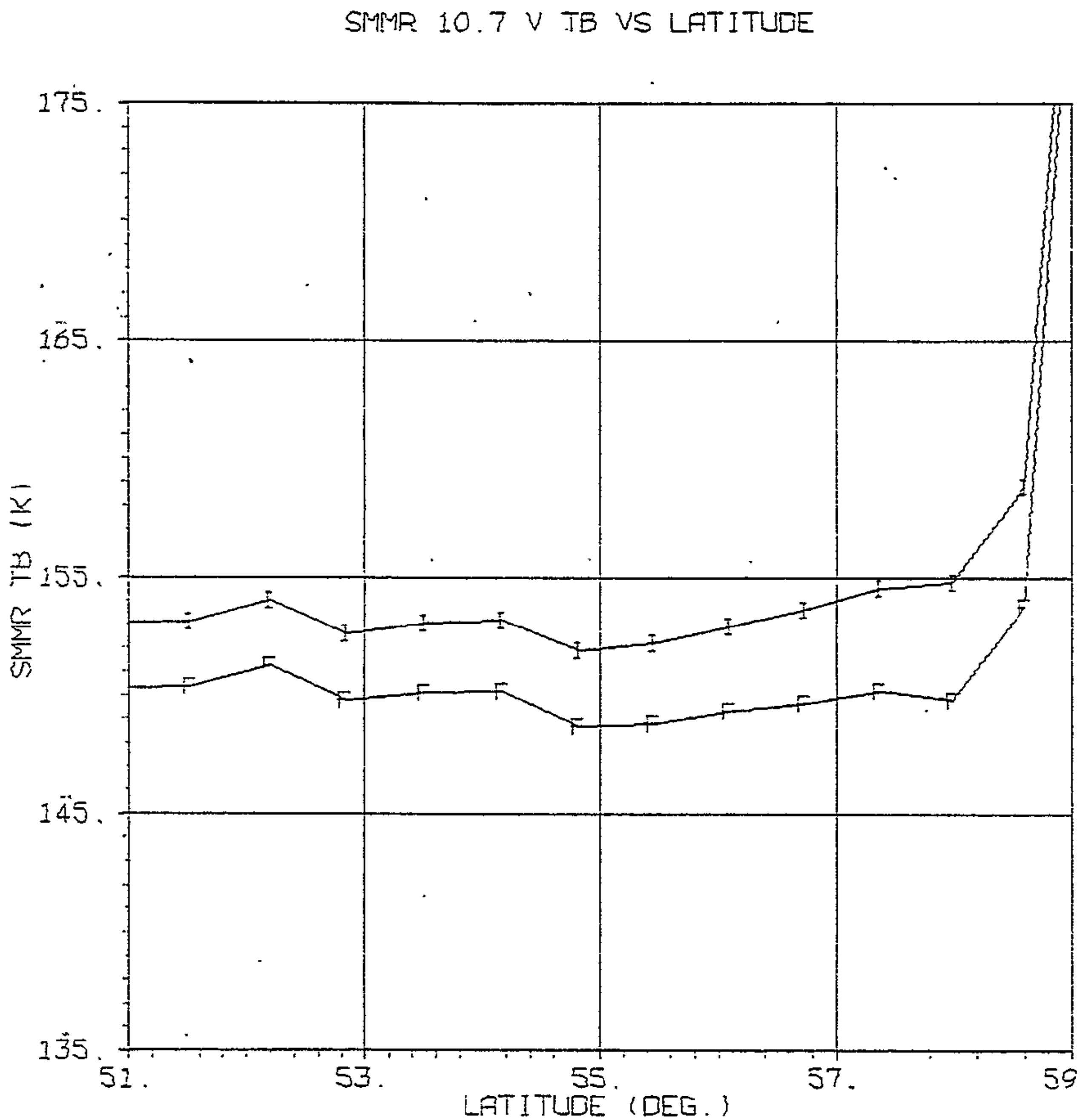

Figure 8.2. Orbit 1212, 55° N, Box and Interim

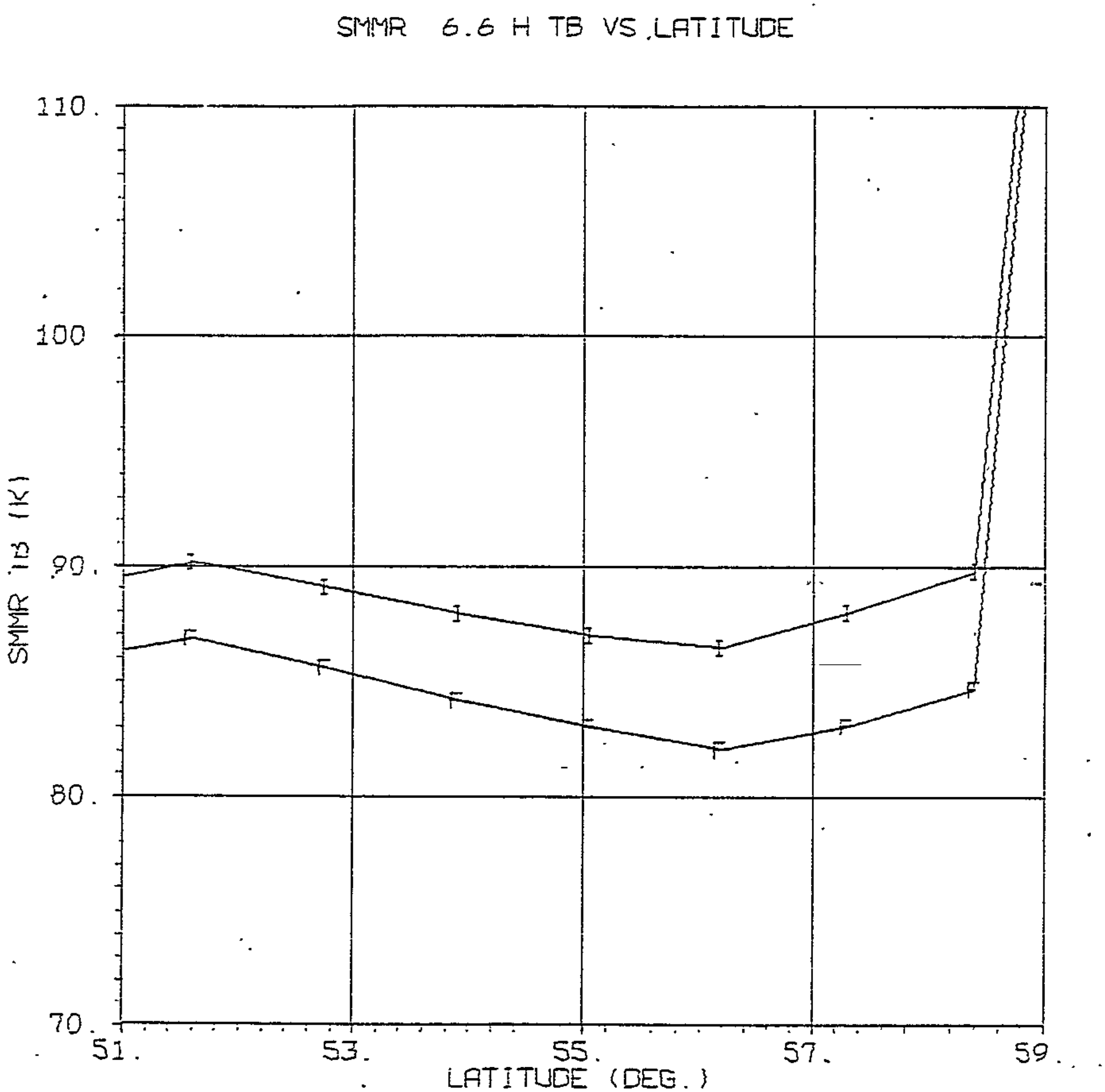

Figure 8.1. Orbit 1212, 55° N, Box and Interim

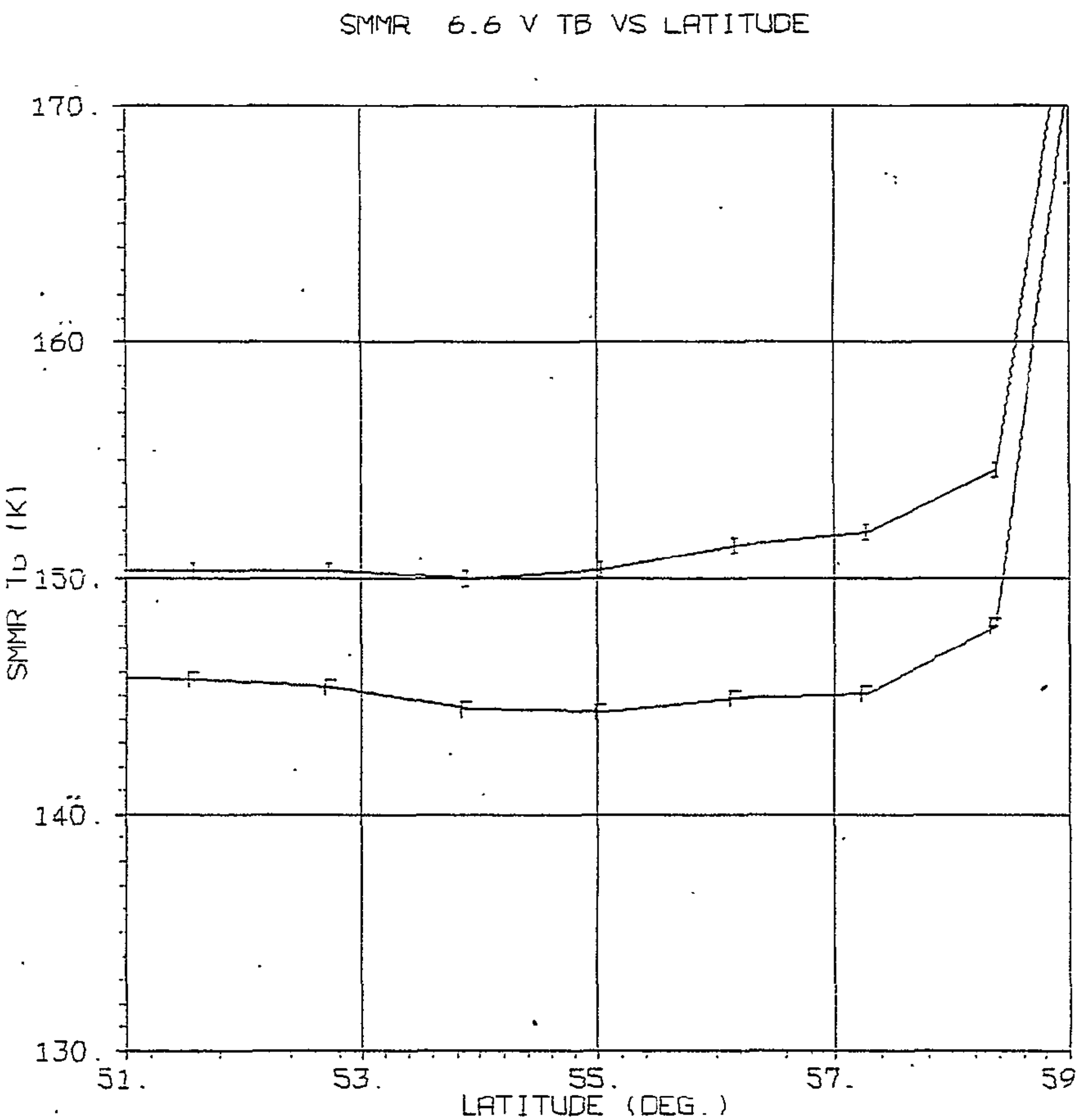

Figure 7.5. Orbit 331, Nominal Mode

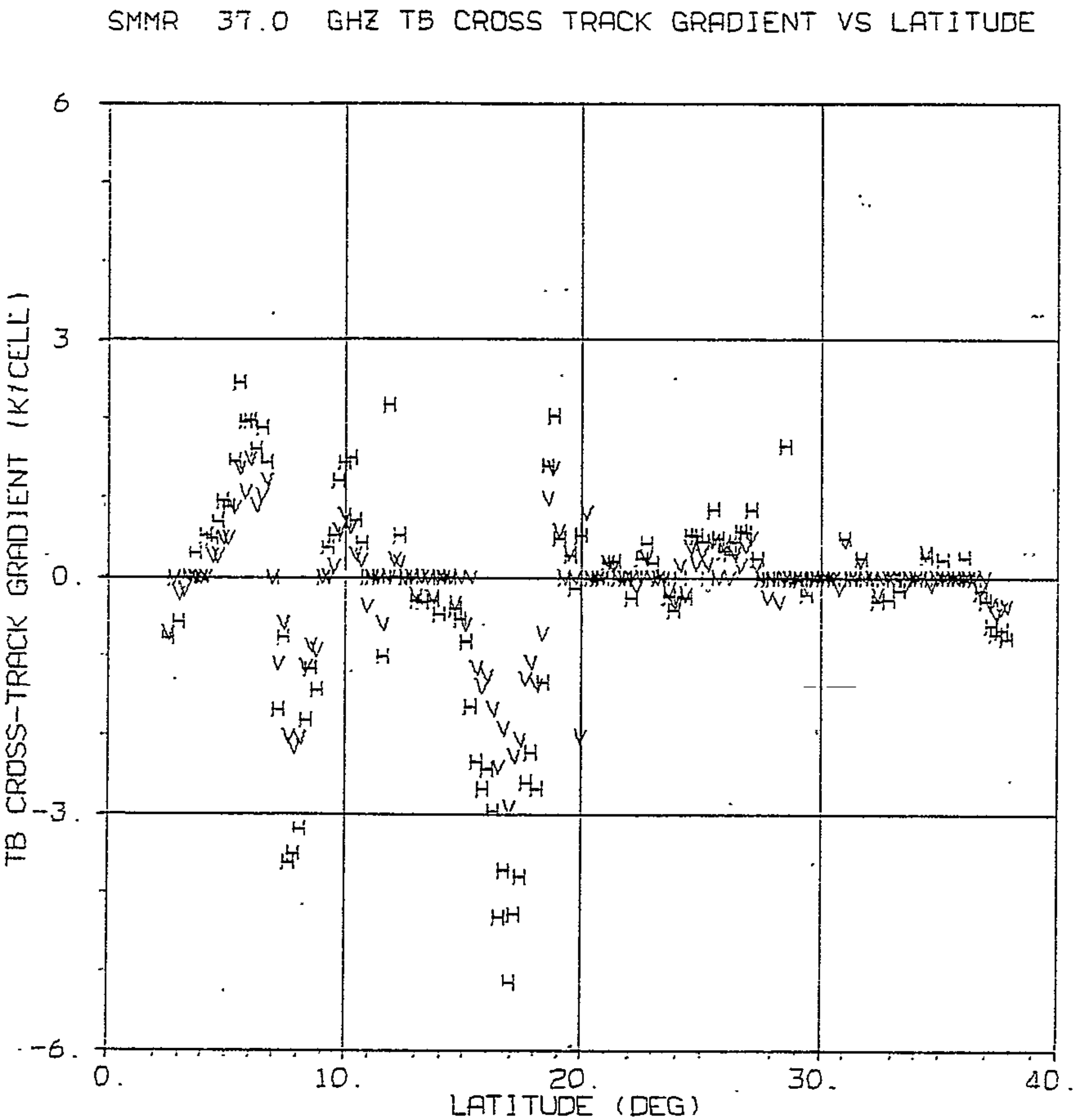

Figure 7.4. Orbit 331, Nominal Mode

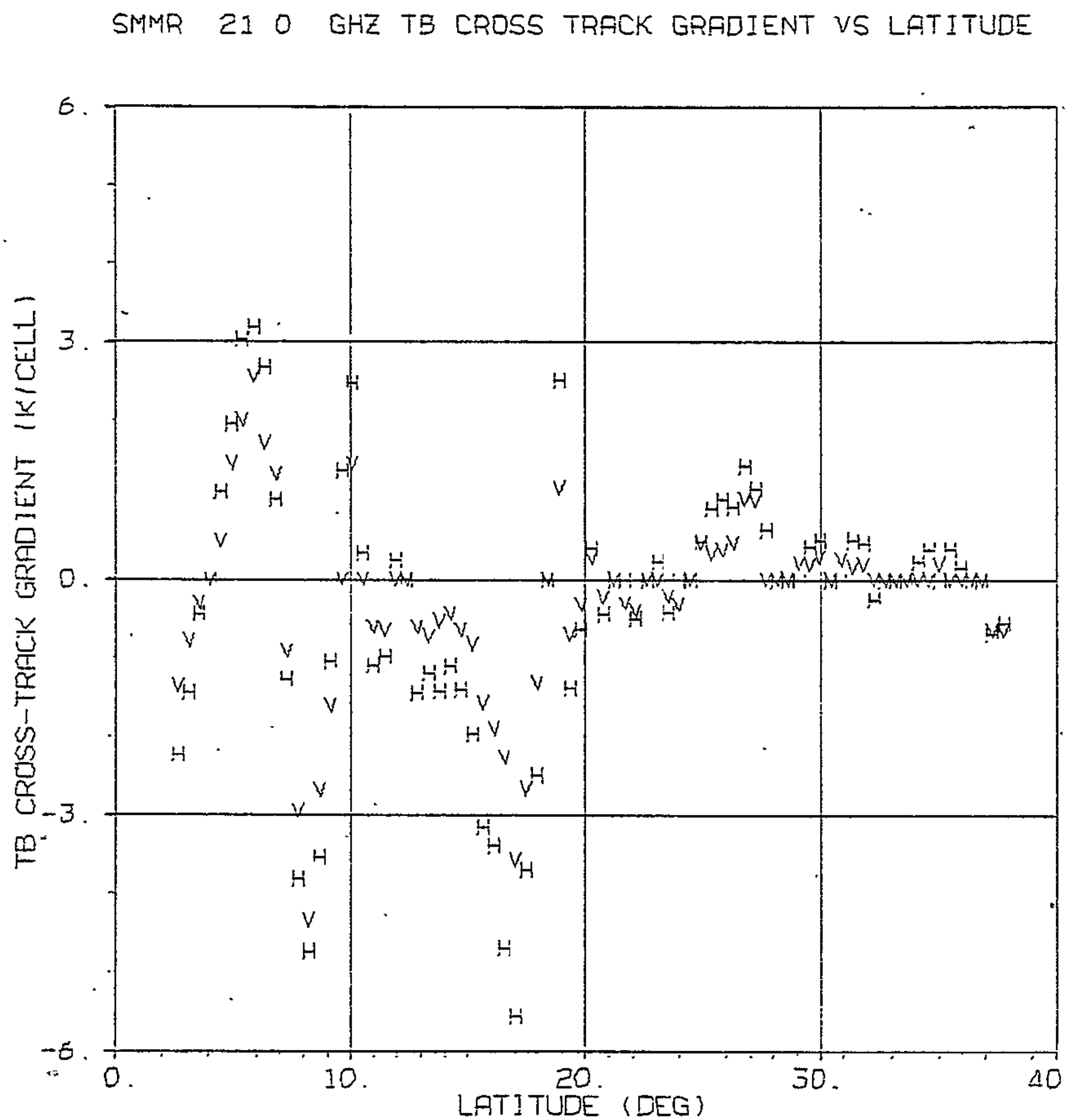

Figure 7.3. Orbit 331, Nominal Mode

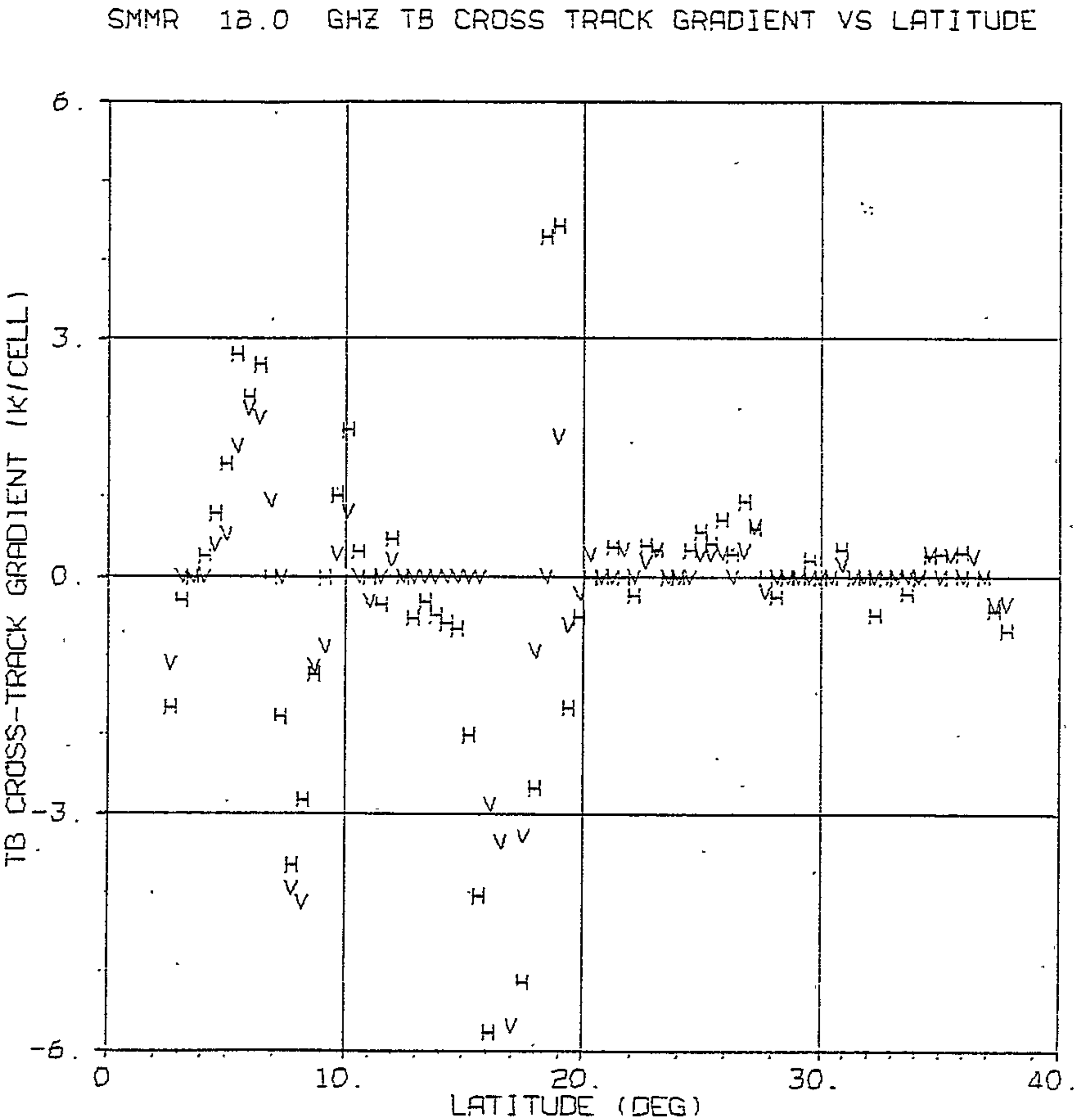

Figure 7.2. Orbit 331, Nominal Mode

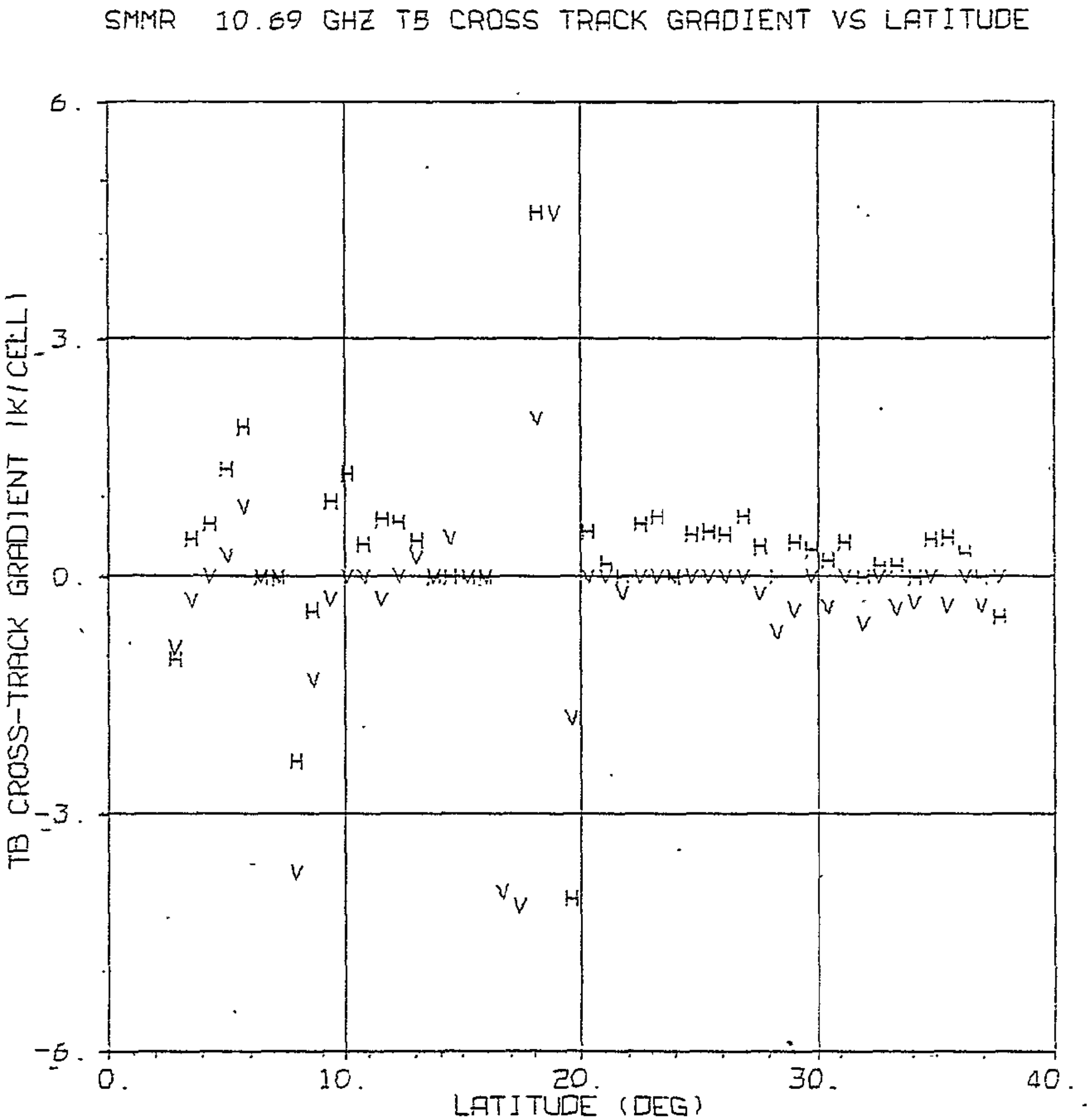

Figure 7.1. Orbit 331, Nominal Mode

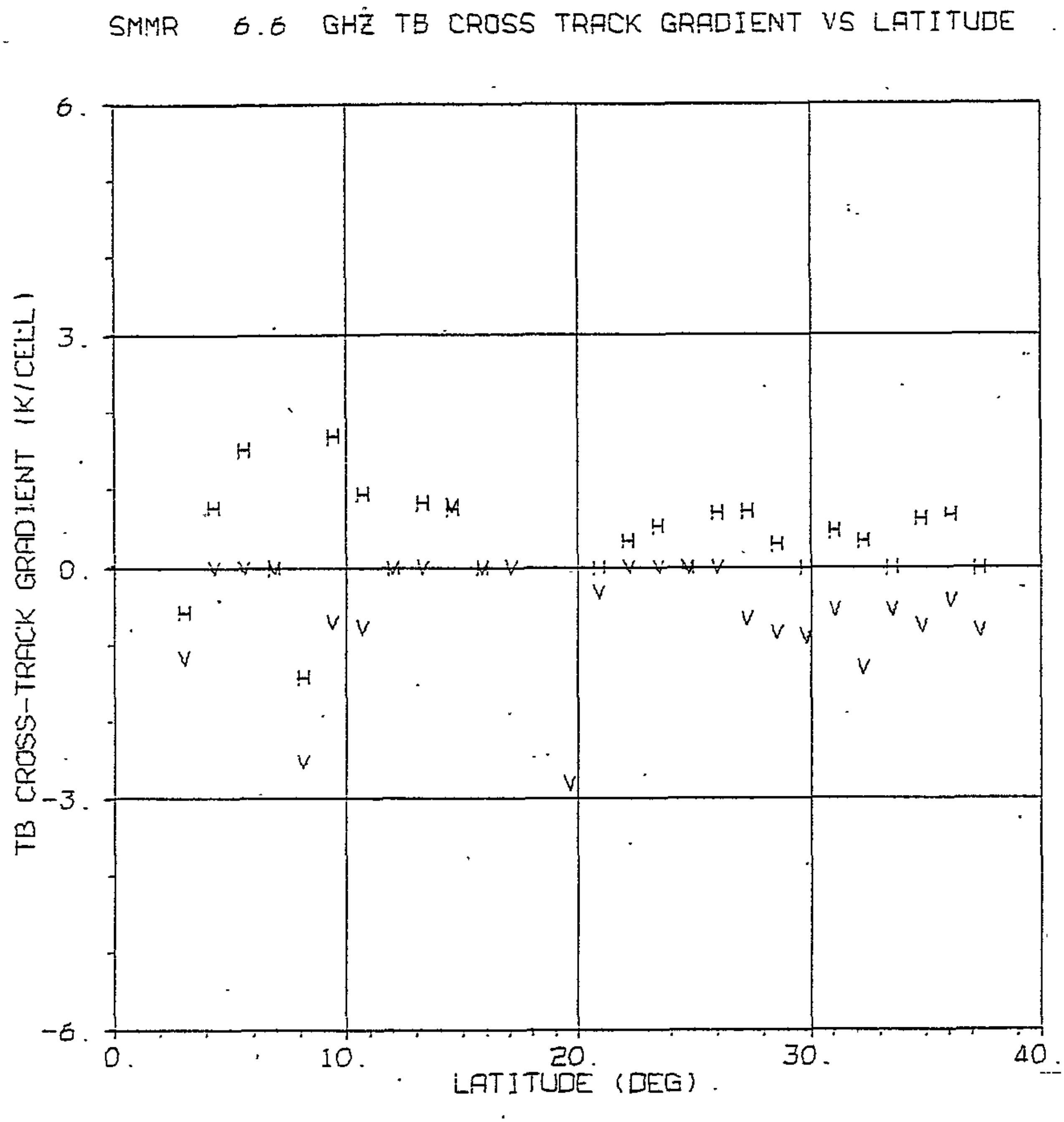

Figure 6.5. Orbit, 331, Cross Mode

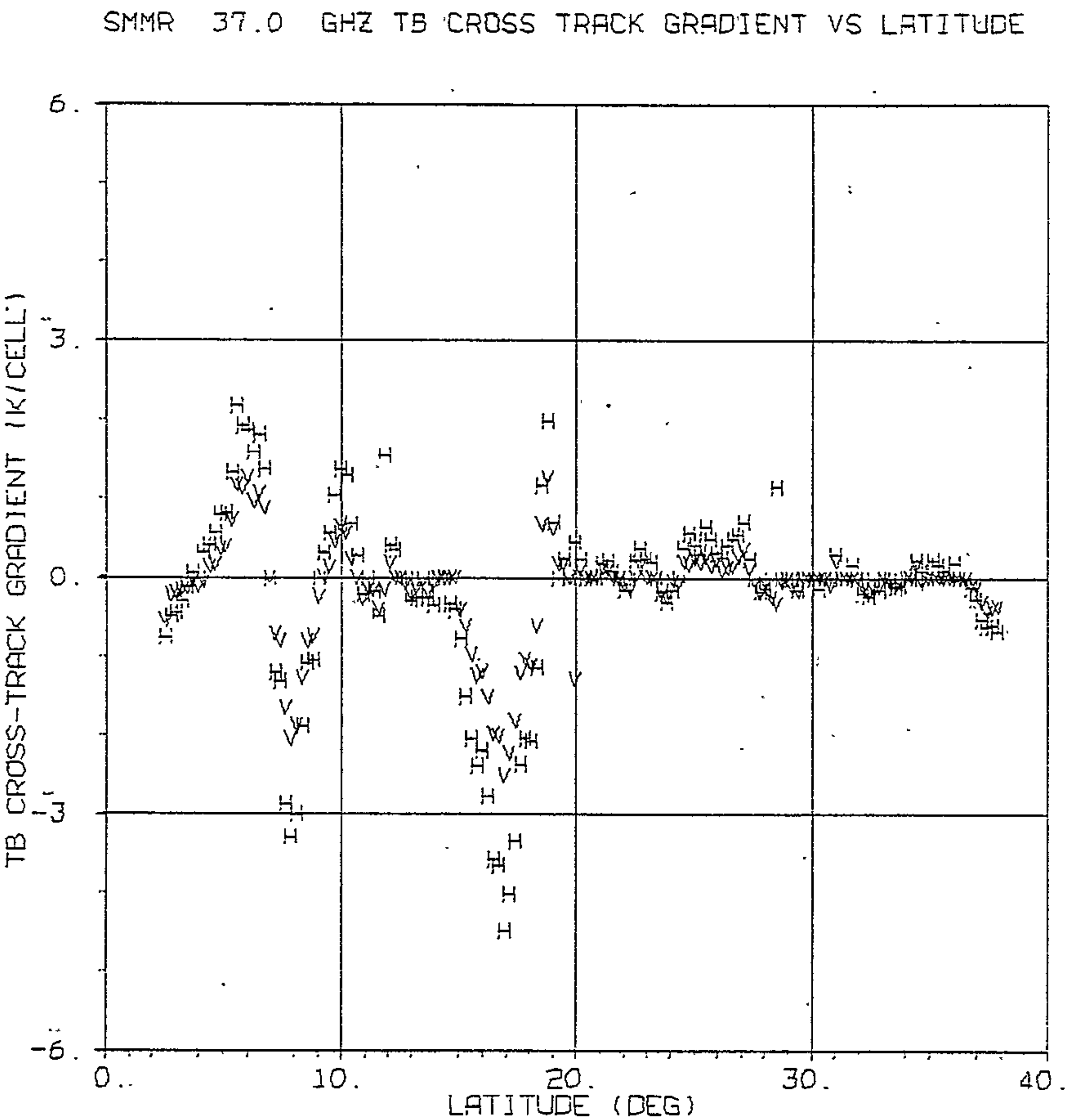

Figure 6.4. Orbit 331, Cross Mode

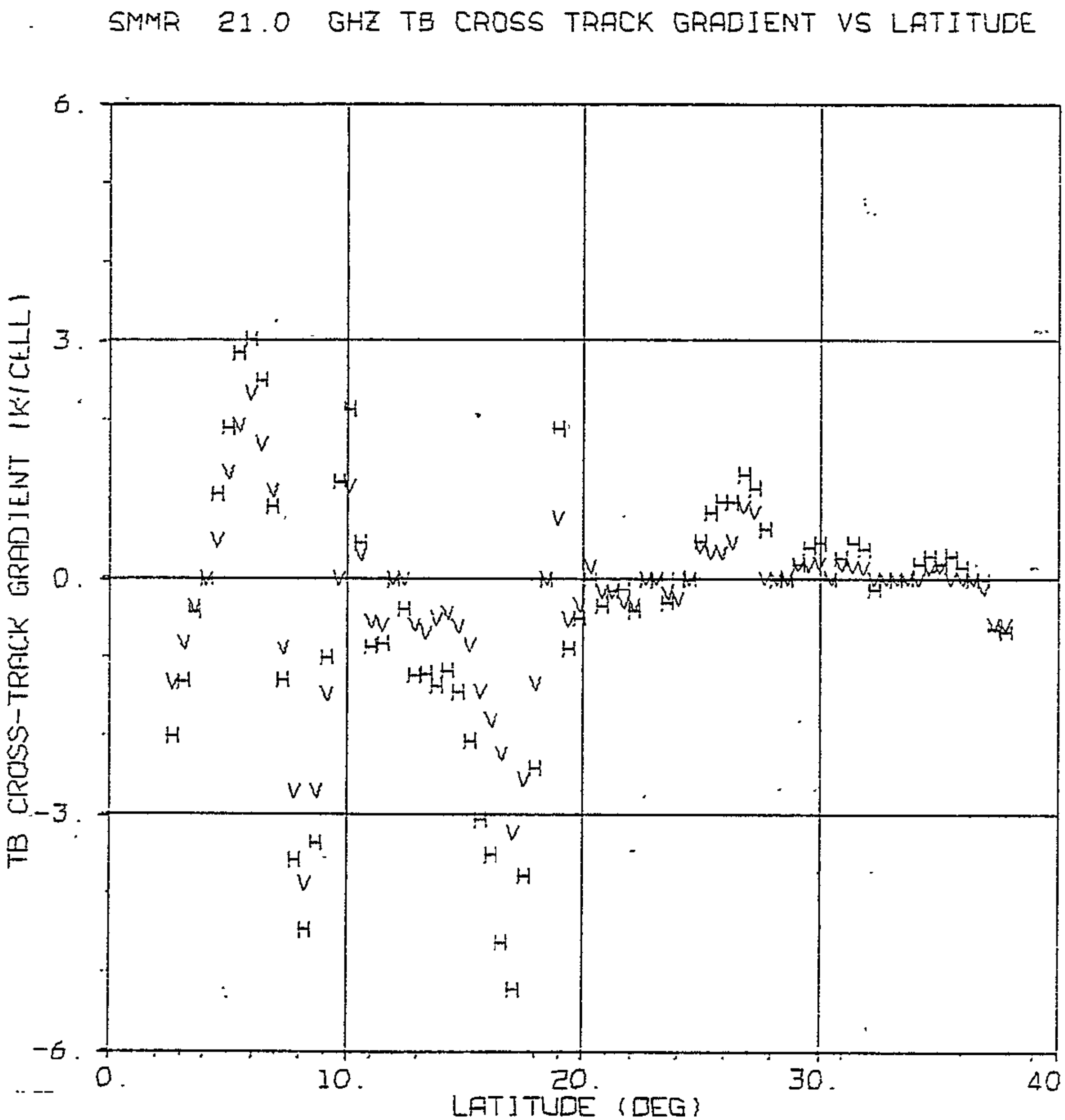

Figure 6.3. Orbit 331, Cross Mode

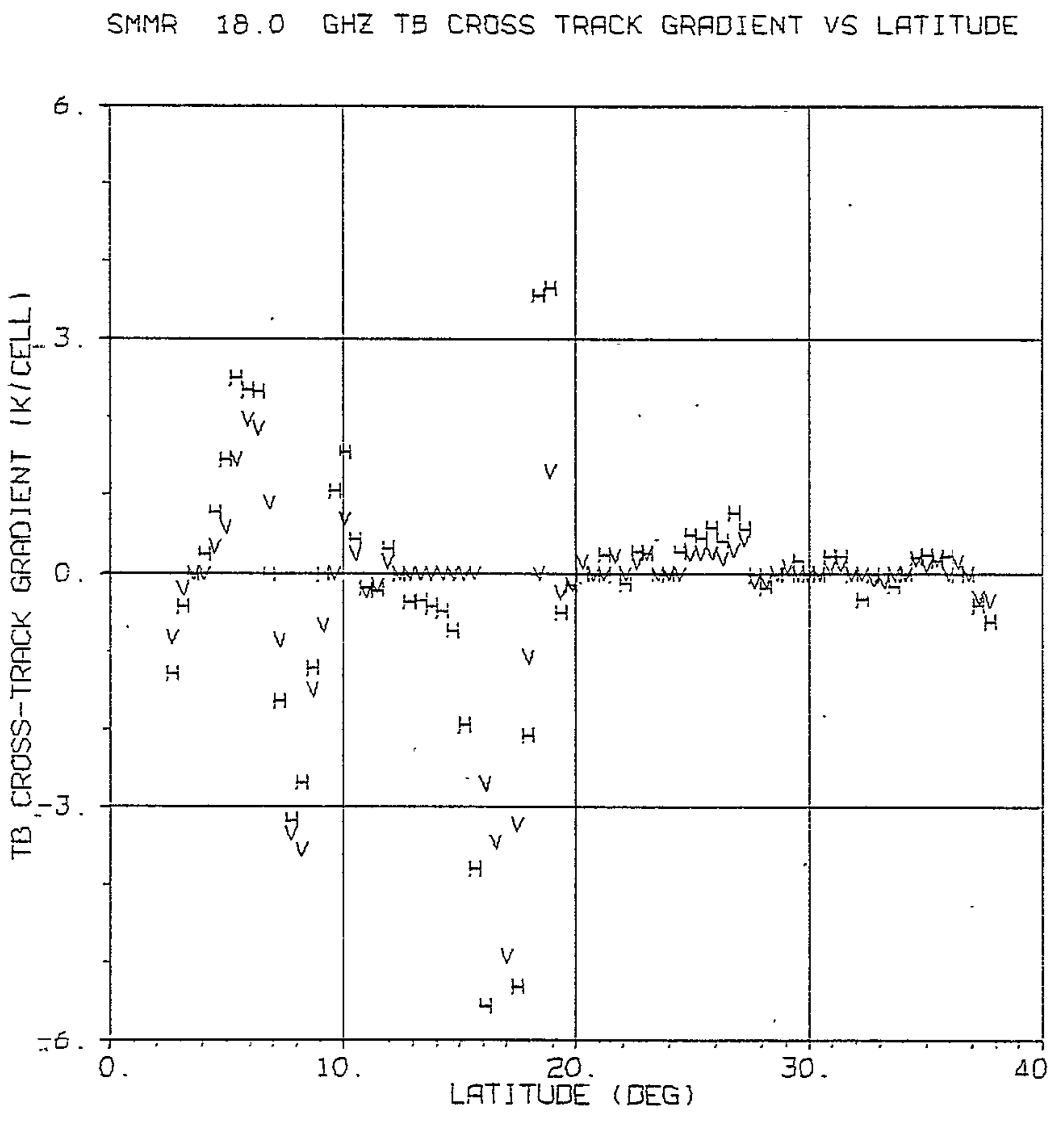

Figure 6.2. Orbit 331, Cross Mode

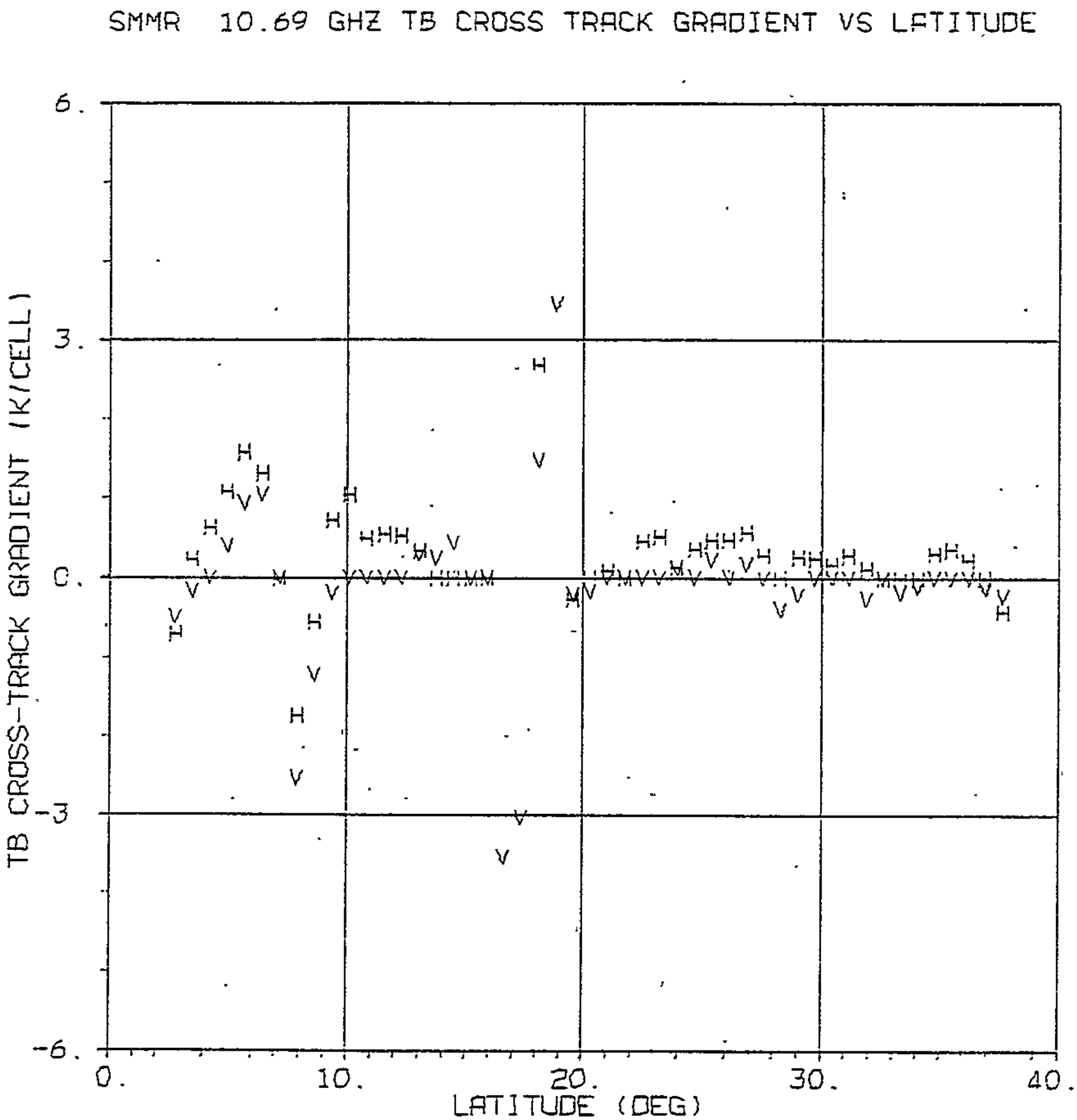

Figure 6.1. Orbit 331, Cross Mode

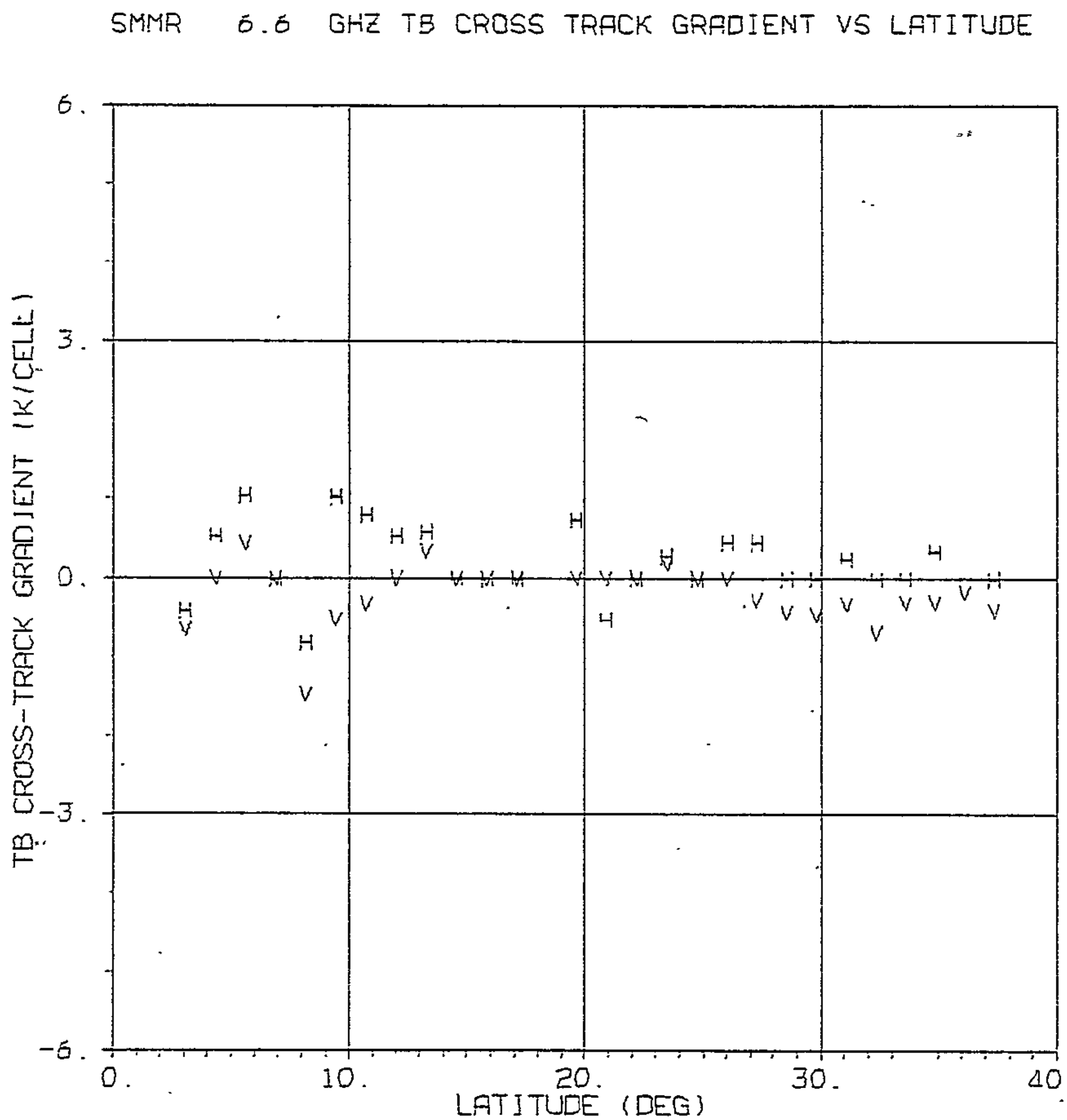

Figure 5.5. Orbit 331, Box Mode

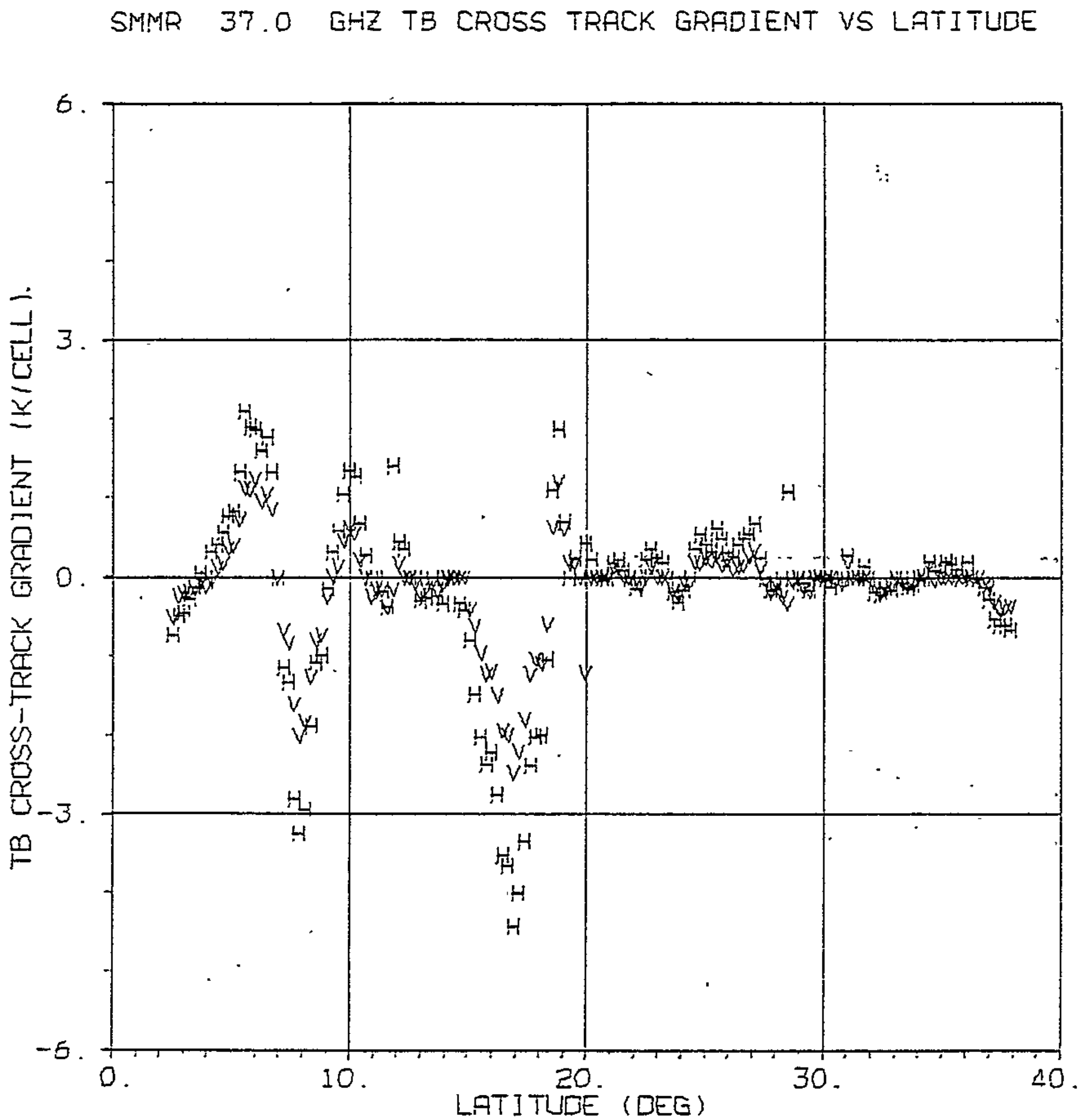

Figure 5.4. Orbit 331, Box Mode

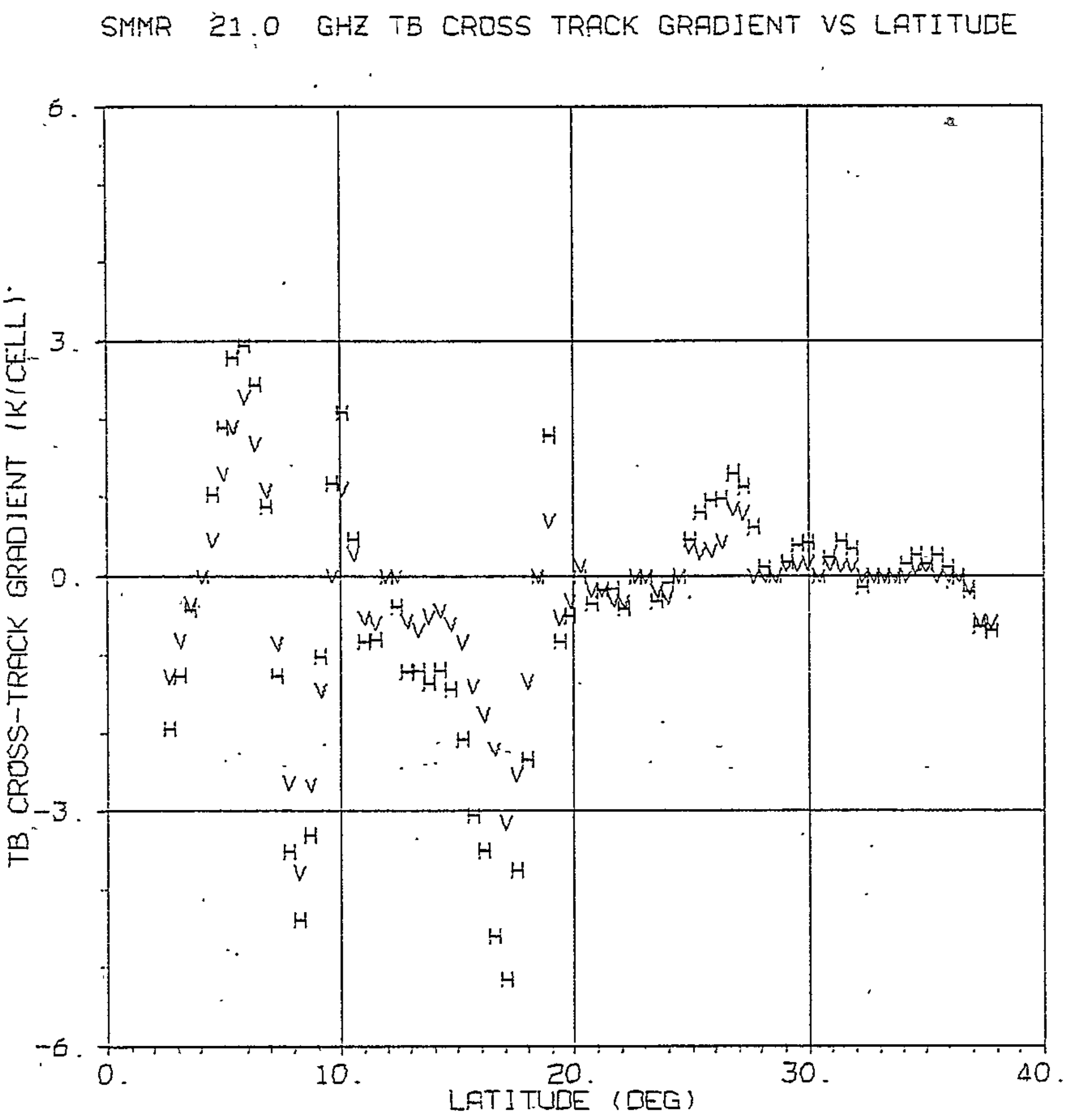

Figure 5.3. Orbit 331, Box Mode

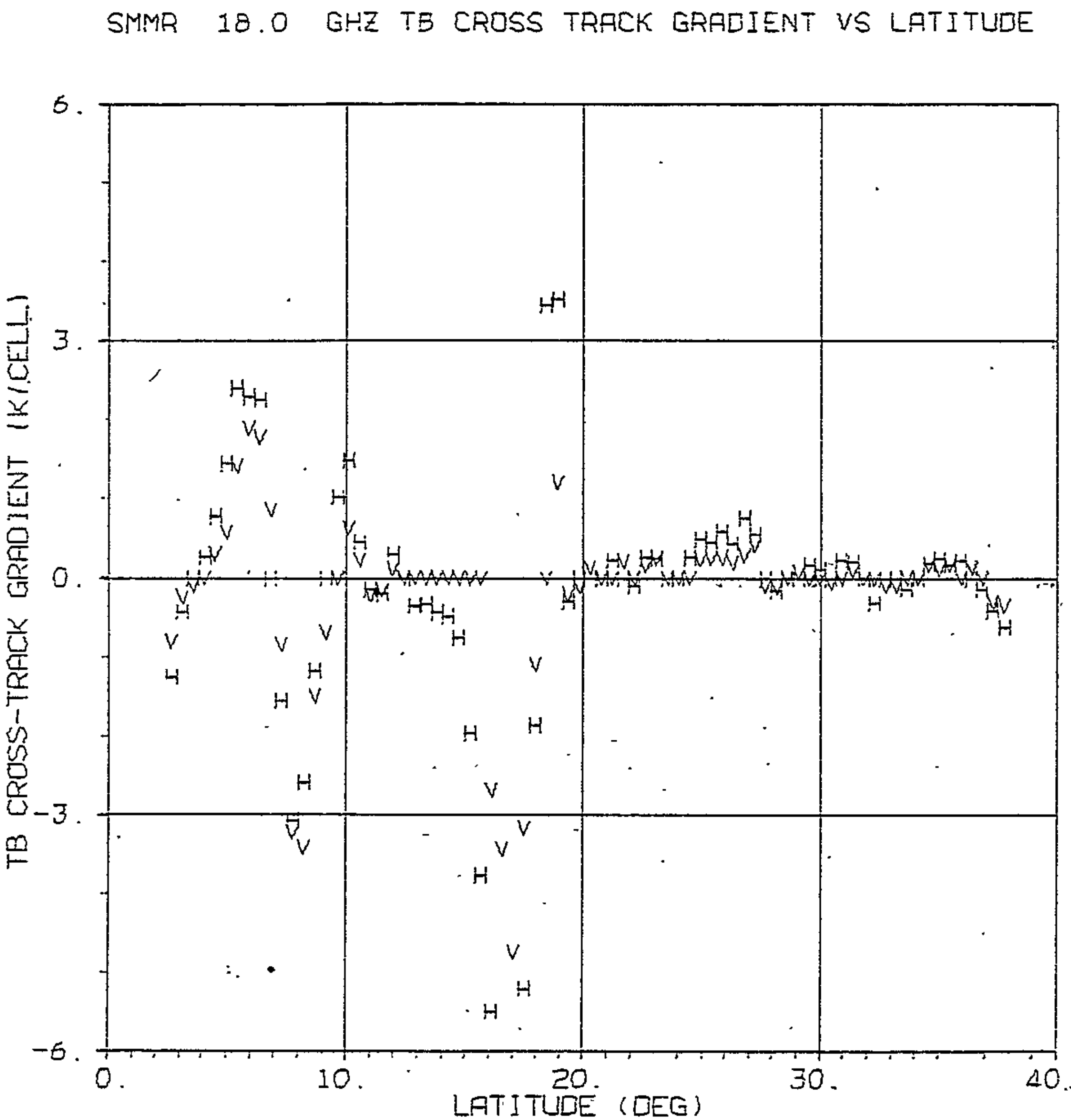

Figure 5.2. Orbit 331, Box Mode

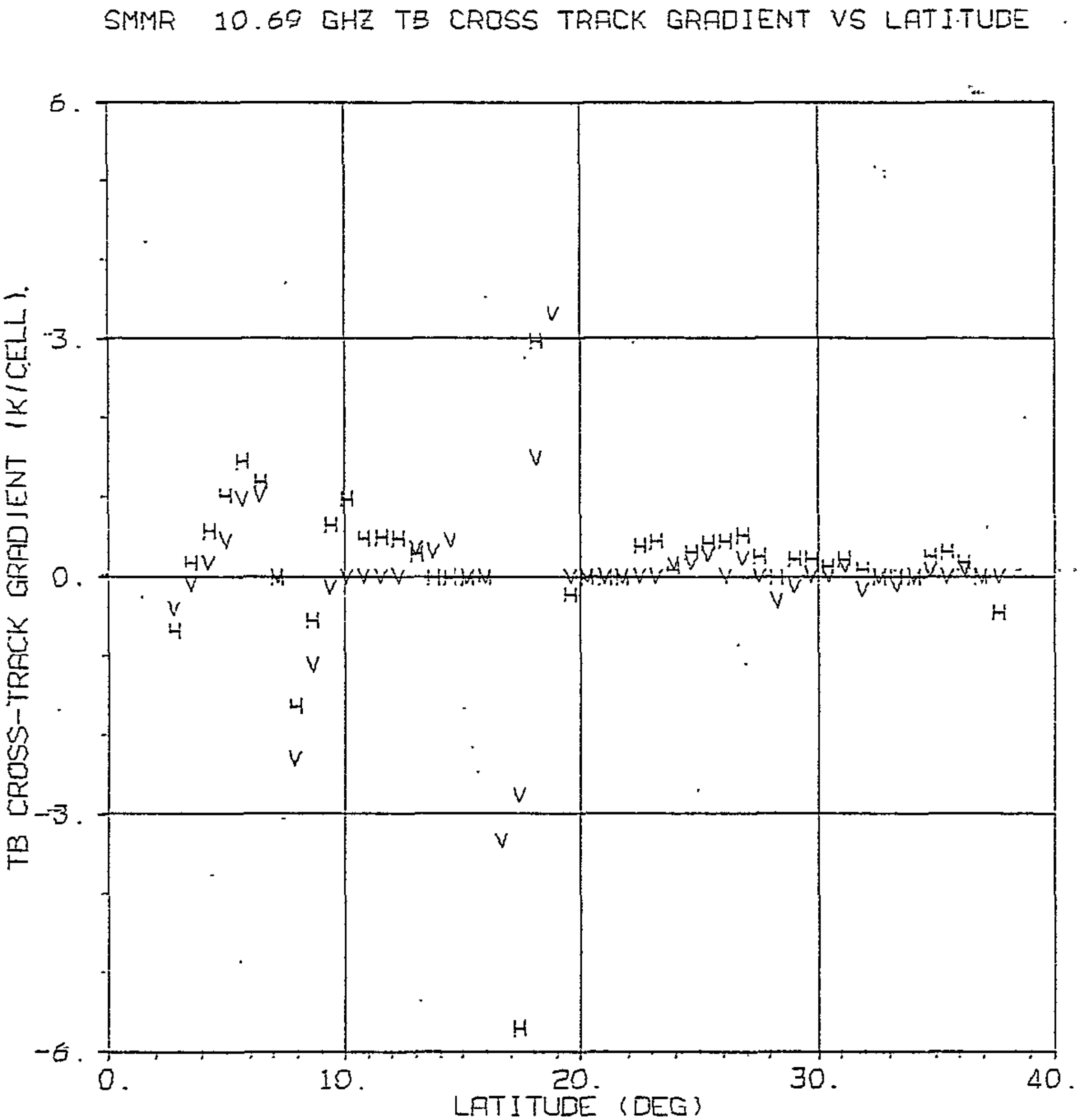

Figure 5.1. Orbit 331, Box Mode

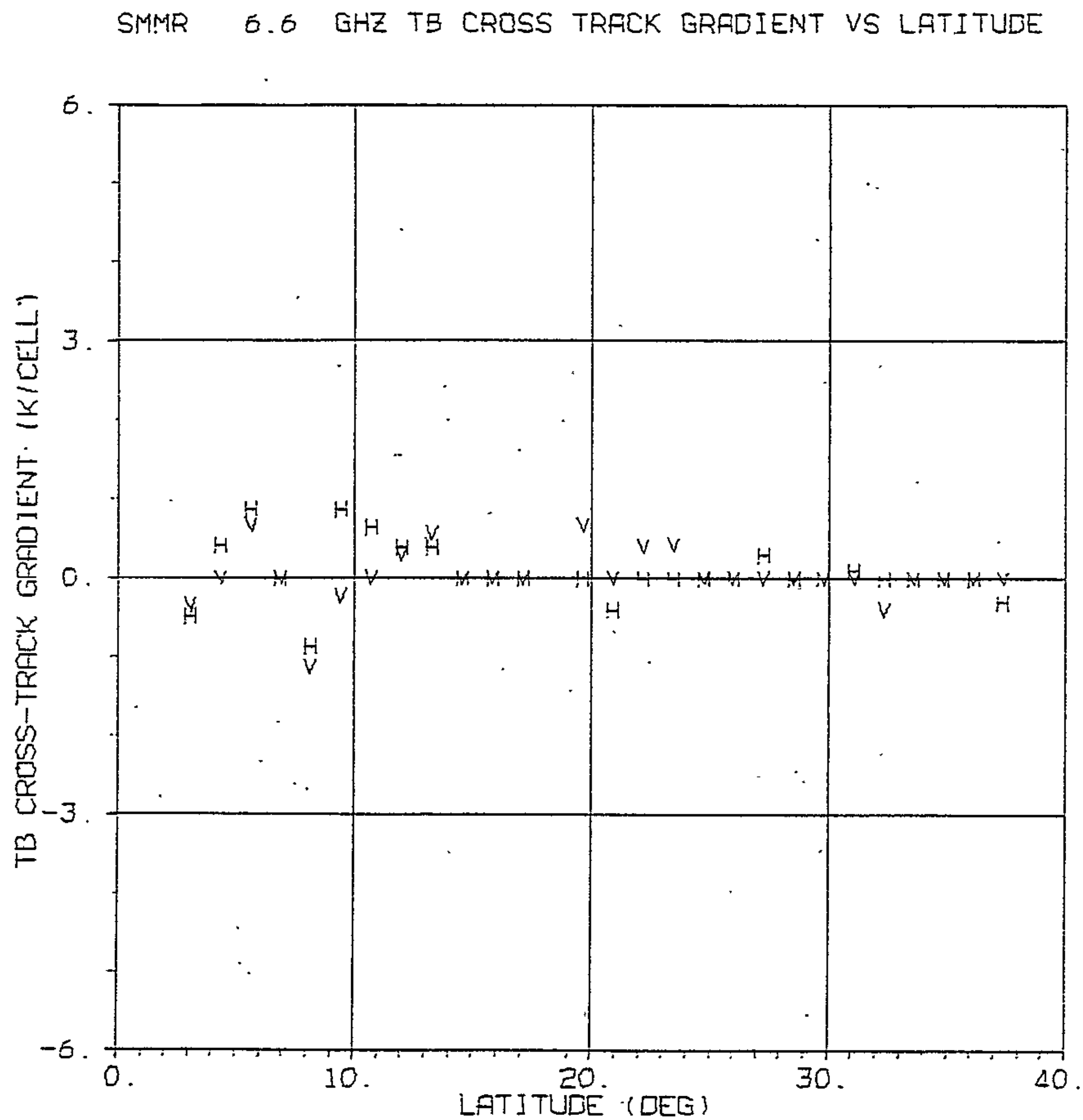

Figure 4.5. Orbit 331, Interim Mode

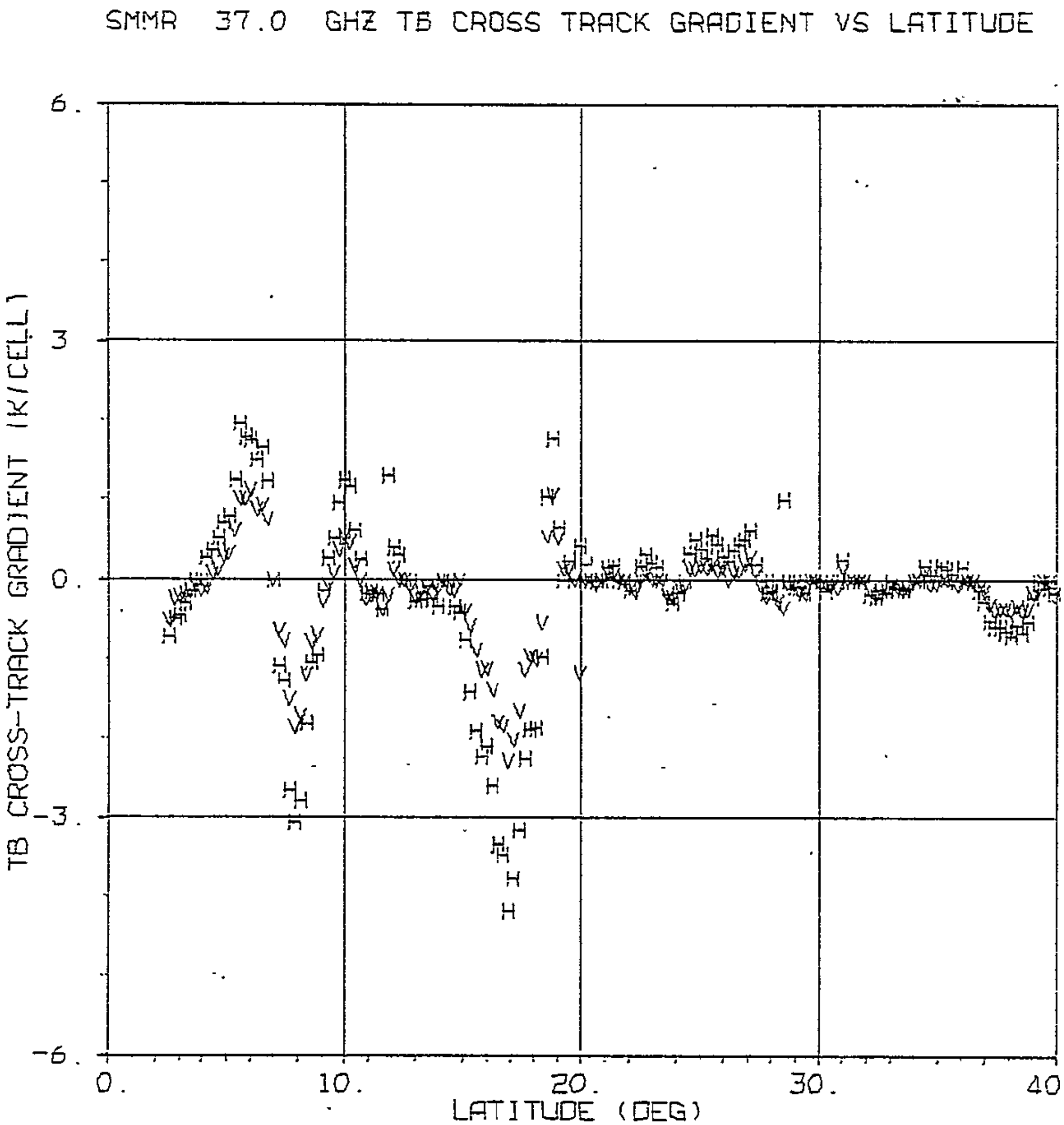

Figure 4.4. Orbit 331, Interim Mode

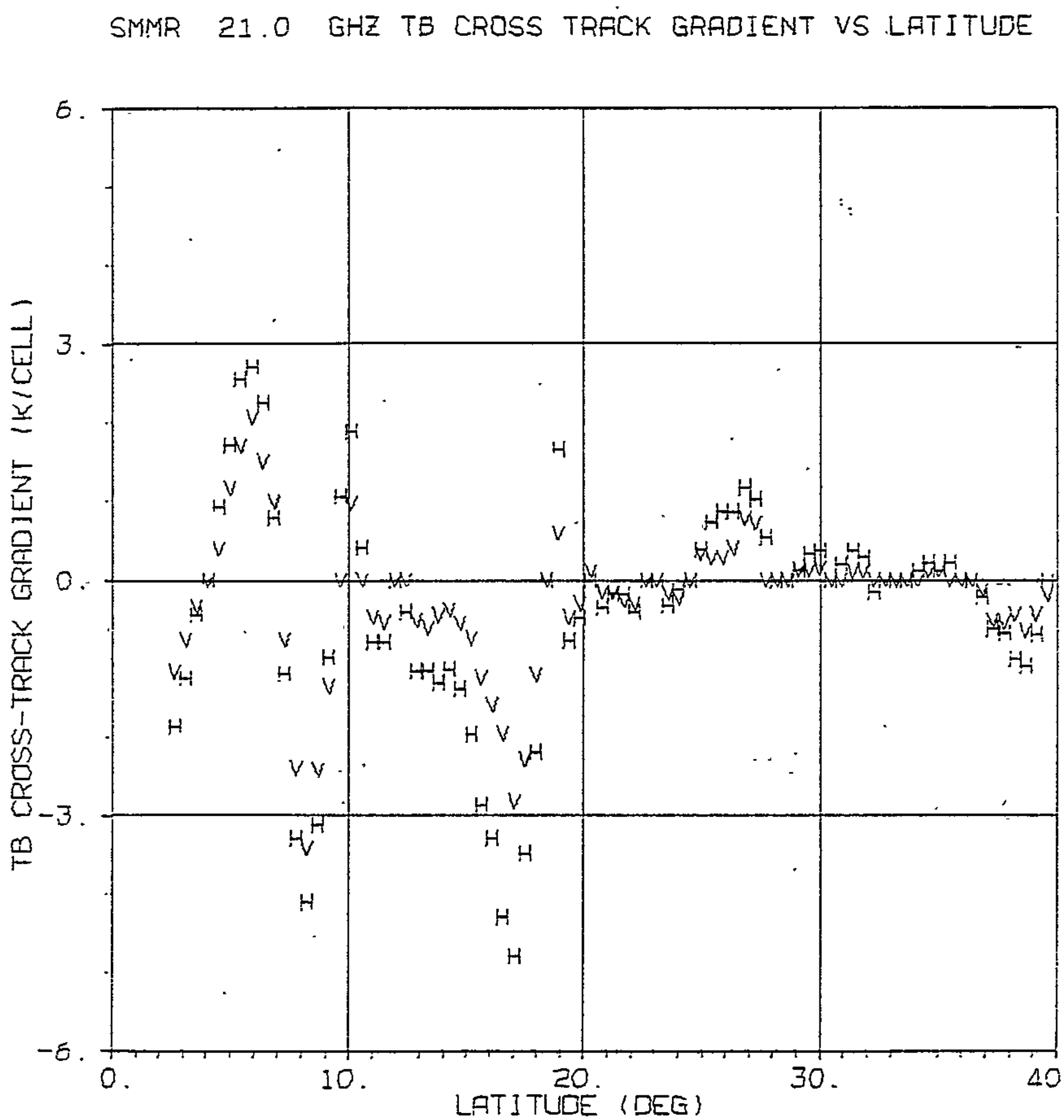

Figure 4.3. Orbit 331, Interim Mode

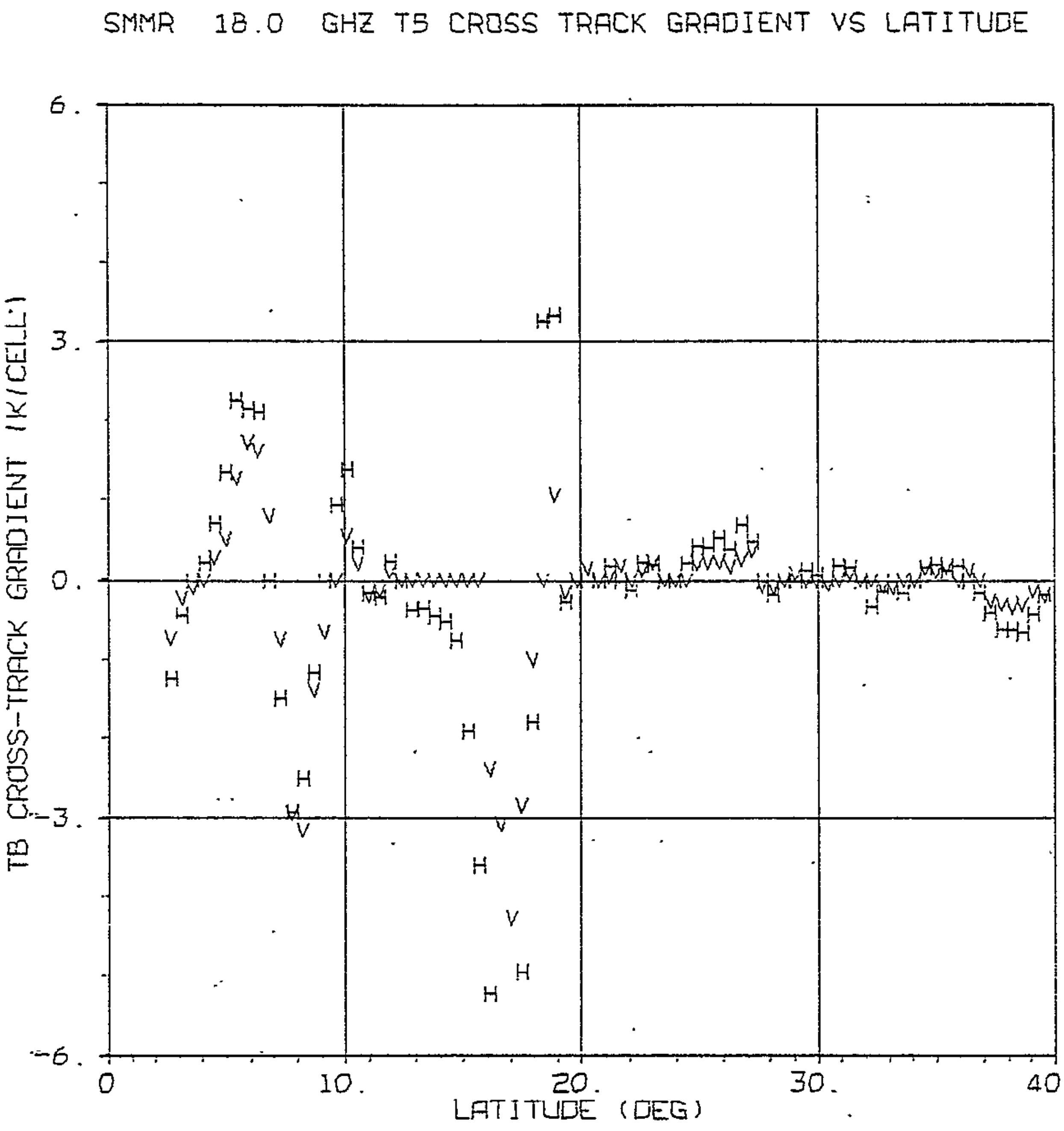

Figure 4.2. Orbit 331, Interim Mode

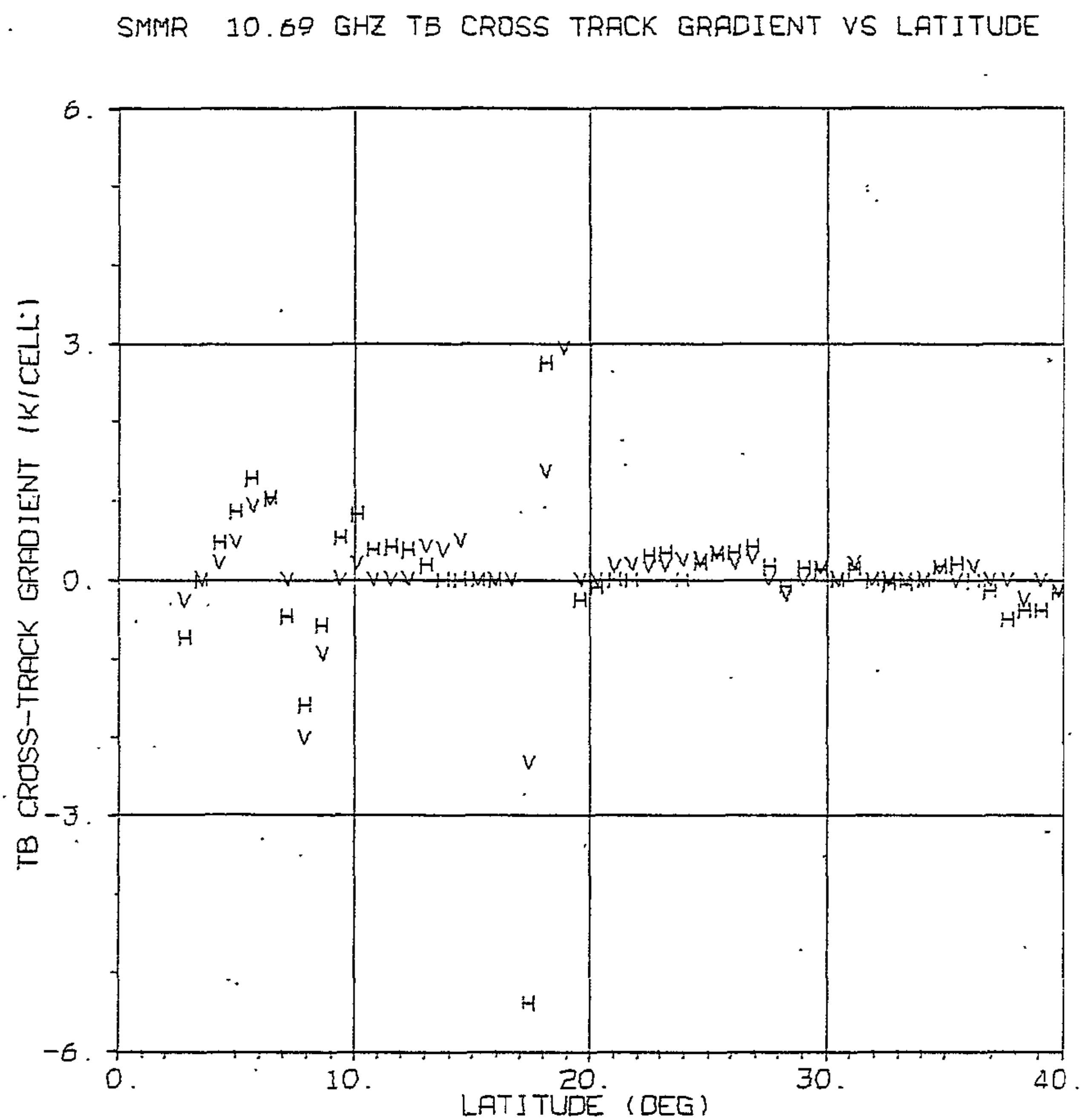

Figure 4.1. Orbit 331, Interim Mode

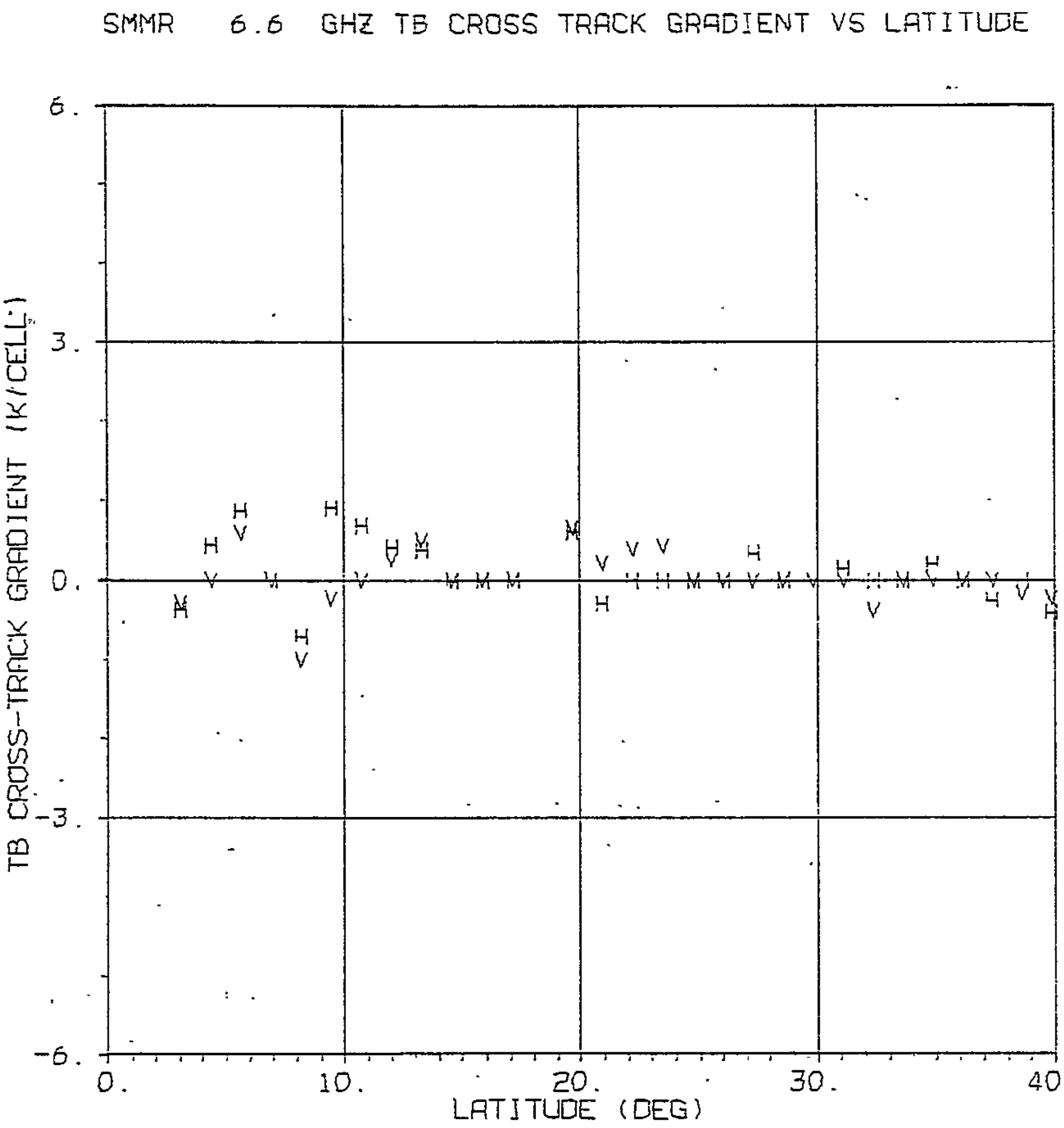

Figure 3.10. Orbit 331, Nominal and Interim

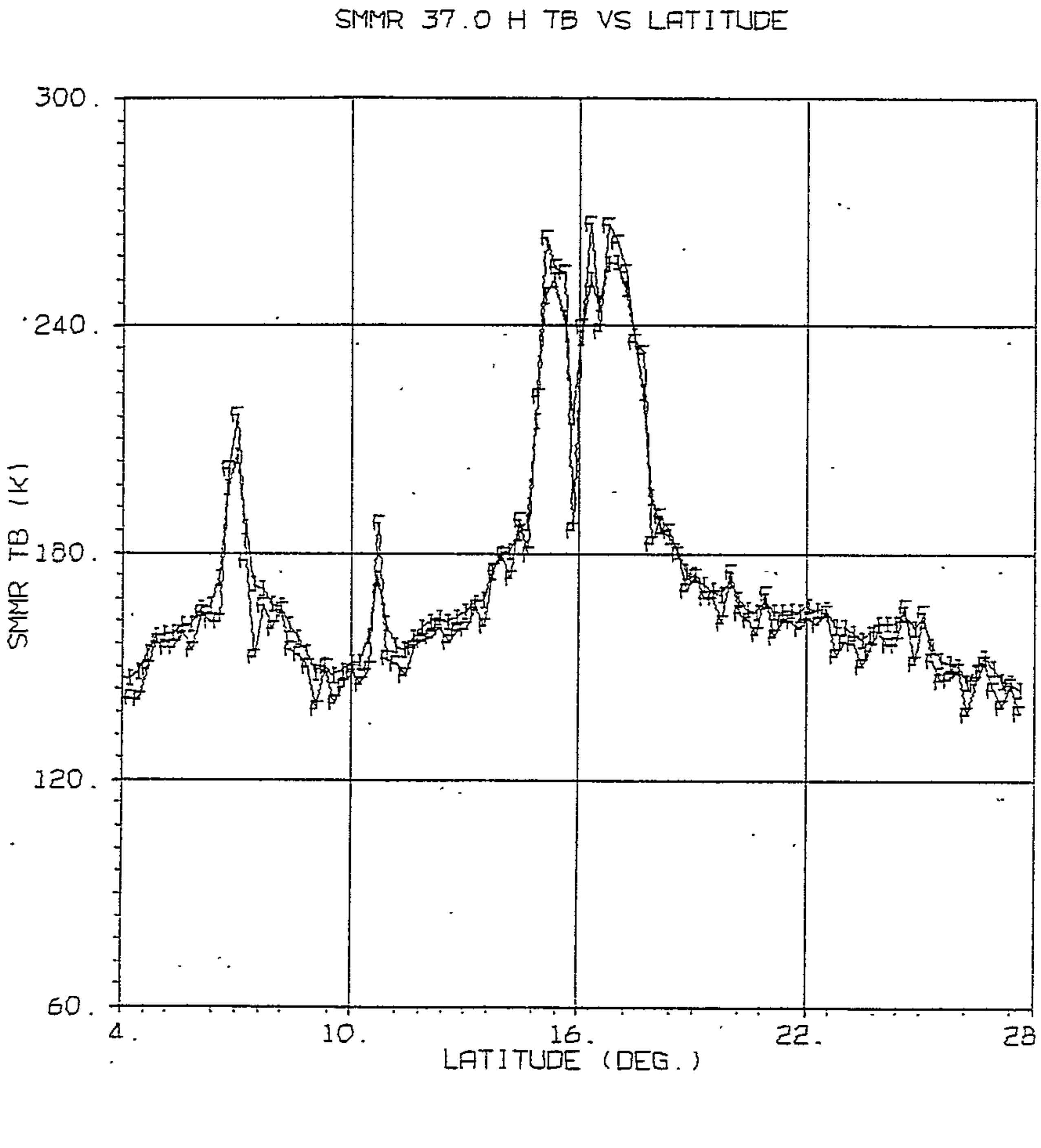

Figure 3.9. Orbit 331, Nominal and Interim

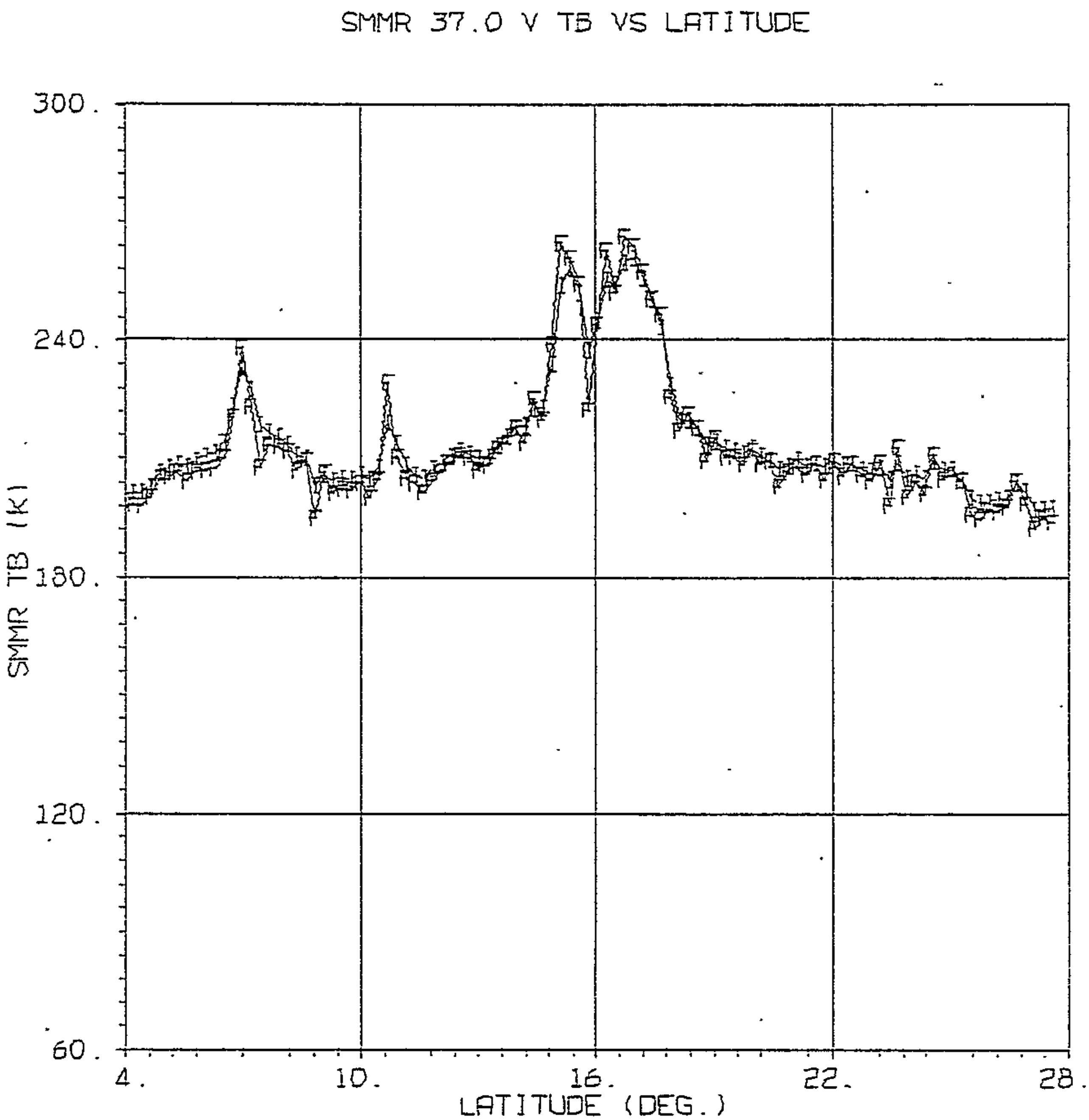

Figure 3.8. Orbit 331, Nominal and Interim

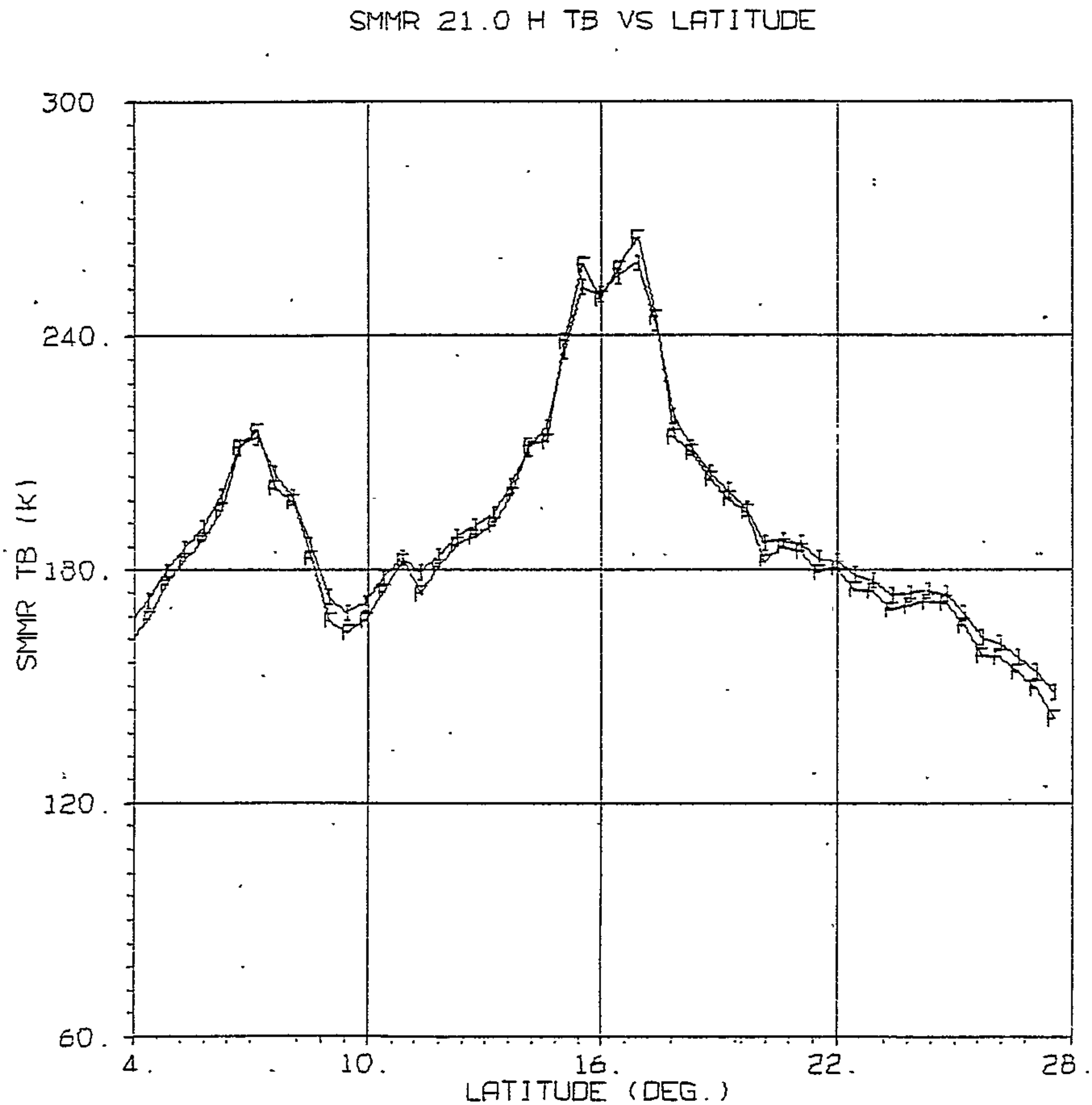

Figure 3.7. Orbit 331, Nominal and Interim

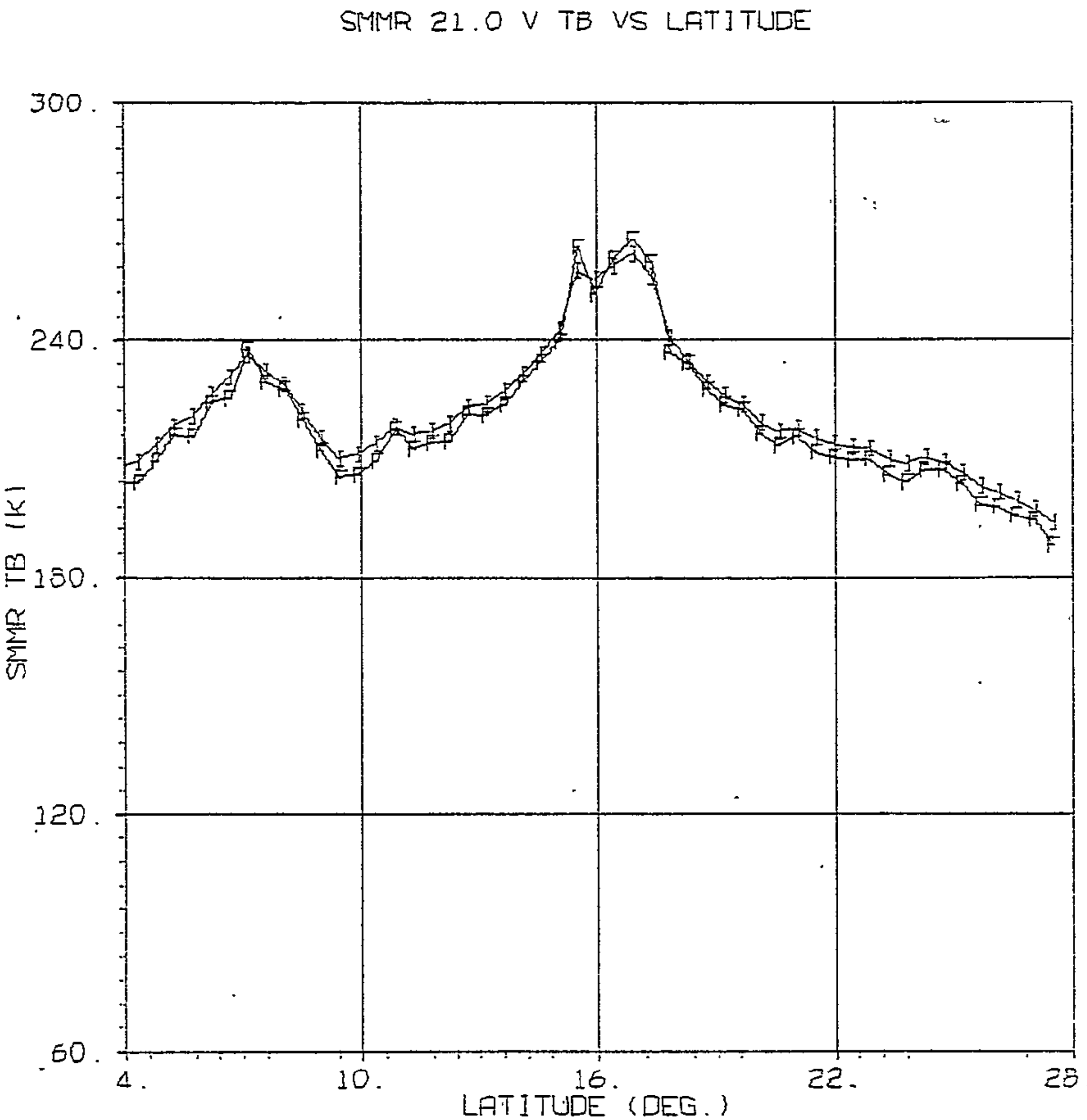

Figure 3.6. Orbit 331, Nominal and Interim

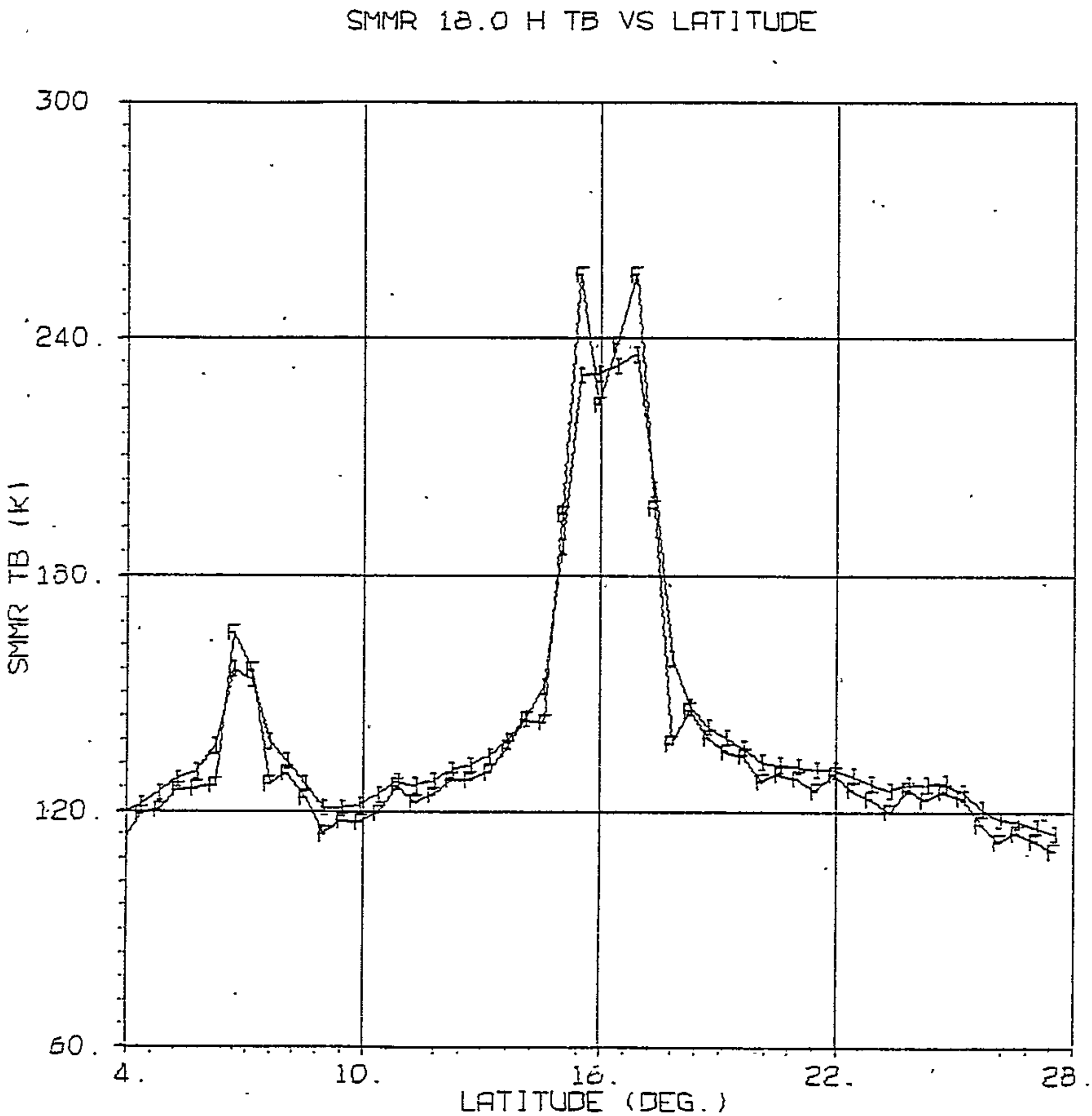

Figure 3.5. Orbit 331, Nominal and Interim

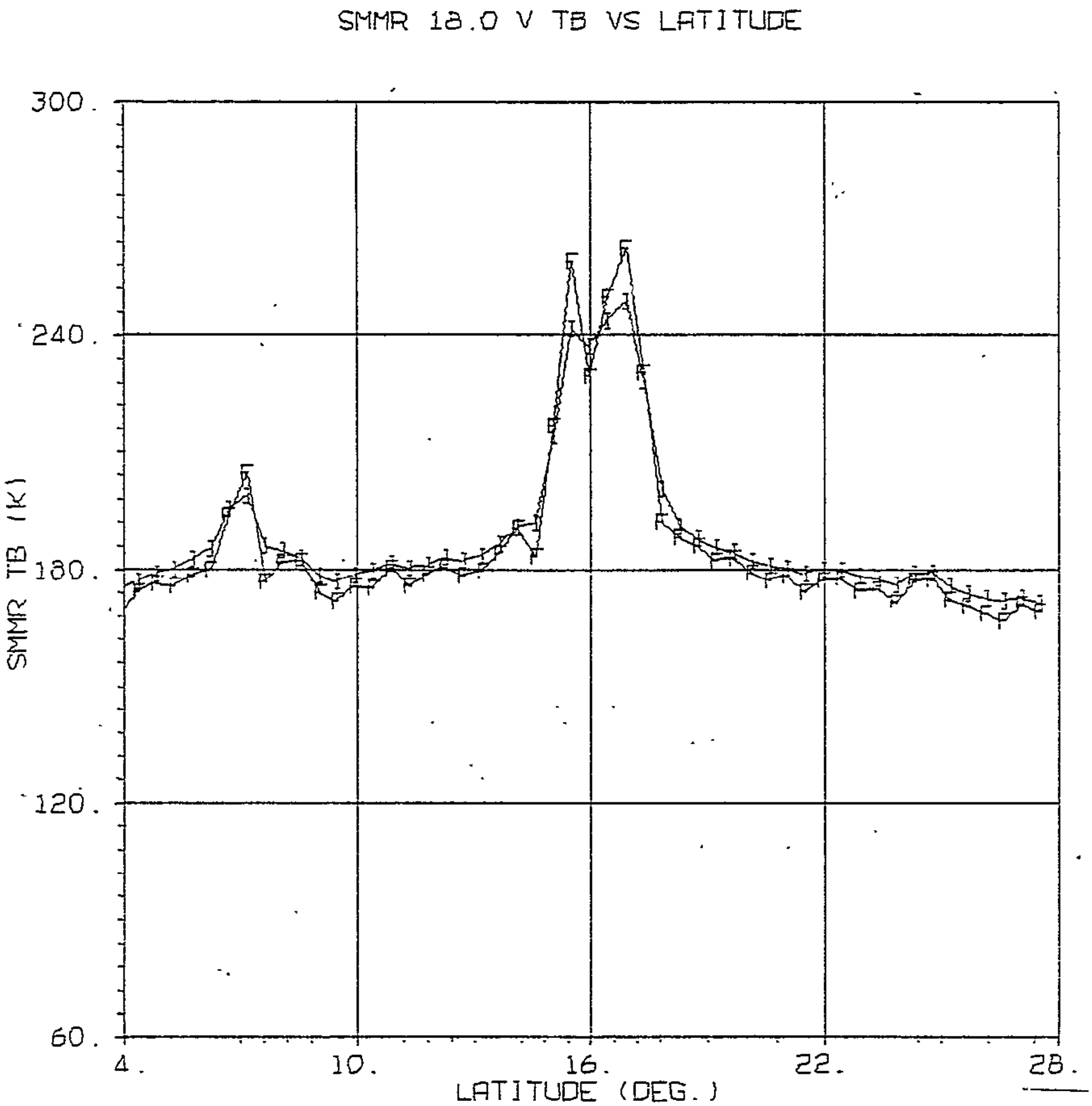

Figure 3.4. Orbit 331, Nominal and Interim

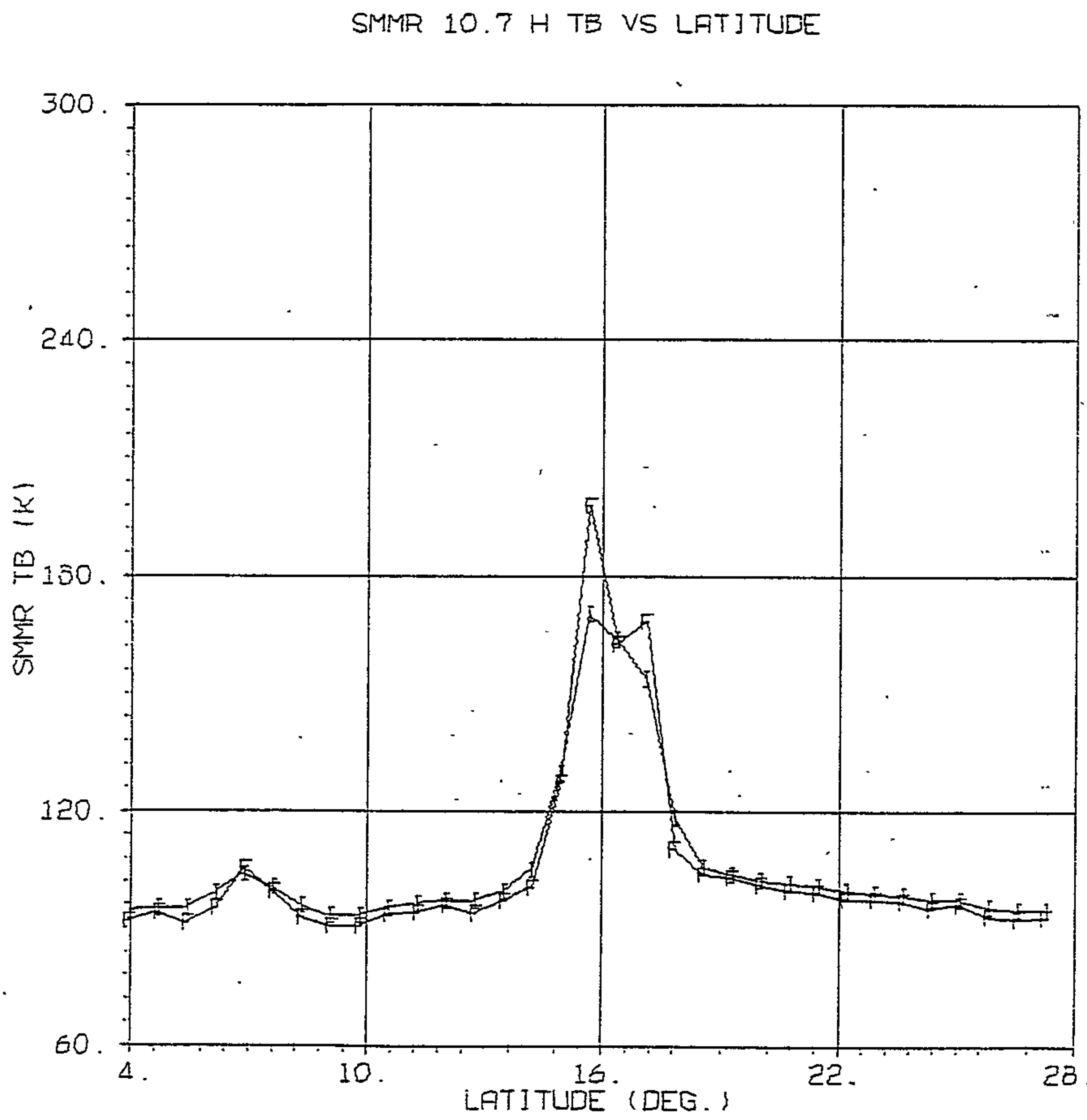

Figure 3.3. Orbit 331, Nominal and Interim

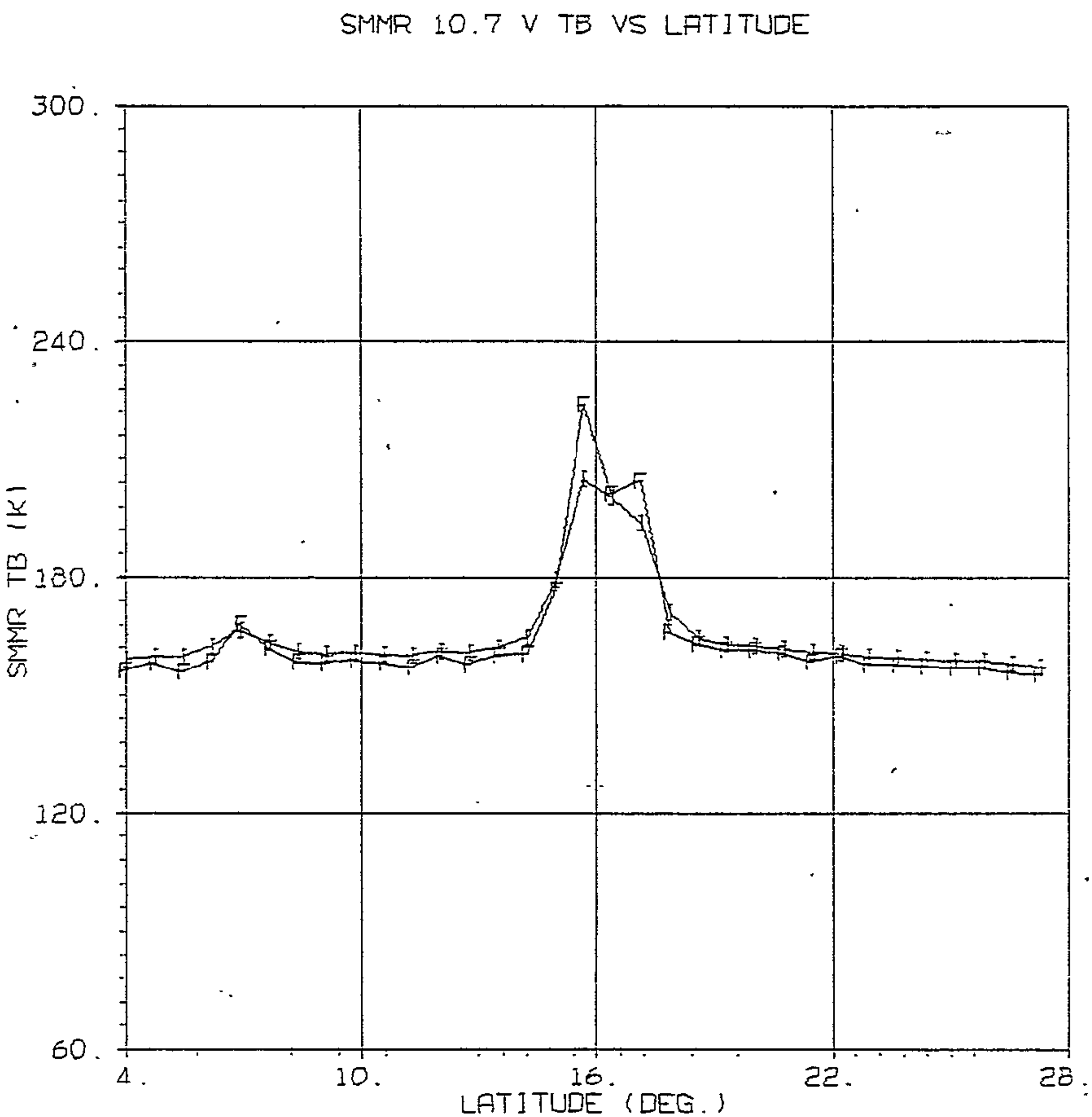

Figure 3.2. Orbit 331, Nominal and Interim

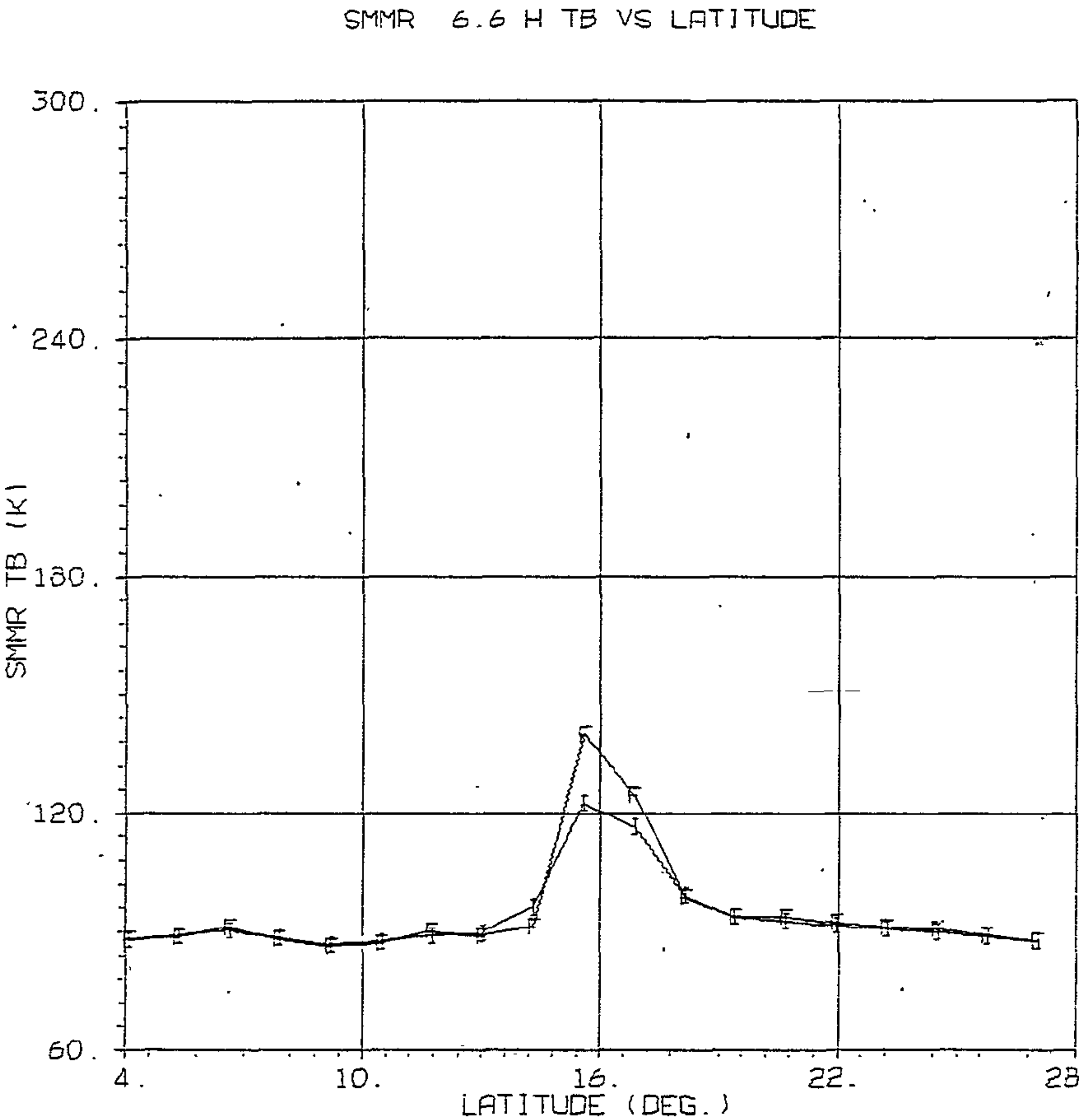

Figure 3.1. Orbit 331, Nominal and Interim

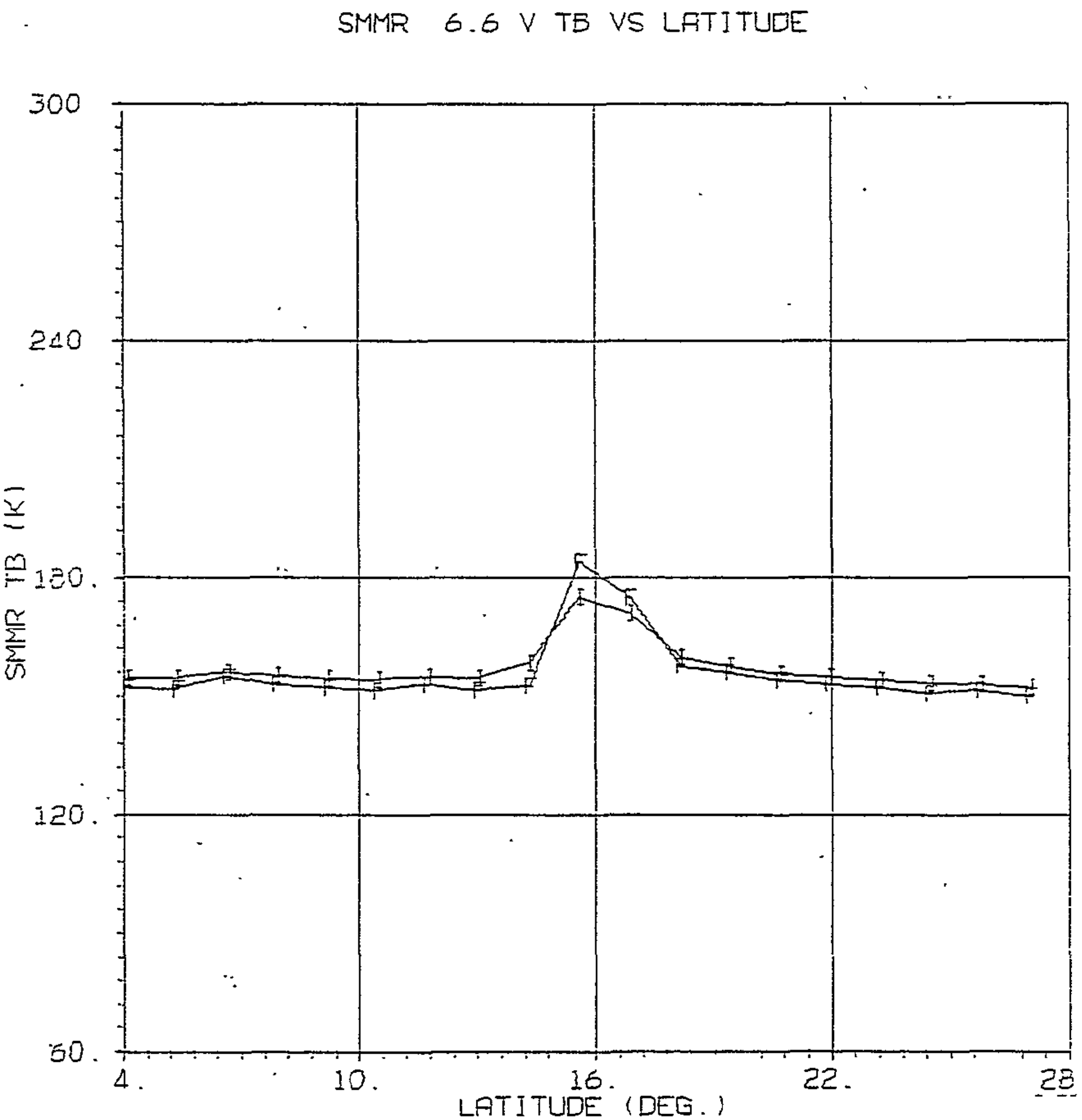

Figure 2.10. Orbit 331, Cross and Interim

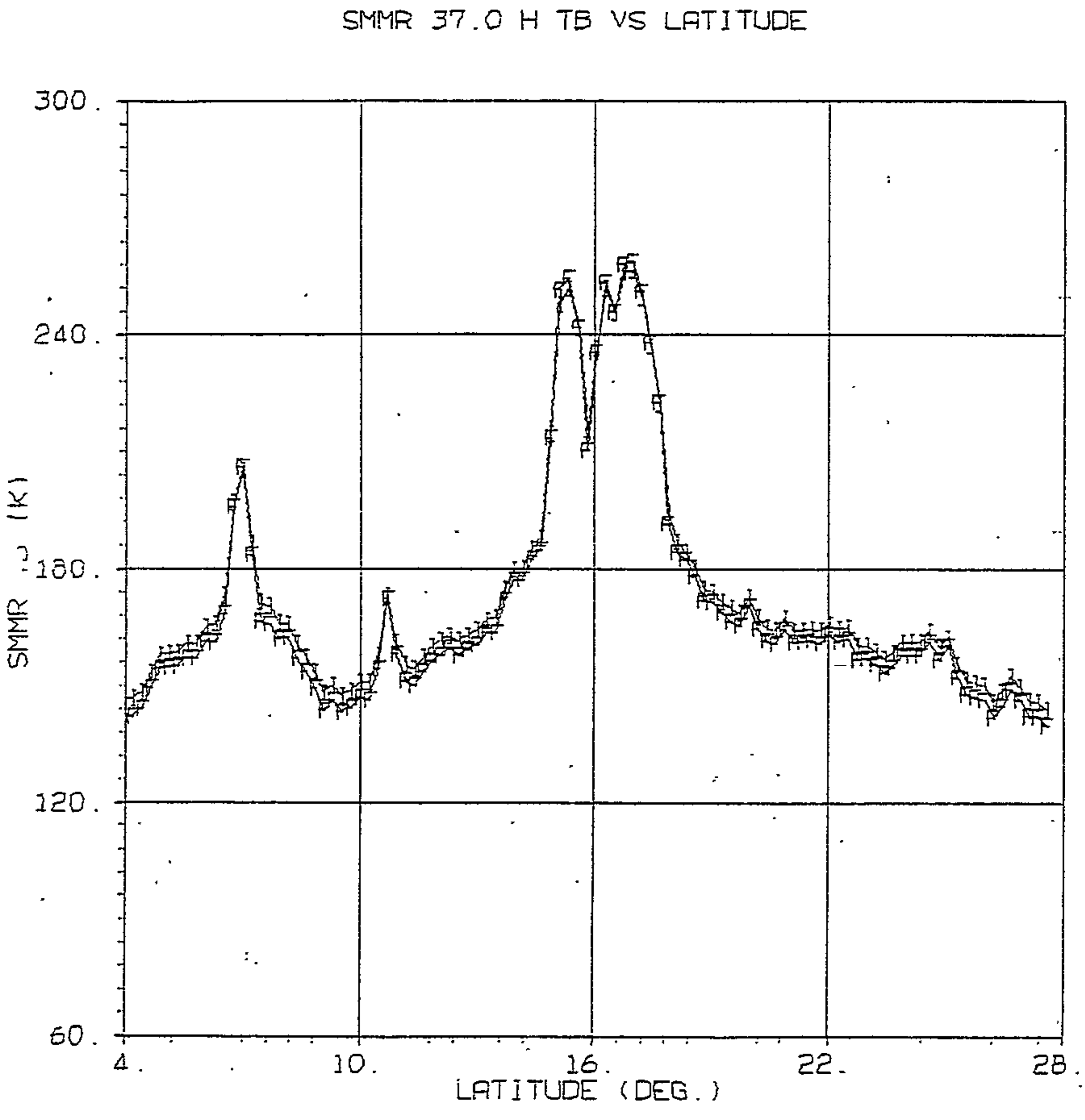

Figure 2.9. Orbit 331, Cross and Interim

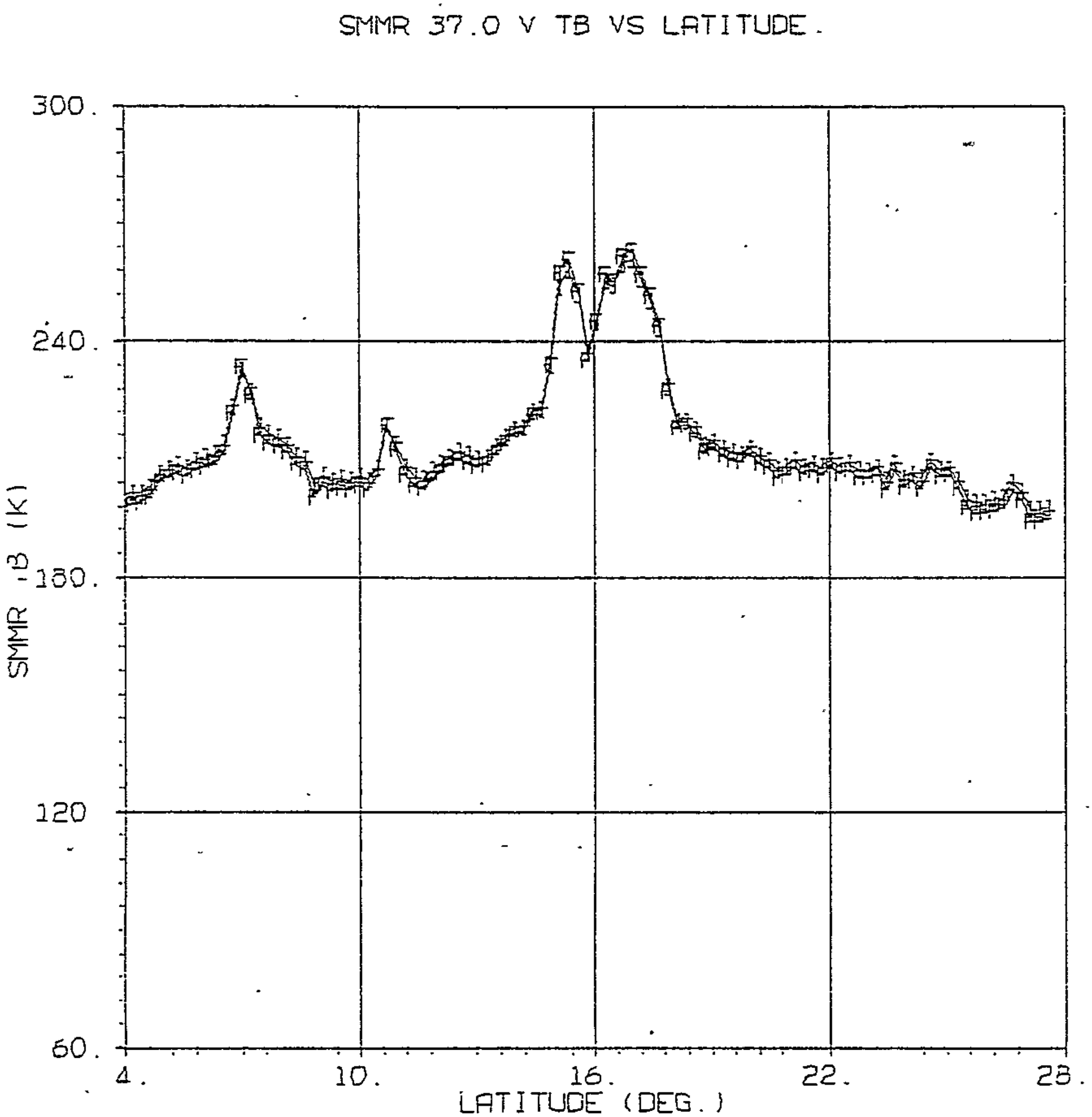

Figure 2.8. Orbit 331, Cross and Interim

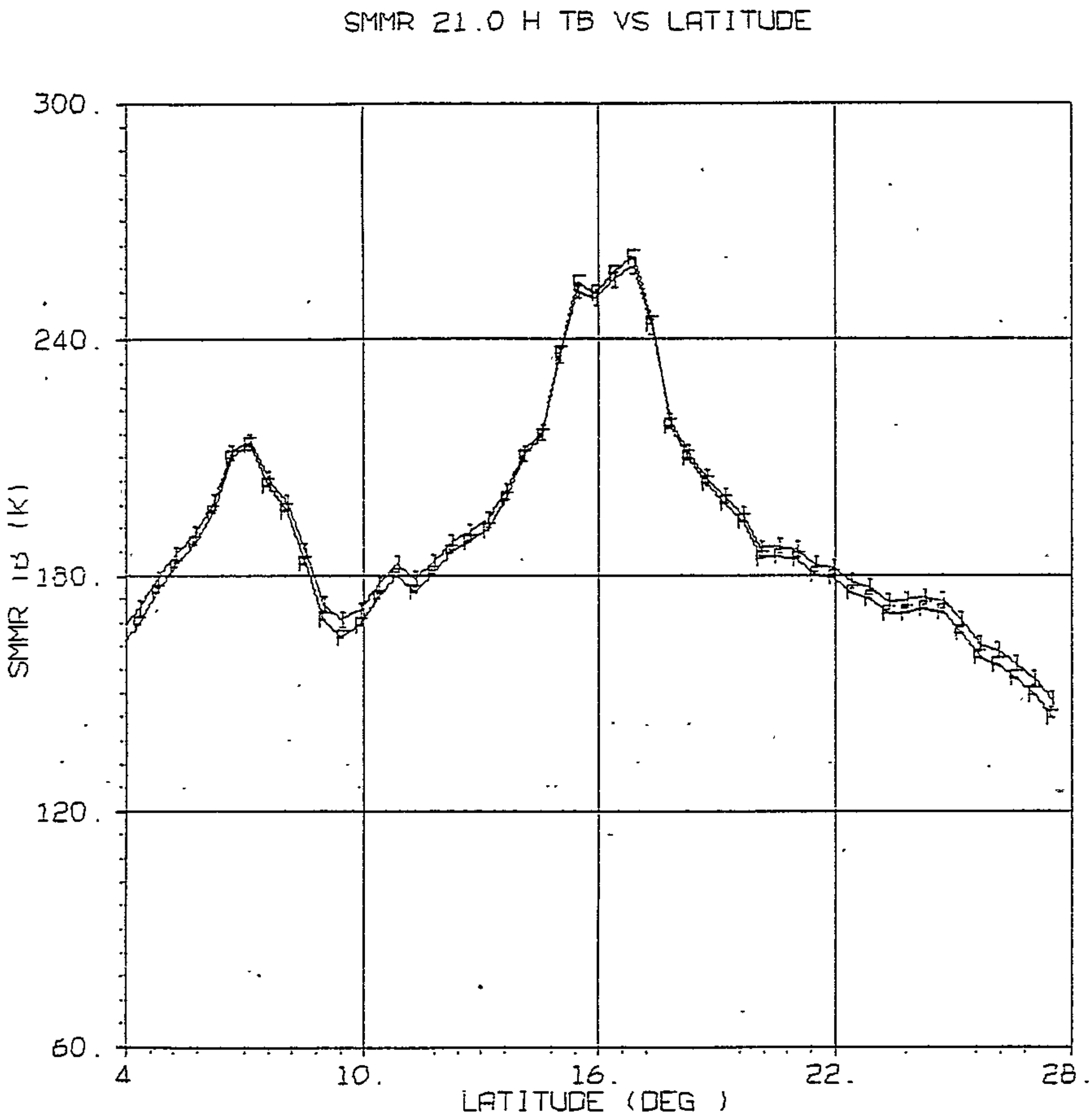

Figure 2.7. Orbit 331, Cross and Interim

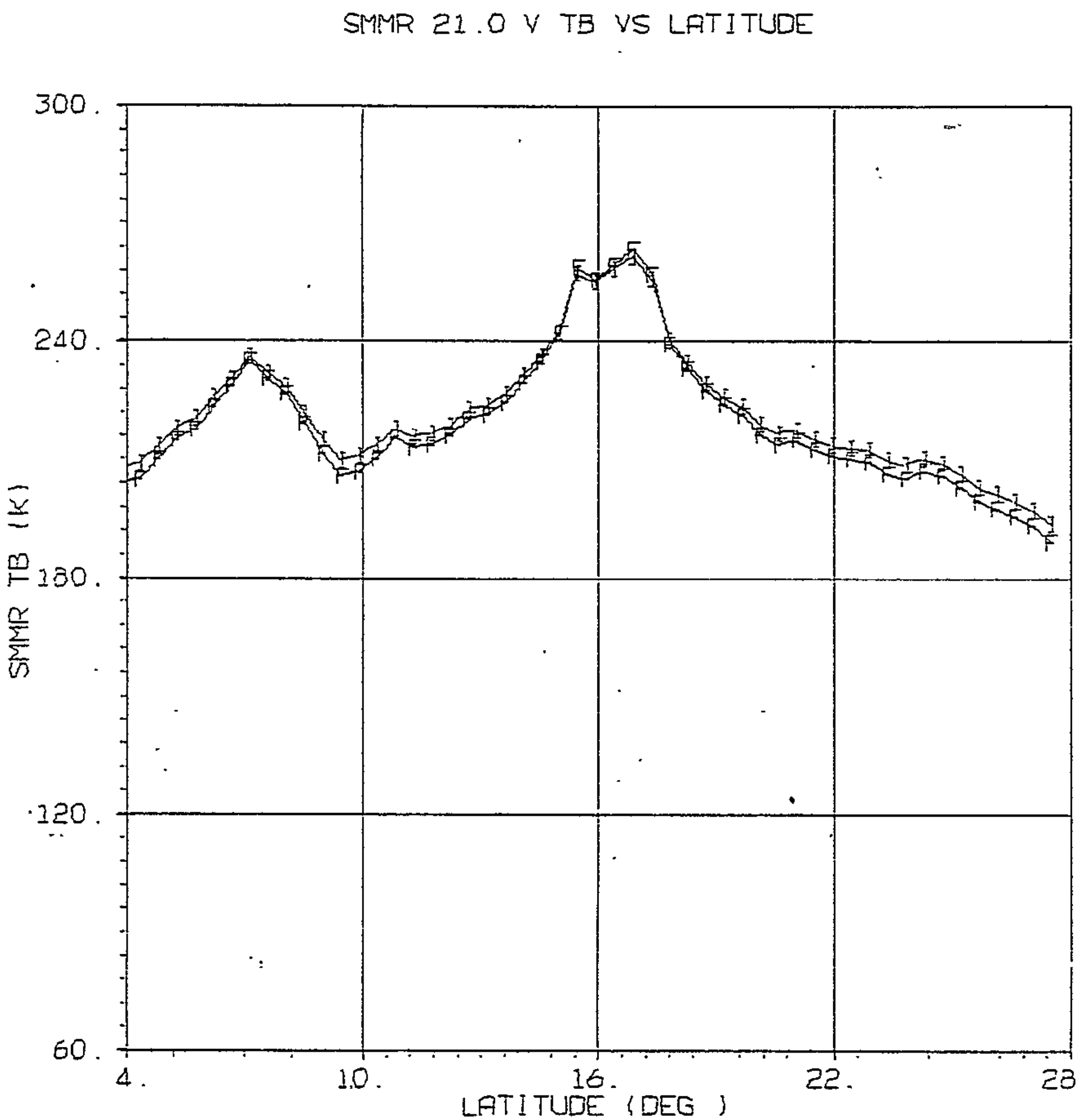

Figure 2.6. Orbit 331, Cross and Interim

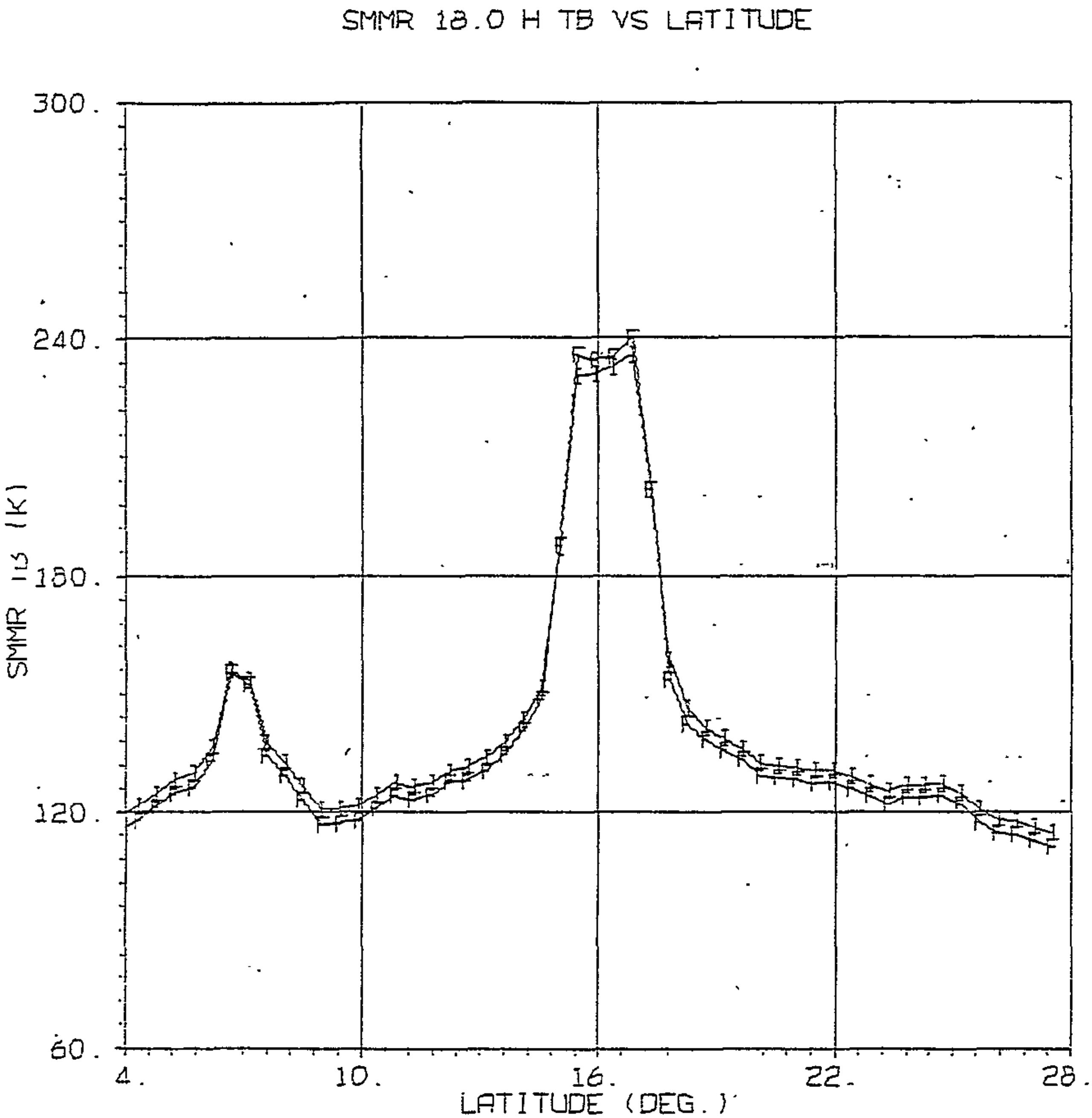

Figure 2.5. Orbit 331, Cross and Interim

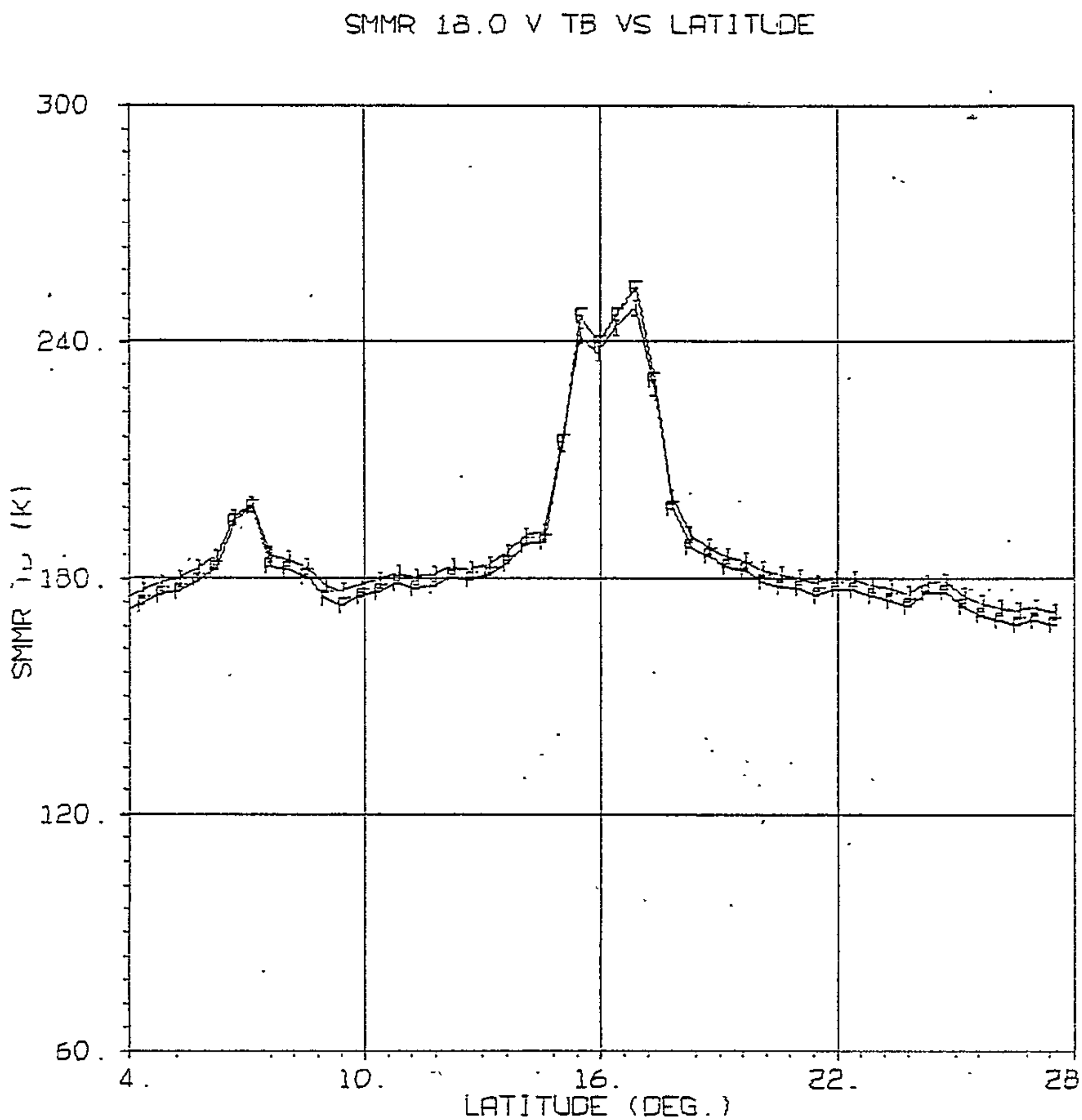

Figure 2.4. Orbit 331, Cross and Interim

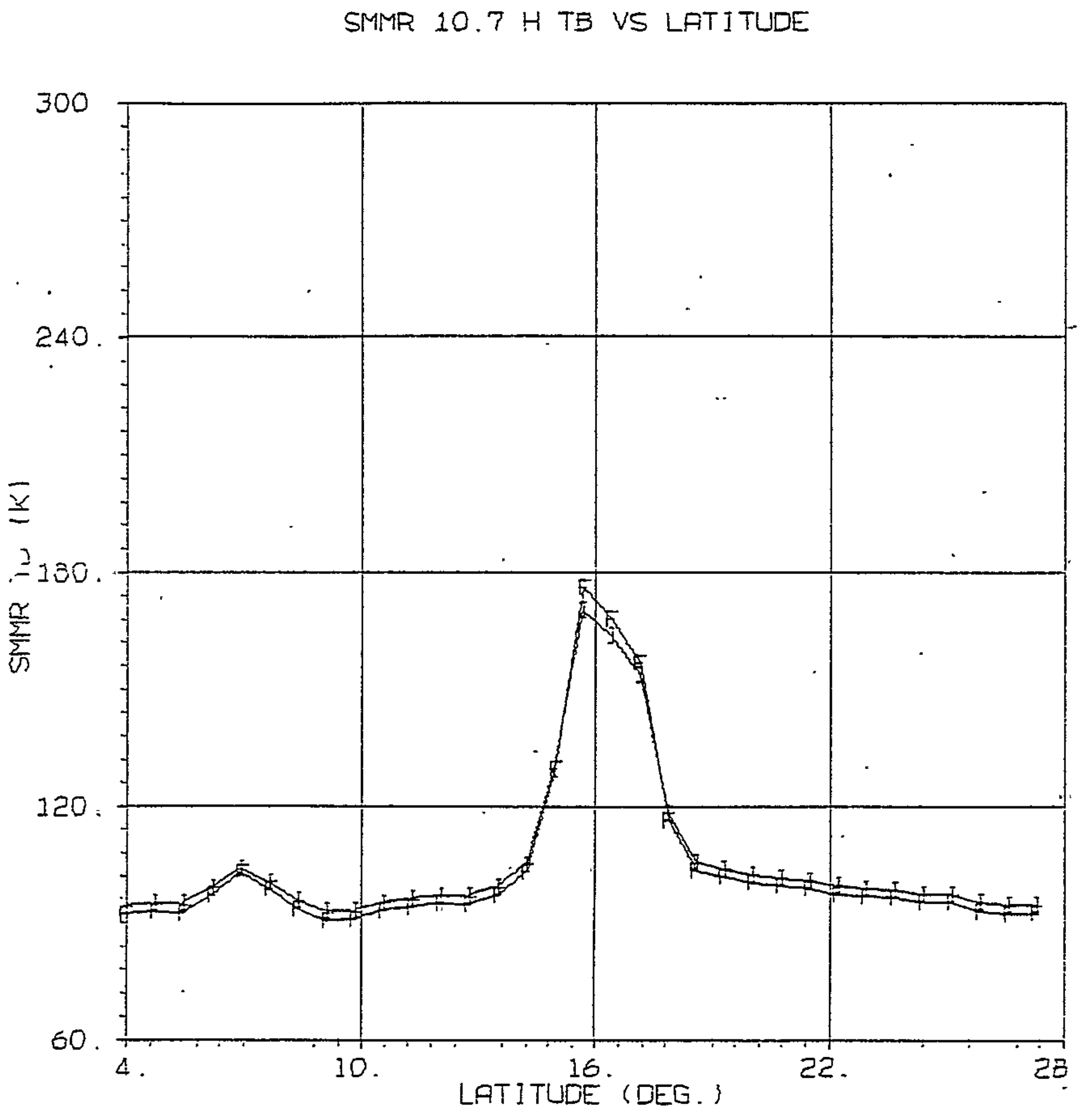

Figure 2.3. Orbit 331, Cross and Interim

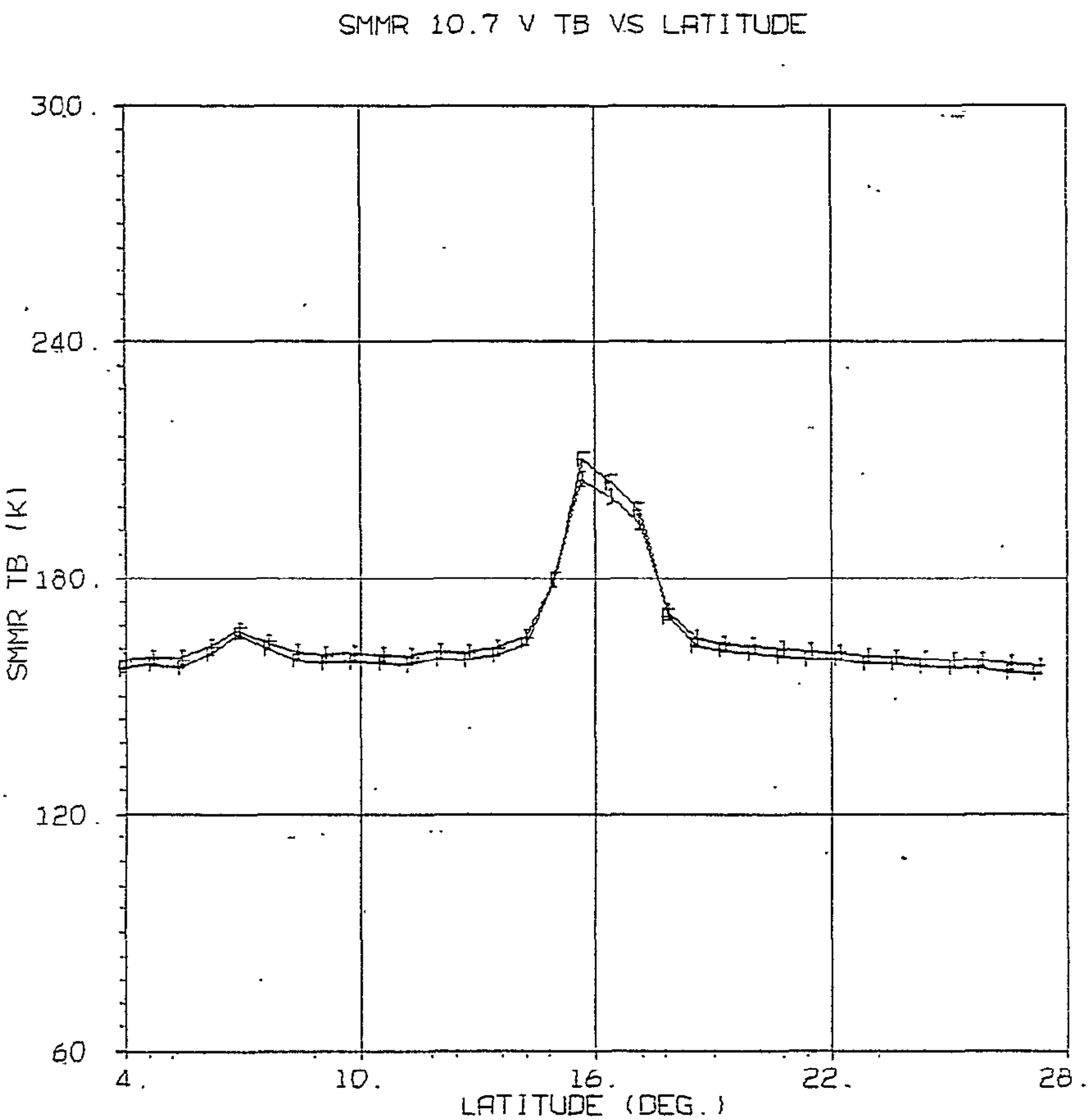

Figure 2.2. Orbit 331, Cross and Interim

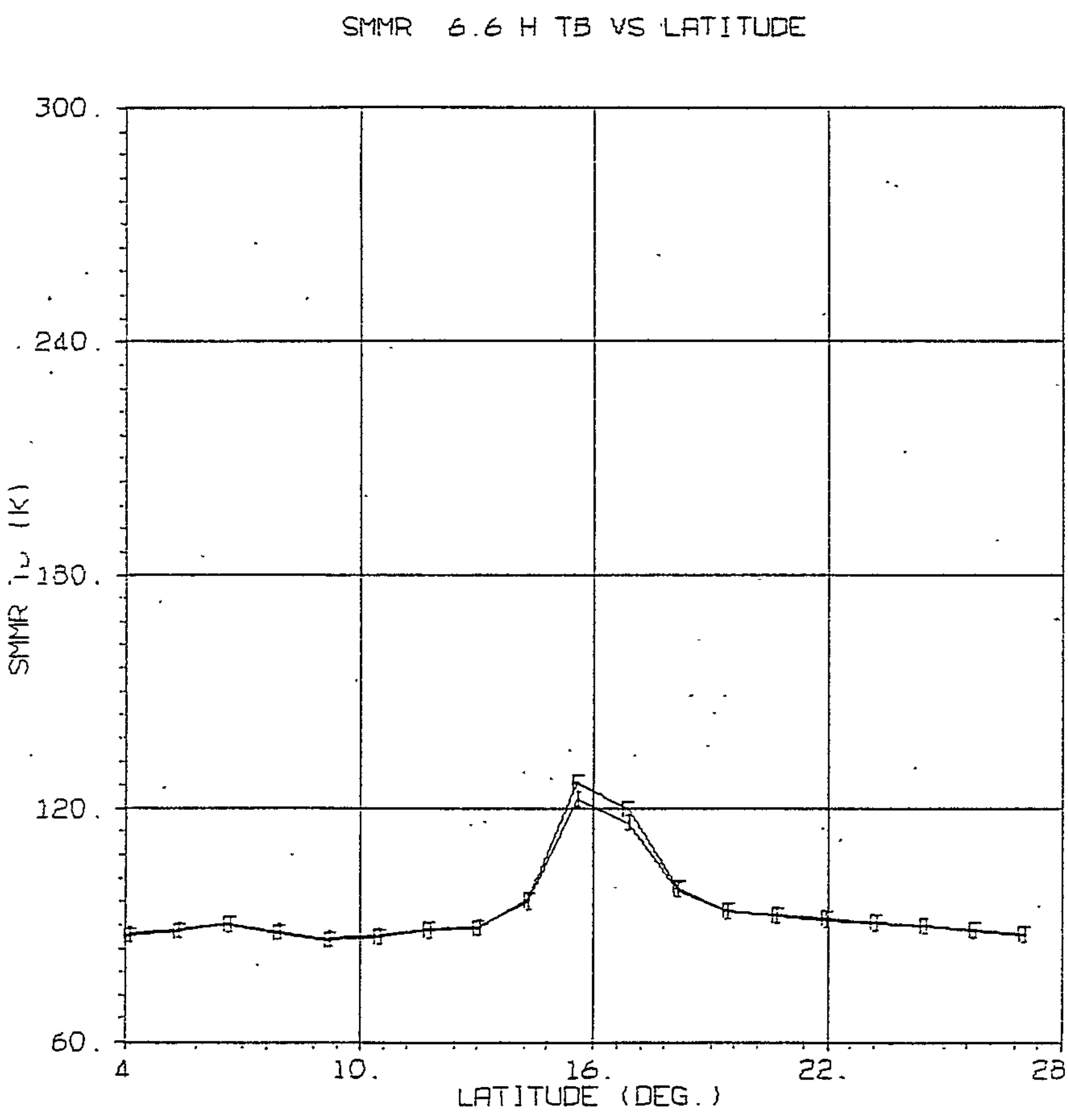

Figure 2.1. Orbit 331, Cross and Interim

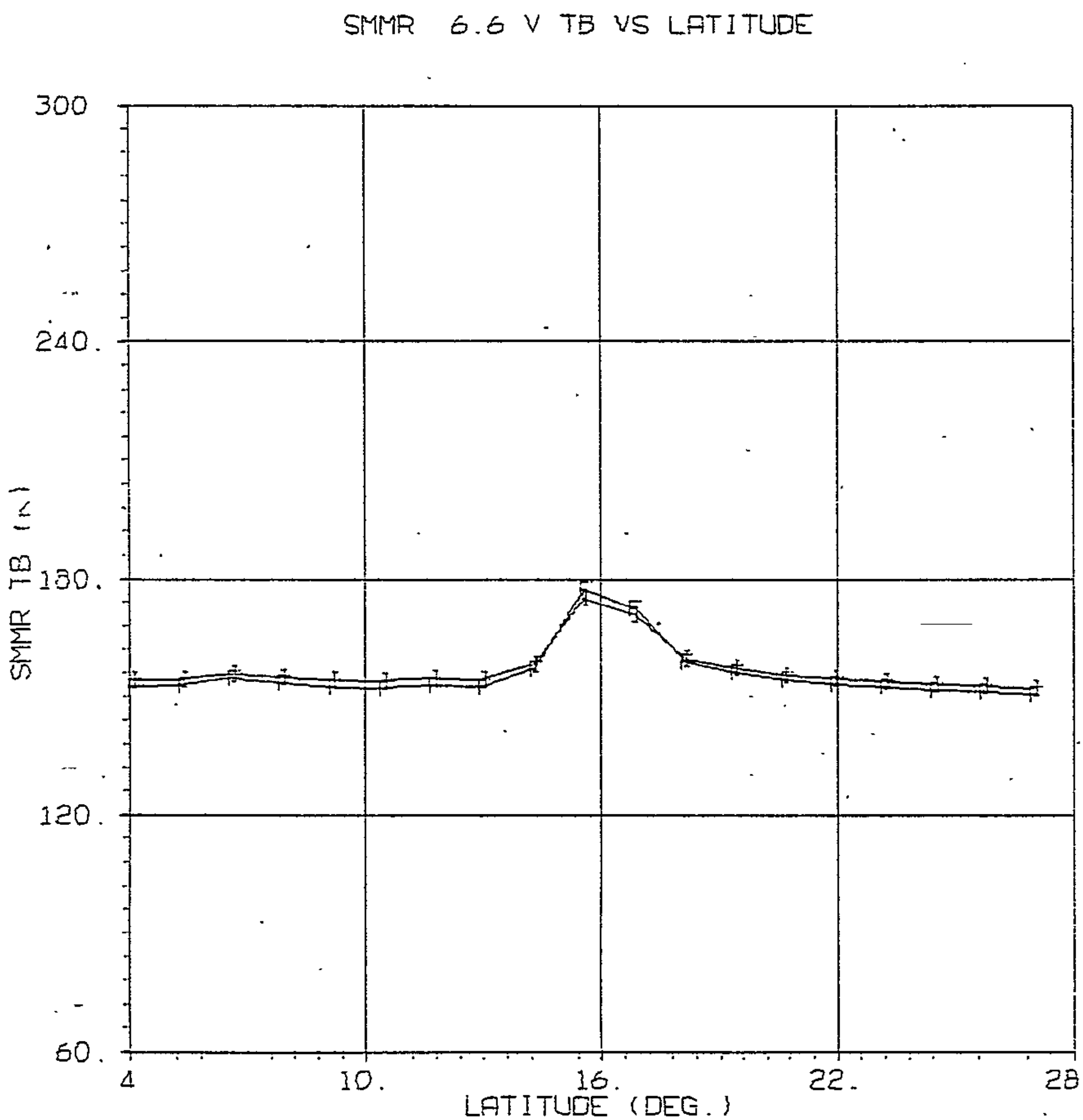

Figure 1.10. Orbit 331, Box and Interim

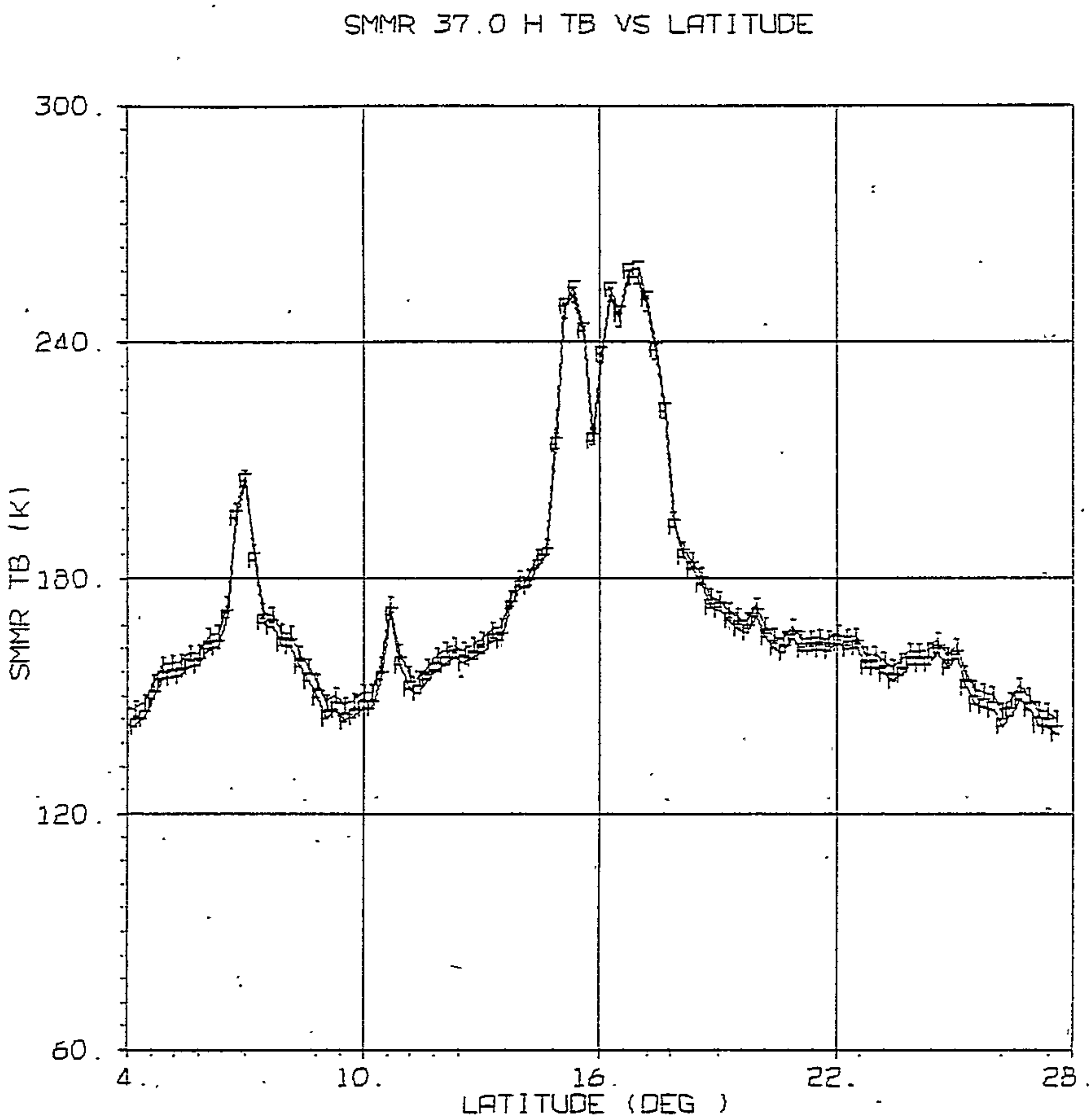

Figure 1.9. Orbit 331, Box and Interim

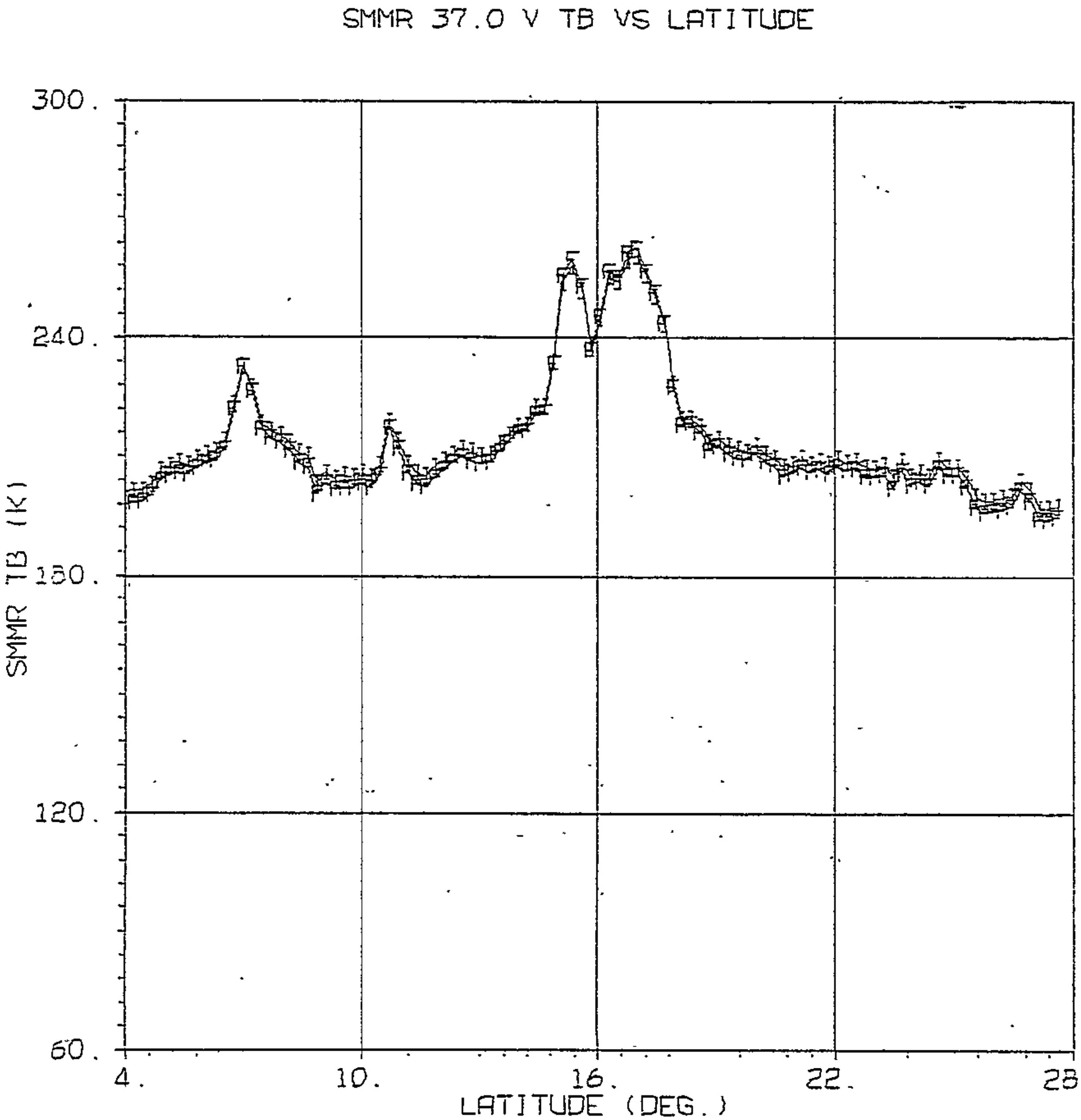

Figure 1.8. Orbit 331, Box and Interim

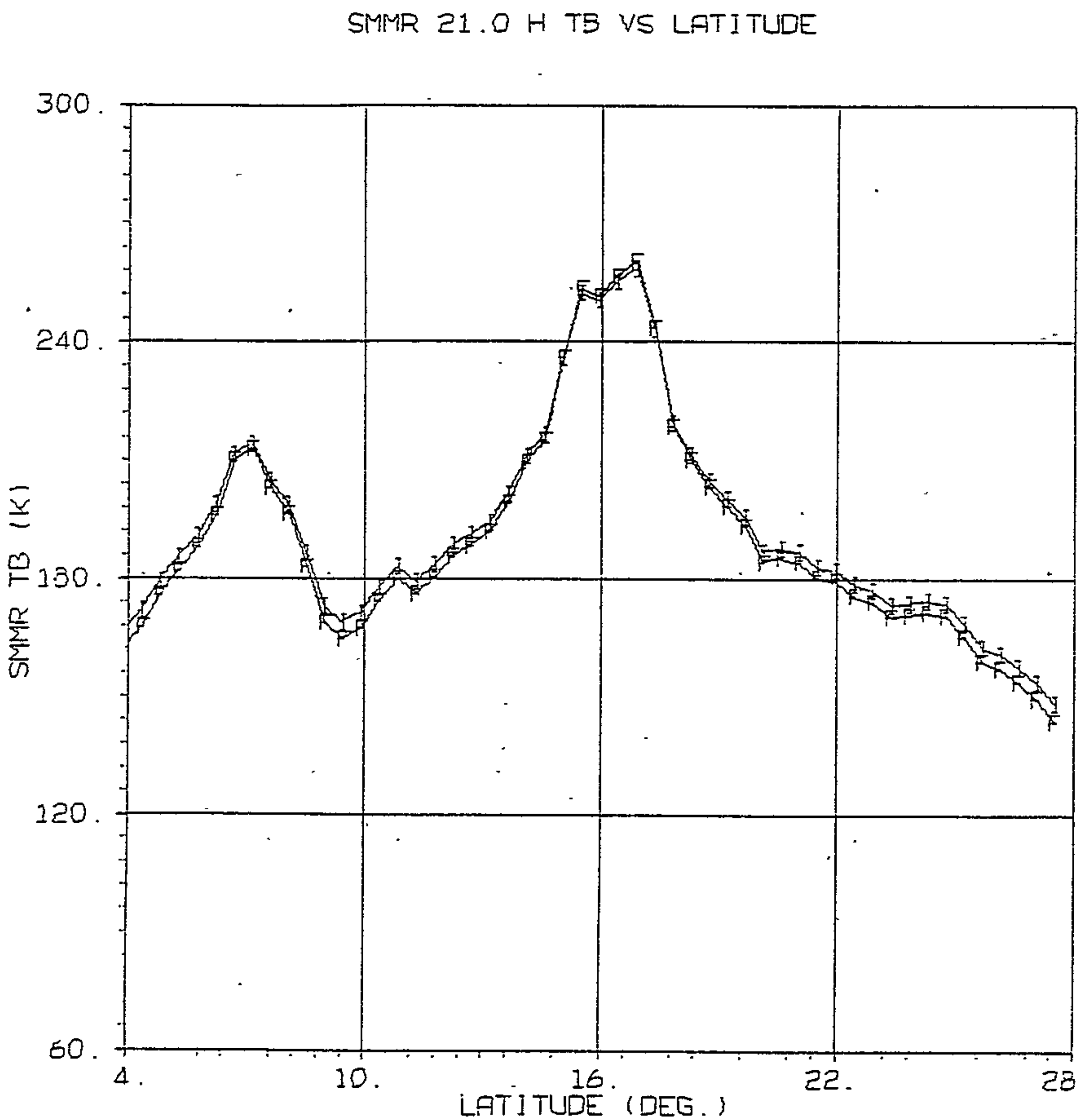

Figure 1.7. Orbit 331, Box and Interim

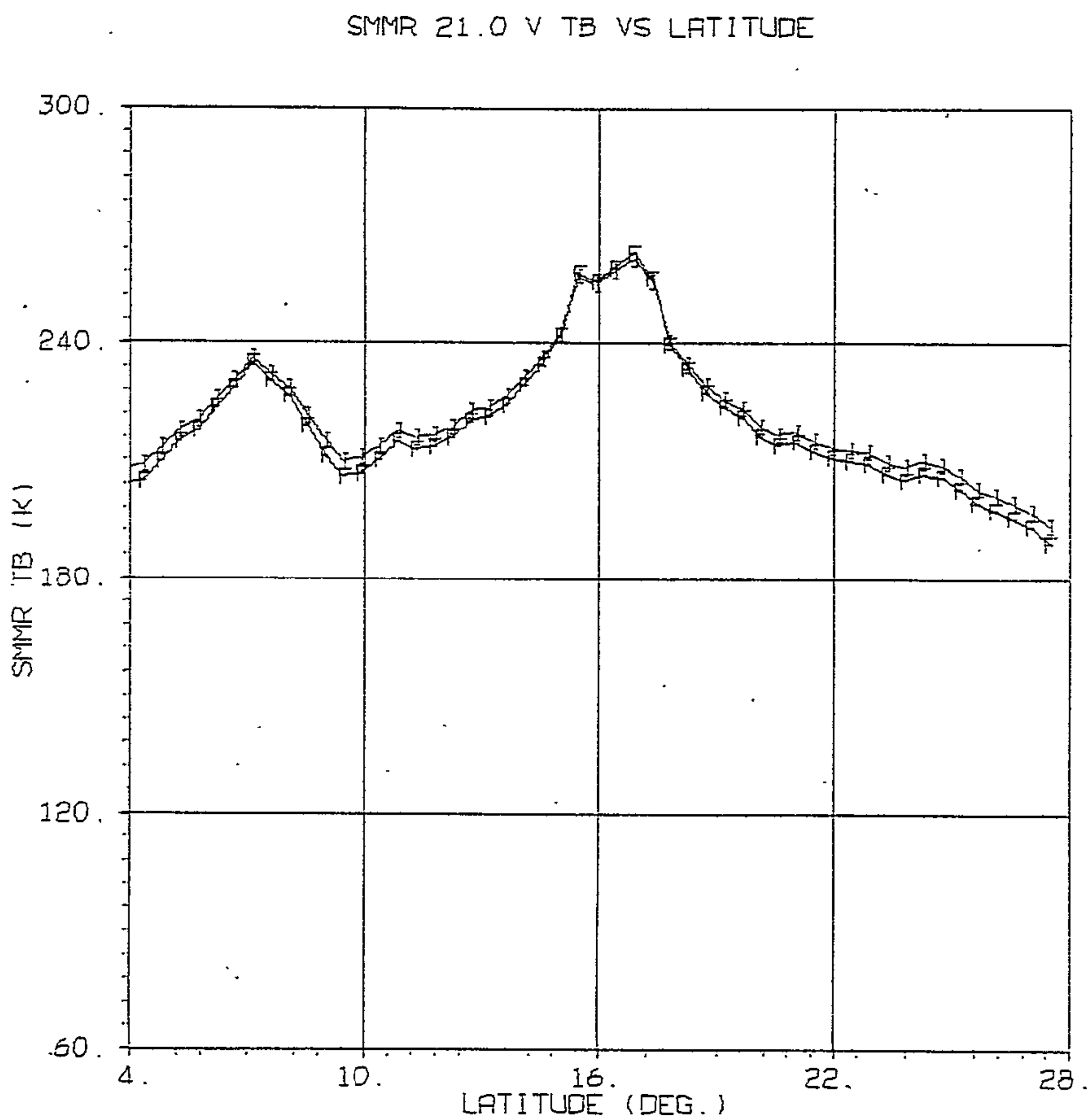

Figure 1.6. Orbit 331, Box and Interim

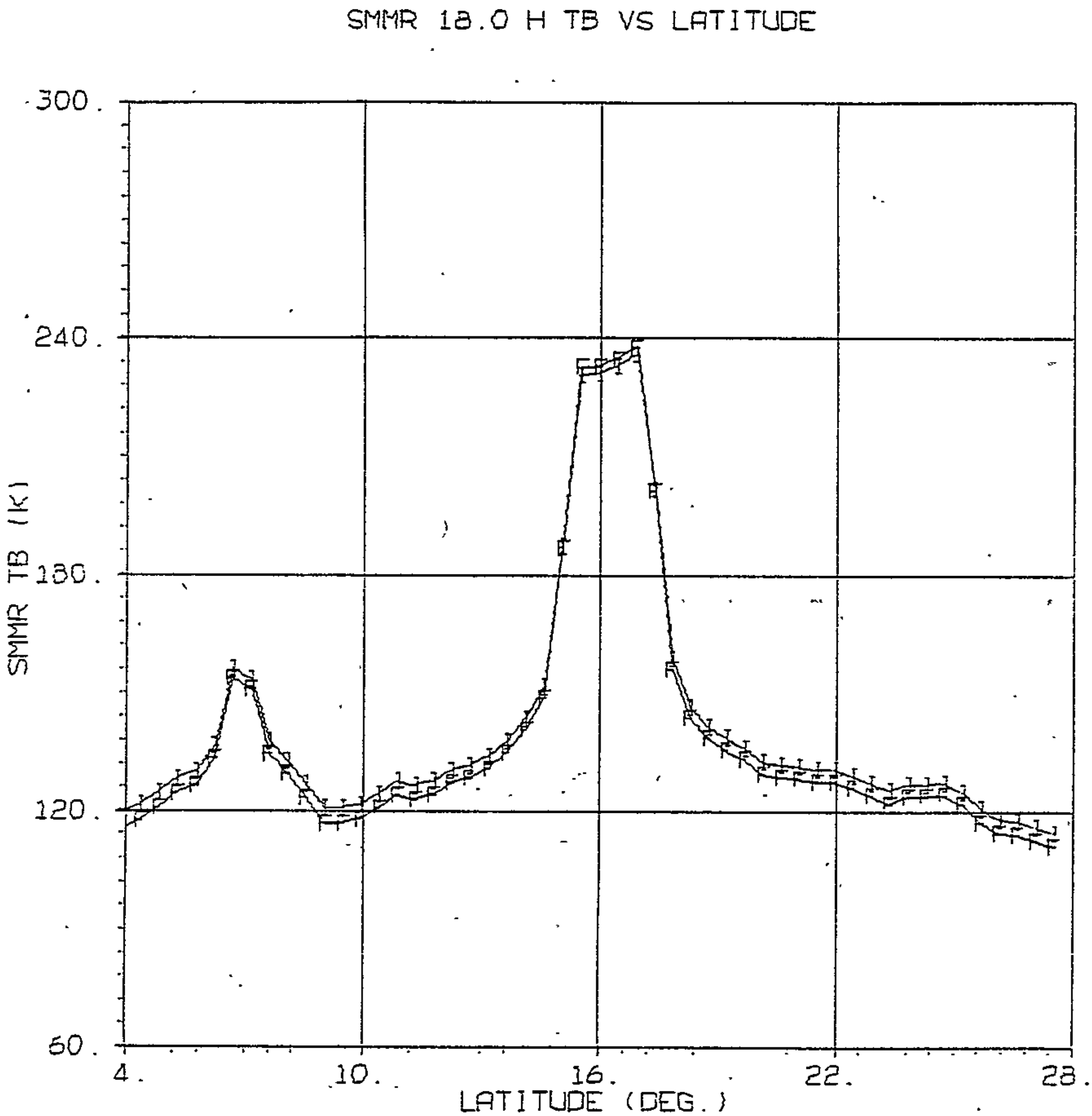

Figure 1.5. Orbit 331, Box and Interim

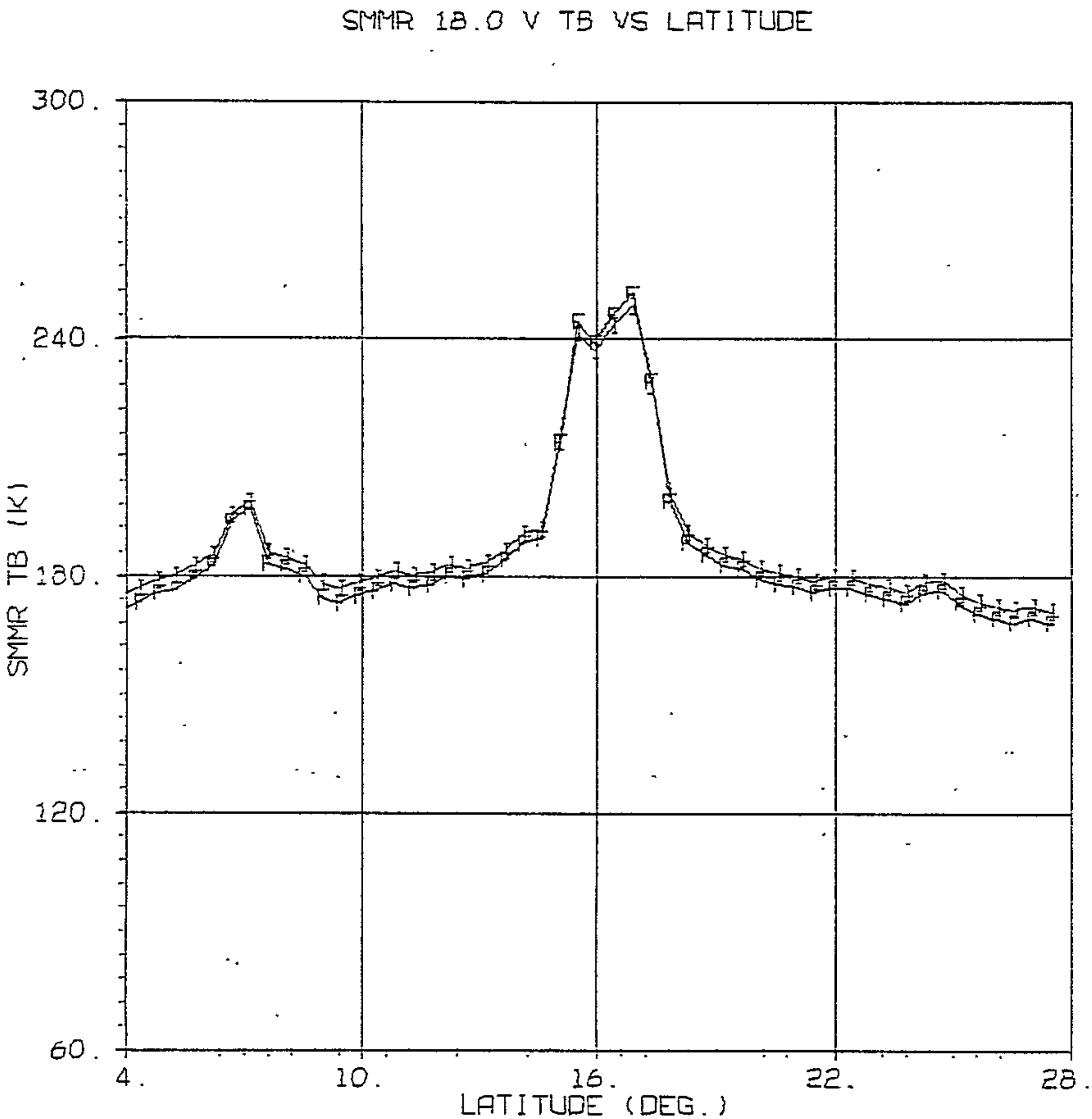

Figure 1.4. Orbit 331, Box and Interim

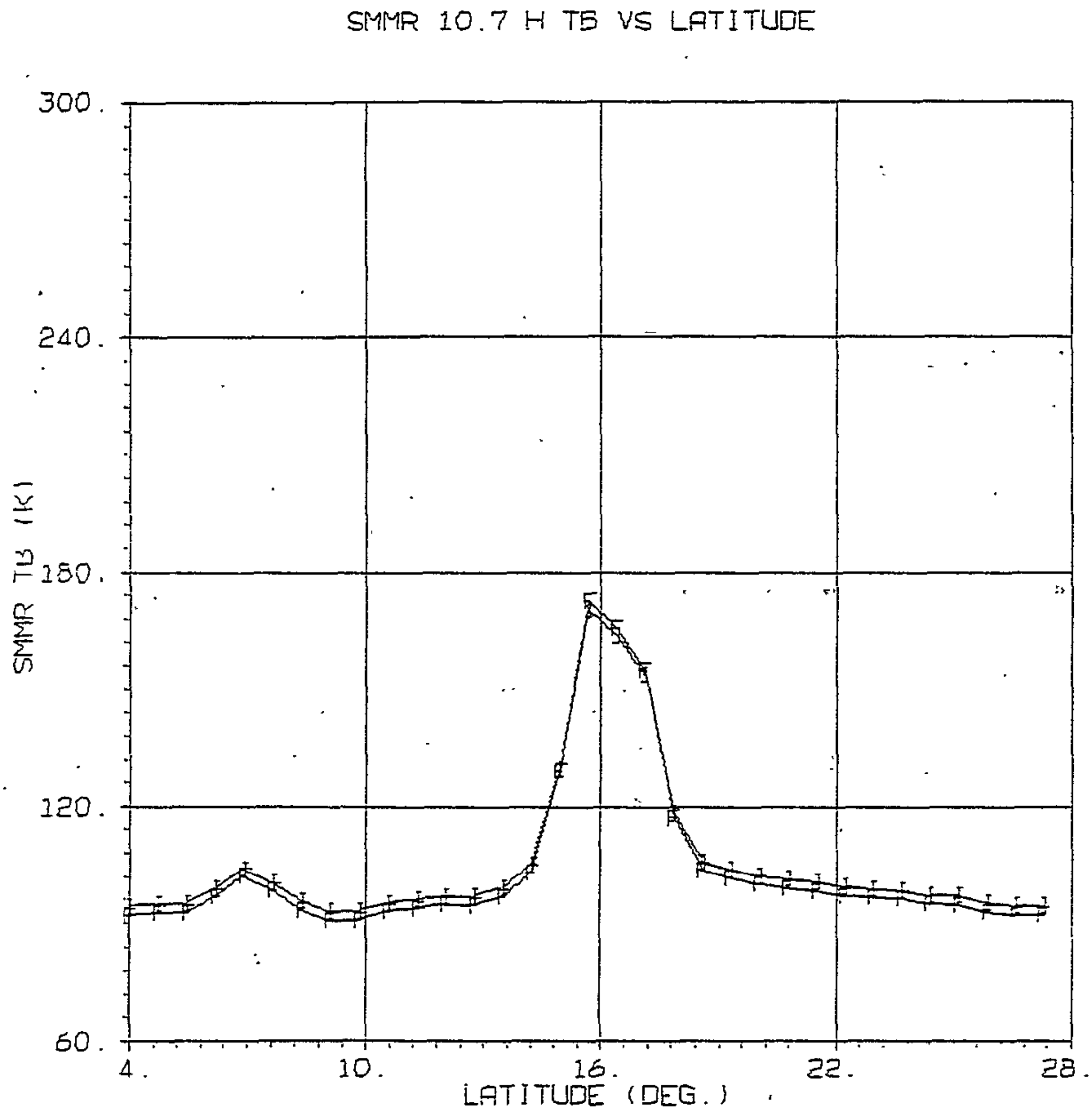

Figure 1.3. Orbit 331, Box and Interim

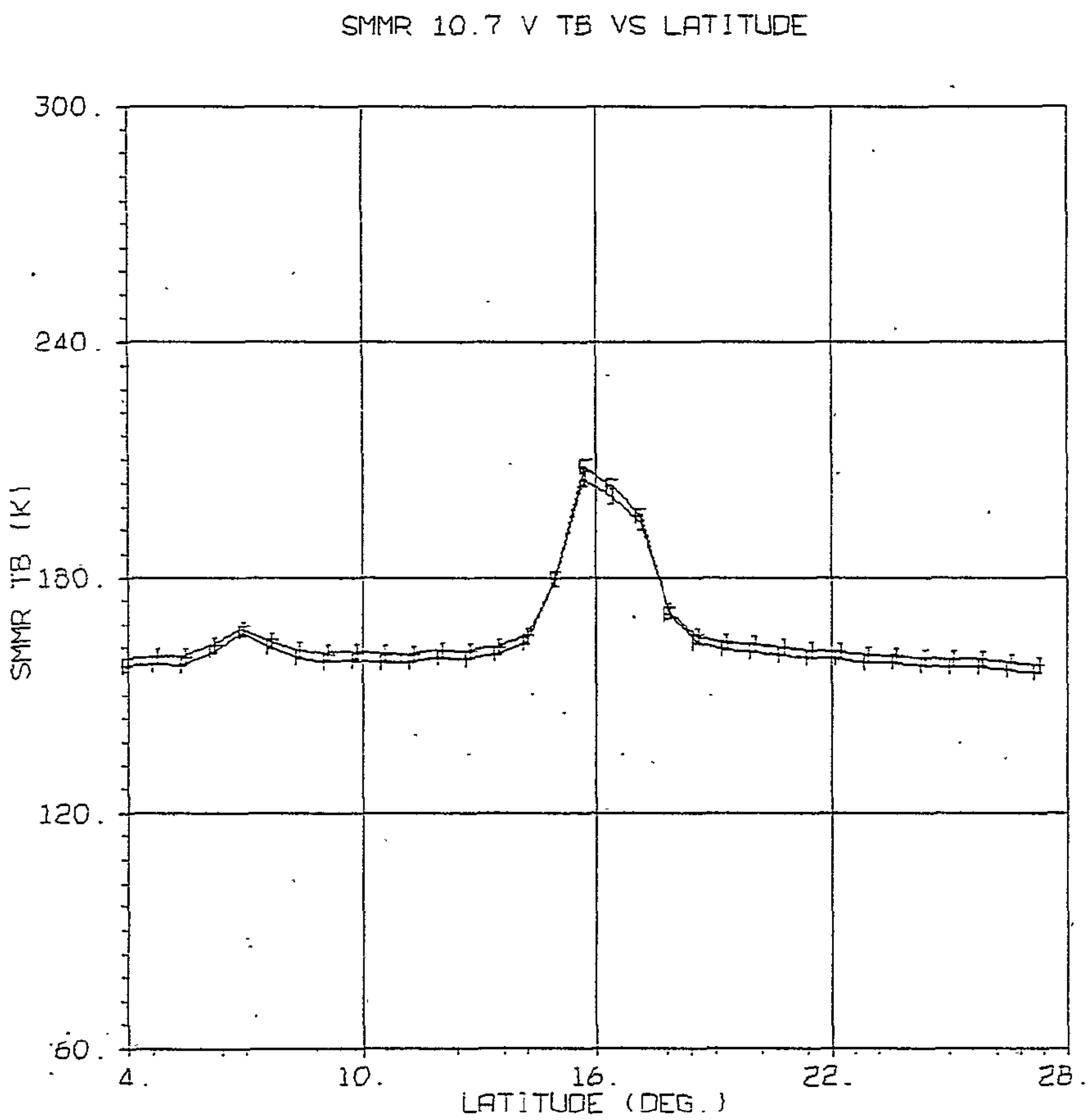

Figure 1.2. Orbit 331, Box and Interim

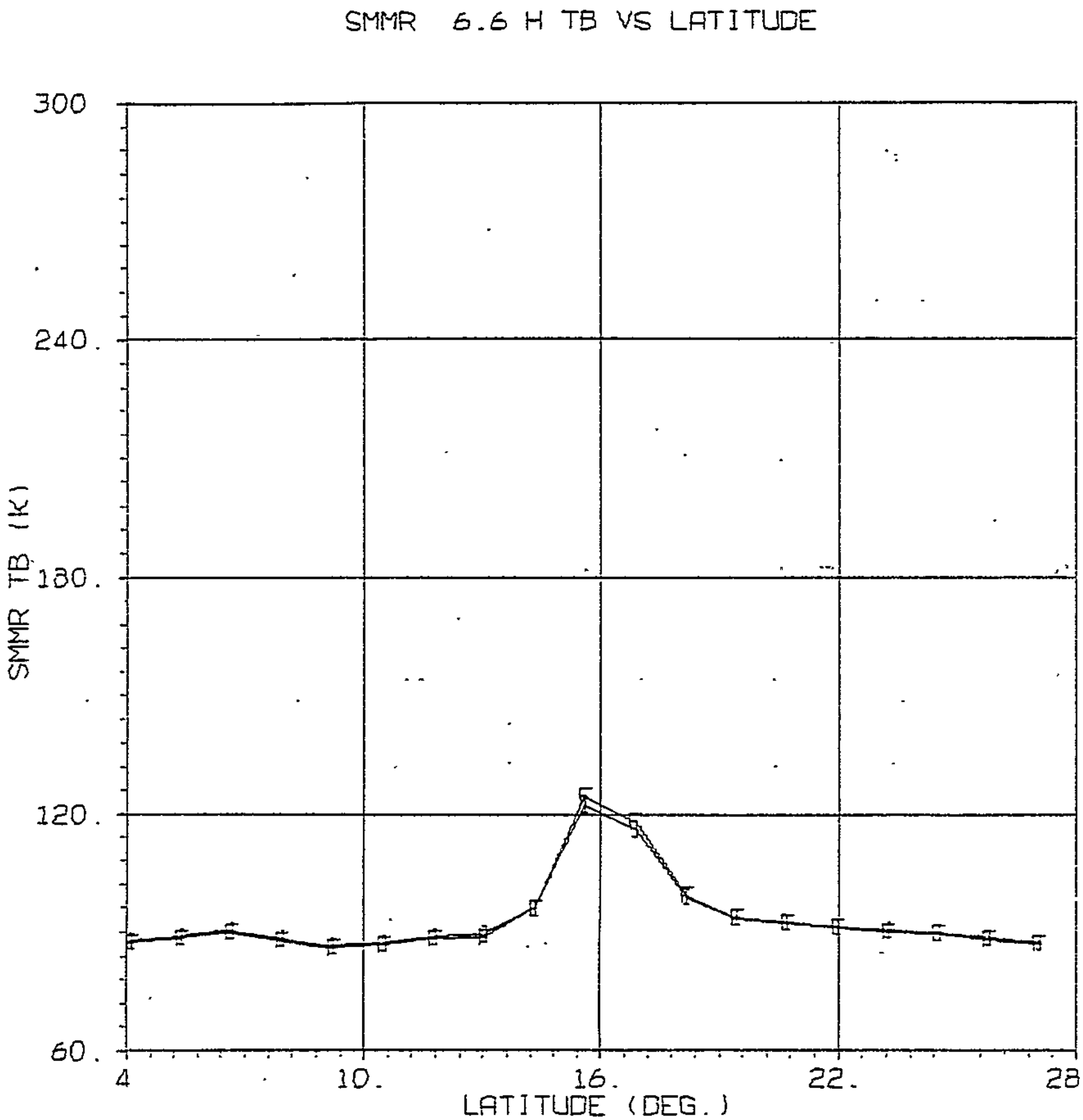

Figure 1.1. Orbit 331, Box and Interim

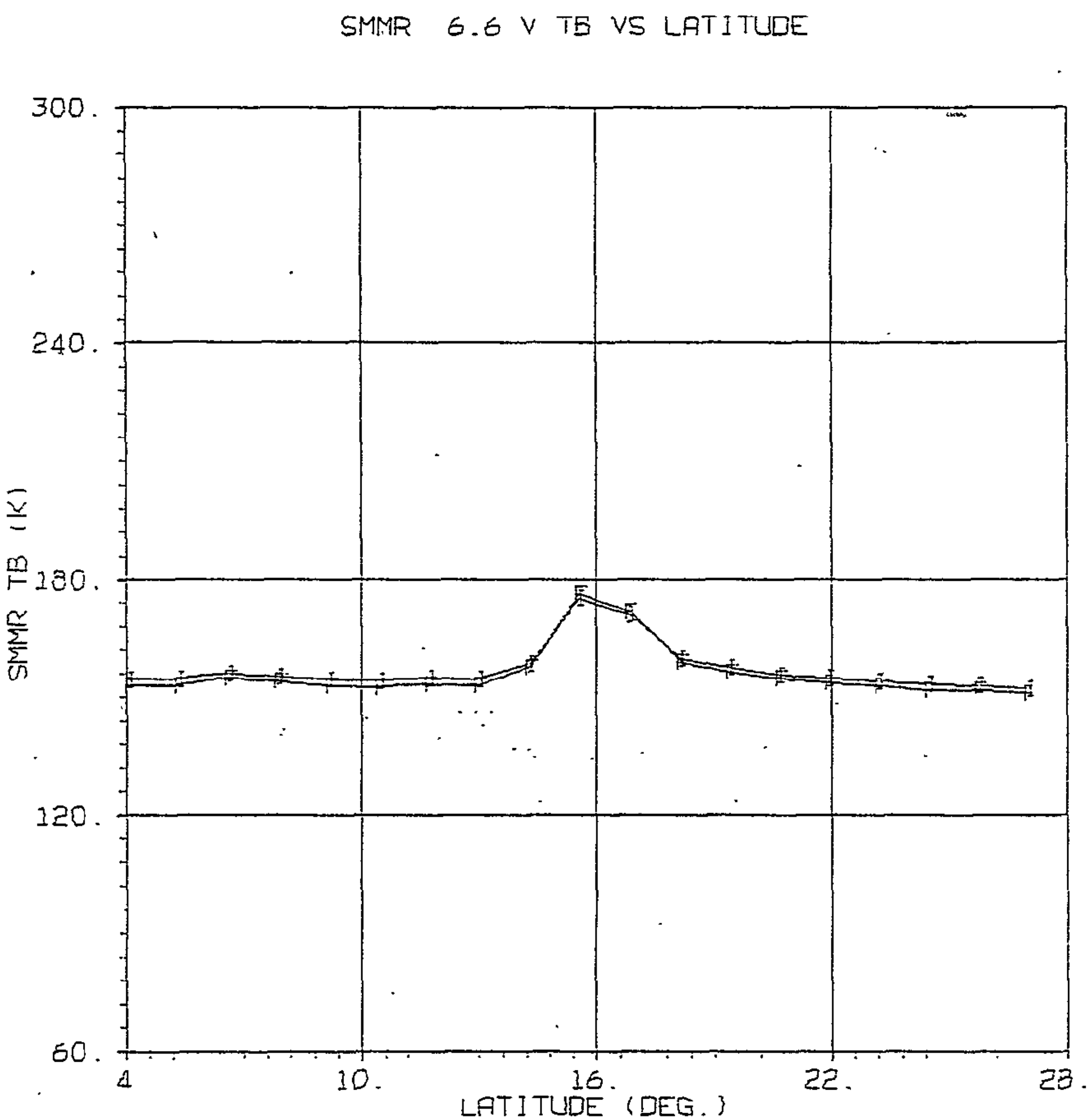

Table 2. Land Sidelobe Effects Orbit 1212, 51°N to 59°N, Column 1

	INTERIM - BOX			INTERIM - CROSS			INTERIM - NOMINAL	
Channel	Open Ocean	N*	Near Land†	Open Ocean	N*	Near Land†	Open Ocean	Near Land†
6.6V	4.50	7	6.50	4.50	7	8.50	4.50	15 **
6.6H	3.25	7	5.00	3.25	7	6.75	2.75	18 **
10.7V	3.00	8	5.00	3.00	8	7.00	3.75	18 **
10.7H	4.00	8	6.00	4.00	10	9.00***	4.00	>20 **
18V	3.00	4	4.00	3.50	4	5.50***	5.00	9
18H	4.50	6	5.50	4.50	6	8.00	5.00	>28 **
21V	3.50	0	3.50	3.50	0	3.50	3.50	14
21H	3.75	5	5.00	3.75	5	5.50	4.00	22 **
37V	3.00	0	3.00	3.00	3	4.00	4.00	24 **
37H	4.00	4	5.00	4.00	4	7.00	4.00	>20 **

† Near Land refers to cell adjacent to land.
* N is the number of cells from land at which the difference first equals the "open ocean difference".
** The near land values for the nominal mode exhibit ringing effects.
*** CROSS mode appears to be overcorrecting for nearby land.

(Box and Cross appear to be identical except for the cell adjacent to land).

Table 1.3. Orbit 331, 33°N to 43°N Interim Minus Nominal Mode (Continued)

CHANNEL	COLUMN	MEAN	STD. DEV.
37.0 V	1	3.50	2.36
	2	3.69	2.81
	3	3.61	3.79
	4	2.73	3.10
	5	2.43	2.27
	6	2.24	1.53
	7	2.24	1.74
	8	2.23	2.18
	9	1.79	2.49
	10	2.64	2.91
	11	2.13	2.75
	12	1.97	1.50
	13	2.46	2.74
	14	2.03	2.71
	15	1.96	2.47
	16	2.32	2.11
	17	1.71	1.93
	18	2.11	1.46
	19	2.02	1.85
	20	2.16	2.27
	21	1.96	1.39
	22	2.65	3.24
37.0 H	1	3.34	2.63
	2	3.01	4.75
	3	2.85	2.96
	4	2.93	4.08
	5	4.43	1.93
	6	3.07	2.45
	7	3.80	2.77
	8	2.55	3.68
	9	3.20	3.28
	10	3.06	2.14
	11	2.57	3.55
	12	2.90	2.76
	13	2.92	3.55
	14	2.87	3.05
	15	3.01	2.04
	16	3.08	3.65
	17	2.58	2.24
	18	3.56	1.99
	19	3.48	5.15
	20	3.01	11.90
	21	4.63	6.38
	22	2.54	13.74

Table 1.3. Orbit 331, 33°N to 43°N Interim Minus Nominal Mode (Continued)

CHANNEL	COLUMN	MEAN	STD. DEV.
18.0 H	1	4.43	1.16
	2	3.38	1.02
	3	3.09	1.25
	4	3.08	1.29
	5	2.98	1.48
	6	2.86	1.32
	7	3.06	1.55
	8	3.15	1.22
	9	3.11	.86
	10	3.35	.83
	11	3.93	1.12
21.0 V	1	4.99	1.62
	2	3.60	.96
	3	3.70	.83
	4	3.69	.89
	5	3.50	1.06
	6	3.50	.88
	7	3.43	1.44
	8	3.86	.92
	9	3.55	.63
	10	3.66	.77
	11	4.37	.95
21.0 H	1	4.25	1.57
	2	3.34	1.11
	3	4.12	1.58
	4	3.70	1.37
	5	3.34	1.14
	6	3.05	1.58
	7	3.19	1.19
	8	3.60	.96
	9	3.26	.87
	10	3.93	1.04
	11	3.17	1.69

Table 1.3. Orbit 331, 33°N to 43°N Interim Minus Nominal Mode

CHANNEL	COLUMN	MEAN	STD. DEV.
6.6 V	1	1.59	.35
	2	1.87	.47
	3	1.85	.29
	4	3.78	.40
6.6 H	1	.20	.29
	2	-.39	.41
	3	-.19	.34
	4	-.94	.31
10.7 V	1	1.50	.51
	2	1.90	.43
	3	2.02	.48
	4	2.14	.75
	5	2.34	.60
	6	1.85	.51
	7	4.76	.44
10.7 H	1	3.31	.52
	2	2.34	.70
	3	2.01	.56
	4	1.97	.62
	5	2.11	.49
	6	2.21	.42
	7	1.46	.41
18.0 V	1	4.06	1.04
	2	2.80	.89
	3	3.12	1.09
	4	2.86	1.72
	5	3.06	1.74
	6	2.91	.95
	7	2.89	.94
	8	3.18	1.14
	9	2.86	1.06
	10	2.73	.73
	11	3.67	.89

Table 1.2. Orbit 331, 33°N to 43°N Interim Minus Cross Mode (Continued)

CHANNEL	COLUMN	MEAN	STD. DEV.
37.0 V	1	2.94	.63
	2	2.26	.43
	3	2.52	.48
	4	1.98	.48
	5	1.91	.44
	6	2.22	.41
	7	2.13	.42
	8	2.08	.35
	9	2.08	.41
	10	2.18	.48
	11	2.10	.47
	12	1.97	.43
	13	2.09	.43
	14	1.93	.43
	15	1.94	.38
	16	1.96	.39
	17	1.90	.38
	18	1.96	.31
	19	1.81	.41
	20	2.07	.37
	21	2.08	.40
	22	2.20	.58
37.0 H	1	3.54	.71
	2	3.71	.65
	3	3.11	.50
	4	3.69	.57
	5	4.25	.46
	6	3.34	.51
	7	3.49	.54
	8	3.10	.51
	9	3.17	.52
	10	3.14	.50
	11	2.90	.58
	12	2.94	.55
	13	2.93	.53
	14	3.04	.51
	15	2.99	.49
	16	3.19	.49
	17	2.87	.54
	18	3.36	.43
	19	3.61	.69
	20	3.33	1.43
	21	3.88	1.12
	22	3.47	1.90

Table 1.2. Orbit 331, 33°N to 43°N Interim Minus Cross Mode (Continued)

CHANNEL	COLUMN	MEAN	STD. DEV.
18.0 H	1	4.30	.37
	2	3.48	.24
	3	3.15	.28
	4	3.10	.27
	5	3.03	.26
	6	3.00	.23
	7	3.04	.25
	8	3.12	.22
	9	3.21	.25
	10	3.44	.26
	11	3.78	.34
21.0 V	1	3.99	.79
	2	3.58	.58
	3	3.67	.56
	4	3.61	.47
	5	3.48	.47
	6	3.55	.48
	7	3.52	.52
	8	3.62	.44
	9	3.58	.46
	10	3.54	.52
	11	3.83	.57
21.0 H	1	4.23	.77
	2	3.50	.60
	3	3.97	.63
	4	3.70	.51
	5	3.37	.55
	6	3.13	.53
	7	3.27	.54
	8	3.43	.48
	9	3.35	.48
	10	3.77	.58
	11	3.55	.68

Table 1.2. Orbit 331, 33°N to 43°N Interim Minus Cross Mode

CHANNEL	COLUMN	MEAN	STD. DEV.
6.6 V	1	1.59	.09
	2	1.45	.09
	3	1.64	.06
	4	2.41	.17
6.6 H	1	.20	.06
	2	-.00	.08
	3	.01	.06
	4	-.15	.09
10.7 V	1	1.50	.07
	2	1.84	.08
	3	1.93	.08
	4	2.05	.08
	5	2.15	.09
	6	2.09	.08
	7	2.73	.10
10.7 H	1	3.12	.07
	2	2.39	.07
	3	2.09	.06
	4	2.03	.08
	5	2.11	.09
	6	2.22	.09
	7	2.12	.12
18.0 V	1	2.89	.39
	2	2.69	.27
	3	2.91	.29
	4	2.78	.25
	5	2.84	.25
	6	2.73	.24
	7	2.82	.27
	8	2.84	.22
	9	2.79	.27
	10	2.68	.25
	11	2.79	.34

Table 1.1. Orbit 331, 33°N to 43°N Interim Minus Box Mode (Continued)

CHANNEL	COLUMN	MEAN	STD. DEV.
37.0 V	1	2.73	.40
	2	2.28	.37
	3	2.46	.36
	4	1.97	.36
	5	1.83	.35
	6	2.20	.36
	7	2.10	.35
	8	2.06	.29
	9	2.16	.31
	10	2.12	.34
	11	2.09	.34
	12	1.99	.36
	13	2.03	.33
	14	1.89	.30
	15	1.93	.28
	16	1.85	.28
	17	2.00	.28
	18	1.94	.27
	19	1.75	.33
	20	2.05	.30
	21	2.12	.33
	22	2.07	.33
37.0 H	1	3.59	.46
	2	3.67	.45
	3	3.15	.39
	4	3.75	.42
	5	4.17	.42
	6	3.37	.42
	7	3.42	.42
	8	3.20	.36
	9	3.13	.39
	10	3.11	.42
	11	2.96	.40
	12	2.94	.40
	13	2.91	.38
	14	3.05	.37
	15	2.97	.35
	16	3.16	.36
	17	2.93	.37
	18	3.32	.36
	19	3.63	.41
	20	3.42	.52
	21	3.66	.41
	22	3.73	.78

Table 1.1. Orbit 331, 33°N to 43°N Interim Minus Box Mode (Continued)

CHANNEL	COLUMN	MEAN	STD. DEV.
18.0 H	1	4.26	.25
	2	3.51	.24
	3	3.16	.24
	4	3.07	.22
	5	3.05	.21
	6	3.04	.20
	7	3.00	.21
	8	3.11	.20
	9	3.22	.21
	10	3.45	.21
	11	3.72	.18
21.0 V	1	3.70	.58
	2	3.60	.57
	3	3.68	.55
	4	3.62	.48
	5	3.50	.46
	6	3.58	.47
	7	3.55	.48
	8	3.60	.44
	9	3.60	.46
	10	3.50	.49
	11	3.74	.47
21.0 H	1	4.23	.66
	2	3.55	.61
	3	3.93	.60
	4	3.68	.53
	5	3.38	.54
	6	3.15	.52
	7	3.26	.52
	8	3.41	.48
	9	3.36	.48
	10	3.76	.53
	11	3.67	.46

Table 1.1. Orbit 331, 33°N to 43°N Interim Minus Box Mode

CHANNEL	COLUMN	MEAN	STD. DEV.
6.6 V	1	1.60	.06
	2	1.22	.07
	3	1.30	.06
	4	1.57	.12
6.6 H	1	.21	.05
	2	.19	.06
	3	.23	.04
	4	.36	.05
10.7 V	1	1.52	.04
	2	1.80	.05
	3	1.90	.04
	4	1.99	.04
	5	2.08	.05
	6	2.02	.05
	7	2.06	.07
10.7 H	1	3.03	.04
	2	2.44	.04
	3	2.14	.04
	4	2.08	.04
	5	2.09	.05
	6	2.25	.05
	7	2.35	.06
18.0 V	1	2.51	.26
	2	2.70	.26
	3	2.93	.26
	4	2.83	.23
	5	2.84	.23
	6	2.75	.22
	7	2.85	.23
	8	2.84	.22
	9	2.83	.24
	10	2.69	.24
	11	2.66	.25

truth data sets. These data sets can then be used along with geophysical models and appropriate assumptions about atmospheric water content to yield a better determination of the bias for each SMMR channel. To facilitate this process, it is recommended that, as new APC output is produced, the LOCATE program be run in a production mode to accumulate additional buoy hits.

6.0 NEW TECHNOLOGY

No new technology has been developed in the course of this study.

7.0 REFERENCES

1. Kitzis, S.N. and Kitzis, J.L., "Evaluation and Analysis of SEASAT-A SMMR APC Algorithm: 6.6 GHz T_B vs. $T_{surface\ truth}$ Comparison Results", March 16, 1979.

2. Kitzis, S.N. and Kitzis, J.L., "Evaluation and Analysis of SEASAT-A SMMR APC Algorithm: T_B Measured vs. T_B Calculated Comparison Results", April 13, 1979.

3. Kitzis, J.L. and Kitzis, S.N., "Evaluation and Analysis of SEASAT-A SMMR APC Algorithm: Interim T_B vs. Final T_B with Gaussian Coefficients", May 25, 1979.

4. Kitzis, J.L. and Kitzis, S.N., "Evaluation and Analysis of SEASAT-A SMMR APC Algorithm: Interim Mode T_B vs. Cross and Nominal Mode T_B", July 27, 1979.

(2) Initial analysis carried out by R. Hofer of data produced by the software described in section 3.2 indicates that there are still significant inter-channel biases in the SMMR data (i.e. residual biases between SMMR T_B values and model-predicted brightness temperatures from surface truth). Simulation runs indicate that these inter-channel biases are not introduced by the APC algorithm. Therefore, these biases are either the result of errors in the model-predicted brightness temperatures or else biases in the data which is input to the APC.

(3) Over open ocean, the only differences observed between the four APC modes are offsets which vary with the mean T_B level. At low T_B levels, the interim mode values are above the other three modes, while at high T_B levels the reverse is true. This changing offset varies smoothly with increasing brightness temperatures.

(4) The box mode outputs are generally similar to those of the interim mode, except that the box mode removes some of the sidelobe contributions from nearby land. No "ringing" effects are observed in the box mode values. Thus, the box mode is superior to the interim mode near land without suffering any ill effects from "ringing."

(5) The cross mode appears to remove more of the sidelobe contributions near land than does the box mode. Unfortunately, the cross mode exhibits "ringing" effects for some channels, thereby making it less desirable than the box mode.

(6) The nominal mode still shows severe "ringing" effects for all channels. Although this mode shows the potential for significantly better resolution than the other modes, the "ringing" renders it unreliable at the present time.

5.0 RECOMMENDATIONS

All of the previous questions regarding the SMMR brightness temperatures have been answered with the possible exception of two. One involves the "ringing" effects observed in the nominal and, to a much lesser degree, in the cross modes near land. At present, this "ringing" phenomenon is not completely understood and should be further investigated unless a final decision is made to completely disregard the nominal and cross modes. This effect can best be studied by simulating a brightness temperature scene which is half ocean and half land, which requires a more sophisticated simulation approach than that currently in use.

The second remaining question concerns the inter-channel T_B biases. These biases should be studied by using the software described in section 3.2 to assemble a large number of matched spacecraft and surface

```
@ASG,A JK*ENI.
@ASG,A JK*TABLE.
@ASG,A 1135*WINDFIELD.
@USE 10.,1135*WINDFIELD.
@ASG,T TAPE.,U9H,SxxxxR  (Tape containing TB data)
@REWIND TAPE.
@USE SMMRTAPE., TAPE.
@CAT,P OUTPUT1.          (Output file for TB data)
@ASG,A OUTPUT1.
@USE 23.,OUTPUT1.
@CAT,P OUTPUT2.          (Output file for surface truth data)
@ASG,A OUTPUT2.
@USE 11.,OUTPUT2.
@XQT JK*ENI.CORAL
 $TIMES
   LWIND = .TRUE., LVAPOR = .TRUE.,
 $END
@ADD JK*TABLE.
```

The output file of T_B data contains two card images corresponding to each grid-1 cell location. The first card image contains an ID number for the point and the ten SMMR brightness temperature measurements. The format of this card is I5, 10F7.2 .

The second card image contains the same ID number and the ten grid column numbers corresponding to the T_B measurements. This card has the format I5, 10I7. The ID numbers range from 101 through 116 for the 16 points from the first block of SMMR data processed, then from 201 through 216 for the points from the second block of data, etc.

The output file of surface truth data contains a single card image corresponding to each grid-1 cell location. This card contains the ID number for the point, the sea surface temperature in degrees Celsius, the water vapor content in grams/cm^2, and the wind speed in meters/second. The format used is I5, 3F7.2 .

4.0 CONCLUSIONS

Several conclusions may be drawn from the results discussed in section 3.0:

(1) Most of the problems in the APC outputs discussed in previous reports have now been eliminated or reduced to insignificant levels. These problems all involved unrealistic variations in brightness temperatures across the SMMR swath. These include unmodeled cos β effects, cross-track gradients induced by the sidelobe correction procedure, and large biases at the edges of the swath also caused by sidelobe corrections. These problems are no longer apparent in the brightness temperature output of the APC.

choose to have the temperatures for all channels taken from grid 1, or alternatively to have temperatures for each channel taken from those cells of its best grid which lie closest to the grid-1 cell locations. In either case, the grid 1 locations are used to interpolate the surface truth fields to produce corresponding surface truth measurements. If a given location is outside the limits of a field, the corresponding surface truth parameter is set to zero.

The namelist $TIMES is required to execute the program and contains the following variables:

Variable Name	Type	Dim.	Default	Description
IT1	Int.	4	0,0,0,0	Beginning time (Days,Hrs,Min,Sec)
IT2	Int.	4	366,0,0,0	Ending time (Days,Hrs, Min, Sec)
ALLGR1	Log.	1	.FALSE.	.TRUE. if T_B measurements for all channels are to be taken from grid 1.
LWIND	Log.	1	.FALSE.	.TRUE. if wind speeds are to be interpolated from a wind field.
LVAPOR	Log.	1	.FALSE.	.TRUE. if water vapor values are to be calculated.

The namelist $TABLE contains the sea surface temperature field data and is made available to the program by @ADD'ing the file JK*TABLE to the runstream. In addition to printed output, the program produces two output files, one containing T_B data and one containing surface truth data.

The following is a sample runstream for orbit 1135, assuming that T_B data is to be read directly from a nine-track tape.

```
@ASG,T TAPE.,T,Q160R
@EZIO,RS JK*ENI.
@REWIND TAPE.
@FREE TAPE.
@ASG,T TAPE.,T,Y317R
@EZIO,RS JK*TABLE.
@REWIND TAPE.
@FREE TAPE.
@ASG,T TAPE.,T,W498R
@EZIO,RS TAPE.,1135*WINDFIELD.,1298*WINDFIELD.
@REWIND TAPE.
@FREE TAPE.
```

these are not measured by buoys and are simply set to zero. The fields are as follows:

Field #	Parameter	Units	Format
1	Air temperature	Tenths of degrees Celsius	I4
2	Dew point	Tenths of degrees Celsius	I4
3	Barometric pressure	Tenths of millibars	I5
4	Wind speed	Hundredths of meters/sec.	I4
5	Wind direction	Tenths of degrees from north	I4
6	Weather code	----	I1
7	Visibility	Tenths of nautical miles	I3
8	Precipitation	Millimeters	I4
9	Solar radiation	Hundredths of Langleys/min (wave lengths from .6 to 4.0 microns)	I3
10	Solar radiation	Hundredths of Langleys/min (wave lengths from 4.0 to 50 microns)	I3
11	Significant wave height	Tenths of meters	I3
12	Average wave period	Tenths of seconds	I3
13	Average wave direction	Degrees from north	I3
14	Highest crest	Tenths of meters	I3
15	Deepest trough	Tenths of meters	I3
16	Sea surface temp.	Hundredths of degrees Celsius	I4
17	Salinity	Thousandths of parts per thousand	I5
18	Conductivity	Thousands of millimhos/cm	I5

The third and fourth cards respectively contain the maximum and minimum values measured during the six-hour window. The fifth card contains the standard deviations of the measurements about their mean values. These three card images use the same format as the second card.

3.2.3 CORAL User's Guide. The program CORAL uses sea surface temperature fields, wind fields, and a simple water vapor model to produce corresponding sets of surface truth values and SMMR brightness temperature measurements. The current sea surface temperature field covers a region in the northeastern Pacific between 21 degrees and 55 degrees north latitude, and between 179 degrees and 245 degrees east longitude. It represents the NMFS monthly average temperatures for September 1978. Figure 15 shows the full extent of the sea surface temperature field. Wind field values have been produced by Vince Cardone and are available for SEASAT orbits 1135 and 1298. Values for water vapor content are calculated as a function of latitude.

Sixteen brightness temperature measurements for each channel are extracted from each block of SMMR data. These measurements are associated with the centers of the sixteen grid-1 cells. The user may

In addition to printed output, a FORTRAN formatted file is produced. An example of the printed output appears in figure 14. The nonzero measurements are respectively air temperature (C), pressure (mb), wind speed (meters/sec), wind direction (degrees from north), and sea surface temperature (C). The value of 1 for JSTAT indicates that measurements are available both before and after the time of overflight within the 6-hour window centered on overflight. A value of 2 would indicate that measurements were found on only one side of the overflight time. The value of NTOT indicates the number of sets of measurements found within the 6-hour window centered on overflight. When no measurements are available, an appropriate message is printed.

The following is a sample runstream:

```
@ASG,T TAPE.,T,Q160R
@EZIO,RS TAPE.,JK*ENI.,SEASAT-ADF*BFILE.
@REWIND TAPE.
@FREE TAPE.
@USE BFILE.,SEASAT-ADF*BFILE.
@ASG,A JK*ENI.
@ASG,A BFILE.  (This buoy file must be assigned to the run under the
                name BFILE.)
@ASG,A OUTPUT.  (Output file)
@USE 22.,OUTPUT.
@ASG,A HITFILE.  (File produced by LOCATE)
@USE 23.,HITFILE.
@XQT JK*ENI.MATCH
```

The output file contains either one or five card images corresponding to each overflight time encountered in the hit file from LOCATE, depending on whether or not buoy measurements are available within 3 hours of overflight. The first card image is formatted as follows:

```
(Buoy ID)       (Days,Hrs,Min,Sec)       JSTAT      NTOT

   I10      5X         4I5            5X    I1    5X   I1
```

A value of 3 for JSTAT indicates that buoy measurements are not available and that no additional cards have been produced for this overflight time. A value of 1 or 2 indicates that measurements are available, and in this case, the 4 cards immediately following contain information regarding this hit.

The second card image contains the interpolated measurements. There are fields for eighteen separate physical parameters, but many of

The following is a sample runstream, when reading T_B data from a 9-track tape.

```
@ASG,T TAPE.,T,Q160R
@EZIO,RS TAPE.,JK*ENI.
@REWIND TAPE.
@FREE TAPE.
@ASG,A JK*ENI.
@ASG,A OLDHITS.     (file of previously accumulated hits)
@USE 25.,OLDHITS.
@CAT,P HITFILE.     (output file - will include old and new hits)
@ASG,A HITFILE.
@USE 23.,HITFILE.
@ASG,T TAPE.,U9H, SxxxxR   (Tape containing TB data)
@REWIND TAPE.
@USE SMMRTAPE., TAPE.
@XQT JK*ENI.LOCATE
 $TIMES
  MERGE = .TRUE.,
 $END
```

Note: If MERGE = .FALSE., no file of previously stored hits is required.

The output file contains 3 card images corresponding to each hit encountered. The first card is formatted as follows:

(Buoy ID)		(Days, Hrs., Min., Sec.)		(Seconds from beginning of year)
I10	5X	4I5	5X	F10.0

The second card image contains the ten brightness temperature measurements and uses the format 10F7.2. The third card image contains the ten grid column numbers, and uses the format 10I7.

3.2.2 MATCH User's Guide. The program MATCH outputs buoy surface truth data corresponding to overflight times listed in a "hit" file produced by LOCATE. Surface truth values are extracted from a buoy file covering the period between July 1 and October 31, 1978, and are interpolated to the exact time of overflight whenever possible. Measurements must be available within 3 hours of overflight in order to produce surface truth output. If measurements are available both before and after the time of overflight, a linear interpolation is performed. If measurements are only available on one side of the time of overflight, those closest to the time are used. The program also outputs the maximum and minimum values measured within 3 hours of overflight and the standard deviations of the measurements about their mean values during the same period. Measurements contained in the buoy file include air temperature, air pressure, wind speed and direction, sea surface temperature, and sometimes significant wave height and average wave period.

to yield valid statistical results. In order to automate the process of accumulating large sets of spacecraft and surface truth data which are co-located in time and space, we have developed a package of three programs. These programs are:

(1) LOCATE - This program identifies times at which the SMMR swath passes over the locations of a predetermined set of buoys.

(2) MATCH - This program produces buoy measurements corresponding to the overflight times output by LOCATE.

(3) CORAL - This program uses digitized surface truth fields to produce corresponding sets of surface truth measurements and SMMR data.

These programs have been designed with the goal of minimizing required user preparation and involvement. They may be used in a production environment in which the only inputs which change for each run are the file names/tape ID's to be processed. Since it is expected that a large number of users may be interested in this software, a user's guide for each program is provided in the following sections. This software has been thoroughly tested and has been used to process all the SMMR T_B data produced for the SMMR Mini-II workshop. These programs are easy to set up and are fast-running.

3.2.1 LOCATE User's Guide. The program LOCATE identifies times at which the SMMR swath passes over the location of any of the buoys listed in Table 3. The outputs of the program include buoy ID, time of overflight, SMMR brightness temperature measurements for all 10 channels, and the grid column numbers corresponding to these measurements for each buoy "hit" encountered. The T_B measurements for each channel are taken from that channel's best grid and represent the grid cell closest to the location of the buoy. A buoy falling outside the SMMR swath may still result in a hit if the buoy is within 13.5 kilometers (one half of a grid 4 cell-width) of the swath's edge. In addition to printed output, the program produces a FORTRAN formatted file for use in a subsequent program.

A namelist input $TIMES is required to execute the program, and includes the following variables:

Variable Name	Type	Dim.	Default	Description
IT1	Int.	4	0,0,0,0	Starting time for processing T_B data (days, hours, minutes, seconds)
IT2	Int.	4	365,23,59,59	Ending time for processing T_B data (days, hours, minutes, seconds)
MERGE	Log.	1	.TRUE.	.TRUE. to merge all hits encountered with file of previously accumulated hits.

Observations regarding these plots are listed below:

(1) The effects of the adjacent land on the interim mode data can be seen as a rise in T_B values occurring between 38° and 40° north latitude. The horizontal channels show larger effects than the vertical channels. In fact, the interim 18V and 21V channels (figures 11.5 and 11.7) show hardly any response to the nearby land. This behavior is unchanged from that previously observed in references 3 and 4.

(2) For all channels except 6.6 GHz, the only difference between the box and interim modes is a constant offset. For the 6.6 GHz channels, this offset diminishes slightly as the SMMR swath approaches the point of closest proximity to land. These observations imply that the box mode sidelobe corrections are not improving upon the performance of the interim mode in this particular case. In fact, the observation concerning the 6.6 GHz channels seems to suggest that the box mode may be more sensitive to the nearby land than the interim mode.

(3) The behavior of the cross mode is somewhat similar to that of the box in that the cross mode values differ from the interim mode values by a nearly constant offset. However, this offset increases near the point of closest proximity to land for the 6.6 H and 18 H channels. This implies that the cross mode is less sensitive to the nearby land than the box or interim mode for these channels. Unfortunately, the cross mode data for the 10.7 H channel exhibits some over- and under-compensation which is reminiscent of the "ringing" discussed for the coastline crossing case.

(4) As noted in prior reports, the nominal mode data exhibits more noise than the other modes. In addition, the nominal mode shows severe over- and under-compensation effects near land for all the horizontal channels. This is particularly evident for the 6.6 H and 10.7 H channels (figures 13.2 and 13.4). This severe over- and under-compensation is undoubtedly related to the "ringing" effects previously discussed.

3.2 <u>Creation of Matched Surface Truth and Spacecraft Data Sets</u>. References 2 and 3 document attempts to determine instrument biases in the SMMR data by comparing SMMR T_B values with surface truth measurements. Such comparisons are difficult to perform due to the frequent lack of adequate atmospheric water measurements. This problem may be partially alleviated by first assembling large quantities of surface truth data. Measurements corresponding to clear atmospheric conditions can then be extracted from the large ensemble, or alternatively, mean values of atmospheric water content can be assumed to hold for the complete data set. In either case, a sufficiently large data set must be available

Observations regarding the complete set of data are listed below:

(1) The box, cross, and nominal mode values are generally below the interim values over the ocean. This is not the case over land, where the relationship is reversed for the lower frequency channels.

(2) As expected, the transition from ocean to land is sharpest for the 37 GHz channels and becomes less sharp with decreasing frequency. In addition, the ocean data exhibits more noise for the higher frequency channels than for the lower frequency channels. This is due to the better resolution of small local weather features afforded by the higher frequencies.

(3) "Ringing" is clearly observed in the nominal mode data near the coastline crossing (figures 10.1 through 10.10). It is present to a much lesser extent in the cross mode data (for 10.7H and 18V), and is not present at all in the box and interim modes.

(4) The differences observed between the interim mode and the other three modes generally increase as the distance from land diminishes. This increase in the differences is due to a gradual rise in the interim mode values as the swath approaches land while the box and cross modes maintain more constant levels. This is good evidence that the sidelobe correction procedure is truly removing contamination from nearby land.

(5) Table 2 summarizes the differences observed for orbit 1212, over open ocean and adjacent to the coast. Note that the land contamination in the interim data extends farthest from the coast for the lower frequency channels (e.g. 7 grid-1 cells ≈ 1000 km. for 6.6 GHz versus 4 grid-4 cells ≈ 100 km for 37 GHz), which is a reflection of their wider beam widths. Also, note that the cross mode appears to remove more of the land contamination than does the box mode, which is evidenced by the larger differences adjacent to land for the cross mode. Unfortunately, the cross mode appears to over-correct for land (i.e. "ring") in the 10.7H and 18V channels. This over-correction becomes much more severe in the nominal mode for all channels.

3.1.3 Paralleling Coastline Case. We have analyzed data from orbit 1212 near 38° north latitude as an example of the SMMR swath following a course parallel and extremely close to land. The right-hand edge of the swath runs parallel to the California coastline and comes within 50 kilometers of San Francisco. There are two points of closest approach to land, one at 38.5° and the other at 40° north latitude. Figures 11, 12, and 13 contain plots of T_B values versus latitude for the four APC modes.

(2) Table 1 also shows that the interim mode values are consistently higher than the corresponding box, cross, and nominal mode values for all channels. The mean differences tend to increase with increasing frequency, and vary between 0° and 4°K. These differences are approximately the same for the box, cross, and nominal modes.

(3) The outer cells for the 18, 21, and 37 GHz channels tend to be somewhat lower than the center cells in the box, cross, and nominal mode outputs.

(4) The cross-track gradients observed in the T_B data appear to be very similar for all four APC modes. A slight enhancement of the interim mode gradients can be seen in the box, cross, and nominal modes (see figures 4 through 7). These gradients for all modes appear to be geophysically realistic, and thus indicate that the final cos β estimates have been properly implemented.

(5) The box, cross, and nominal modes appear to introduce small (<1°K) opposing cross-track variations in the 10.7 V and H data (see Table 1). This is the only remaining evidence that the sidelobe correction procedure is introducing undesired effects. Note, however, that all of the previously observed problems (see reference 4) have been corrected.

(6) As noted previously in references 3 and 4, the difference between the interim mode and the other modes decreases with an increasing average T_B level. In fact, if the T_B level increases high enough, the box, cross, and nominal mode values will be consistently above the interim mode data. An excellent example can be seen in figures 1, 2, and 3, where T_B data is plotted through the eye of hurricane Fico. Note that the interim values are above the other mode values away from Fico, but are below them near the eye of Fico, with a smooth transition in between.

(7) An additional comment is in order regarding the pass over Fico. The nominal mode appears to achieve a better resolution of the eye of the hurricane than do the other modes. This is readily apparent in figures 3.1 through 3.10, and especially in figures 3.3, 3.4, and 3.6. The box and cross modes generally show the eye to the same extent as the interim mode, whereas the nominal mode shows a significant improvement in resolution.

3.1.2 Coastline Crossing Case. We have analyzed data from orbits 1178 and 1212 as examples of the SMMR swath crossing a coastline. We have produced plots of T_B versus latitude corresponding to these two orbits for different positions across the scan and for each of the APC modes. A set of expanded-scale plots produced for the left-hand edge of the SMMR swath for orbit 1212 are displayed as figures 8, 9, and 10. The sharp rise in T_B values near 50°N is due to the SMMR swath crossing the Kenai Peninsula on the Alaskan coast.

A third analysis tool calculates mean T_B values for each cell of the ten channels for two modes of the APC, and associated standard deviations. The program also calculates the mean differences between the two modes and associated standard deviations. This program is typically used to compare interim mode results with results of one of the other modes. An example of the program's output may be found in Table 1.

The comparisons presented here have been performed for the purpose of evaluating the effects of the different sidelobe correction procedures. The following results are expected from these types of comparisons:

(1) All four modes of the APC should produce generally similar results over open ocean, in terms of both mean T_B levels and any gradients which may exist in the data. However, the nominal mode is expected to exhibit more point-to-point variation than the interim mode, with the box and cross modes being intermediate between the two.

(2) When crossing a land-sea interface, the sharpest transition is expected for the nominal mode, a somewhat less sharp transition for the cross and box modes and the smoothest transition for the interim mode. The cross and box modes are expected to remove the ringing phenomena observed in the nominal mode and discussed in references 3 and 4.

(3) When paralleling a coastline, the nominal mode should be least sensitive, the cross and box modes slightly more sensitive, and the interim mode most sensitive to the nearby land.

This section contains the results of a direct comparison of interim mode data with nominal, cross, and box mode data from the APC. Separate comparisons are made for the open ocean, land-crossing, and land-paralleling cases listed above.

3.1.1 Open Ocean Case. For the open ocean case, we have analyzed data from two SEASAT passes over the Gulf of Alaska, orbits 1178 and 1212, and a third pass over hurricane Fico near Hawaii, orbit 331. For each pass, we have produced plots of brightness temperature versus latitude and of cross-track gradients versus latitude. In addition, we have calculated mean differences between the various modes for each grid cell. Examples of these three types of output for the hurricane pass may be found in Figures 1 through 7 and Table 1.

Observations regarding the complete set of data are listed below:

(1) As expected, the nominal mode data exhibits more noise than any of the other modes. As seen in Tables 1.1, 1.2, and 1.3, the noisiness of the box and cross modes is only slightly greater than that of the interim, while the nominal exhibits significantly more noise than the others.

Report 4 - The fourth report (reference 4) extended the evaluation to the Nominal and Cross modes of the APC. Both of these modes were compared directly with Interim APC output for the three environmental regimes. As observed for the Gaussian APC, the Nominal and Cross mode T_B values were biased low with respect to Interim values, and exhibited cross-track gradients significantly different from those observed in Interim T_B output. In general, these effects were less severe for the Cross than for the Nominal APC. "Ringing" was again observed in Nominal output near coastline crossings. Two parallel efforts showed that the world T_B map agrees well with actual SMMR data, and that the cos β correction effectively removes the previously observed opposing cross-track gradients.

Report 5 - This present report evaluates the latest versions of the Interim, Cross, Box, and Nominal modes of the APC. Most of the problems observed in report 4 have been corrected. The biases between the Interim and the other modes are significantly reduced, and the gradients previously introduced by the sidelobe correction procedure are no longer apparent. "Ringing" is still observed in the Nominal, is greatly reduced in the Cross, and does not appear at all in the Box APC. For the first time, cases have been observed which show that the implemented sidelobe correction procedure removes land contamination effects such that the Nominal, Cross and Box mode data is preferable to the Interim data when near land. In addition, due to the need for larger surface truth data sets, new software has been developed which facilitates the production of matched spacecraft and surface truth data sets which are co-located in time and space.

3.0 TECHNICAL DISCUSSION

3.1 Intercomparison of APC Modes. The comparisons presented here are a continuation of the work previously discussed in section 3.1 of reference 4. Several software analysis tools have been used to facilitate these comparisons.

One of these tools produces plots of brightness temperatures versus latitude for two modes of the APC. Typically, these plots display interim mode data along with either nominal, cross, or box mode data. Examples of these plots are shown in figures 1.1 through 1.10. For all plots presented here, the symbol "I" represents interim mode data, while "F" represents either box, cross, or nominal mode data, as indicated in the plot title.

A second analysis tool produces plots of T_B cross-track gradients versus latitude. These gradients are calculated by fitting a straight line to each row of T_B data cells. The gradients are plotted in units of degrees Kelvin per grid cell. Examples of these plots are shown in figures 4.1 through 4.5. In each plot, the symbol "V" represents gradients for the vertical polarization and "H" represents gradients for the horizontal polarization for the frequency indicated in the plot title.

Of course, each of these versions has incorporated changes over time as problems have been uncovered and the resulting corrections implemented. For example, the Nominal, Cross, and Interim modes of the APC discussed in this report are slightly different from those of the same names discussed in the last report (reference 4). These changes are a reflection of problems identified in this prior report, as well as problems uncovered in independent investigations. Even though the present report concludes this particular evaluation effort, it is expected that the APC will continue to change following the publication of the report. Therefore, the results presented here should not be construed as representing the final state of the APC algorithm, but only its status as of this time.

The following is a short history of the valiant attempts of this evaluation to keep pace with the ever-changing APC algorithms.

Report 1 - This first report (reference 1) documented the initial evaluation of the Interim APC 6.6 GHz channels. SMMR data was compared with sea surface temperature values obtained from the NMFS monthly average sea surface temperature map for September, 1978. This comparison yielded the first indication of the existence of opposing cross-track gradients. A brief survey of T_A data suggested that the source of the gradients may lie in the T_A data.

Report 2 - The second report (reference 2) extended the evaluation to all ten of the Interim APC channels. This portion of the evaluation established the basic software analysis tools to be used throughout the following stages of the study. SMMR data was compared with NDBO buoy measurements, using a geophysical model to convert the buoy measurements into predicted brightness temperatures. This initial attempt at determining T_B biases was frustrated by a lack of atmospheric water vapor and cloud liquid water measurements. However, this comparison still indicated the existence of T_B biases which vary from channel to channel, with the horizontal channel biases being more positive than the corresponding vertical channel biases. In addition, opposing cross-track gradients were observed for the 18 and 21 GHz channels as well as the 6.6 GHz channels.

Report 3 - The third report (reference 3) represented the first evaluation of the sidelobe corrections implemented in the Gaussian APC. Gaussian APC output was directly compared with corresponding Interim APC output for the three basic environmental regimes of open ocean, crossing a coastline, and paralleling a coastline. The Gaussian T_B values were found to be significantly lower than corresponding Interim values, and in addition, gradients observed in the Gaussian data were significantly different from those observed in Interim data. Both observations suggested that the sidelobe correction procedure was introducing errors into the T_B data. This conclusion was reinforced by the first observations of "ringing," seen in the Gaussian T_B data at coastline crossings. In a parallel effort, first estimates of cos β values were obtained by fitting T_A data to the narrow beam antenna equations. These cos β values correlated well with the opposing cross-track gradients previously observed in the Interim APC.

1.0 SUMMARY

This report contains an evaluation of the latest versions of the SEASAT-A SMMR Antenna Pattern Correction (APC) algorithm, and concludes the APC evaluation previously documented in references 1 through 4. The report focuses on two principal efforts: 1) the intercomparison of the interim, box, cross, and nominal APC modes, and 2) the development of new software to facilitate the creation of matched spacecraft and surface truth data sets which are co-located in time and space.

The more important conclusions of the report are:

(1) Most of the problems in the APC outputs discussed in the previous reports have now been eliminated or reduced to insignificant levels.

(2) The box mode is superior to the interim mode in that it removes some of the sidelobe contamination effects due to nearby land without exhibiting "ringing."

(3) The cross and nominal modes are unreliable near land due to the presence of "ringing" effects.

2.0 INTRODUCTION

The work described in this report concludes the current evaluation of the APC algorithm which is documented in references 1 through 4. Over the course of this evaluation, the APC has evolved through several stages of development. The following presents a synopsis of this stepwise evolution.

a. The first version of the APC to be implemented is known as the Interim APC. This version of the algorithm does not include corrections for Earth sidelobe contributions, although it does correct for sidelobe contributions from cold space.

b. The Gaussian APC is the first version which applies Earth sidelobe corrections. The actual antenna patterns are not used, but are approximated by smooth Gaussian functions.

c. The Nominal APC is identical to the Gaussian version except that the actual antenna patterns are used in performing Earth sidelobe corrections. Corrections are applied for all cells outside the cell being corrected.

d. The Cross APC is a refinement of the Nominal, developed for the purpose of eliminating algorithm sensitivity to small errors in the sidelobe contributions from the four cells nearest the one being corrected.

e. The Box APC is a further refinement of the Nominal, which eliminates sensitivity to small errors in all eight adjacent cells.

CONTENTS (CONTINUED)

CONTENTS (CONTINUED)

CONTENTS (CONTINUED)

FIGURE

CONTENTS (CONTINUED)

CONTENTS (CONTINUED)

FIGURE

CONTENTS (CONTINUED)

CONTENTS

ABSTRACT

This report contains an evaluation of the latest versions of the SEASAT-A SMMR Antenna Pattern Correction (APC) algorithm, and concludes the current APC evaluation effort. The report focuses on two principal efforts: 1) the intercomparison of the interim, box, cross, and nominal APC modes, and 2) the development of new software to facilitate the creation of matched spacecraft and surface truth data sets which are co-located in time and space. The major conclusion of the report is that most of the problems discovered in earlier versions of the APC have now been corrected.